Proceedings of the Session on

Construction Materials and Systems

6th International Conference on

Structural Engineering and Construction Management 2015

Kandy, Sri Lanka

11th to 13th December 2015

Abstracts of 6th International Conference on Structural Engineering and Construction Management 2015

Vision

Promoting innovative research for tomorrow's development

Mission

To meet experts, colleagues and friends in the field and to exchange findings, concepts and ideas on research for the development of a sustainable world

ISBN: 978–955–589–210-0

Printed at: Nethwin Printers (Pvt) Ltd.,
Gampola Road, Peradeniya, Sri Lanka
E-mail: nethwin@yahoo.com

Preface

It is with great pleasure that we present the Proceedings of the 6th International Conference on Structural Engineering and Construction Management (ICSECM 2015). This is the sixth conference consecutively organized following the 1st International Conference on Sustainable Built Environment in 2010, 2nd International Conference on Structural Engineering and Construction Management in 2011, 3rd International Conference on Sustainable Built Environment in 2012, 4th International Conference on Structural Engineering and Construction Management in 2013 and the 5th International Conference on Sustainable Built Environment in 2014, keeping its tradition of adhering to engineering excellence.

Taking a step forward from the last four events, the coverage of specialty areas of this conference has been diversified. This book contains the abstracts of research papers from ten different sub specialties in Construction Management, Construction Materials and Systems, Structural Health Monitoring, Structural and Solid Mechanics, Earthquake Engineering, Fatigue Damage of Materials, Water Safety, Hydraulic Structures, Tall Building and Urban Habitat and MSW and Landfill Management. We expect that all these abstracts will be presented in parallel sessions from 11th to 13th December 2015.

We would like to express our appreciation to all keynote lecturers for their invaluable contribution for the development of a sustainable world. We are very much grateful to the authors for contributing research papers of high quality. The research papers of these abstracts in the publication have been peer-reviewed. The enormous work carried out by the reviewers is gratefully appreciated. We are also pleased to acknowledge the advice and assistance provided by the members of the international advisory committee, members of the editorial committee along with many others who volunteered to assist to make this very significant event a success. Finally, we acknowledge the financial sponsorship provided by many organizations that has been extremely helpful in successfully organizing this international conference.

It is the earnest wish of the editors that this book of abstracts and volumes of proceedings would be used by the research community and practicing engineers who are directly or indirectly involved in studies related to Construction Management.

Editorial Committee

6th International Conference on Structural Engineering and Construction Management 2015

11th December 2015.

**Message from
Conference Chairmen**

It is a pleasure for us to welcome all the participants to the 6th International Conference on Structural Engineering and Construction Management 2015 in Kandy, Sri Lanka. We, the co-chairs would gratefully like to mention the previous successful conferences, the 1st International Conference on Sustainable Built Environment 2010, 2nd International Conference on Structural Engineering and Construction Management 2011, 3rd International Conference on Sustainable Built Environment 2012, 4th International Conference on Structural Engineering and Construction Management 2013 and the 5th International Conference on Sustainable Built Environment in 2014, all held in Kandy, Sri Lanka.

The theme selected for the conference - Structural Engineering and Construction Management- is extremely relevant for today's world. With the vision of promoting innovative research for tomorrow's development, we organize this conference as a meeting place of talents, knowledge and dedication. Therefore, we trust that the conference will produce great ideas from a variety of research and exchange the knowledge of experts, colleagues and friends who are working for the world's sustainable development.

The conference focuses on ten different sub topics in Structural Engineering and Construction Management: Construction Management, Construction Materials and Systems, Structural Health Monitoring, Structural and Solid Mechanics, Earthquake Engineering, Fatigue Damage of Materials, Water Safety, Hydraulic Structures, Tall Building and Urban Habitat and MSW and Landfill Management. The proceedings of the conference are peer reviewed. The full papers are published in five volumes in paper format with a book of abstracts.

The host city of the conference, Kandy, is a world heritage city famous for its unique architecture, culture, natural beauty and climate. We hope that you will enjoy your time in Kandy during the conference.

We, the conference co-chairs express our sincere thanks to our guests, keynote speakers, authors, members of the international advisory committee, members of the editorial committee financial sponsors and many others who volunteered to assist to make this very significant event a success.

Prof. Ranjith Dissanayake
Prof. S.M.A. Nanayakkara
Prof. Priyan Mendis
Prof. Janaka Ruwanpura
Dr. Y.G.S. De Silva
Eng. Shiromal Fernando

Co-chairs

6th International Conference on Structural Engineering and Construction Management 2015
11th December 2015.

Message from
Dean, Faculty of Engineering, University of Peradeniya.

I am glad to submit this message for the Sixth International Conference on Structural Engineering and Construction Management (ICSECM-2015), which is a continuation of the efforts of the organizers to share knowledge and research in the sectors. This time too, the conference is held in historic city of Kandy, in Sri Lanka.

The ICSECM - 2015 is organized as a joint effort of a number of professionals, and a number of institutions; including Engineering Faculties of Peradeniya, Moratuwa and Ruhuna Universities in Sri Lanka. The topic covered and the keynotes delivered by professionals in the field add more depth to the objectives and outcomes of the conference.

I take this opportunity to thank the organizers for their commitment and persistent effort to make the conference a success. These events facilitate a forum for many young undergraduate and postgraduate students to receive a good initial exposure to present their work, and for some few, to get a flavor of organizing events of global importance.

I believe that the organizers of ICSECM-2015 will continue their dialog of bringing concerned professionals from diverse fields, from different parts of the worlds, into the discussion forum of ICSECM.

I wish the conference a great success.

Prof. Leelananda Rajapaksha

Dean,
Faculty of Engineering,
University of Peradeniya,
Peradeniya,
Sri Lanka.

Table of Contents

SECM/15/138
INVESTIGATION OF STRENGTH PARAMETERS AND PHYSICAL PROPERTIES OF NON-CLASS TIMBER SPECIES IN SRI LANKA
Ruwanpathirana B.S, Rathnayaka R.M.C.P, Sudhira De Silva and Subashi De Silva

SECM/15/139
EFFECT OF RICE HUSK ASH (RHA) ON STRUCTURAL PROPERTIES OF BURNT CLAY BRICKS
B.V.A. Perera, K.G.S. Madhushanka, G.H.M.J. Subashi De Silva and G.S.Y.De Silva

SECM/15/141
EVALUATING SUBCONTRACTOR PERFORMANCE IN CONSTRUCTION INDUSTRY
L. Chamara, A. Waidyasekara and H. Mallawaarachchi

SECM/15/143
USE OF RICE HUSK ASH BLENDED CEMENT TO MANUFACTURE CEMENT-SAND CELLULAR BLOCKS
A. Dolage, A. Alirajay and A. Parvathakeethan

SECM/15/147
STUDY ON MODERN METHODS OF CONSTRUCTIONS USED IN SRI LANKA
H.M.M.Uthpala and T.Ramachandra

SECM/15/152
POTENTIAL OF USING SRI LANKAN APATITE AS A DE-FLUORIDATION AGENT AGAINST VARIOUS APATITE MATERIALS
A.A.G.D. Amarasooriya, Hikaru Miyazaki and Tomonori Kawakami

SECM/15/155
DETERMINATION OF TENSILE STRAIN CAPACITY OF FRESH CONCRETE ; A NEW TEST METHOD
T. G. P. L. Weerasinghe and S. M. A. Nanayakkara

SECM/15/159
EXPERIMENTAL STUDY ON INTEGRATED METHOD OF NSM AND EBR TECHNIQUES FOR FLEXURAL STRENGTHENING OF CONCRETE BEAMS USING CFRP
N.A.Amarasinghe and J.C.P.H. Gamage

SECM/15/160
ACI GUIDELINES TO ASSESS THE PERFORMANCE OF CFRP-STRENGTHENED CONCRETE BEAMS WITH TRANSVERSE END U WRAPS
M.R.E.F. Ariyachandra and J.C.P.H. Gamage

SECM/15/024

Analysis of Strain Rate Dependent Tensile Behaviour of Polyurethanes

H. M. C. C. Somarathna[1], S. N. Raman[2*], K. H. Badri[3,4], A. A. Mutalib[1]

[1]Department of Civil and Structural Engineering, Universiti Kebangsaan Malaysia
43600 UKM Bangi, Selangor, Malaysia
[2]Department of Architecture, Universiti Kebangsaan Malaysia
43600 UKM Bangi, Selangor, Malaysia
[3]School of Chemical Sciences and Food Technology, Universiti Kebangsaan Malaysia
43600 UKM Bangi, Selangor, Malaysia
[4]Polymer Research Centre (PORCE), Universiti Kebangsaan Malaysia,
43600 UKM Bangi, Selangor, Malaysia
*E-Mail: snraman@gmail.com, hmccsomarathna@gmail.com; TP: +603 8911 8403

Abstract: The stress-strain behaviour of elastomeric polymers, such as polyurethane (PU), exhibit high rate dependency, stress–strain non-linearity, and high pressure dependency when compared to other construction materials. Since these polymers exhibit the potential to be applied as retrofitting and protective material for various types of structural materials, in enhancing their load-carrying capacity, ductility and structural survivability under different loading regimes, it is essential to comprehensively investigate their mechanical behaviour at varying strain rates. This study was undertaken to investigate the tensile stress-strain characteristics of elastomeric PU at varying strain rates, ranging from 0.001 s^{-1} to 0.1 s^{-1} (low to intermediate). The primary emphasis of this study was on the strain rate sensitivity of the tensile properties, including the Young's modulus, tangent modulus, ultimate tensile stress, fracture strain, and strain energy modulus. The findings indicated that stress-strain behaviour of the PU exhibited high dependence to variations in strain rates and stress–strain non-linearity. The behaviour of PU also provided good concurrence with recent studies, which explored the strain rate dependency of other elastomeric polymers.

Keywords: Dynamic loading, Polyurethane, Strain rate, Stress-strain behaviour, Tensile behaviour.

1. Introduction

Elastomeric polymers, such as polyurethane (PU), are currently considered amongst promising materials for several types of structural applications, where these polymers provide extra structural capacity, and resistance against severe environmental conditions. Typical examples for applications of elastomeric polymers in numerous industries vary from building structural elements (masonry, concrete, steel and composite elements), vehicles, infrastructures including underground structures (such as pipelines), marine constructions, etc. [1-3]. The conventional technique of enhancing the capacity of a structural element is by increasing the mass and the stiffness of the element. Though it is used commonly, it forms obstacles such as; high initial cost, high materials and resources consumption, and inappropriateness for the existing structures [3]. Consequently, structural and material engineers have been investigating to find more appropriate solutions as alternative for those techniques.

Based on the prior investigations, it can be observed that increasing the energy absorption capacity of the element is an efficient technique to reduce the level of destruction and fragmentation effect of failures under impulsive loading conditions [2,3]. To achieve high energy absorption in structural elements, it is essential to use materials which possess high stiffness and strain capacity. Although cementitious materials are known to have high stiffness values, they fail via tensile cracking when overloaded, since cementitious materials have low tensile strain capacity (with tensile strain of about 0.0001, nearly one-tenth that of compressive strain), and with low fracture toughness approximately 0.01 kJ/m^2, compared with other construction materials such as mild steel (100 kJ/m^2), they are extremely brittle [4]. Elastomeric polymers including PU have been of great interest among the structural and material engineers, and are also considered for the blast protection of several structural elements. Since PU exhibits characteristics such as high toughness-to-density ratio under high strain rate conditions, and leads to enhancement in the dynamic performance and failure resistance under impulsive conditions. [2,3]. PU readily adheres to numerous types of surfaces including concrete, masonry, metal, and wood, and has a fast curing time with straight forward techniques of preparation and application. Therefore this technique shows a better concurrence to be used as a strengthening material for existing structures to enhance the blast and ballistic resistance of structures [2,3].

The properties of most types of elastomers are highly variable. They depend on many factors including chemical combination which were used to synthesise, temperature, loading rate which is applied during testing, etc. Therefore, a major challenge is, however, to select the best material since the characteristics of the elastomers are rate dependent, and are considerably non-linear. Prior to investigating the dynamic response and the resistance mechanisms of elastomeric PU as a retrofitting material, it is important to study the behaviour of the PU elastomer at a wide range of strain rates to simulate the behaviour of the material under static and dynamic loading regimes. Considering that structures experience different loading conditions during their service life, and impact loading being one of the critical. In addition, PU elastomers exhibit wide range of mechanical properties, generally from soft (or lower stiffness) to hard (or higher stiffness), depending on the chemical composition and their characteristics. At room temperature, elastomeric PU is highly flexible, elastic, and resistant to impact, abrasion, and weather [1]. Therefore, the evaluation of structural behaviour of elastomeric PUs, and their response under wide range of temperatures, strain-rates and pressures conditions should be clearly understood.

Though the mechanical performance of elastomeric polymers under essentially static loads can be evaluated using a variety of specifications and techniques, standard test methods available for determining the dynamic response of those materials are scarce. Over the last few decades, various instrumentations and testing procedures have been developed to investigate the dynamic response of elastomeric materials. Among the various techniques used for this purpose are: Universal test machine, the Hopkinson bar testing system, the high speed impact or drop hammer testing system, the Zwick screw drive mechanical tester, various servo-hydraulic testing systems, as well as other types of customized high speed test configurations [5-16]. According to the findings of the above studies on the behaviour and the strain rate sensitivity of the elastomeric polymers, the researchers have highlighted, that the stress-strain response of most elastomeric polymer materials exhibits significant non-liner rate sensitivity under low, intermediate and high strain rate conditions [5-13].

In the present study, the authors have focussed to investigate on the tensile behaviour of two types of elastomeric Pus, from low to intermediate strain rate ranges (0.001 to 0.1 s^{-1}), using a hydraulic universal testing machine (Instron 5566 universal testing machine).

2. Experimental Programme

2.1 Materials

Palm-based polyol (PKO-p) was supplied by the Polymer Research Centre (PORCE) of Universiti Kebangsaan Malaysia. 4,4-diphenylmethane diisocyanate (MDI) was obtained from Cosmopolyurethane Sdn. Bhd., Malaysia. Acetone (industrial grade) and polyethylene glycol (PEG: Mw 200 Da) were purchased from Sigma Aldrich (M) Sdn. Bhd., Malaysia.

2.2 Preparations of the polyurethane elastomer

Two types of polyurethane (PU) resins were prepared by solution casting technique, from the rapid reaction between PKO-p and MDI in the presence of PEG as the plasticizer via pre-polymerisation technique. They were labelled as PU-A and PU-B comprising of 6 and 8 % w/w of PEG, respectively. The PKO-p, MDI and acetone were formulated at the ratio of 100: 80: 35. Clear yellowish and bubble-free PU films were obtained, and let to condition at ambient temperature for further characterization.

2.3 Tensile test

The uniaxial tensile tests were carried out in an Instron model 5566 testing machine under displacement controlled conditions (different crosshead speed were used to obtain different strain rates) [Figure 1(a)]. The cured pre-cast PU sheets of 3 mm thickness were cut to dumbbell shaped specimens (Die C) for tension tests as per ASTM D 412: Method-A specification [Figure 1(b)], in the same direction of the sheets, in order to minimise the effect of anisotropy or grain directionality due to the direction of the flow during the preparation and the processing of the PU sheets. The median of three measurements were used for the dimensions (width and thickness) of each samples. All test specimens were clamped to the grip automatically with a clamping distance of 65 mm, and tested at ambient temperature with uniform rates of 1.5, 15 and 150 mm/min to attain strain rates of 0.001, 0.01, and 0.1 s^{-1} respectively. The time, load, and deflection data were recorded until the rupture of specimens.

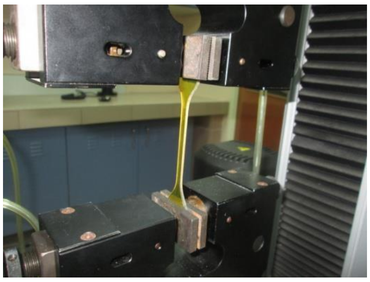

(a)

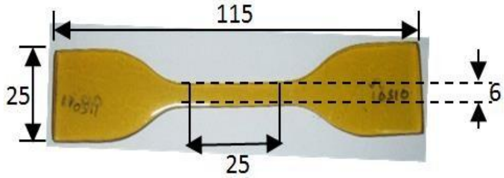

(b)

Figure 1: The: (a) Uniaxial tensile test; and (b) Dimensions of specimens (in mm).

3. Results and Discussion

The tensile characteristics of PUs were analysed based on the experimental data and the values was obtained as an average of five sets of tests for each category

3.1 Tensile Characteristics

The tensile responses (engineering stress-strain relationship) of PU-A and PU-B are shown in Figures 2 and 3 respectively at lower to intermediate strain rates (0.001 to 0.1 s^{-1}). All stress-strain curves follow the behaviour of typical elastic-plastic material. Figures 2 and 3 indicated that the all PUs exhibited significant hysteresis behaviour during loading. The is further supported by the findings in Figure 4(a-e), which depict the variation of the Young's modulus, stress at elastic limit, tangent modulus, ultimate tensile stress, and failure strain as a function of strain rate at various increasing strain rates. In addition, the tensile strain energy response and characteristics, which are the cumulative strain energy density, resilience and toughness modulus and their ratios at increasing strain rates are illustrated in Figures 5 and 6.

3.1.1 Young's modulus

The engineering stress-strain curves indicated that the initial response in each case depicted a linear elastic region, with the average Young's modulus approaching 25.0, 44.1, and 85.8 MPa for PU-A, and 22.6, 34.5, and 70. 5 MPa for PU-B at strain rates of 0.001, 0.01, and 0.1 s^{-1} respectively. The variation of the Young's modulus of PUs with varying strain is shown in the Figure 4(a).

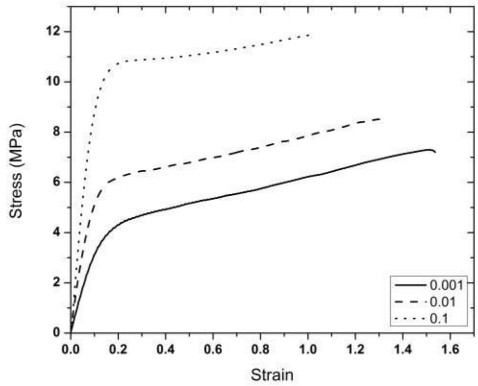

Figure 2: The engineering stress-strain curves of PU-A at varying strain rates.

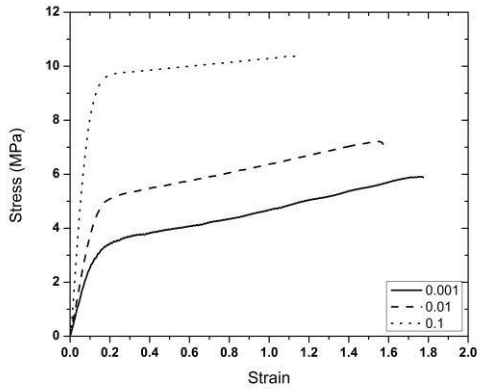

Figure 3: The engineering stress-strain curves of PU-B at varying strain rates.

As illustrated in Figures 2 and 3, both PU-A and PU-B show similar behaviour, and the Young's modulus was increased significantly with the increasing strain rate. Findings indicate the 1.8, and 3.4 increment of PU-A, and 1.5, and 3.1 increment of PU-B for strain rates of 0.01 and 0.1 s^{-1}, when compared with the Young's modulus at 0.001 s^{-1}, and they exhibited strain hardening mechanism.

3.1.2 Stress at elastic limit

Subsequently after the linear region, the PUs started yielding after reaching considerable stress and elongation for all cases [Figure 4(b)]. Within this region, it can be concluded that, the stress at elastic limit increases significantly with increasing strain rates. In this case, the variation of the stress at elastic limit is similar for both PUs, and with the increasing trend of Young's modulus at varying strain rates. The stress at elastic limit for 0.01 and 0.1 s^{-1} strain rates, of PU-A was 1.4, and 2.6 times higher, and for PU-B was 1.6, and 2.9 times higher, than the value at 0.001 s^{-1} strain rate, though the yield strains were almost similar for all cases .

3.1.3 Tangent modulus

All PUs underwent a brief period of yielding which resulted in permanent or inelastic deformation under all strain rate conditions. Further increase in the stress above the elastic limit caused molecular breakdown of the material and result in permanent deformation. The tangent modulus defines the behaviour of the material at stress beyond its elastic limit. The variation of tangent modulus with strain rates was obtained using the findings obtained above; the respective results are presented in Figure 4(c). The tangent modulus was influenced significantly by the strain rate effects, and it decreased with increasing strain rates for both PU-A, and PU-B. In addition, PU-A showed a rapid reduction between the strain rates of 0.01 and 0.1 s^{-1} in comparison to PU-B. PU-B is more ductile due to its higher content of plasticizer. Moreover, all PUs yielded over wide range of strains. Although each PU system underwent permanent deformations, it was still able to withstand more load prior to ultimate failure.

3.1.4 Ultimate Tensile Stress

The variation of ultimate tensile stress, against strain rates is presented in Figure 4(d). Higher strain rates resulted in an increase in ultimate tensile stress, up to more than 17% and 82% for PU-A and 24% and 88% for PU-B at strain rates of 0.01 s^{-1} and 0.1 s^{-1}, when compared to ultimate tensile stress at 0.001 s^{-1}. PU-A which contains lower content of plasticizer, shows higher ultimate tensile stress at all strain rates.

3.1.5 Failure Strain

The failure strain of a material is one of the key characteristic to evaluate its behaviour under different loading conditions and indicates its capability to undergo the required deformation prior to fracture. Engineers often select more ductile materials for retrofitting applications under dynamic loading events, since those materials are capable of absorbing energy or shock imparted. In addition, if the material is overloaded, it will usually provide "signs" through its deformation before failure.

The plot of failure strain versus strain rate is shown in Figure 4(e). The failure strain of PUs decreased with increasing strain rates. The materials exhibited viscoelastic characteristics, which were inclined to fail at a higher stress, but at a lower strain.

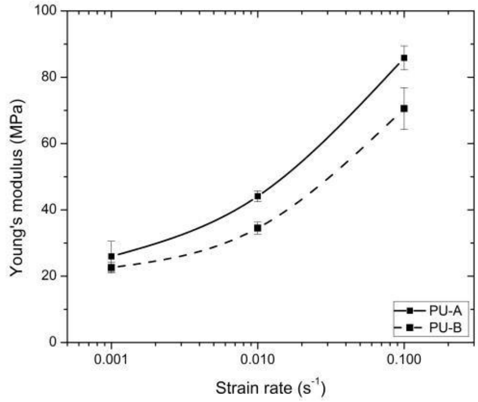

(a)

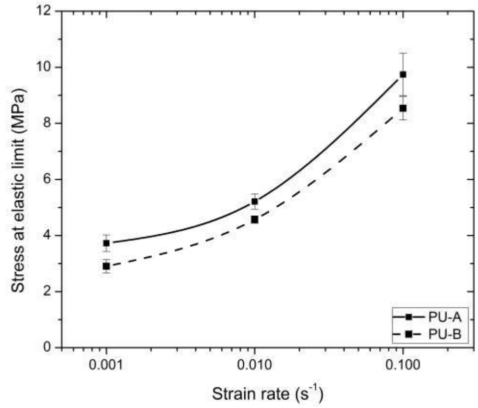

(b)

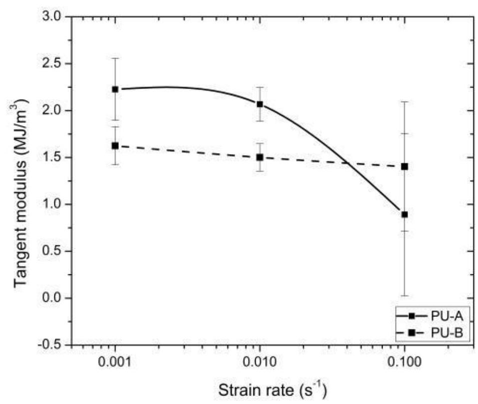

(c)

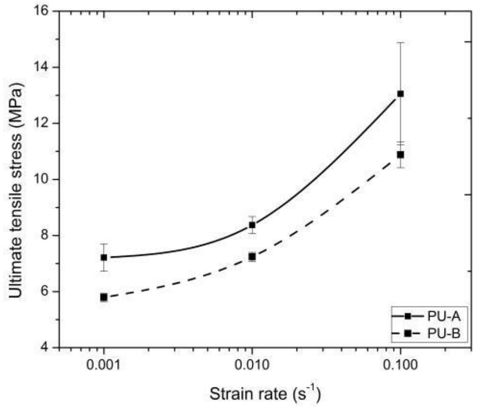

(d)

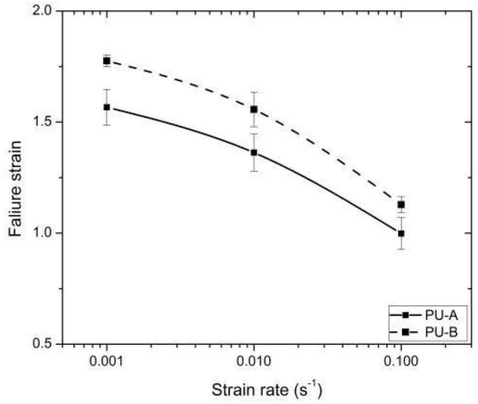

(e)

Figure 4: The tensile characteristics of the PUs at varying strain rates: (a) Young's modulus; (b) Stress at elastic limit; (c) Tangent modulus; (d) Ultimate tensile stress; and (d) Failure strain.

Similar observations were reported by Roland et al. [11] based on their experimental findings of uniaxial tensile behaviour of elastomeric polyurea in over a range of strain rates from 0.06 to 573 s^{-1}. Moreover, PU-B showed higher failure strain at all strain rates. The addition of plasticizer increases the chain length of the polymer, and leads to the PU sample to have a higher mobility in its molecular structure, thus reducing the stiffness of the sample.

3.2 Strain energy

The energy stored internally in a material due to change of its original shape is known as the strain energy. The strain energy per unit volume is referred to as the strain energy density, and is computed by integrating the area underneath the specific stress-strain curve up to the reference point of deformation. The energy absorption and dissipation ability of a material are a key properties that should be considered in the retrofitting application for a structural element subjected to dynamic loadings. The applied load on a material is stored as strain energy throughout its volume. The comparison of cumulative strain energy density against strain for PU-A and PU-B, is shown in Figure 5, for the three different strain rates.

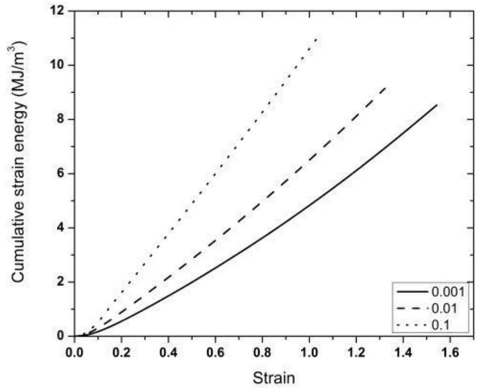

(a)

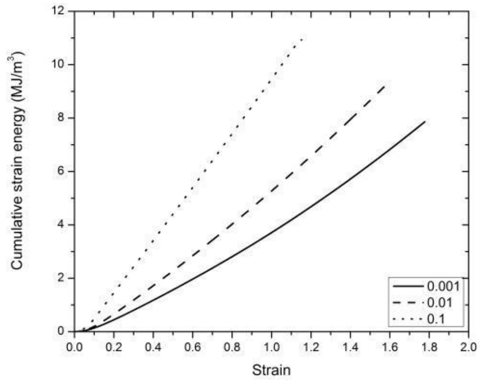

(b)

Figure 5: Cumulative strain energy versus strain at varying strain rates, for: (a) PU-A; and (b) PU-B.

3.2.1 Resilience Modulus

In particular, due to the application of loads, the resulting deformation up to the elastic limit of the stress-strain curve, was only accompanied by the absorption of energy. The resilience modulus (U_r) is defined as the strain energy density when the stress reaches the proportional limit, and is computed by taking the area under the stress-strain curve from zero to the proportionality limit [17]. The variation of the U_r of PUs with enhancing strain rates is exhibited in Figure 6(a). Based on the results, it was deduced that the U_r tends to be increased with increasing strain rates. In addition, the difference of the U_r values of PU-A and PU-B decreased with the increasing strain rate.

3.2.2 Toughness Modulus

The toughness modulus (U_t) at varying strain rates is shown in Figure 6(b). Physically, the U_t

represents the strain energy density just before the rupture of the material, and quantify the entire area underneath the stress–strain diagram [17]. With increasing strain rate, the PUs exhibited increments in their toughness moduli.

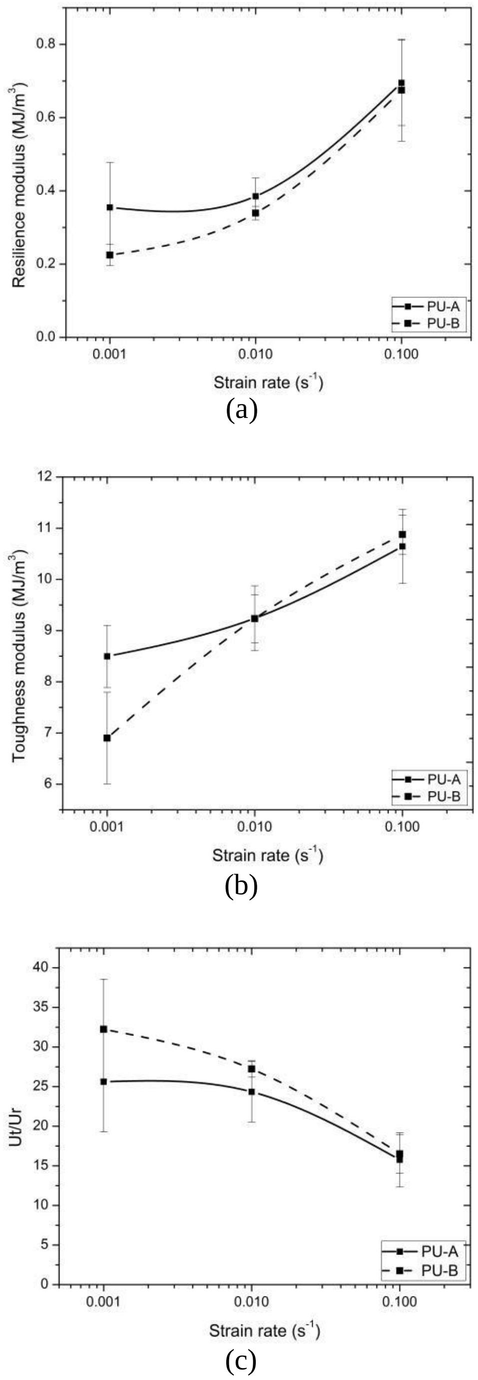

(c)

Figure 6: Strain energy characteristics of the PUs at varying strain rates: (a) Resilience modulus; (b) Toughness modulus; and (c) Ratio between toughness and resilience modulus.

While at low strain rates, PU-A exhibited lower U_t compared to PU-B, both PUs recorded almost similar values at 0.01 s^{-1}. Subsequently, at 0.1 s^{-1}, PU-B showed higher U_t value compared to PU-A. This may be due to the higher content of plasticizer in PU-B resulting in it exhibiting higher ductility. Though the U_r and U_t were enhanced with increasing strain rates, the ratio between the toughness and resilience modulus decreased for both PU-A and PU-B with increasing strain rates [Figure6(c)]. Moreover, PU-B showed higher ratio at all strain rates. While at lower strain rates, PU-B exhibited ratio which was almost 1.3 times compared to PU-A, the ratio were much closer at higher strain rates.

These outcomes suited with the objectives of the present study, to deliver PU as a retrofitting material for structures subjected to dynamic loadings. The findings implied that PU would be able to absorb considerable amount of energy throughout elastic-plastic deformations (even after yielding of the material), before undergoing total failure.

4. Conclusions

The analysis of the tensile behaviour of two types of PUs under varying strain rates which were undertaken in this research indicated the following salient points:

- Both PU-A and PU-B exhibited significant rate dependency in terms of tensile properties, namely the Young's modulus, stress at elastic limit, ultimate tensile stress, tangent modulus, failure strain and strain energy modulus.
- The stress–strain behaviour of both PU-A and PU-B at varying strain rates was considerably non-linear.
- For both types of PU, the Young's modulus, stress at elastic limit, and ultimate tensile stress were enhanced, while the tangent modulus, and failure strain was reduced, with increasing strain rates.
- Even though the U_r and U_t increased with increasing strain rates, the ratio between U_t and U_r decreased. The increment of strain energy with increasing strain rate gives a good agreement as a characteristic of strengthening or retrofitting material to resist dynamic loadings.

Acknowledgement

The authors would like to express their gratitude to the Ministry of Higher Education, Malaysia in providing the necessary funding for this research through the ERGS Grant Scheme (ERGS/1/2013/ TK03/UKM/02/6), and to the Polymer Research Centre of UKM for the generous supply of palm-based polyol through the grant ETP-2013-026.

References

[1]. Chattopadhyay, D. K. & Raju, K. V. S. N. "Structural engineering of polyurethane coating for high performance applications". Progress in Polymer Science, Vol. 32, pp. 352-418, 2007.

[2]. Raman, S. N., Ngo T. amd Mendis, P., "Elastomeric Polymers for Blast and Ballistic Retrofitting of Structures". Electronic Journal of Structural Engineering, Vol. 11, pp. 69-80, 2011.

[3]. Somarathna, H. M. C. C., Raman S. N., Mutalib, A. A. and Badri, K.H., "Elastomeric Polymers for Blast and Ballistic Retrofitting of Structures". Jurnal Teknologi (Sciences & Engineering), Vol. 76, pp. 1-13, 2015.

[4]. Li, V. C., Lim, Y. M. and Chan Y. W., "Feasibility study of a passive smart self-healing cementitious composite". Composites: Part B, Vol. 29B, pp. 819-827, 1998.

[5]. Hoo Fatt, M. S. and Bekar, I., "High-speed testing and material modelling of unfilled styrene butadiene vulcanizates at impact rates". Journal of Materials Science, Vol. 39, pp. 6885- 6899, 2004.

[6]. Yi, J., Boyce, M. C., Lee, G. F. and Balizer, E., Large deformation rate-dependent stress-strain behaviour of polyurea and polyurethanes. Polymer, Vol. 47, pp. 319-329, 2006.

[7]. Sarva, S. S., Deschanel, S. Boyce, M. C. and Chen, W., "Stress-strain behaviour of a polyurea and a polyurethane from low to high strain rates. Polymer, Vol. 48(8), pp. 2208-2213, 2007.

[8]. Somarathna, H. M. C. C., Raman S. N., Mutalib, A. A. and Badri, K. H., "Tensile Behaviour of Polyurethane under Varying Strain Rates". Proceedings of the 7th Asia Pacific Young Researchers and Graduates Symposium 2015, 20-21 August 2015, Kuala Lumpur, Malaysia, 8 pgs, 2015.

[9]. Somarathna, H. M. C. C., Raman S. N., Mutalib, A. A. and Badri, K.H., "Mechanical Characterization of Polyurethane Elastomers: For Retrofitting Application against Blast Effects". The Third Conference on Smart Monitoring, Assessment and Rehabilitation of Structures (SMAR 2015). 7-9 September 2015, Antalya, Turkey. pp. 82-89.

[10]. Shim, J. & Mohr, D., "Using split Hopkinson pressure bars to perform large strain compression tests on polyurea at low, intermediate and high strain rates". International Journal of Impact Engineering, Vol. 36(9), pp. 1116-1127, 2009.

[11]. Roland, C. M., Twigg, J .N. Vu, Y. and Mott, P. H., "High strain rate mechanical behaviour of polyurea". Polymer, Vol. 48(2), pp. 574-578, 2007.

[12]. Ruan, D., Lenung, M. Y., Lu, G., Yu, T., Cao, J, & Blicblau, A. S., "Impact Tests on Lincoln Wool Fibers Using a Mini Split Hopkinson Tensile Bar". Textile Research Journal, Vol. 79(5), pp. 444-452, 2009.

[13]. Raman, S. N., Ngo, T. Lu, J. and Mendis, P., "Experimental investigation on the tensile behavior of polyurea at high strain rates". Materials and Design, Vol. 50, pp. 124-129, 2013.

[14]. Omar, M. F., Akil, H. M. & Ahmad, Z. A., "Measurement and prediction of compressive properties of polymers at high strain rate loading". Materials and Design, Vol. 32, pp. 4207-4215, 2011.

[15]. Naik, N. K., Shankar, P. J., Kavala, V. R., Ravikumar, G., Pothnis, J. R. & Arya, H., High strain rate mechanical behaviour of epoxy under compressive loading: Experimental and modelling studies. Materials Science and Engineering A, Vol. 528, pp. 846-854, 2011.

[16]. Ravikumar, G., Pothnis, J. R., Joshi, M., Akella, K., Kumar, S., Naik, N.K., "Analytical and experimental studies on mechanical behaviour of composites under high strain rate compressive loading". Materials and Design, Vol. 44, pp. 246-255, 2013.

[17]. Hibbeler, R. C. Mechanics of Materials, 8th Ed., Pearson, Singapore, 2011.

SECM/15/028

Synthesis of Ultra-High Performance Cementitious Composite incorporating Carbon Nanotubes

J. L.G. Lim[1], S. N. Raman[2]*, R. Hamid[1], M. F. M. Zain[2], F. C. Lai[3]

[1]Department of Civil and Structural Engineering, Universiti Kebangsaan Malaysia, 43600 UKM Bangi, Selangor, Malaysia
[2]Department of Architecture, Universiti Kebangsaan Malaysia 43600 UKM Bangi, Selangor, Malaysia
[3]Hume Concrete Products Research Centre, 46700 Petaling Jaya, Selangor, Malaysia
*E-Mail: snraman@gmail.com; TP: +603 8911 8403

Abstract: Ultra High-Performance Concrete (UHPC) is a type of special concrete developed to meet the demand for niche applications in the industry, where this type of concrete comes with enhanced durability and superior mechanical characteristics in comparison to conventional normal- and high-strength concrete. However, UHPC has its drawbacks in terms of lower tensile strength ratio and brittleness. Nanomaterials such as carbon nanotubes (CNT) with their superior mechanical properties are potential candidates to act as nano-reinforcement in Ultra High-Performance Cementitious Composite (UHPCC) matrix, to create a more denser and ductile UHPCC system. However, prior to arriving at the "desired" UHPCC mix design, attention has to be paid to the process of dispersing the CNT into the fresh composite mix since the dispersion of CNT in cement-based material is a challenge due to their agglomerating behaviour. This paper presents on the synthesis of UHPCC mix design which optimizes on its packing density of its constituent materials. The influence of different dispersion methods of CNT on the mechanical strength and microstructure of UHPCC are also reported. It was found that samples reinforced with CNT exhibit higher compressive and tensile strengths and denser microstructure compared to control samples without CNT.

Keywords: Carbon nanotubes (CNT); Ultra High-Performance Cementitious Composites (UHPCC); Mechanical properties; Microstructure; Nanoengineered

1. Introduction

A new class of cementitious composites, namely Ultra High-Performance Concrete (UHPC) was developed based on the advancement in sciences and engineering of concrete. The mechanical and durability properties of UHPC makes it feasible to be used in various kind of construction. UHPC is typically produced with high volume of cementitious materials (or binder), water, ultra-fine aggregates, fibre reinforcements (in large quantities) and rheology modifying admixtures. Unlike the generic type of concrete (as mentioned earlier), UHPC contains no coarse or fine aggregates in its mix. Instead, its matrix is packed with powdery sand or quartz-sand (at the micro scale), in most instance, with particle sizes of 0.600 mm or lower. This material is typically an ultra high-strength fibre reinforced cementitious composite, exhibiting a 28th day characteristic compressive strength of 150 MPa or higher [1].

One of the most important aspect of UHPC production is its fibre composition. While in the early decades, the use of fibres in concrete were focused towards the utilisation of steel (most widely used), carbon, glass, aramid and various types of natural fibres, which were in the centi- and mili-scale, the use of micro-scaled fibres was popularised by the commercialisation of Reactive Powder Concrete (RPC) in construction from mid-2000s onwards [1,2].

The discovery of carbon nanotube (CNT) by Iijima in 1991 [3], has given researchers in concrete engineering and technology a new avenue to further enhance and innovate this cementitious composite. The excellent mechanical properties of CNT, as well as the high aspect ratio allows the CNT to be an ideal nano-reinforcement for the development of UHPC even at lower dosages. However, studies have shown inconsistent and sometimes contradictory results of the effects of CNT on concrete properties, on the compressive and tensile strengths in particular [4]. The nano-scaled particle of CNT is a challenge to be dispersed homogenously and effectively into the cementitious matrix. Past studies have shown that ultrasonication is one of the effective method to disperse CNT in colloidal form. However CNT tends to agglomerate and thus result in concrete mix to record lower compressive strength. This can be improved by incorporating a surfactant during the dispersion process [4,5]. The presence of nano-scaled particles have the tendency to increase the early strength and improve the micro-structure of the matrix [4,6]. However, past research have shown that lower amount of CNT used will result in better dispersion. With only an addition of 0.5% of multi-walled CNT (by weight of cement) have resulted in the enhancement of compressive strength [4,7,8].

This paper explores the utilisation of nano-scaled fibres in the form of carbon nanotubes (CNT) in cementitious composites. This nano-engineered cementitious composite technology is still in the lab stage, where much of its engineering, mechanical, durability and dynamic properties is yet to be investigated in detail. This study was initiated to develop UHPCC with a compressive strength of 150 MPa and higher, under normal curing conditions and to investigate the effect of CNT on the strength properties of UHPCC.

2. Experimental Programme

2.1 Material and Mix Design

Three mix designs with different water/cement (w/c) ratios, designated as UHPC 0.28, UHPC 0.25 and UHPC 0.22 were designed and evaluated to obtain the optimum mix for the UHPC under normal curing conditions. The optimized mix design for the UHPC was then used for the mix design to investigate the effect of CNT on the properties of UHPC. Two mixed designs based on the selected UHPC mix namely UHPC-CNT-A and UHPC-CNT-B were developed (Table 1). Two mixes of UHPC-CNT-A were used. One mix design incorporates CNT-A produced using ultrasonification dispersion method while the other incorporates CNT-A produced via ultrasonification plus surfactant dispersion method. Meanwhile, mix design UHPC-CNT-B incorporates CNT-B produced using only the ultrasonification dispersion method. The details of the mix proportions are presented in the Table 1.

The materials used in this study were ordinary Portland cement (CEM I OPC), graded sand and superplastizer, and CNT. CNT-A was produced through chemical vapour deposition (CVD) method while CNT-B was produced by using plasma method. The CNT were dispersed using method described earlier to produce two variations of UHPCC incorporating CNT-A and one type of UHPCC with CNT-B. Figure 1 shows the type of CNT that was produced with different dispersion method in this study.

Table :1 UHPCC mix proportions

% by weight	UHPC 0.28	UHPC 0.25	UHPC 0.22	UHPC CNT-A	UHPC CNT-B
Cement	1	1	1	1	1
Graded sand	0.5	0.5	0.5	0.5	0.5
Water	0.28	0.25	0.22	0.22	0.22
Superplastizer	0.008	0.009	0.01	0.01	0.01
CNT				0.00066	0.00066

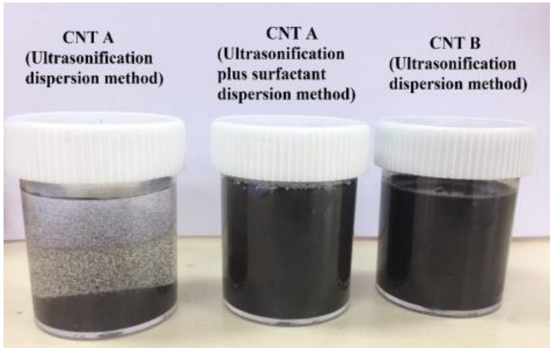

Figure 1: Type of CNT used

2.2 Specimen Preparation and Testing

Cement and micro-silica sand were first mixed together in a 5-litre capacity Hobart planetary mixer. After dry mixing, water (with or without CNT) was added into the mixer followed by superplasticizer and mixed until the fresh mixture achieved a consistent and uniform state. The flow value was measured to ensure a consistency flow expansion within 30 seconds. The fresh mix was then placed into the designated moulds with mild compaction on a vibration table. The moulds were then covered with PVC sheets at the top for the initial curing. All specimens were demoulded after 24 hours and were cured in water at 25^{o}C until the day of testing.

The compressive strength test was undertaken in accordance to ASTM C109/C109M-13 in which a 50 mm cubic specimen was rotated by 90 degrees and tested without capping or any surface treatment. Three specimens were tested for each mix and the average cube strength, f_{cu}, was determined. The three point bending test was performed in accordance with ASTM C348, using 40 × 40 × 160 mm prisms. Three specimens were tested for each mix design and the flexural strength, f_t, was calculated based on the following equation:

$$f_t = 0.0028\ P \tag{1}$$

Where P = maximum load, N

The particle size analysis of the cement and graded sand was performed using the Malvern Master Sizer 2000 Laser granulometry analyser. Meanwhile, the chemical compositions of the cement was determined using the XRD technique and are as summarised in Table 2.

Table 2: Chemical composition of cement

Composition	OPC, CEM I 42.5 N (%)
C_3S	75.3
C_2S	6.5
C_3A	5.6
C_4AF	7.8
Gypsum	4.5
$C_3S + C_2S$	81.8

An optimum packing density was achieved by considering the following equation:

$$P(d) = \left(\frac{d}{D}\right)^q \tag{2}$$

Where;
P = Fraction that is finer than size d
D = Maximum particle size of aggregate
q = Parameter q that has a value between 0 and 1

The grading by Fuller is obtained when q = 0.5 whereas the modified version by Andreasen and Andersen can be obtained when q = 0.37 [9].

In this analysis, the cumulative mass of both cement and graded sand was calculated based on the Fuller's curve equation to achieve optimum packing as presented in Figure 2.

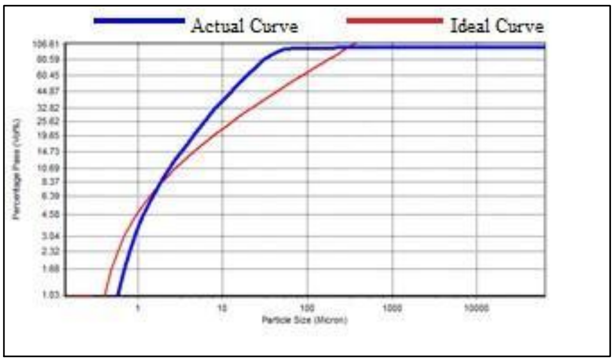

Figure 2: Optimum packing grading

3. Results and Discussions

3.1 Effect of w/c ratio

The 7th and 28th day compressive strength of the UHPC produced in this study with different w/c ratio are presented in Figure 3. It can be observed that UHPC mix with w/c 0.28 recorded the lowest compressive strength, which measured at only 108 MPa at 7 days and 132 MPa at 28 days. Meanwhile, the mix design with 0.22 w/c ratio recorded the highest strength with 128 MPa at 7 days and 151 MPa at 28 days.

Meanwhile, Figure 4 shows the flexural strength recorded at 28 days, and the ratio of 28th day flexural strength (f_t) to the compressive strength (f_{cu}). UHPC with w/c 0.22 achieved the highest flexural strength of 11.3 MPa but recorded the lowest f_t/f_{cu} ratio of 7.3%. This is due to the enhanced brittleness of the composite when it is driven to achieve higher strength with a much denser matrix. The flexural strength to compressive strength ratio can be expected to be decreased with the increase in compressive strength [10].

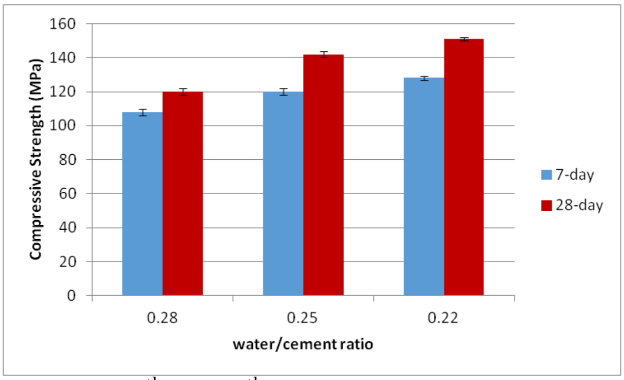

Figure 3: 7th and 28th day compressive strength of UHPC mixes produced with different w/c ratio

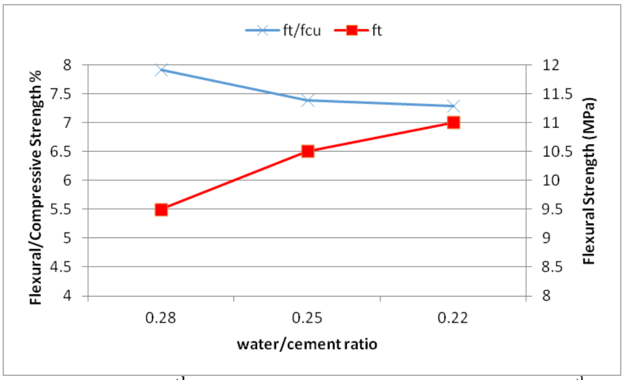

Figure 4: 28th day flexural strength, and the 28th flexural/compressive strength ratio

3.2 Effect of CNT types and dispersion methods

3.2.1 Compressive Strength

Figure 5 shows the 7th and 28th day compressive strength of UHPCC mixes, incorporating CNT produced with different dispersion techniques practiced in this study. It can be observed that UHPC-CNT-A (CNT-A dispersed via ultrasonification only) recorded the lowest compressive strength of 111 MPa at 7 days strength and 133 MPa at 28 days. On the other hand, UHPC-CNT-A with a much stable dispersion (CNT-A dispersed via ultrasonification + surfactant), achieved a slightly lower compressive strength compared to the control UHPCC specimen. This is possibly due to the presence of surfactant in the mix, which does not provide good bond characteristics with the cementitious structure [4]. The highest compressive strength was recorded by UHPC-CNT-B mix, where the CNT also underwent the ultrasonification dispersion method, with a compressive strength measured at 133 MPa at 7 days strength and 155 MPa at 28 days.

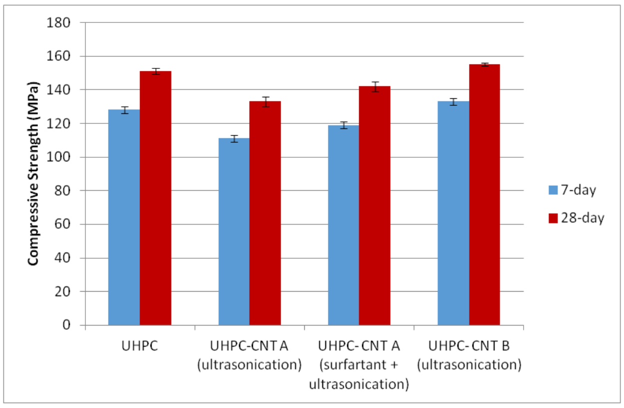

Figure 5: CNT-A and CNT-B under different dispersion methods

The Field Emission Scanning Electron Microscope (FESEM) micrographs of UHPC-CNT-A and UHPC-CNT-B are presented in Figures 6 and 7. It can be observed from Figure 6 that CNT-A likely underwent "agglomeration" in the matrix, which affected the structure of the UHPCC. This improper dispersion of CNT will affect the denser structure of UHPCC and leads to a decrease in the compressive strength.

The particle size of the CNT properties is another factor, with CNT-A consisting of generally uniform particles (approximately in the range of 40 nm), whereas CNT-B provided a better size distribution of nano particles and stable dispersion (Figures 6 and 7). Hence the nano materials existed in the matrix at the optimum stage. FESEM illustrated the good bond between CNT-B and the UHPCC matrix, whereas CNT-A with a smaller size distribution may not have had "excellent" bonding with the surrounding matrix.

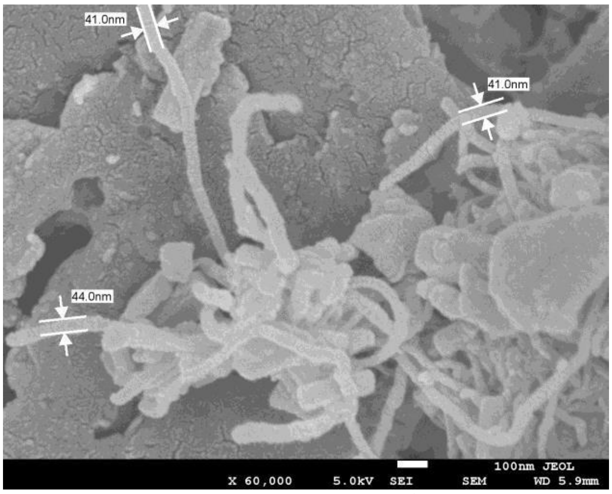

Figure 6: FESEM micrograph of CNT-A in the UHPCC matrix

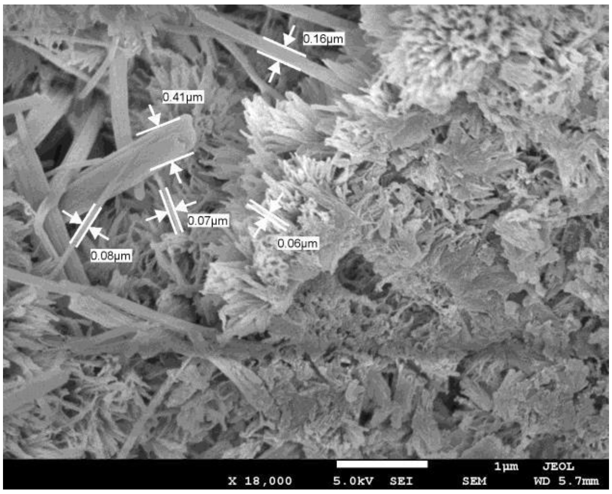

Figure 7: FESEM micrograph of CNT-B in the UHPCC matrix

3.2.2 Flexural Strength

Figure 8 presents the flexural strengths, and the corresponding flexural/compressive strength ratio at the age of 28 days. The flexural strength of both UHPC-CNT-A and UHPC-CNT-B was enhanced in comparison to the control UHPC. UHPC-CNT-B achieved the highest flexural strength of 21 MPa, a 70% enhancement compared to the control UHPC. As shown in Figure 7, CNT-B provided an effective bridging capacity with the surrounding matrix. With the effective bridging effect at nano-scale, the flexural/compressive strength ratio was enhanced to 13%. However, the flexural strength of UHPC-CNT-A was much lower due to ineffective dispersion of CNT-A, and the existence of weak bond between CNT-A and the cement matrix.

Figure 9 concludes overall findings based on the contribution of CNT-A and CNT-B on the compressive strength and flexural strength under the different dispersion methods. It is obvious that ultrasonication dispersion of CNT-B is the most effective way to disperse CNT, by achieving highest compressive strength and flexural strength. Good dispersion will result in better bonding between CNT and cement matrix, leading to increase in compressive strength. However, poor dispersion causes agglomeration of CNT which act as defect sites and result in poor bonding between CNT and cement matrix, thus lower the strength characteristics.

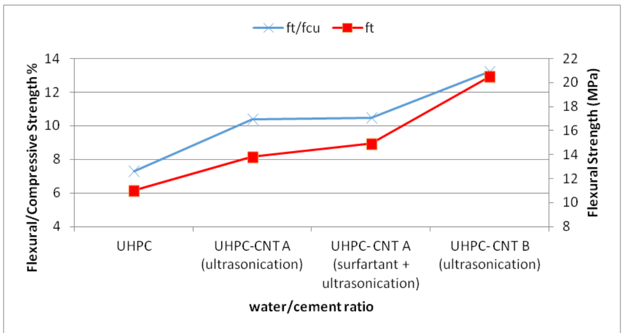

Figure 8: CNT-A and CNT-B respect to the control specimen

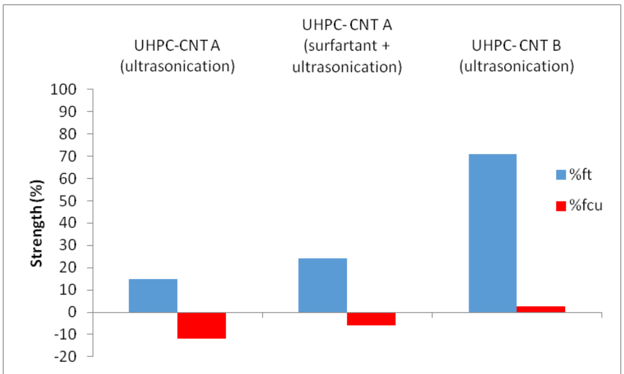

Figure 9: The effect of CNT-A and CNT-B on the strength

5. Conclusions

This study was undertaken to synthesise the mix design of UHPCC incorporating CNT, with a compressive strength higher than 150 MPa under normal curing conditions, and to investigate the effect of CNT on the properties of UHPCC. It was found that the characteristics of the CNT and its homogeneous dispersion method can contribute leads to significantly to the UHPCC characteristics. The findings from this research also indicated that even though the use of CNT as nanoreinforcement, in some cases resulted some minor negative effect to the compressive strength (decrease in the compressive strength of up to 11%), the flexural strength was improved significantly (up to 70%) compared to the control UHPCC mix. The overall findings of the research assert that CNT contributes in positive effect to the strength characteristics of UHPCC and is feasible to enhance the post-crack behaviour of the composite.

Acknowledgement

The authors would like to extend their gratitude to the Universiti Kebangsaan Malaysia for providing the necessary funding for this research through the DLP Grant Scheme (DLP-2014-005).

References

[1] Raman, S. N., "New Generation Concrete in Construction: 150 MPa and Beyond". in *In Between: Form + Being* (Edited by M. F. Mohamed & S. N. Raman): Faculty of Engineering and Built Environment, UKM, Bangi, Selangor, Malaysia, 2012, pp. 120-123.

[2] Voo, Y. L., Nematollahi, B., Mohamed Said, A. B. B., Gopal, B. A. and Yee, T. S., "Application of Ultra High Performance Fiber Reinforced Concrete – The Malaysia Perspective", International Journal of Sustainable Construction Engineering & Technology Vol. 3(1): pp. 26-44, 2012

[3] Iijima, S., "Helical microtubules of graphitic carbon", Nature 354, pp. 56-58, 1991.

[4]. Siddique, R. and Mehta, A. "Effect of carbon nanotubes on properties of cement mortars", Construction and Building Materials, Vol. 50, pp. 116-129, 2014.

[5] Collins, F., Lambert, J. and Duan, W.H., "The influences of admixtures on the dispersion, workability, and strength of carbon nanotube–OPC paste mixtures", Cement & Concrete Composites, Vol. 34, pp. 201-207, 2012.

[6]. Du, H., Du, S. and Liu, X., "Durability performances of concrete with nano-silica", Construction and Building Materials, Vol. 73, pp. 705-712, 2014.

[7] Kumar, S., Kolay, P, Malla, S. and Mishra, S., "Effect of multiwalled carbon nanotubes on mechanical strength of cement paste", ASCE Journal of Materials in Civil Engineering, Vol. 24, pp. 84-91, 2012.

[8]. Chuah, S., Pan, Z., Sanjayan, J. G., Wang, C. M., and Duan, W. H., "Nano reinforced cement and concrete composites and new perspective from graphene oxide", Construction and Building Materials, Vol. 73, pp. 113-124, 2014.

[9]. Brouwers, H. J. H. and Radix, H. J., "Self-Compacting Concrete: Theoretical and experimental study", Cement and Concrete Research, Vol. 35(11), pp. 2116–2136, 2005.

[10]. Mindess, S., Young, J. F., and Darwin, D, "Concrete, 2nd Ed.", Prentice-Hall, Upper Saddle River", NJ, US, 2003.

SECM/15/037

Feasibility of Using Palmyrah and Bamboo Strips as Reinforcement in Lintels

H. Y. V. Dias[1], M. A. S. S. Munasinghe[2] and K. Baskaran[3]

[1, 2, 3]University of Moratuwa, Katubedda, Sri Lanka

yomaldiaz@gmail.com, TP: +94716837096

Abstract: Timber species such as Palmyrah, Bamboo and Babadua have been identified to have potential to replace reinforcing steel in concrete elements. This research was conducted to assess the feasibility of using Palmyrah and Bamboo strips as reinforcing material in lintels. The low ductility of such timber specimens, as observed during the experiments, governed this selection of a lightly loaded low risk structural element for the study. Tensile strength, water absorption and desorption characteristics, associated dimensional variations, anchorage bond strength and flexural strength of Palmyrah and Bamboo strips coated with different water repellents were evaluated using a series of laboratory experiments. Having identified double varnish coated water repellent technique to give the highest anchorage bond strength and lowest water absorption, four lintels were cast keeping two as unreinforced control specimens and two reinforced with Palmyrah and Bamboo strips. While both reinforced beams exhibited under-reinforced behaviour, one with Bamboo reinforcement achieved an incremental moment capacity of 250% and the beam with Palmyrah reinforcement achieved that of 168% compared to their respective unreinforced beams. Hence, it was concluded that both Palmyrah and Bamboo shows potential to be used as reinforcement for lintels.

Key Words: Timber Reinforcement, Bamboo, Palmyrah, Lintel

1. Introduction

Construction industry is one which consumes significant amounts of non-renewable resources. With growing concerns on developing sustainable and cost effective solutions, much focus has been given during the last two to three decades to identify renewable materials, which can successfully replace conventional construction materials.

Steel is one such conventional construction material that is imported to Sri Lanka. Its uses within the country range from low cost rural housing schemes to high rise buildings in the heart of Colombo. The reason for steel to be considered the “go to” solution in structural and even non-structural applications could be the availability of a comprehensive and accurate knowledge base of its properties and the convenient availability of the material throughout the country [1]. Ghavami (2005) [2] specifically identified this lack of knowledge and research on locally available materials in developing countries as a key factor leading to the eventual use of industrialized materials for every application.

There have been a number of studies conducted in the past to determine the engineering properties of some natural fibres. Research conducted on Bamboo, Babadua, Raffia, Palm, Jute Wood have established a comprehensive knowledge base with respect to their mechanical properties [3-7].

In the Sri Lankan context, some research has been conducted to identify the mechanical properties of Bamboo and Palmyrah species found at various regions within the island, and to assess the performance of Palmyrah reinforced concrete beams and slab panels.

The present study was conducted to assess the feasibility of using Bamboo and Palmyrah strips as reinforcement in lintels. The choice of this structural element depended on the mechanical properties of timber species tested. Both Bamboo and Palmyrah specimens exhibited low ductility compared to steel during testing stages [1, 2, 8, 9]. It was decided to adopt a lightly loaded common concrete element with low structural significance for the study due to this reason.

2.Review of Literature

2.1 Bamboo as a reinforcing material

Tests on mechanical properties of bamboo have been conducted by various researchers in the past. Table 1 summarizes the findings by past researchers with respect to strength and stiffness properties of Bamboo.

Table 1 - Mechanical Properties of Bamboo

		Ghavami [3]	Harish et al. [8]	Pratima et al. [9]
Ultimate Tensile Strength (N/mm^2)		< 370	115-128	139-164
Modulus of Elasticity (GPa)			9.5-19	5.1
Ultimate Compressive Strength (N/mm^2)			108	
Pull Out Strength (N/mm^2)	Treated	0.73 - 2.75	0.9-1.3	
	Non Treated	0.52	0.95-1.07	
Shear Strength (N/mm^2)			29	

The ultimate tensile strength of Bamboo is comparable with that of Mild steel. Thus, the strength to weight ratio of Bamboo could be six times higher than that of Steel [3].

The modulus of elasticity established from previous researches for both Bamboo and Palmyrah species are comparatively low. They are in fact lower than that of concrete, and does not make a considerable contribution to the flexural stiffness of the reinforced beam [2]. In general, modulus of elasticity of Bamboo is considered to be approximately 1/15 of that of Steel [10].

Another issue associated with using timber in engineering applications is the damage due to insect attack. Bamboo with moisture content less than 15% is less likely to be susceptible to such attacks [3]. The service life of Bamboo in contact with ground can be as low as 1 year [10].

Testing of Bamboo reinforced beams have shown that prime cause of failure is the tensile failure of concrete and Bamboo. Even the over reinforced test specimens have not developed compression failure due to the impossibility of creating perfect bonding between concrete and Bamboo [3].

Absorption, desorption of moisture and associated dimensional variations are also major shortcomings that prohibit the use of Bamboo bars as reinforcement in concrete in their raw form. Stresses induced in the hardened concrete due to volumetric changes in timber reinforcement may introduce cracks, impairing the durability of the element [4, 5].

With effective treatment techniques, Bamboo-concrete bonding has found to increase by more than 100%. A reinforcement percentage of 3% has found to increase the ultimate load capacity of Bamboo reinforced beams by 400% compared to their unreinforced control specimen [3].

Bamboo reaches its full growth in a few months and maximum mechanical resistance is developed in a few years. It is also the fastest growing woody plant on the planet belonging to the grass family [11].

The colour of Bamboo is an indication of the maturity of the plant and could be used as a basis when identifying suitable specimens for engineering applications. Brown coloured trunk is an indication that the tree is at least three years old.

The properties of Bamboo vary depending on the nature of growth, climate conditions and soil moisture conditions. Therefore, although there exists a considerable amount of reliable information from past researches, it is required to establish reliable strength parameters pertaining to local conditions as past research may not be representative of local Bamboo species.

2.2 Palmyrah as a reinforcing material

Palmyrah growth in Sri Lanka is predominant in the dry zone, quite notably in the northern region. Generic uses of Palmyrah in building construction range from roofing elements such as rafters and purlins to earth retaining walls in bunkers.

Table 2 - Mechanical Properties of Palmyrah

	Baskaran et al. [1]
Tensile Strength parallel to grain (N/mm^2)	40-170
Modulus of Elasticity (GPa)	8-20
Compressive Strength parallel to grain (N/mm^2)	72-90
Flexural Strength (N/mm^2)	40-190

Baskaran et al. [1, 2] conducted experiments on Palmyrah samples from Jaffna and Puttlam from which the basic engineering properties shown in table 2 were established. The authors adopted the guidelines set out in BS EN 338: 1995 [12] in classifying the strength class of the specimen. Although the characteristic strength values conformed to the minimum strength limits of G70, hardwood of Palmyrah was categorized as G40, as the Elastic modulus of the tested specimens only achieved the limiting values of G40 class. The authors further stated that the tested specimens, despite originating from different regions in the island, exhibited similar mechanical properties.

3. Methodology

3.1 Tensile Strength Testing

Simple tensile strength tests were performed to evaluate the tensile strengths of Bamboo and Palmyrah strips. Three Palmyrah strips with approximately 12mm x 12mm cross sectional dimensions were tested using the Amsler machine.

Fifteen Bamboo specimens extracted from top, middle and bottom parts of the tree were tested using the tensometer. A fractured Bamboo specimen is shown below in figure 1.

Figure 1: A failed Bamboo specimen under tensile strength testing

3.2 Water Absorption and Desorption Testing

3.2.1 Palmyrah

Two series of tests were conducted on both softwood and hardwood samples of Palmyrah, coated with a variety of water repellent agents. Single and double coats of sanding sealer, varnish, black oil, bitumen, water paint and oil paint were utilized under this scheme.

Initially, the weights and the dimensional measurements of Series 1 Palmyrah samples were recorded. These samples were then put in the oven. Weights and dimensional measurements of these samples were recorded every 15 minutes. The oven dried Palmyrah samples were then immersed in water and similar readings were taken with time under absorption testing.

Series 2 contained a different set of treated and untreated Palmyrah samples. Here, the absorption test was conducted prior to the desorption test.

3.2.2 Bamboo

Water absorption tests were conducted on 63 treated and untreated Bamboo samples extracted from top, middle and bottom parts of the trunk. The test specimens were submerged in water for a total duration of 96 hours and weight measurements were taken within the test duration.

A separate set of 15 untreated Bamboo samples were used for desorption testing where the samples were oven dried for 24 hours and weight measurements were taken.

3.3 Pull Out Test

These pull out tests were carried out considering the guidelines established in BS EN 12504-3, (2005) [13]. Three varnish double coated Palmyrah specimens with approximately 12 mm x 12 mm cross sectional dimensions were tested using the Amsler testing machine, after 28 days from their casting date. Anchorage lengths of 50 mm, 100 mm and 150 mm were provided for the three specimens to assess the variation of pull out force with anchorage length. Figure 2 below shows the Pull out test setup and a failed sample split in to two to see the anchorage slip.

a b

Figure 2: (a) Pull out test setup, (b) Failed test specimen

Seven Bamboo specimens with different water repellent treatments and nodal arrangements were tested with each having 200 mm anchorage.

3.4 Bond Strength under Flexure

In order to investigate the behaviour of bond strength between the two types of timber reinforcing bars and concrete, the guidelines stated in BS EN 12269-1 (2000) were adopted. For each type of reinforcement, four beams were cast with the following properties.

i. Plain unreinforced concrete beam
ii. Beam reinforced with an untreated reinforcing bar, having an anchorage length of 600 mm
iii. Beam reinforced with a treated reinforcing bar, having an anchorage length of 400 mm
iv. Beam reinforced with a treated reinforcing bar, having an anchorage length of 600 mm

The tensile reinforcement area was 144 mm^2 and 300 mm^2 for Palmyrah and Bamboo reinforced beam specimens respectively. The Bamboo reinforced beam was of 1400mm x 150mm x 100mm dimensions whereas the Palmyrah reinforced beam had dimensions of 2000mm x 200mm x 150mm. Water repellent technique used for all 8 beams was varnish double coating. Palmyrah reinforced beams were cast with grade 35 concrete and tested 7 days after casting. The ones reinforced with Bamboo were cast with grade 25 concrete and tested 38 days after casting.

Two point loading system, as indicated in figure 3, was used when testing the beam specimens. Under this loading scheme, the portion of the beam between the two loading points is under pure flexure. This is desirable as the test is required to investigate the bond behaviour under flexure. Central deflection, crack initiation load and failure load were recorded.

Figure 3: Testing for bond strength under flexure of a Bamboo reinforced specimen

3.5 Testing of Lintels

Theoretical flexural moment capacity of an unreinforced concrete section assuming a triangular stress distribution can be derived as;

$$M_t = \frac{f_{ct} b {h_m}^2}{6} \qquad (1)$$

Where;

hm is the height of the section at mid span

The tensile strength of concrete, fct was found using equation 2, as per the guidelines of BS 8110; Part 1, (1985).

$$f_{ct} = 0.45\sqrt{f_{cu}} \qquad (2)$$

Flexural capacity of an under reinforced section was evaluated using equation 3.

$$M_t = A_s f_t \left[d - \frac{k_2 A_s f_t}{k_1 f_{cu} b}\right] \qquad (3)$$

Where;

A_s is the provided reinforcement area

f_t is the tensile strength of reinforcement material

d is the effective depth of section

k_1 is the factor to account for maximum compression strength at flexure

k_2 is the depth factor

k_1 is taken as 0.67 and k2 is taken as 0.45 as per the guidelines of BS 8110; part 1, (1985) [14].

Experimental moment capacity under flexure at mid span, M_t is derived as;

$$M_t = \frac{wl^2}{8} + \frac{Pl_w}{4} + \frac{Rl_e}{2} \qquad (4)$$

Where;

w is the self-weight of the beam

P is the load at failure

l is the total length of the beam

l_e is the distance between supports

l_w is the distance between loading points

R is the support reaction

A design was carried out considering a typical lintel opening using the guidelines provided in BS 5977-1 (1981) and BS 8110-1 (1985). The Palmyrah reinforcement was of 400 mm^2 cross sectional area where as Bamboo reinforcement was made up of two bars with each having 150 mm^2 cross sectional area.

Concrete beams reinforced with varnish double coated Palmyrah and Bamboo bars were cast using grade 35 concrete. For each reinforced beam, an unreinforced control beam specimen was cast from the same concrete. All the beams had 1400 mm x 150 mm x 100 mm dimensions. Testing was done 7 days after casting.

Two point loading system was used in testing and central deflection, initial cracking load and ultimate failure load were recorded.

4. Experimental Results

4.1 Tensile strength

Tensile strength testing yielded much cohesive results for Palmyrah samples with an average tensile strength parallel to grain of 86.5 N/mm^2 and a maximum of 103.0 N/mm^2.

However, Bamboo exhibited a much wider distribution of tensile strength values among its 15 tested samples with a minimum of 29.9 N/mm^2 and a maximum of 226.2 N/mm^2, resulting in an average of 109.7 N/mm^2 and a standard deviation of 54.0 N/mm^2. The samples extracted from the bottom of the trunk showed relatively cohesive tensile strength values, also greater than those exhibited by the samples from middle and top portions of the trunk.

4.2 Water absorption and desorption

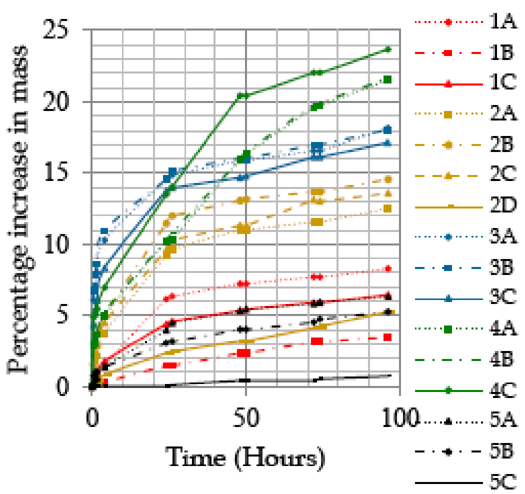

Figure 4: Water absorption characteristics of Palmyrah specimens – Series 1

Table 3: Specimen groups for Figure 4

Group	Treatment Type
1	1st coat varnish, 2nd coat sand sealer
2	Solignum coated
3	Untreated hardwood
4	Untreated softwood
5	1st coat sand sealer, 2nd coat varnish

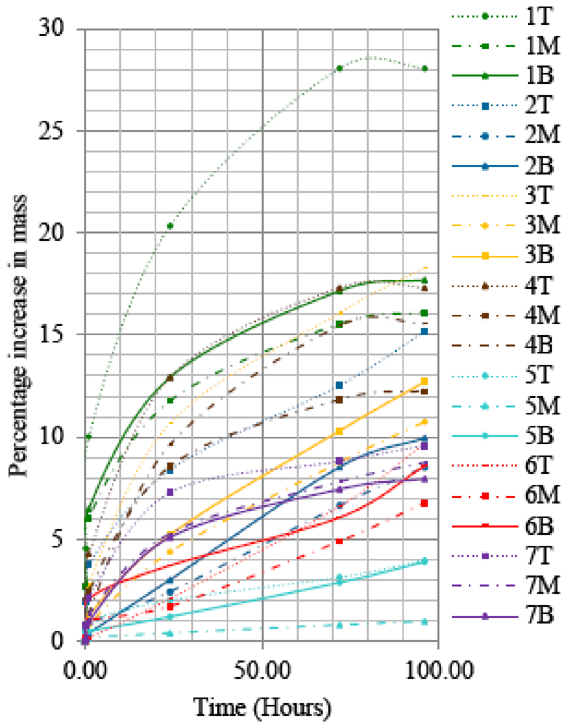

Figure 5: Water absorption characteristics of Bamboo specimens

Table 4: Specimen groups for Figure 5

Group	Treatment Type
1	Untreated specimen
2	Sand sealer single coat
3	Varnish single coat
4	Black oil single coat
5	Sand sealer double coat
6	Varnish double coat
7	Black oil double coating

The potential for swelling was evaluated for these different water repellent techniques by measuring the mass of the test specimen with time and the results were plotted as in Figures 4, 5 and 7. The results indicate that for both Palmyrah and Bamboo species, untreated specimens exhibit the greatest water absorption amounts. Combined sand sealer and varnish coating appears to be the most effective water repellent technique among the tested, with the potential to limit water absorption to 8% by mass at 100 hour exposure for both timber species.

The volumetric changes were calculated using the measured changes in the cross sectional dimensions and lengths of the samples and plotted as shown in figures 6 and 8.

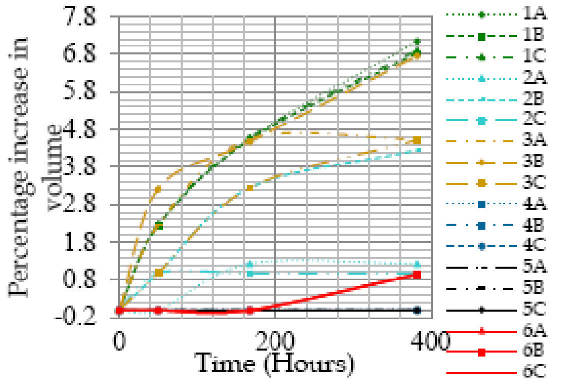

Figure 6: Swelling potential of treated Palmyrah specimens – Series 2

The percentage increase in volume of varnish and bitumen coated specimens was less than 1% after being submerged in water for 400 hours.

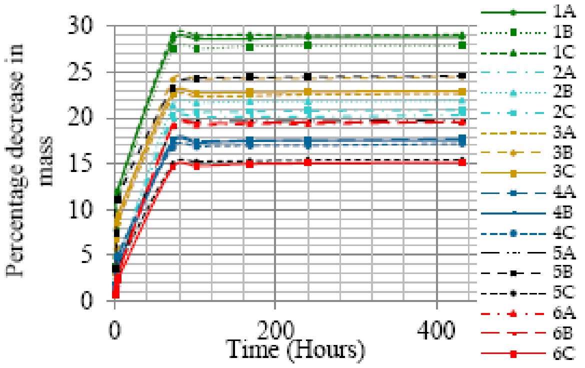

Figure 7: Water desorption characteristics of Palmyrah specimens – Series 2

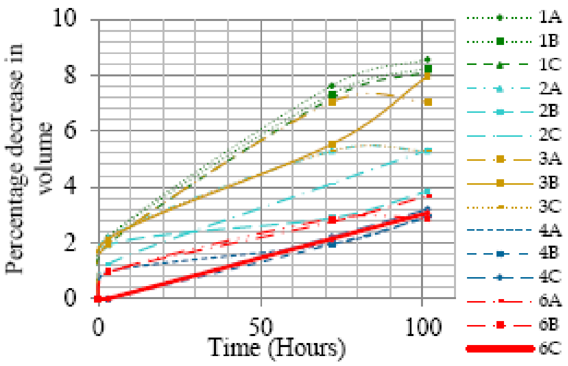

Figure 8: Shrinking potential of treated Plamyrah specimens – Series 2

Table 5 - Specimen groups for Figures 6, 7 and 8

Group	Treatment Type
1	Untreated specimen
2	Solignum coated
3	Water paint and oil paint
4	Sand sealer coated
5	Varnish coated
6	Bitumen coated

Percentage reduction of mass during desorption testing was less than 20% for both bitumen and sand sealer coated specimens. Corresponding reductions in volume were under 6%.

4.3 Anchorage Strength

Pull out tests conducted on varnish double coated Palmyrah strips with 12mm x 12 mm cross sectional dimensions yielded the results shown in table 6. The reduction in pull out load, with the reduction of anchorage length however, as expressed in table 6, is very low.

Table 6 - Anchorage strength of Palmyrah strips

Specimen	Anchorage length (mm)	Pull out load (kN)
A	150	5.9
B	100	5.4
C	50	4.7

Results of the anchorage strength tests conducted on Bamboo strips are tabulated in table 7.

Table 7 - Anchorage strength of Bamboo strips

Specimen	Anchorage length (mm)	Pull out load (kN)
A	200	8.4
B (with node)	200	14.6
C	200	8.4
D (with node)	200	16.1
E	200	7.7
F (with node)	200	12.7
G (Corrugated)	200	11.9

The Bamboo specimens with nodes exhibit pull out loads greater by 65% - 90% compared to the ones without nodes.

4.4 Bond Strength under Flexure

Flexural strength test specimens failed exhibiting under reinforced behaviour. Crack initiation for all beams occurred at mid span. However, Bamboo reinforced beams developed a noticeable crack spanning from one of the loading points at the top to the bottom of the beam, which lead to the ultimate failure. Further investigations revealed that such cracks occurred across spans containing nodes in the Bamboo reinforcement bar. The resulting stress concentration at such locations could have caused such failure patterns. The addition of both types of timber bars, as tensile reinforcement, has increased the failure load as well as provided ductility to the beams.

4.5 Testing of Lintels

A longitudinal crack was visible along the centre of the bottom surface of the Palmyrah reinforced beam at failure. This undesired drawback was eliminated in the Bamboo reinforced beams by providing two reinforcing bars with smaller cross sectional areas rather than one bar with larger cross sectional area. In addition to the flexural crack at mid span, Bamboo reinforced beam exhibited a diagonal crack similar to the one experienced under testing for anchorage strength under flexure. This crack, as shown in figure 9, spanned from one of the loading points to the bottom surface of the beam diagonally. Further investigation by removal of concrete around the crack revealed the existence of nodes in both Bamboo strips. Local stress concentration due to these nodes could have caused this crack.

Figure 9: Additional crack across the beam in Bamboo reinforced specimens

The initial crack in all the tested beams occurred at approximately 5 kN. The Palmyrah reinforced beam failed at an ultimate load of 12.8 kN with an enhancement of 156% from its unreinforced counterpart. For the Bamboo reinforced beam, with an ultimate failure load of 20 kN, this enhancement amounted to 300%.

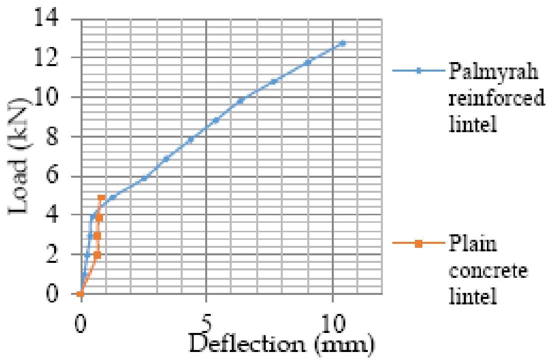

Figure 10: Load vs. Deflection curve for Palmyrah reinforced lintel

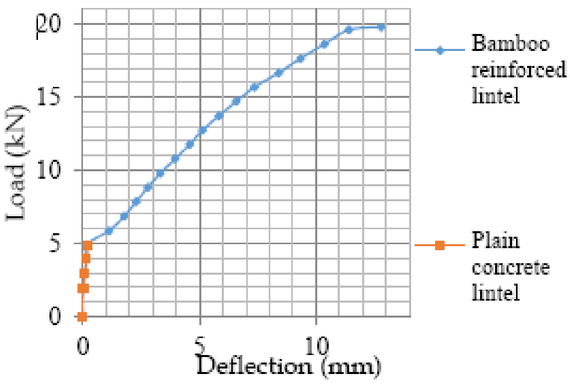

Figure 11: Load vs. Deflection curve for Bamboo reinforced lintel

In Figure 10 and Figure 11, the gradients of the curves for the two lintels in each figure are very similar within the elastic region. Hence, both types of timber reinforcement considered here have negligible effect on the stiffness enhancement of the lintels. The load causing initial crack is approximately the same for both reinforced and unreinforced lintels. However, the addition of the timber strips have provided significant ductility to both reinforced lintels compared to their unreinforced counterparts.

Theoretical and experimental moment capacities of Palmyrah reinforced lintel and its control specimen were evaluated and the values are given in table 8. Here, the compressive strength and the tensile strength of concrete were evaluated to be 36.4 N/mm^2 and 2.5 N/mm^2 respectively. Uniaxial compressive strength test and splitting tensile strength test were used to derive these values.

Table 8: Theoretical and experimental moment capacities of Palmyrah reinforced lintel

Specimen	M_t (kNm)	M_e (kNm)	$(M_e-M_t)/M_t$ x100%
Unreinforced lintel	1.12	1.44	28.6
Bamboo reinforced lintel	3.03	5.02	65.7

The experimental moment capacity of the Palmyrah reinforced concrete beam differs only by - 1.2% compared to its theoretical moment capacity.

Testing for Bamboo reinforced lintel yielded the moment capacities presented in table 9. Here, the average compressive and tensile strengths of concrete were 43.2 N/mm^2 and 3.0 N/mm^2 respectively. These too were also derived using the uniaxial compressive strength test and splitting tensile strength test.

Table 9: Theoretical and experimental moment capacities of Bamboo reinforced lintel

Specimen	Mt (kNm)	Me (kNm)	(Me-Mt)/Mt x100%
Unreinforced lintel	1.12	1.44	28.6
Bamboo reinforced lintel	3.03	5.02	65.7

The experimental flexural capacity is greater by 65.7% in comparison to the theoretical moment capacity of the Bamboo reinforced concrete lintel.

5. Conclusions and Recommendations

The following conclusions were made from the results of the experimental study.

i. Both Palmyrah and Bamboo reinforcement increase the flexural capacity of lightly loaded lintels

ii. Although the introduction of these reinforcing timber strips had negligible effect on the initial cracking load, the ultimate failure occurred with the failure of tensile reinforcement, exhibiting under reinforced behaviour

iii. Varnish and bitumen coating have the potential to limit water absorption to 8% by mass and limiting dimensional variations to negligible proportions

From the experimental results, it can be concluded that both Palmyrah and Bamboo exhibit strong potential to be used as reinforcement in lightly loaded concrete lintels with minor structural importance. However, it should be noted that the tests conducted under this study primarily address the short term behaviour of tested elements. Long term behaviour and properties are of significant importance, as the practical applications of these would at least have a design life time of 50 years, as in the case of residential houses.

References

[1]. Baskaran, K., Mallikarachchi, H., Jayasekara, M. & Madushanka, G., "Study on Palmyrah as a Material for Construction". Proceedings of the second annual sessions, Society of Structural Engineers – Sri Lanka, pp. 7-16, September 25th 2012, Colombo, Sri Lanka.

[2]. Baskaran, K., Mallikarachchi, H., Jayasekara, M. & Madushanka, G., "Feasibility of Using Palmyrah Strips as Reinforcing Material in Cost Effective Houses" *Journal of Construction Engineering*, Volume 2014, pp. 1-8, 2014.

[3]. Ghavami, K. & Hombeeck , R., "Application of bamboo as a construction material: Part I-Mechanical properties and water repellent treatment of bamboo, Part II-Bamboo reinforced concrete beams". Sa˜o Paulo, CIB, pp. 50-65, 1981.

[4]. Ghavami, K., "Bamboo as reinforcement in structural concrete elements" *Cement & Concrete Composites* , Volume 27, pp. 638-650, 2005.

[5]. Ghavami, K., "Ultimate load behaviour of Bamboo-reinforced lightweight concrete beams", *Journal of Cement and Concrete Composites*, Volume 17, pp. 281-288, 1995.

[6]. Ramasamy, H.S., Ahuja, B.M., Krishnamoorty, S., "Behaviour of concrete reinforced with Jute, Coir and Bamboo Fibres", *The International Journal of Cement Composites and Lightweight Concrete*, Volume 5, No 1, pp. 3-13, 1983.

[7]. Kankam, C.K., Ewuakye, B.O., "Structural behaviour of babadua reinforced concrete beams", *Construction and Building Materials*, Volume 13, pp. 187-193, 1993.

[8]. Harish, S., Togati, N.V.V.K., Reddy, I.V.R., "Investigation of properties of Bamboo reinforcing material in concrete", *International Journal of Engineering Research and Applications*, Volume 2 (1), pp. 077-083, 2012.

[9]. Pratima, P.A., Maiwala, A.R., Gajera, V.J., Patel, J.A., Magdallawala, S.H., "Performance evaluation of Bamboo as reinforcement in design of construction element", *International Refreed Journal of Engineering and Science*, Volume 2 (4), pp. 55-63, 2013.

[10]. Nayak, A., Bajaj, A.S., Jain. A., Khandelwal, A., Tiwari, H., "Replacement of steel by Bamboo reinforcement", *IOSR Journal of Mechanical and Civil Engineering*. Volume 8 (1), pp. 50-61,2013.

[11]. Sabnani, C., Latkar, M., Sharma, U., "Can Bamboo replace steel in concrete, for the key structural elements in a low cost house, designed for the urban poor?", *International Journal of Chemical, Environmental and Biological Sciences*. Volume 1 (2), pp. 257-262, 2013.

[12]. British Standard Institution. *Structural Timber, Strength Classes*. BS EN 338: (1995). London, 12 pages, 1995.

[13]. British Standard Institution. *Testing concrete in structures – Part 3: Determination of pull-out force*. BS EN 12504-3: (2005). London, 14 pages, 2005.

[14]. British Standard Institution. *Structural use of concrete*. BS 8110: *Part 1: 1985. Code of practice for design and construction*. London, 124 pages, 1985.

[15]. British Standard Institution. *Lintels—Part 1: Method for assessment of load*. BS 5977-1, 1981, 12 pages London, 1981.

SECM/15/042

LABORATORY PERMEABILITY TESTING OF GRANULAR SLAG AND GRAVEL SUB BASE COURSES (GSB)

G. Kavitha[1*], Krishnamurthy[2] and B.R Srinivasamurthy[3]

[1]Assistant Professor, RASTA, Center for Road Technology, Bangalore
[2] Professor, RASTA, Center for Road Technology, Bangalore
[3] Technical Advisor, RASTA, Center for Road Technology, Bangalore
*E-Mail: kavi_gsy@yahoo.com, TP: +9731339914

Abstract:

Granular Sub Base Course (GSB) provided as one of the structural layer of pavements should also serve as an effective drainage layer. In India current guidelines recommend using natural sand, crushed gravel, stone or slag or combination of these, in the GSB layer. While the above combinations may fulfil the structural requirement, it is not clear whether they meet the minimum drainage requirements of 300 m/day as per AASHTO specifications.

This paper summarizes the laboratory permeability carried out on 1) Crushed stone aggregates and slag in different combinations with non plastic fines such as quarry dust and 2) Gravel- Aggregate combination in the ratio 60:40. The first combination was tried for Grade III requirements as per MORT&H specification (5th Revision) for High volume roads. The second combination was tried for Grade III requirements as per rural roads Manual, IRC SP 20, used for low volume roads in India.

The objective is to compare the permeability characteristics of GSB gradations prepared with different mixes in order to assess their ability to drain, based on the permeability criteria. Horizontal and vertical permeability were tested in the laboratory for these GSB mixes and the results have been reported.

From the study it is observed that while all the combinations of crushed stone – slag mixes meet the minimum permeability criteria in the horizontal as well as vertical directions, 100% granulated steel slag (GLDS) does not meet the requirement in the vertical direction. Also while the Gravel – Aggregate combination (60:40) just meets the minimum permeability requirement in the horizontal direction, there is negligible discharge in the vertical direction.

Keywords: Permeability, Quarry dust, Slag, Gravel, Horizontal, Vertical

1. Introduction

Granular Sub base course (GSB) is an important structural layer as well as the drainage layer in pavements. Most of the pavements in India fail prematurely mainly due to ineffective functioning of this drainage layer. The current guidelines, Ministry of Road Transport & Highways, MORT&H (5th Revision)[1] recommends 6 gradations for using in the GSB layer which are mostly close graded (with more fines passing 2.36mm sieve) compared to AASHTO specifications[2]. It also recommends using natural sand, crushed gravel / stone or slag or their combinations in the GSB layer. Although these combinations are recommended in the ministry, such combinations are seldom used in actual practice. It is not clear whether these gradations and the combination of materials recommended, fulfil the minimum permeability criteria of 300 m/day (AASHTO specification) particularly when the material combination includes gravel with fines having plasticity. Also slag being available as a waste product in the iron and steel manufacturing plants may be best used in combinations in the GSB layer , if it fulfils both the strength requirement as well as drainage requirement.

Hence in the present study an attempt is made to study the permeability characteristics of

1) different combinations of crushed stone aggregate and slag with quarry dust for fines and 2) Gravel - aggregate combination with 60% gravel and 40% crushed aggregates.

2. Objectives

1. To compare the horizontal and vertical permeability of different combinations of Aggregate slag mixes and Gravel – Aggregate mixes (60:40)

2. To identify the most optimum combination based on the minimum permeability requirement of 300 m/day as per AASHTO specifications.

3. Experimental Investigations

3.1 Materials & Methods

1. Aggregates were collected from Tippagondanahalli quarry near Magadi in Bangalore District.
2. Gravel was obtained from Jigani, Bangalore and
3. Air Cooled Blast Furnace slag (ABFS) and Granulated Linz Donawitz Steel slag (GLDS) were procured from M/s Jindal Steel Works, Bellary, Karnataka

Rothfutch method of proportioning was adopted for the crushed stone aggregates (CA) and slag combinations to meet the Grade III requirements for GSB as mentioned in the MORT&H specifications (Table 1)

The following combinations were tried

i) CA : GLDS : ABFS…..50 : 25 : 25
ii) CA : GLDS : ABFS…..30 : 35 : 35
iii) 100% GLDS

Rothfutch method of proportioning was also adopted for the Gravel – Aggregate combination in 60:40 proportions, to meet the Grade III requirement as per IRC SP 20. Since Grade III being close graded is commonly provided for rural roads. The same was adopted in the present study also.

The physical properties of the aggregates tested are shown in Table 5.

3.2 Test Set up

Two Test approaches were planned in the Laboratory

1) Horizontal Permeability Test and
2) Vertical Permeability Test

3.2 Horizontal Permeability Test– was conducted in the laboratory using a horizontal permeameter[4] mould of size 0.6m X 0.3m X 0.3m specifically fabricated to accommodate GSB gradations with aggregates more than 26.5mm size.

Two perforated brass plates are provided at a distance of 0.15m from the inlet and outlet end of the flow providing an effective specimen space of 0.3m X 0.3m X 0.3m. Once the GSB mix is compacted in layers in the mould to get the required density, it is closed with a cover on top with rubber gasket of 6mm thickness to make it leak proof.

Permeability test was conducted at 3 hydraulic gradients for the different combinations of the GSB mixes after subjecting it to saturation. Permeability for the different gradations were determined by Darcy's equation.

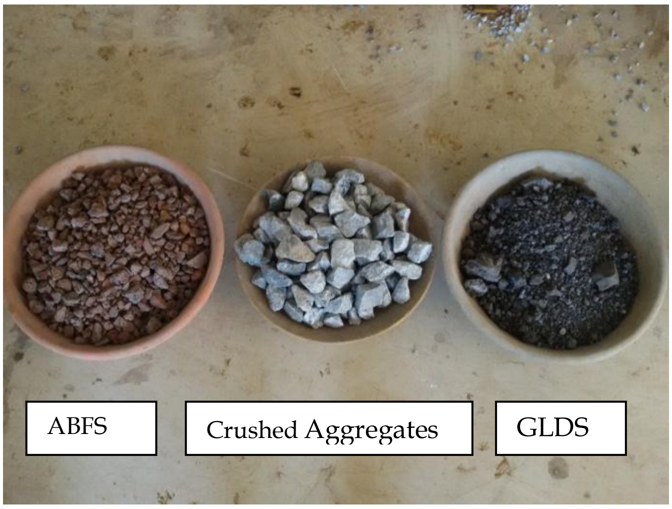

Figure 1: Slag and Crushed Aggregates selected for the Study

Figure 2: Specimen compaction in progress – Horizontal Permeability Test

Figure 3: Specimen compaction in progress

Figure 4: Horizontal permeability Test in progress

3.3 Vertical Permeability Test – was conducted in the laboratory using a Vertical permeameter[4] mould of 0.3m diameter and a height of 0.3m Two perforated brass plates are provided at a distance of 0.075m from the inlet and outlet end of the flow providing an effective specimen space of 0.3m dia and a height of 0.15m. Once the GSB mix is compacted in layers in the mould, it is closed with a cover on top with rubber gasket of 6mm thickness to make it seal proof. The entire setup was ensured leak proof during the progress of test using M.Seal on all the welded portions. Permeability test was conducted at different hydraulic gradients for all the six gradations recommended in MORT&H after subjecting it to saturation. Permeability for the different combinations of GSB mixes was determined by Darcy's equation.

Figure 5: Vertical permeability Test in progress

Table 1: – Grading of Granular Sub-base materials as per Table 400-1 of MORT&H (5^{th} Revision)

IS Sieve Size	Grade III Percent by Weight Passing IS Sieve
75	100
53	100
26.5	55-75
9.5	…
4.75	10-30
2.36	…
0.85	…
0.425	…
0.075	<5

Table 2: Gradations of the Slag and Gravel used in the Present Study

SIEVE SIZES in mm	Blast Furnace Slag ABFS % passing	Steel slag GLDS % passing	Gravel A
75	100	100	100
53	100	100	100
26.5	93.1	76.88	100
9.5	1.6	66.05	-
4.75	0.05	35.3	70.9
2.36	0	25.13	60.7
0.425	0	13.7	45.8
0.075	0	5.15	29.1

Table 3: Components of Slag (Source: JSW, Bellary)

Components	CaO	MgO	SiO2	Al2O3	Fe2O3
BF Slag	41	6	35	14	1
LD Slag	38	9	13	3	26

Table 4: Physical properties of Slag

Property	ABFS	GLDS
Impact Test	27%	26%
Liquid Limit and Plastic Limit	Non plastic	Non plastic
Specific Gravity	2.26	2.66
Water absorption	3.93	3.58
CBR	19%	38%

Table 5: Basic Physical Properties of Aggregates

Description of tests conducted	Test Method	Test Result	Requirements as per MORT&H 5th Revision
Aggregate impact value (%)	IS 2386 (Part-4)	27.6	Maximum 40%
Water absorption (%)	IS 2386 (Part-5)	0.43	Maximum 2 %
Atterberg Limits	IS 2720 (Part-5)	Non Plastic	LL-25% maximum PL-6% maximum

Table 6: Properties of Granular Slag Combinations

Property	**30% (aggregate)+35%(GLDS)+35%(ABFS)**	**50% (aggregate)+25%(GLDS)+25%(ABFS)**
Modified Compaction Test OMC (%), MDD (gm/cc)	OMC - 3.0% MDD – 2.15	OMC - 2.0% MDD – 2.12
CBR (%)	62	69

Table 7: Physical properties of Gravel

Property	
Wet Sieve Analysis	
Gravel (%)	29
Sand (%)	38
Fines (%)	33
Atterberg Limits	
Liquid Limit (%)	23
Plastic Limit (%)	15
Plasticity Index (%)	8
Compaction Test	
Maximum Dry Density (g/cc)	1.97
Optimum Moisture Content (%)	11
CBR	15%

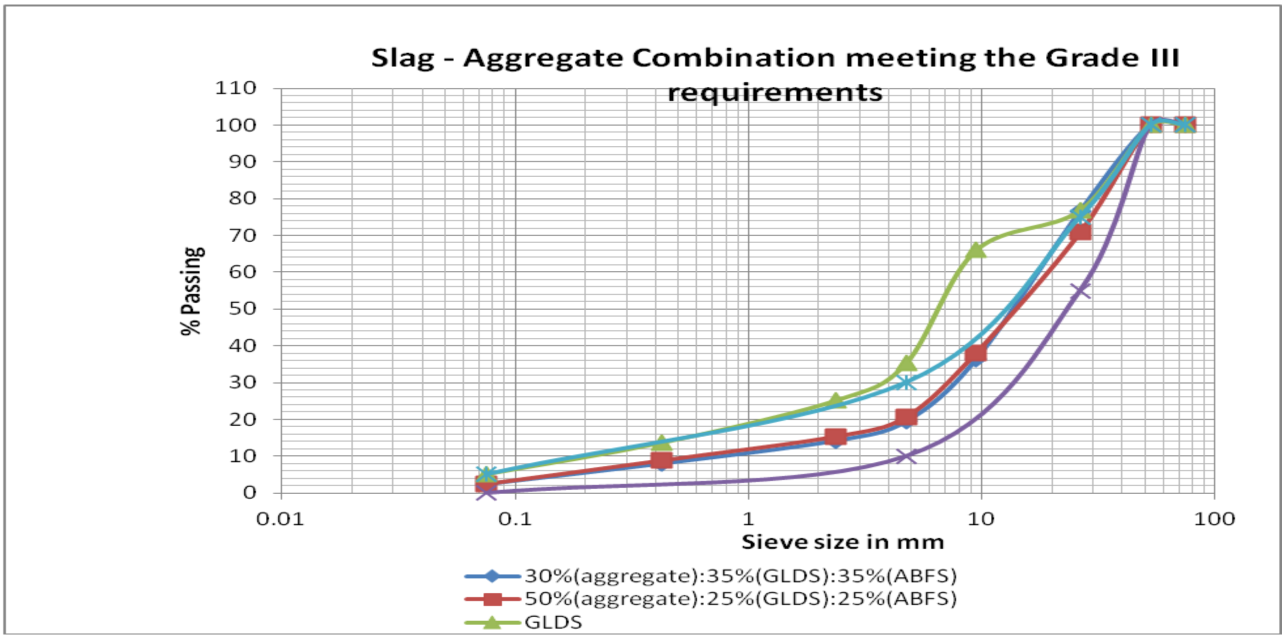

Figure 6: Gradation curves of Slag Aggregate combinations meeting Grade III requirements

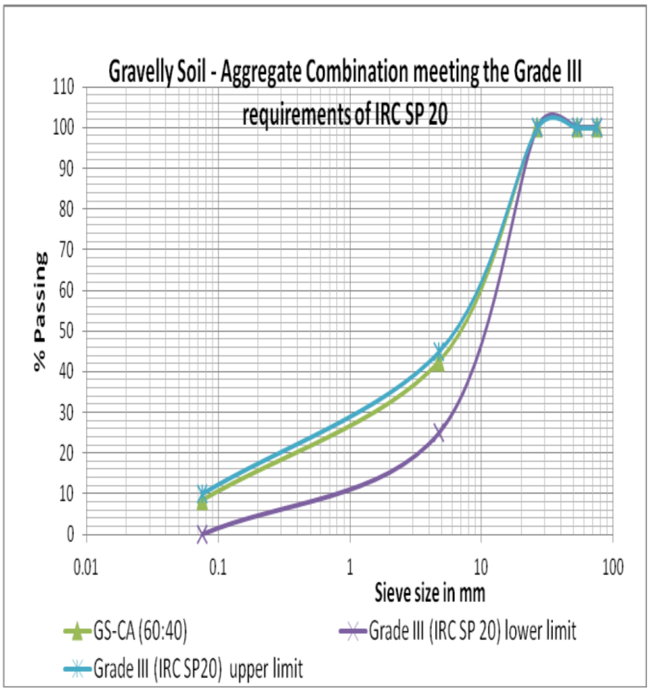

Figure 7: Gravelly soil and aggregate combination meeting the Grade III requirements (IRC SP 20)

Table 8: Horizontal Permeability of various Granular slag and aggregate combinations

Horizontal permeability, k_{20}, cm/s (m/day)			
GSB Gradation	**Hydraulic gradient**		
	0.025	**0.04**	**0.05**
CA:ABFS:GLDS -50:25:25	0.73 (631)	0.79 (688)	0.88 (760)
CA:ABFS:GLDS -30:35:35	0.90 (775)	0.89 (766)	0.87 (748)
only GLDS	0.82 (709)	0.82 (709)	0.81 (700)
Crushed aggregates	0.89 (772)	0.80 (691)	0.81 (700)

Table 9: Results of Vertical permeability at different hydraulic Gradients

Vertical permeability, k_{20}, cm/s (m/day)			
GSB Gradation	**Hydraulic gradient**		
	0.025	**0.04**	**0.05**
CA:ABFS:GLDS -50:25:25	0.67 (579)	0.63 (544)	0.72 (622)
CA:ABFS:GLDS -30:35:35	0.79 (683)	0.58 (501)	0.58 (501)
only GLDS	No Traceable discharge		
Crushed aggregates	0.75 (648)	0.89 (769)	0.87 (752)

Table 10: Permeability values of Gravel aggregate combination

60% gravel + 40% aggregate meeting Grade III, as per IRC Sp 20			
Permeability k_{20}, cm/s (m/day)	Hydraulic gradient		
	0.025	0.04	0.05
Horizontal	0.37 (316)	0.41 (350)	0.43 (375)
Vertical	No traceable discharge		

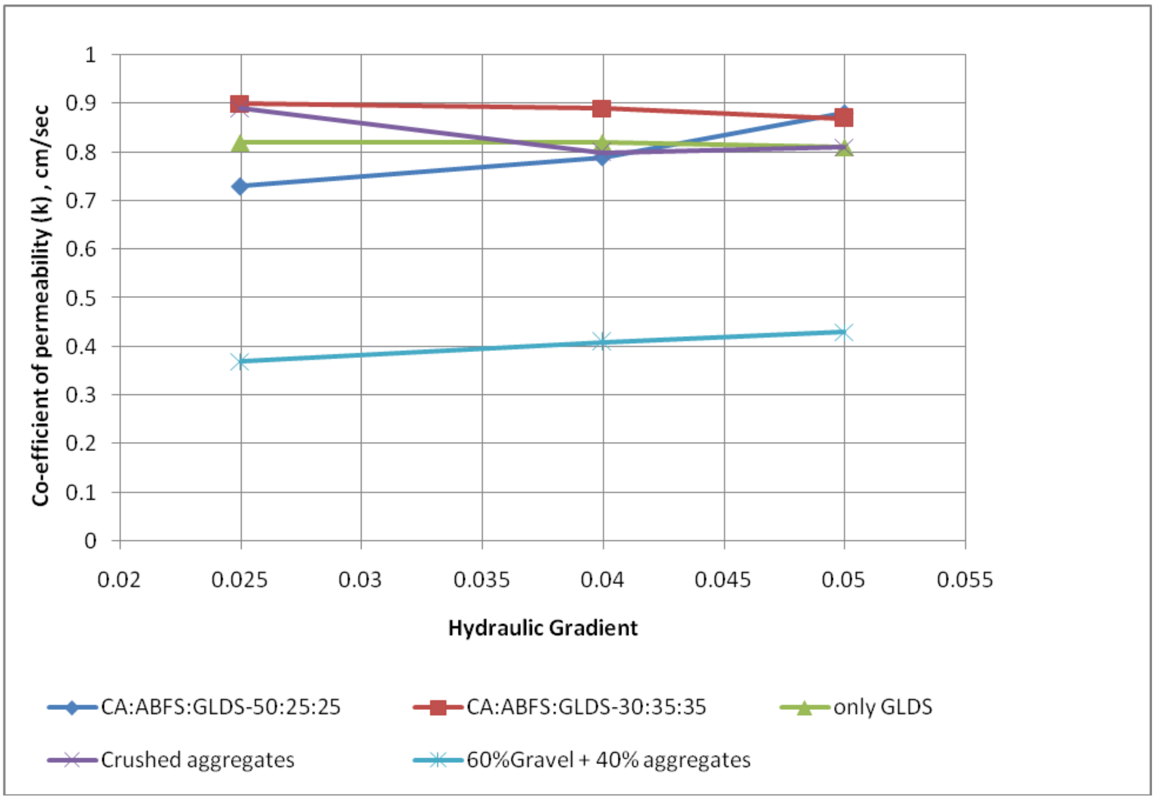

Figure 8: Horizontal Permeability with hydraulic gradients for various combinations

4 Discussions

i) The horizontal permeability values (Table 8) obtained for the different combinations of Slag and aggregates such as CA:ABFS:GLDS – 50:25:25, (50% slag replacement) CA:ABFS:GLDS – 30:35:35 (70% slag replacement) and only GLDS (100% slag), show values almost equal to or even greater compared to the horizontal permeability values obtained for crushed aggregates meeting grade III requirements.

ii) The vertical permeability values (Table 9) obtained for the above combinations of slag and aggregates is lesser compared to that obtained for crushed aggregates meeting grade III requirements.

This may be due to stratification and greater segregation of particles along the vertical flow that results in possible settling of fines at the bottom, and hindering the flow.

iii) Vertical permeability Tests on GLDS (100% slag) also showed negligible discharge at all gradients.

This may be because in addition to the stratification and segregation of particles along the vertical flow, the cementing action of the granulated steel slag which is hydraulic bound in nature may result in an impervious matrix. Further, it was also observed that during compaction there was break down of particles under the impact of the rammer, which could further speed up the self binding process.

iv) Permeability tests results on the gravel aggregate combination (Gravel:aggregate-60:40) , as per the requirements of rural roads specification IRC SP:20 from Table 10 indicates that while the horizontal permeability of the gravel aggregate combination meets the minimum permeability criteria of 300 m/day, there is negligible discharge in the vertical direction.

5 Conclusions

The horizontal permeability values obtained for 50% and 70% slag in the slag- aggregate combinations meet the minimum permeability criteria; hence can be tried for use in the GSB layer. However there is a need to check the long term permeable characteristics of these slag – Aggregate combinations as their permeability may reduce gradually in the due course of time due to cementing action of the slag.

The combination of gravel and aggregates in 60:40 proportions were just meeting the minimum threshold for permeability only in the horizontal direction. Hence care should be taken in selecting the right combination of crushed aggregates, gravel and moorum , for using it as GSB in low volume roads, as it may not meet the minimum desired permeability criteria and hence may not be effective in draining.

6 References

[1]. Ministry of Road Transport and Highways, (MORT&H), "Specifications of Road and Bridge works", Indian Roads Congress, Fifth Revision

[2]. Federal Highway Administration. 1992. Drainable Pavement Systems-Participant Notebook. Report FHWA-SA-92-008. Washington, DC: Federal Highway Administration

[3]. Indian Roads Congress Special Publication 20, "Rural Road Manual", 2002

[4]. Design Manual for Roads & Bridges, (1990) HA41/90, "A permeameter for Road Drainage layers", Vol 4, section 2 Jones, R. H., (1995),

[5]. A.K Sinha et al, "Steel Slag Waste Material for the Construction of Road" Indian Highways , Vol 41, No. 10, October 2013

[6]. M.C Nataraja et al " A Study on the Strength properties of Paver blocks made from unconventional materials", IOSR, Journal of Mechanical and Civil Engineering (IOSR – JMCE) ISSN: 2278-1684 PP 01-05

[7]. U Arunkumar et al " Utilization of Industrial Waste material in GSB layer" , International Journal of Engineering Research and Applications. ISSN: 2248-9622, Vol 4, Issue -8 (version 3), Aug 2014. Pg 61-64

[8]. Vijay Keshav Joshi, "Properties on Performance of Slag pavements", University of Wollongong, Research online. Thesis Collections (1997)

SECM/15/043

Determination of Binder Film Thickness for Bituminous Mixtures prepared with various Types of Fillers

Jaya R.S. [1], Asif [2]

[1] Asst. Prof., RASTA-Centre for Road Technology, VOLVO Construction Equipment Campus, Peenya Indl.Area, Bangalore, India

[2] M.Tech student, RASTA-Centre for Road Technology, VOLVO Construction Equipment Campus, Peenya Indl.Area, Bangalore, India

E-mail:jayars@rastaindia.com; Mob: 9448510511

Abstract: Roads form the lifeline of any country. It is considered to be an engineered structure and the pavement is expected to serve its designed life and meet the performance criteria for better economy. Various materials constitute the different layers of the pavement and their characterization becomes important for durability. In spite of these considerations however, many factors contribute to early pavement failure and improper material characterization is just one of them.

The Bituminous mix which is used for the surface and binder courses is formed as a conglomeration of the binder, graded aggregates and voids which forms a stable mixture which can resist wear and tear as well as heavy wheel loads when used in the field. The bituminous mix needs to meet the volumetric requirements to attain stability. When bitumen is mixed with aggregates in a heated condition, the binder forms a coating around the aggregate particle which is termed as Asphalt film thickness (AFT) which is not measured but calculated. Bitumen due to its visco-elastic nature should be used at the optimum and the specified temperature to provide a minimum uniform film thickness to ensure proper bonding in the Bitumen mastic.

Fillers play a major role in determining the properties and the behaviour of the mixture, especially the binding and aggregate interlocking effects. The filler has the ability to increase the resistance of particle to move within the mix matrix and/or works as an active material when it interacts with the asphalt cement to change the properties of the mastic. Mineral fillers serve a dual purpose when added to asphalt mixes, the portion of the mineral filler that is finer than the thickness of the asphalt film blends with asphalt cement binder to form a mortar or mastic that contributes to improved stiffening of the mix.

In the present study the film thickness was determined by Hveem method by determining the total surface area and the effect of fillers thereon is discussed. The effect of types of fillers in varying percentage, in the performance of hot-mix-asphalt is also studied. Three types of fillers namely, Hydrated lime, Ordinary Portland Cement, and Fly ash were used as fillers in the present study. Their percentage by weight of aggregates was varied as 2%, 4% and 6% to study their effect on the mix prepared for BC Grade II. The optimum binder content was determined for the various fillers and moisture susceptibility of bituminous mixtures was evaluated..

The results of film thickness determination reveals that an average film thickness of 6 μm is obtained for all fillers which is necessary for durability of the mixes. The Fatigue results show that Lime at 4% can be used for enhanced performance and 2% is recommended, when cement or fly ash is used as filler material.

Keywords: Asphalt Film thickness, volumetric properties, aggregate surface area, Stone binder interaction, durability, fillers

1. Introduction

In recent years, many countries have experienced an increase in truck pressure, axle loads, and traffic volumes. Tire pressure and axle load increases means that the bituminous layer near the pavement surface is exposed to higher stresses. High density of traffic in terms of commercial vehicles, overloading of trucks and significant variations in daily and seasonal temperature of pavements have been reasonable for development of distress indications like ravelling, undulations, rutting, cracking, bleeding, shoving and potholing of bituminous surfaces. Appropriate material combinations of aggregates, binders and fillers have been found to results longer life for wearing courses depending upon the percentage of filler and type of fillers used [8].

Fillers, in particular, as one of the ingredients in HMA, have only been thought to fill voids in the aggregate. However, studies indicated that the role of fillers in bituminous mixture performance is more than filling voids depending on the type used. The filler also influences the optimum binder content(OBC) in bituminous mixtures by increasing the surface area of mineral particles and, at the same time, the surface properties of the filler particles modify significantly the rheological properties of asphalt such as penetration, ductility, and also those of the mixture, such as resistance to rutting. In order to improve the pavement performance, it is necessary to ensure that adequate behavior of the bituminous mixtures is achieved, which depends essentially on their composition. Therefore, selecting the proper type of filler in bituminous mixtures would improve the filler's properties.

It is generally believed that asphalt paving mixes should have an adequate asphalt film thickness around the aggregate particles to ensure reasonable durability of the mixture. The minimum asphalt film thickness generally recommended ranges from six to eight microns [1].

2. Objectives of Present study

i. To study the effect of the different types of fillers on increase in surface area and film thickness.
ii. To evaluate the mechanical properties of the Bituminous mixes by Marshall Mix design.
iii. To study the effect of varying filler type & content on the mechanical and volumetric properties of bituminous mixes.
iv. To study the change of moisture sensitivity with varying filler type and content.
v. To evaluate the performance enhancement of the mixes with the use of varying filler type and content as an effect of variation in film thickness.

3. Literature Review

3.1 Boris Radovskiy, et.al., [2] reviewed the history of VMA and average film thickness where he stated that the minimum VMA requirement has been a property proposed since 1950's for use in bituminous mix design provisions, but problems in achieving VMA in mixtures have led to several new research studies. Some researchers recommend using the average binder film thickness to supplement the minimum VMA criteria in the volumetric mix design and the conventional calculation of the film thickness does not require any information on porosity of mixture or on degree of compaction. He concluded that a new definition of film thickness is proposed. A model for film thickness calculation is developed. The results of calculations are logical and agree with some important data reported in previous publications.

3.2 Kandhal ,et.al [3] in their review of literature stated that thicker asphalt binder films produced mixes which were flexible and durable, while thin films produced mixes which were brittle, tended to crack and ravel excessively, retarded pavement performance, and reduced its useful service life. On the basis of the data they analysed, average film thicknesses ranging from 6 to 8 microns were found to have provided the most desirable pavement mixtures. They calculated average film thickness by dividing volume of asphalt by surface area of aggregate. Surface area of aggregate depends on the gradation of aggregate being used in the mixture and surface area factor for each sieve, where surface area calculated by multiplying per cent passing of aggregate for a certain sieve by surface area factor of that sieve. Asphalt Institute proposed surface area factors to be used in calculating surface area of aggregate. They also concluded that the film thickness decreases as the surface area of the aggregate is increased. Studies have shown that asphalt mix durability is directly related to asphalt film thickness.

3.3 Satish Chandraand Rajan Choudhary, et.al[4],in their study have made an attempt on the possible use of three industrial wastes such as marble dust, fly ash and granite dust along with hydrated lime and conventional stone dust from quartzite, as filler in bituminous mix preparations. Bituminous concrete (BC) mixes were designed according to the Marshall method at four different percentages for the five types of fillers. The performances of bituminous concrete mixes were studied through moisture susceptibility, static creep, flexural fatigue, and wheel-tracking tests. The results suggest that marble dust, granite dust, and fly ash can be used as filler in bituminous mixes. Among the three industrial wastes, marble dust shows most potential filler and will shows very economical also, as mixes with marble dust have the least optimum binder content (OBC).

3.4 Talal H. Fadhil, et.al [5] in their study White Cement Kiln Dust was used as filler in Hot Mix Asphalt (HMA) production which results in more economy and leads to maintain the environment clean and healthy. In this research, various percentages of WCKD taken from Fallujah cement plant were used in addition to two filler types such as Cement and Limestone powder to prepare bituminous concrete mixes. Five tests were carried to evaluate the performance of these different bituminous concrete mixes, standard Marshall Test at 60^0C and 70^0C, to test immersed samples for four days in water at room temperature (24^0C), Indirect Tensile Strength (ITS) to test conditioning and un-conditioning samples. All the test results were satisfactory and within the AASHTO and Iraqi roads specifications. The results showed that using WCKD as a filler could save the environment and give confidence to the HMA producers to use this cheap material in their works.

3.5 Debashish Kar, Mahabir Panda and Jyoti Prakash Giri, [6], in their study cement and stone dusts are used as filler material in bituminous mix. A study has been carried out in this study to investigate the use of fly ash, a by-product of a coal based thermal power plant in bituminous paving mixes. For comparison, conventional mixes with cement and stone dust have also been considered. Marshall Test has been adopted for the purpose of mix design as well as evaluation of bituminous mixes. Other performance tests such as indirect tensile strength and retained stability have also been conducted. It was noticed that the mixes with fly ash as filler show slightly inferior properties compared to conventional mixes and full fill the desired criteria as per specifications. Therefore, it has been suggested to utilize fly ash wherever accessible, not only lowering the cost of execution, but also somewhat resolve the fly ash utilization and dumping problems.

3.6 B.Durga Priyanka, et.al[7], studied the likelihood of using fly ash as filler in Bituminous mixes where in general cement, stone dust are used. For comparison, stone dust also used to prepare conventional mix. Marshall stability test is adopted to obtain the properties like stability, flow value, % air voids, voids in mineral aggregate (VMA), voids filled with bitumen (VFB) for a Dense Bituminous Macadam (DBM) mix of Grading I. The tentative work is carried out by using specifications from MORTH. By substituting the stone dust with fly ash at various percentages like 4%, 8%, 12% the results were analyzed. The variation of mechanical properties, optimum bitumen content and fly ash contents were evaluated. It was observed that the mixes with fly ash as filler not differ much in properties when compared with conventional mix and satisfy desired criteria specified by a much higher margin. Hence, it has been recommended to utilize fly ash wherever available, not only reducing the cost of execution, but also partly solve the fly ash utilization and disposal problems.

Based on the above literature review, it was understood that film thickness has to be adequate for better durability, and to reduce the ageing effect. When the mix gradation tends to be open with more permeability, the air voids would increase, having thinner bitumen film thickness and results in excessive ageing. The portion of mineral filler that is finer than the thickness of bitumen film blends with bitumen to form a mortar that contributes to improved stiffening of the mix. This study is intended to evaluate the effect of different fillers namely ordinary Portland cement, hydrated lime and fly ash passing 0.075mm sieve in varying contents on the bitumen film thickness calculated by the empirical method given by Hveem. The Marshall and Moisture susceptibility tests were used to investigate the mixture in the laboratory.

4. General

In this present investigation, the adopted gradation was Bituminous Concrete Grade II as per MORTH specification and the BC mixes were prepared using VG30 grade binder with different types of fillers with varying percentage.

4.1 Material Characterisation

a. Aggregate: The aggregate test results were determined and are tabulated in Table 4.1

Table 1: Test values of aggregates

Sl. No.	Test	Method of Test adopted	Results Obtained	Specification Requirement as Per MORTH (V Revision)
1	Impact value in %	IS:2386 part 4	26.5	Max 24%
2	Loss Angeles abrasion in %	IS:2386 part 4	28.76	Max 30%
3	Combined index in %	IS:2386 part 4	34.7	Max 35%
4	Specific gravity			

	a. 9 mm down aggregates b. 12.5 mm down aggregates c. 6.3 mm down aggregates d. Quarry Dust 4.75 mm down	IS:2386 part 4	2.625 2.600 2.610 2.680	-------- -------- -------- --------
5	Water absorption	IS:2386 part 4	0.65	Max 2%

b. Bitumen: For the present study bitumen VG30 grade was used in the preparation of HMA mixture. The bitumen was tested for its basic properties and found satisfactory according to IS.

c. Filler: The fillers which are finer than 75 micron in size used in the study were hydrated lime, ordinary Portland cement and fly ash. The filler content added in three different percentages (2, 4 and 6) by weight of aggregate for the preparation of BC mixes. The fillers are checked for specific gravity test using density bottle or specific gravity bottle and the results are tabulated in table 4.2

Table 2: Specific gravity of the fillers

Type of filler used	Specific gravity
Hydrated Lime	2.3
Ordinary Portland Cement	3.10
Fly ash	2.09

4.2 Procedure

The specimens were prepared using different types of fillers at varying percentages. The different fillers used were Lime, Ordinary Portland cement and fly ash at 2%, 4% and 6% by weight of aggregates. Marshall Method of mix design is used for the present study and accordingly the specimens were prepared. Compaction of specimen is done by giving 75 blows on either side of the mould. Specimens prepared were then subjected for stability and flow test using Marshall Stability equipment at test temperature of 60^0C. After that the test values were used for density voids analysis to determine OBC.

For moisture damage evaluation the specimens were prepared at OBC. Compaction of the specimen is done at 7% air voids. Then the prepared specimens were subjected to freezing and thawing cycle and followed by testing the specimens for Indirect Tensile Strength test.

Repeated indirect tensile strength test was carried out for studying the mixes for their fatigue behavior.

Asphalt film thickness calculations were done to study the effect of fillers on asphalt film thickness for the durability of the bituminous mixes.

The Marshall Test results obtained are as tabulated below in Table 4.3, 4.4, 4.5

Table 3: Marshall Properties at Optimum Binder Content – Lime Filler

Filler type/ Properties	Lime			Requirement as per MORTH
	2%	4%	6%	
OBC, %	5.69	5.66	5.706	5.4 minimum
Stability, Kg	1820.4	1905.1	1967.08	900
Flow, mm	3.37	3.5	3.35	2-4
Air voids %	3.920	3.277	3.622	3-5
Gt, gm/cc	2.462	2.404	2.412	-------
Gb, gm/cc	2.331	2.341	2.325	-------
VMA, %	17.05	16.466	16.71	14 minimum
VFB, %	77.01	80.095	78.335	65-75
Film thickness	7.891	7.218	6.735	-------

Table 4: Marshall Properties at Optimum Binder Content – Cement Filler

Filler type/ Properties	Cement			Requirement as per MORTH
	2%	4%	6%	
OBC, %	5.82	5.76	5.703	5.4 minimum
Stability, Kg	1808.1	1630	1730.9	900

Flow, mm	3.5	3.95	4.1	**2-4**
Air voids %	4.05	3.09	3.67	**3-5**
Gt, gm/cc	2.434	2.423	2.447	-------
Gb, gm/cc	2.361	2.367	2.35	-------
VMA, %	17.504	16.719	17.256	**14 minimum**
VFB, %	76.85	81.51	78.68	**65-75**
Film thickness	8.071	7.343	6.721	-------

Table 5: Marshall Properties at Optimum Binder Content – Fly Ash Filler

Filler type/ Properties	**Fly ash**			**Requirement as per MORTH**
	2%	**4%**	**6%**	
OBC, %	5.75	5.603	5.636	5.4 minimum
Stability, Kg	1306.7	1905.1	1502.9	900
Flow, mm	3.97	3.6	3.8	**2-4**
Air voids %	3.918	3.118	2.353	**3-5**
Gt, gm/cc	2.419	2.412	2.399	-------
Gb, gm/cc	2.324	2.337	2.343	-------
VMA, %	17.152	16.425	15.695	**14 minimum**
VFB, %	77.162	81.014	85.013	**65-75**
Film thickness	7.981	7.137	6.660	-------

4.3 Asphalt film thickness calculation

The technique used in calculating for asphalt film thickness is by Hveem Method of Mix design. The film thickness is the function of surface area of aggregate and the percent of binder used in the mixture. Table 4.6 below shows the surface area factors and total surface area calculation.

Table 6: Surface area factors and obtained surface area 'SA' in m^2/Kg

Hveem method of Surface area determination			
Sieve Size (mm)	**% Passing**	**Surface area Factor**	**Surface Area 'SA', m^2/kg (Surface factor x Passing %)**
26.5	100	0.41	0.41 x 1 = 0.41
19	100		
13.2	86.59		
9.5	83.43		
4.75	65.49	0.41	0.27
2.36	51.75	0.82	0.42
1.18	39.46	1.64	0.65
0.6	34.36	2.87	0.99
0.3	19.81	6.14	1.22
0.15	11.7	12.29	1.44
0.075	5.3	32.77	1.74
Cement	2	32.77	0.6554
Total Surface area SA'm^2/kg'			**7.37**

** Total surface area for 4% and 6% fillers are 8.03 and 8.68 in m^2/Kg and these values are same for other two fillers at 2%, 4% and 6%

$$TF = \left(\frac{Vasp}{SA * W}\right) * 1000 \qquad (8)$$

Where,

TF= Average film thickness in µ

Vasp= Effective volume of binder (lt)

SA= Surface area of the aggregate in m^2/Kg

W= Weight of aggregate

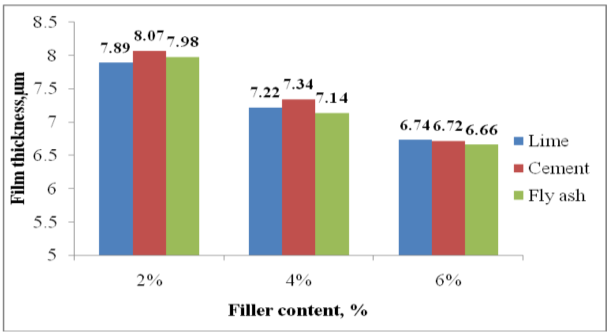

Figure 4.1 Variation of Film thickness with Filler content

4.4 Indirect Tensile Strength test

It is a design tool for evaluating moisture susceptibility of HMA mixes. In this test Marshall Specimens are subjected to compressive loads, which act along the vertical diametrical plane, which were tested unconditioned and conditioned as per standard procedure AASHTO 283

The load at failure was recorded and ITS values were calculated using the expression below.

$$\sigma x = \frac{2000*P}{\pi*d*t} \qquad (10)$$

Where,

σ_x= Horizontal tensile stress, KPa

P= Applied load in N

d= Dia of specimen, mm

t= Thickness of specimen

The result thus obtained is represented in the bar chart shown in Fig 4.2

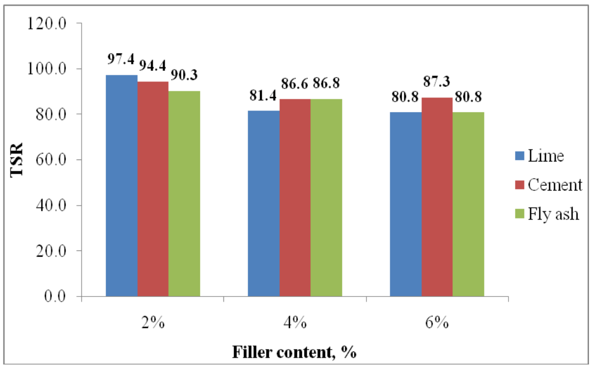

Figure 4.2 Variation of TSR with Filler content

3.5 Fatigue Test for Bituminous mixes

The test is carried out on the bituminous mixes for evaluating the fatigue life of BC mixes by subjecting the specimen to repeated loading at 250C test temperature. In this present investigation the fatigue life is tested for the specimens prepared for different types of fillers at different percentages. The input load for the test will be the failure load of ITS value of conditioned specimens prepared at OBC. And 30% of this ITS value is taken as stress level.

The result thus obtained is represented in the bar chart shown in Fig 4.3

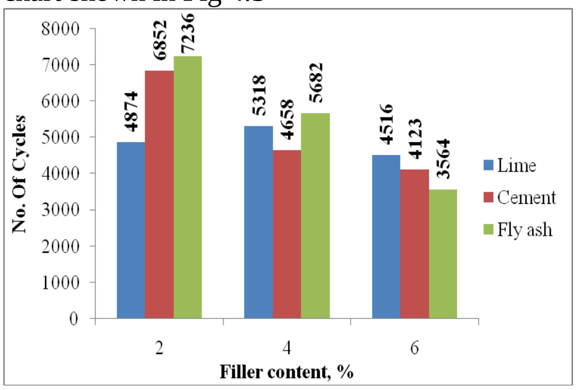

Figure 4.3 Variation of Fatigue life with Filler content

5. Conclusions

1. Mixes with cement filler requires higher bitumen content that makes them to be costly from practical point of view.This is probably due to the fact that there is higher bitumen absorption when mixes prepared with Cement. Hence higher optimum bitumen content values were required to fulfil the Marshal requirements. Whereas, mixtures prepared with lime or Fly ash filler, optimum asphalt content are relatively the same. The optimum bitumen content requirement in case of fly ash is less. Considering the free and abundant availability of fly ash particularly at places near thermal power plants and where coarse aggregates are scarce, use of fly ash shall be cheaper compared to other two types of fillers.
2. Stability values of mixes prepared with fly ash is found to be increasing up to maximum and then decreasing with the increase in the amount of filler content starting from 2% this is due to the fact that voids at lower filler content is too high and aggregates tend to be finer as filler content increases, hence both effect tend to reduce the stability values. Whereas, the stability values of mixes containing lime keeps increasing with the filler content. Higher stability values were obtained for mixtures containing lime for all filler contents. Mixes prepared with fly ash provide higher stability values for filler content 4%.
3. From the figure 4.1 it is observed that as filler content increases the film thickness coating over the aggregate is decreased. On comparing all fillers, at filler content 6% film thickness is lowest for Fly ash and at 2% film thickness is highest.
4. The method of calculation of film thickness is empirical, as it assumes aggregate particles to be spherical and cubical. The weight of aggregates and the effective volume of bitumen are determined from the bulk density of the mix at OBC. It is generally observed that Film thickness is above 6µm, for the various trials with different fillers.
5. Higher TSR values were obtained from mixtures prepared with lime as compared to crushed stone.
6. It is observed that the value of Tensile Strength Ratio (TSR) for mixes prepared with lime as filler offers highest Tensile Strength Ratio

value followed by cement and fly ash filler. However, the variations are so small to be considered significant and all the mixes satisfy the minimum TSR value requirement i.e. 80%. It means all the mixes including that with fly ash as filler have very good resistance to moisture induced damages.

7. When lime is used as a filler fatigue resistance increases from 2% to 4%. But at higher percentage of lime content as filler reduces the fatigue resistance and this can be attributed to stiffening of mix to a greater extent at 6% and mix becomes too stiff to compact which has resulted in the reduced fatigue resistance. Cement as filler should be limited to 2%. Because too much cement as filler reduces the interaction between aggregate and binder as coating of aggregate by fillers will increase the OBC hence weakening the mix and seen as reduced fatigue resistance. Fly ash as filler in BC mixes shows decreasing fatigue resistance as filler content increases. On comparing with other fillers fly ash has the better fatigue resistance for all filler contents except at 6% filler content it is lowest this can attributed to that too much cement as filler reduces the interaction between aggregate and binder as coating of aggregate by fillers and hence reducing the fatigue resistance.

6 Acknowledgement

The authors would like to express their respectful and profound gratitude to our guide ***Dr.Krishnamurthy***, Professor-PG Studies, RASTA - Centre for Road Technology, Dr. ***Dr. B.R.Srinivasamurthy***, Technical Advisor, RASTA, for their constant encouragement and also valuable guidance. Owing our sincere gratitude to all the faculties and staff of RASTA for their co-operation and support throughout the work.

References

[1]. Prithvi S. Kandhal, Kee Y Foo and Rajib B Mallick. (1998). “A Critical Review of VMA Requirements inSuper pave.” NCAT Report No. 98-1

[2] John P. Zaniewski, Carlos H. Reyes. (2003). “Evaluation of the Effect of Fines on Asphalt Concrete.” Asphalt Technology Program, Department of Civil and Environmental Engineering, Morgantown, West Virginia.

[3] Boris Radovsk

iy. (2003), “Analytical Formulas for Film Thickness in Compacted Asphalt Mixture”. Transportation Research Board, 82nd Annual Meeting, Washington, D.C.

[4] Satish Chandra and Rajan Choudhary, 2013. “Performance Characteristics of Bituminous Concrete with Industrial Wastes as Filler,”Journal of Materials in Civil Engineering, Vol. 25, No. 11, November 1, 2013. © ASCE, ISSN 0899- 1561/2013/11-1666-1673

[5] Dr. Talal H. Fadhil, Salah S. Jasim, Dr. Kahlil E. Aziz, Ahmed S. Ahmed, 2013. “Influence of using white cement kiln dust as mineral filler on hot asphalt concrete mixture properties, “International Journal of Civil Engineering and Technology (IJCIET), ISSN 0976 – 6308 (Print), ISSN 0976 – 6316(Online) Volume 4, Issue 1, January-February (2013), © IAEME

[6] DebashishKar, Mahabir Panda and Jyoti PrakashGiri, 2014. “Influence of fly-ash as a filler in bituminous mixes,”ARPN Journal of Engineering and Applied Sciences, VOL. 9, No. 6, JUNE 2014.

[7] B.DurgaPriyanka, P.V.Ajay Kumar, 2015. “Use of fly ash as mineral filler for bituminous paving mixes”, International Journal of Research in Engineering and Technology, Volume: 04 Special Issue: 01 | NCRTCE-2014 | Feb-2015.

SECM/15/045

APPICATIONS OF ENVIRONMENTALLY FRIENDLY CELLULAR CONCRETE IN CONSTRUCTION

Rupa Purasinghe[1], F. Shimose[2], H. Lum[2], J. Shamma[2]

[1]California State University at Los Angeles, CA 90032, USA

[2]California State University at Los Angeles, CA 90032, USA

[1]E-Mail: rpurasi@calstatela.edu, TP: +001-323-343-4459

Abstract: Cellular concrete is a cost effective construction material that is continuously gaining traction and popularity in the US and elsewhere. Cellular concrete is a material consisting of Portland cement, water, and foam. When it hardens, the concrete has an oven-dry density ranging from approximately 50 lbs/cubic feet to 90 lbs/cubic feet. Some applications have achieved an even lower density that 50 lbs/cubic feet. Recipes may also include aggregates such as fly ash. Admixtures are used as well depending on the final use of the product. Cellular concrete has numerous applications in the building construction industry and as an underground backfilling material, but lately other uses in the infrastructure field have been gaining popularity especially as a stabilizer around transmission conduits. Popular application of cellular concrete includes insulation, fire retarding, and sound proofing for a variety of structures. Cellular concrete systems provide better drainage, increased fire resistance, increased wind uplift ratings, improved seismic values, efficient thermal insulation, and improved sound attenuation in an environmentally friendly manner. In underground applications, cellular concrete is used as a cost effective filler material in lieu of soil without the compaction effort required when using soil. Most recently the infrastructure field introduced cellular concrete as a backfill and filler material around underground structures such as segmental tunnel liners and pipelines. Cellular concrete can be used as backfill material at pipeline fault crossing by allowing localized ground deformation without overstressing the pipe section. This application can minimize damage to the pipeline or tunnel transmission structure that results from a shear failure of the pipe. However, the low compressive strength of cellular concrete limits its application as a structural material. The paper discusses material behavior and characteristics, state of the art construction methods, and advantages and disadvantages of using cellular concrete as a construction material in current times.

Keywords: Cellular concrete, fire resistance, green roofs, pipeline backfill, thermal insulation, tunnel annular space backfill.

1. Introduction

1.1 Process and Mixture of Cellular Concrete

The cement used in the preparation of cellular concrete is designed to meet the requirements of ASTM C150 (Portland cement), C 595 (blended cement), or C 1157 (hydraulic cement). The water/cement ratio ranges from 0.5 to 0.6 and is similar to that of the normal weight concrete. Low-density cellular concrete may include lightweight aggregates such as vermiculite meeting the requirements of ASTM C332.

Cellular concrete is produced by adding a chemical admixture to a hydraulic cement and water such that the resultant concrete is a low density product through air-entrainment. The air entrainment forms air voids inside the structural matrix giving it its low density. Usually this added chemical or material is a proprietary foaming agent. The resultant product, when hardened, has a density ranging from 50 lbs/cubic feet to 90 lbs/cubic feet. Compressive strengths range from 160 psi to 300 psi. Some contractors have been able to reduce the density further by modifying their foam and mixing processes. Others have created more elaborate recipes that include materials such as fly ash, special admixtures, and lightweight aggregates. Cellular concrete can be pumped over long distances with proper air-entrainment, thus allowing it to be used in a variety of applications not conducive if using regular concrete.

2. Properties of Cellular Concrete

2.1 Physical Properties

Cellular concrete is a low density product and behaves like a viscous fluid where the interaction between molecules offers little resistance to sheer deformation prior to hardening. This property allows cellular concrete to have self-leveling properties, good workability, and most importantly self-consolidation which eliminates the need for compaction and vibration. The texture/color of air dry cellular concrete is of a rough light gray color riddled with air voids as shown in figure 1 below.

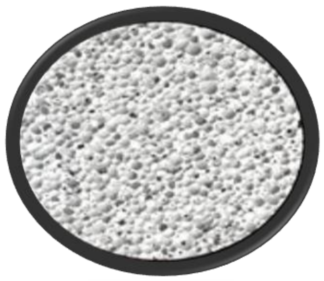

(Courtesy of ACI 523.3R-14)
Figure 1: Texture/Color of Cellular mix

2.2 Temperature & Curing

ACI 523.3R-14, discusses precautions to be taken when concreting in cold weather and recommends not to place cellular concrete in rain, or snow. In fast drying conditions, a wet curing or curing compound should be used. For mass fill applications such as in geotechnical or underground applications, curing takes place in between fresh lifts placed on successive days (ACI 523.3R-14, Chp.4.4).

2.3 Density and Compressive Strength

Compressive strength is dependent on water-cement ratio, density, type of cement used, and aggregate types. Cellular concrete may be designed for densities varying from 50 lbs/cubic feet up to about 90 lbs/cubic feet. For roof insulating concrete and underground fill projects the density is normally below 60 lbs/cubic feet. This helps to maintain its lightweight material properties with improved workability. The use of fly ash, sand and other lightweight aggregates can be added to further enhance its density and strength.

3. Equipment and Mixing on Site

3.1 Equipment Used

Equipment for the production of cellular concrete is varied depending on the use, application, and/or capacity requirements of the task. Many large jobs utilize production plants that are skid mounted and can be moved around the site with ease. Most of these plants are automated in order to achieve the desired consistency for the particular job.

4. Cellular Concrete Applications

4.1 Construction of Buildings Applications of Cellular Concrete

4.1.1 Insulating Concrete Roof Application

A common application of cellular concrete is as insulation material for roofs. In most applications cellular concrete is either used by itself or coupled with insulation foam to provide required insulation. Usually cellular concrete is placed atop a galvanized steel deck and topped off with a roofing material. The cellular concrete is permanent as it does not deteriorate with time and does not require replacement over the life of the structure.

4.1.2 Floors and Decks

Cellular concrete is used for decks and floors where thermal insulation and noise control are requirements of the designer. This is due to its ability to dampen noise and act as an insulator. The use of cellular concrete provides a cost effective way to install floors in apartment buildings and high rises since the material is low density and has great workability. Cellular concrete as an insulator can be used in applications that require an insulating material that has integrity and strength.

4.1.3 Fill Material

Currently, cellular concrete is gaining confidence among the engineering and geotechnical community as a geotechnical fill or ground improvement material. Its popularity is even more so due to its low cost, no compaction requirement, and rapid construction.

4.1.4 Wall Panels

Cellular concrete is also utilized in the construction of precast wall systems for residential and commercial buildings. Its lightweight nature coupled with its resistance to moisture damage makes it a practical and an environmentally friendly product. British Columbia researchers (Dr. Rishi Gupta, P.Eng. of British Columbia Institute of Technology), has developed the use of precast light gage steel wall systems using cellular concrete as filler (Figure 2). Hospitals, high rise building, gas stations, commercial buildings, retail outlets, ATM kiosks, modular washrooms, modular cabins, and site offices and customized buildings are all conducive for the use of cellular concrete wall systems. The lightweight nature of the product allows it to be placed in site or shipped to the site after being formed and poured at a precast facility. This type of construction has proved to be economical in many applications.

Research have determined that the use of cellular concrete in light gage steel wall systems provides an increase in the axial load carrying capacity helping the building structurally. Also, cellular concrete serves as an efficient fire proofing insulator, providing a one hour fire rating per inch of thickness. It also has thermal resistance capabilities that help protect the occupants of a building in case of a fire. The use of cellular concrete wall systems is believed to also reduce the deteriorations of walls due to environmental aspects.

(Courtesy of British Columbia Institute of Technology. http://metro-panels.com/media/ARTICLE%20BY%20FACULTY%20AT%20BRITISH%20COLUMBIA.pdf)

Figure 2: Light Gage Steel with Cellular Concrete in-fill

4.2 Geotechnical Applications of Cellular Concrete

Cellular concrete has a lower density than compacted soil, and it is an efficient void-filling material without surcharging existing facilities or pipelines. Cellular concrete can be used to replace soil and the engineers can prepare it such that it has the desired strength for any particular application including jobs that require it to supplement existing soil strength.

4.3 Underwater Applications of Cellular Concrete

Cellular concrete has been successfully used underwater in such applications as those requiring the encapsulation of timber thus insulating the timber for underwater organisms that contribute to its deterioration. Because cellular concrete remains cohesive during pumping and placing allows it to work well underwater. The most important requirement when placing cellular concrete under water is that is has a higher density than water allowing it to displace water and not disperse. This also gives it the ability to fill in small underwater voids.

4.4 Pipeline and Tunnel Backfill

4.4.1 Pipeline Trench Backfill

For pipeline construction in a vertical trench support system, the space between the pipeline and vertical shoring and/or the trench wall may be too tight to allow proper compaction of soil backfill. In cases like this, cellular concrete can be used to fill the void surrounding the pipeline. Cellular concrete can be an economical solution to fill the voids while providing corrosion protection for the pipe. With the proper mix design, cellular concrete can be pumped over a long distance which helps when performing work in tight areas or when the construction schedule is a constraint.

4.4.2 Conduits at Fault Crossings

For conduit (pipeline and tunnel) construction across active faults, cellular concrete can be used as annular filler around a pipeline to accommodate ground movement during fault offset without damaging the pipeline. This is usually done by creating a chamber around the pipeline or oversizing a trench area and then filling the cavity around the pipeline with very low density cellular concrete. When a seismic event occurs, the cellular concrete will crush and deform to accommodate the displacement while maintaining alignment of the existing pipeline.

4.4.3 Tunnel Annular Backfill

For a two-pass tunnel lining system for water or wastewater construction, the primary liner (such as concrete segmental liner) provides the initial ground support while the final liner (such as welded steel pipe) is constructed inside the primary liner. The gap between the primary liner and the final liner is known as the annular space. Cellular concrete is widely used as backfill material to fill the annular space to provide corrosion protection, final liner support and a continuous load path between the pipeline and the surrounding ground. Cellular concrete is pumped for a long distance inside the final liner and flows through grout ports along the liner to fill the voids. The placement sequence of concrete backfill is tightly controlled inside the liner to ensure proper dissipation of heat of hydration and prevent pipe floatation associated with the low fluid density of cellular concrete.

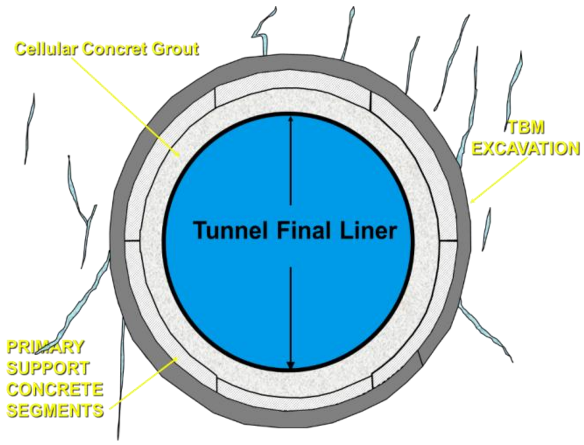

(Courtesy of Howard Lum)
Figure 3: Typical Tunnel Cross-Section showing cellular concrete grout

(Courtesy of Howard Lum)
Figure 4: Cellular concrete pumped in the annular gap of a tunnel

5. Cellular Concrete – Advantages and Disadvantages

5.1 Advantages

Cellular concrete is finding its way in many aspects of the construction industry and has been replacing a variety of materials. Some of the reasons for cellular concrete are:

- Low density characteristic
    - o Low density results in reduced loading on substructures
- Lightweight characteristic
- Easy to pump
    - o Fluidity and air content make it easy to pump over long distances
- Self-leveling
- Easy to use to fill small voids
- Does not need to be compacted
- Easy placement with proper pumping equipment
- An insulator
    - o Reduces noise transmission
    - o Thermal insulation
- Can be safely removed and reused
- Provides shock and energy absorption. If compressed during impact, resistance increases and kinetic energy is absorbed.
- Cost efficient.

5.2 Disadvantages

- Low compressive strength compared to normal weight concrete
- Not as durable and will not resist structural loads
- Requires more precise control in pumping and placement

6. Summary

Cellular concrete is getting increased attention as a construction material due to its versatility, lightweight nature, low cost, and environmentally friendliness. Cellular concrete is a material consisting of Portland cement, water, and foam. Recipes may also include admixtures such as fly each to accommodate a variety of applications. Cellular concrete has numerous applications in the building construction industry and as an underground backfilling material, but lately other uses in the infrastructure field have been gaining popularity especially as a stabilizer around transmission conduits. Popular application of cellular concrete includes insulation, fire retarding, and sound proofing for a variety of structures. Cellular concrete systems provide better drainage, increased fire resistance, increased wind uplift ratings, improved seismic values, efficient thermal insulation, and improved sound attenuation in an environmentally friendly manner. In underground applications, cellular concrete is used as a cost effective filler material in lieu of soil without the compaction effort required when using soil. Most recently the infrastructure field introduced cellular concrete as a backfill and filler material around underground structures such as segmental tunnel liners and pipelines. Cellular concrete can be used as backfill material at pipeline fault crossing by allowing localized ground deformation without overstressing the pipe section. This application can minimize damage to the pipeline or tunnel transmission structure that results from a shear failure of the pipe. However, the low compressive strength of cellular concrete limits its application as a structural material.

References

[1]. American Concrete Institute ACI 523.3R-14, April, 2014, Guide for Cellular Concretes above 50lb/ft^3.

[2]. American Concrete Institute ACI 523.1R-06, August, 2006, Guide for Cast-in-place Low-Density-Cellular Concrete

[3]. Institute of Technology, Nirma University, Ahmedabad. “The Innovative Precast Light Gauge Steel Wall System Combined with Cellular Concrete” Dr. Rishi Gupta, P.Eng. British Columbia Institute of Technology, December, 2011 *http://metro-panels.com/media/ARTICLE%20BY%20FACULTY%20AT%20BRITISH%20COLUMBIA.pdf*

[4]. Cell-Crete Corporation, www.cell-crete.com

[5]. Elastizell Corporation of America, www.elastizell.com

[6]. Geofill LD Marine, www.geofill.com

[7]. L.R.E. Ground Services Inc., www.lregsi.com

SECM/15/053

INVESTIGATION OF ADMIXTURES EFFECT ON DEGRADATION OF CEMENT PASTE IN SAGD AND CCS WELLS

Miharu Tsukahara[1*] and Shingo Asamoto[2]

[1]Saitama University, Saitama, Japan
[2]Saitama University, Saitama, Japan
*E-Mail: s15me108@mail.saitama-u.ac.jp, TP: +81488583556

Abstract: In recent years, Steam Assisted Gravity Drainage (SAGD) and Carbon dioxide Capture and Storage (CCS) projects are being developed in oil and gas fields. SAGD is a heavy oil recovery technology to reduce heavy oil viscosity and extract it from underground. CCS is a technology to inject CO_2, emitted from plants, into a couple of 1000m deep ground through well. The deterioration of well in SAGD and CCS projects may cause leakage of deleterious gas.
In this study, mechanical and chemical degradation of hardened cement paste made of Oil Well Cement (OWC) and Geothermal Well Cement (GWC) containing silica flour in the wells was studied experimentally. In order to imitate the underground condition of SAGD, the cement paste was exposed to the drying and moist sealed condition at 200°C. In addition, the cement paste was exposed to supercritical CO_2 to reproduce the condition to inject CO_2 gas in CCS well. The compressive strength tests after exposure to 200°C and thermal analysis to study carbonation after exposure to supercritical CO_2 suggested that the replacement of silica flour to cement is effective to be applied to both SAGD and CCS injection wells.

Keywords: Cement paste, fly ash, polymer, supercritical CO_2, 200°C steam.

1. Introduction

In recent years, Steam Assisted Gravity Drainage (SAGD) and Carbon dioxide Capture and Storage (CCS) projects are being developed in oil and gas field. SAGD is a recovery technology of heavy oil which consists of two horizontal underground wells at depth of a few of 100 m, the injector and the producer as shown in Figure 1. The conventional oil exploration methods is not appropriate to extract heavy oil with high viscosity that is expected as alternative energy source to petroleum. The process of SAGD is to reduce heavy oil viscosity by the injection of hot steam at 200°C thorough the well injector and extract it from underground through the well producer as indicated in Figure 1. CCS is also an underground technology to inject CO_2 emitted from factories into a geological reservoir at more than 1000 m deep underground through the injection well as shown in Figure 2. The injected CO_2 is anticipated to be stored in the reservoir for a long time in order to isolate the CO_2 to be reacted with the mineral. The CCS project has been ongoing in Norway, Canada and Algeria in order to the reduction of

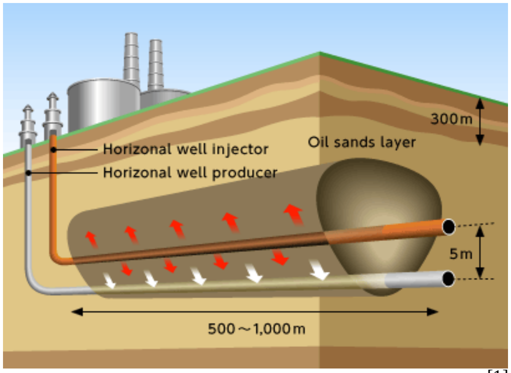

Figure 1: The overview of SAGD project[1]

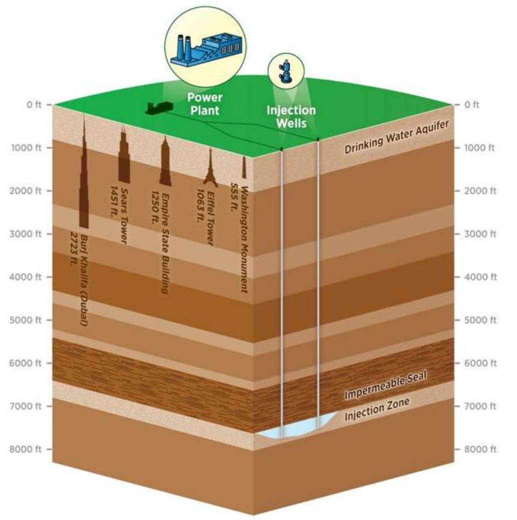

Figure 2: The overview of CCS projects[2]

CO_2 emission. In Japan, the survey of possible sites and the demonstration project have been carried out based on the contraction with the Ministry of Economy, Trade and Industry aiming to prevent global warming.

Wells in SAGD and CCS projects are exposed to severe condition in the underground with high temperature, high pressure, and high concentration of CO_2 gas in CCS well. Thus, the wells will be chemically and physically deteriorated during service. If wells are severely deteriorated, the deleterious gas such as high concentration of CO_2 and H_2S in the underground may be leaked to the ground through the deteriorated well. The prevention from the gas leakage is the most important issue in SAGD and CCS projects because the risk is high to threaten the life of living beings on the ground.

The underground wells consist of steel casing and surrounding cement paste to fill between steel casing and ground. Oil Well Cement (OWC), standardized by the American Petroleum Institute, is generally used for cementing around the casing to be stabilized as well. According to the previous study, the compressive strength of the cement paste with OWC greatly decreases when exposed to moist sealed condition at 200°C, simulating the possible surrounding condition in the SAGD project. In this study, Geothermal Well Cement (GWC) containing silica flour in the OWC is investigated focusing on the strength under SAGD condition and the resistance to high concentration of CO_2 under CCS conditions. In addition, the effect of admixtures such as fly ash and polymer are also examined experimentally.

2. Experimental procedure

In the experiment, the commercial GWC manufactured by Japanese cement company was mainly used as the base cement. For the comparison, the OWC was also studied. The effect of fly ash on the cement paste in the well were also examined. The replacement ratio of fly ash to GWC was changed from 10% to 40% with an increment of 10% (named GWCFA10, 20, 30 and 40). In the experiment to simulate CCS condition, the effect of polymer that may be used to increase the bond between cement paste and casing was investigated. The polymer types used in the experiment were polyvinyl emulsion (PVA) and ethylene-vinyl acetate copolymer emulsion (EVA). The polymer mixing ratio was 1% of cement weight.

In the case of SAGD simulation experiment, the possible extreme surrounding conditions around the cement paste in the injection well during SAGD operation were assumed to be the drying condition at 200°C for dried soil and the moist sealed condition at 200°C for moist soil. The water-to-binder ratio (W/B) of the cement paste was set to 44% because the W/B of about 45% is generally used in oil wells. The specimen size were two types, ϕ50 x 100 mm cylinder and 20 x 20 x 50 mm rectangular. After 7 days curing under

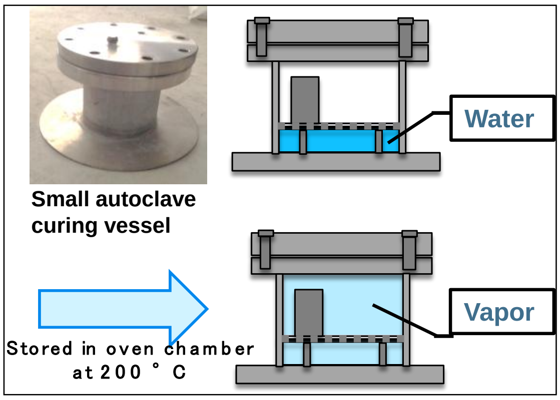

Figure 3: The exposure method to the moist sealed condition at 200°C

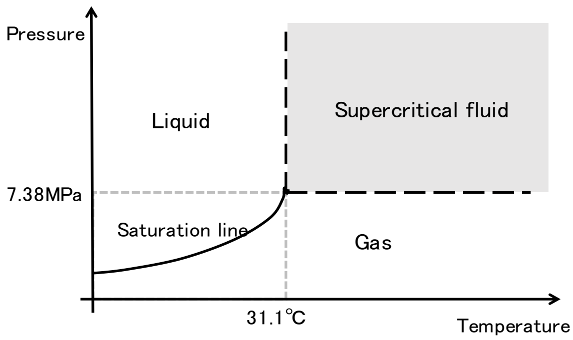

Figure 4: Phase change of the CO_2

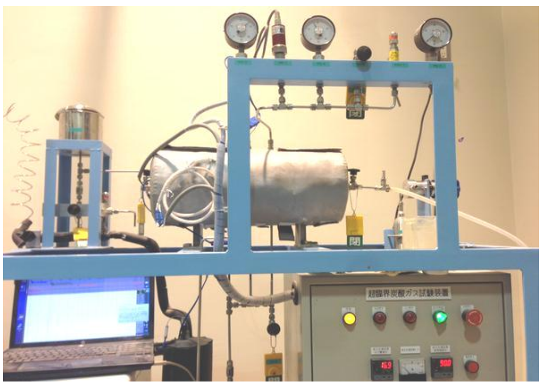
Figure 5: Supercritical CO_2 generator and vessel

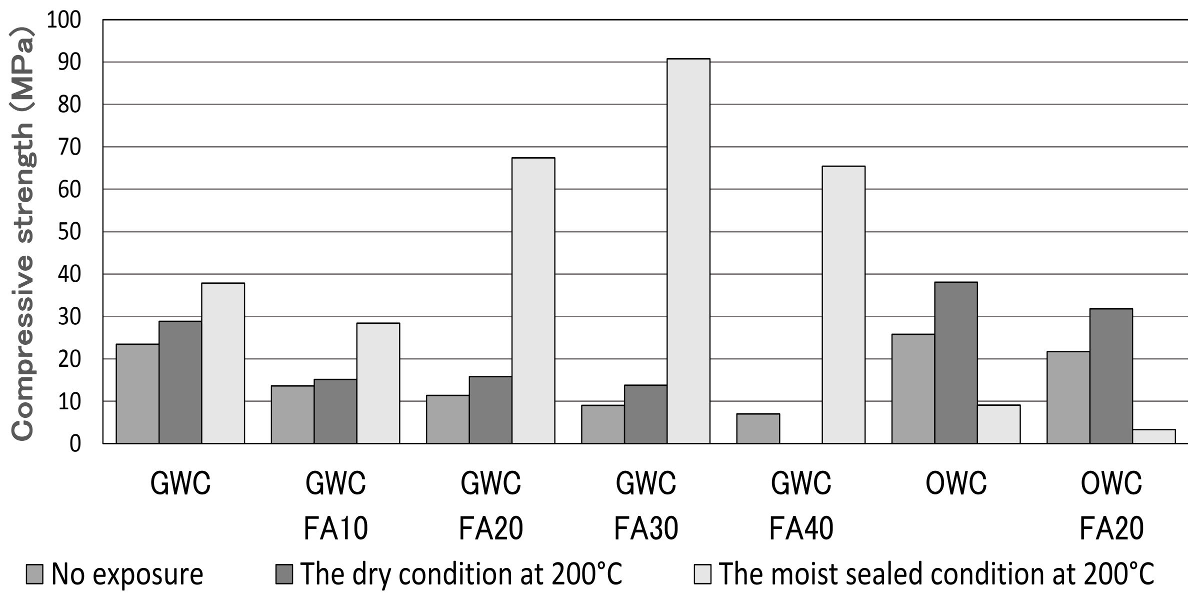

Figure 6: Compressive strength test results

sealing condition at 20°C, the specimens were exposed to the dry condition at 200°C or the moist sealed condition at 200°C (Figure 3) for 3 days. After the exposure, the compressive strength test was done using ϕ50 x 100mm specimens, and the X-ray diffraction analysis and Scanning Electron Microscope (SEM) observation were conducted using crushed 20 x 20 x 50mm specimens.

In the case of CCS simulation experiment, the possible surrounding conditions around the cement paste in the injection well during CCS operation was assumed to be exposure to the supercritical carbon dioxide. The supercritical carbon dioxide is intermediate fluid with characteristics of both liquid and gas (Figure 4). In order to accelerate the carbonation effectively for a short time, very small specimens of ϕ4 x 4 mm cylinder were used and the W/B was set to 55 % even though general W/B is about 45 % as explained above. After 7 days curing under sealing condition at 80°C, the specimens were subjected to the supercritical carbon dioxide at 80°C, 14MPa in the vessel for 7 days (Figure 5). Then, specimens were grinded into powder and set in Thermal Gravity-Differential Thermal Analysis (TG-DTA) test machine. The temperature was risen from room temperature to 100°C with 20°C /min, and remained for 10 minutes to evaporate the liquid water in the sample. Then, the temperature was risen to 900 °C with the same temperature rise velocity. The amount of $Ca(OH)_2$ and $CaCO_3$ due to the dehydrogenation and decarbonized reaction were obtained by the mass loss at 400-500 °C and 600-850 °C, respectively.

3. Experimental results

3.1 Exposure to dry condition and moist sealed condition at 200°C

The compressive strength test results after exposing to drying and moist conditions at 200°C are shown in Figure 6.

In the case of the exposure to the dry condition at 200°C for 3days, the compressive strength was increased, while hydration products of all specimens were not changed due to the exposure as explained later. The reason to increase the compressive strength may be because the severe drying can evaporate the water in fine pores to increase of the solid surface energy of the cement paste and lead to the increase of crack fracture stress based on Griffith crack theory.

In the case of the exposure to the moist sealed exposure at 200°C for 3 days, the compressive strength of GWC was also increased. On the other hand, the compressive strength of cement paste with OWC decreased significantly after exposing to the moist sealed condition at 200°C as shown in Figure 5. Thus, it is suggested that the partial replacement of silica to the oil well cement is effective to improve the compressive strength under moist sealed condition at 200°C. In addition, the compressive strength of GWCFA with fly ash was increased with increase of replacement ratio of fly ash under moist sealed condition at 200°C and then compressive strength of GWCFA30 cement

Cement type	GWC	GWCFA10
Hydration products found by X-ray diffraction	Xonotlite	Xonotlite and Tobermolite
Hydration products observed by SEM	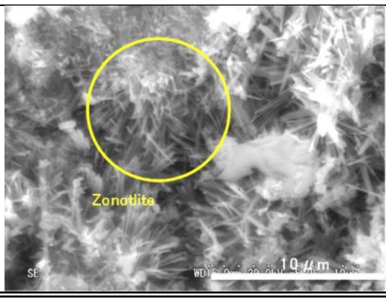	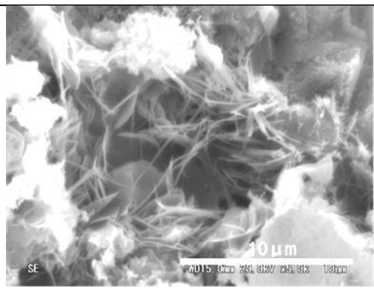
Cement Type	**GWCFA20**	**OWC**
Hydration products found by X-ray diffraction	Tobermolite	C_5S_2H, C_3SH and $C_5S_2H_6$
Hydration products observed by SEM	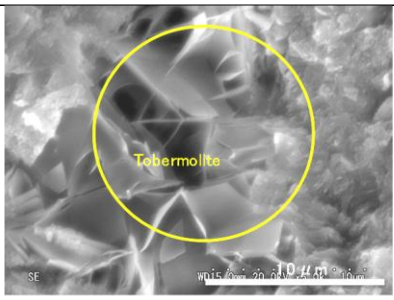	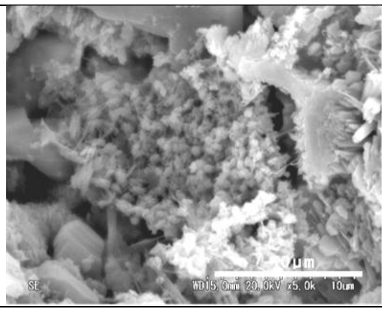

Figure 7: Hydration products after moist sealed exposure at 200°C

paste was the highest when the replacement ratio was changed from 10 % to 40 %. These results suggest that the compositive replacement of silica and fly ash to the oil well cement can be more effective to improve compressive strength under moist sealed condition at 200°C than sole replacement of them.

X-ray diffraction was carried out to identify hydration products precipitated in the cement paste after the exposure at 200°C. In addition, the hydration products were carefully observed using SEM. The results are shown in Figure 7. According X-ray analysis and SEM observation, Zonotlite was identified in GWC and GWCFA10 and Tobermolite in GWCFA10 and GWCFA20. Both Zonotlite and Tobermolite are calcium silicate hydrate. Then, Tobermolite is plate crystal while Zonotlite is column crystal. The previous studies reported that the cement paste matrix consisting of Tobermolite has higher strength than that with Zonotlite[3]. It is attributed to the increase of compressive strength of GWC cement paste with fly ash. On the other hand, Tobermolite and Zonotlite were not found in OWC and granular products such as C_5S_2H and $C_5S_2H_6$ were observed after moist sealed exposure at 200°C. The experimental results indicate that the granular hydration products cannot improve the strength and concludes that the hydration products precipitated by the high temperature exposure affect compressive strength significantly.

3.2 Exposure to supercritical carbon dioxide condition

The carbonation of cement paste under the supercritical carbon dioxide is much more progressive than the general carbonation in the atmosphere because supercritical carbon dioxide has high permeability into hardened cement [4]. The carbonation is the reaction of main hydration products of $Ca(OH)_2$ and C-S-H with CO_2 and results in precipitation of $CaCO_3$ in the cement paste. The reactions are represented below.

$$Ca(OH)_2 + CO_2 \rightarrow CaCO_3 + H_2O \quad (1)$$
$$\text{C-S-H} + CO_2 \rightarrow CaCO_3 + H_2O \quad (2)$$

The exposure to the severe supercritical carbon dioxide can promote both reactions simultaneously even though the C-S-H is little carbonated in the normal atmosphere. When the carbonation of C-S-H represented by equation (2) proceeds, pores structure can be coarsened due to the destruction of C-S-H matrix [5]. Thus, the understanding of the C-

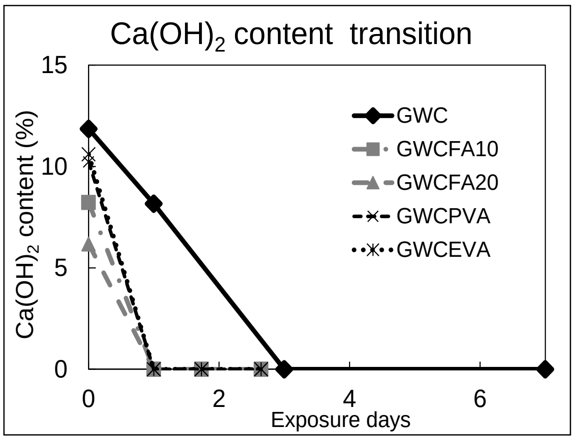

Figure 8: $Ca(OH)_2$ content transition

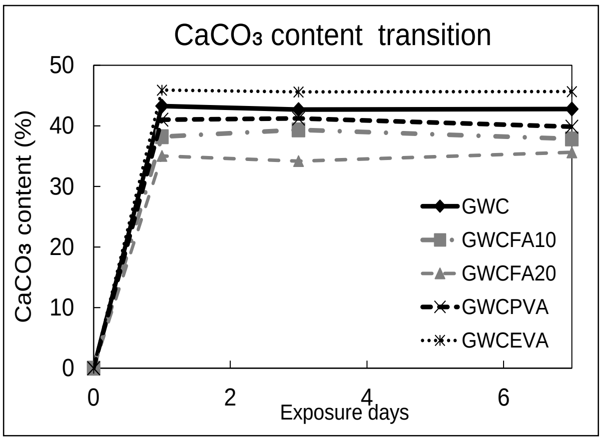

Figure 9: $CaCO_3$ content transition

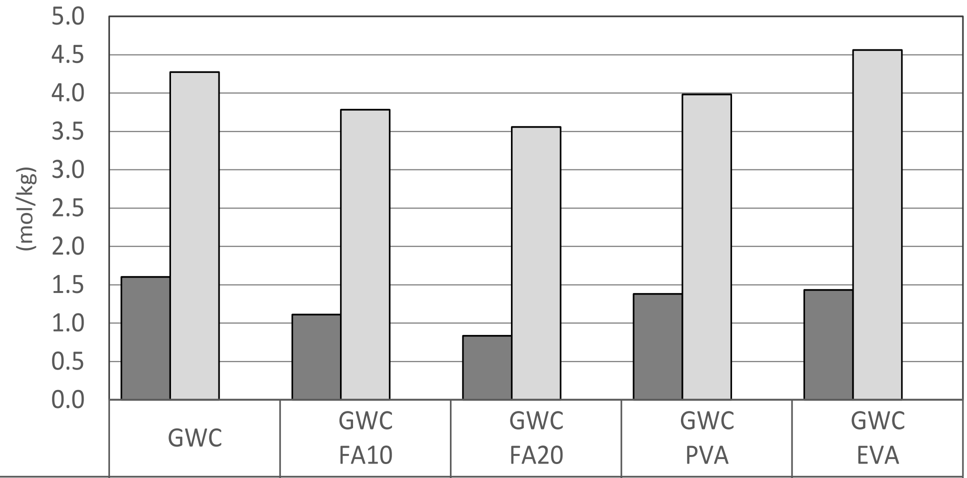

	GWC	GWC FA10	GWC FA20	GWC PVA	GWC EVA
Ca(OH)2 before exposure	1.60	1.11	0.83	1.38	1.43
CaCO3 after exposure	4.27	3.78	3.56	3.98	4.56
The difference	2.67	2.67	2.72	2.60	3.13

Figure 10: The difference between molar mass of $Ca(OH)_2$ before the exposure and molar mass of $CaCO_3$ after exposure for 7 days

S-H carbonation progress is important to avoid the deleterious gas leakage through the coarse pores.

Figure 8 shows the relationship between $Ca(OH)_2$ amount variation and square root of exposure days and Figure 9 shows the relationship between $CaCO_3$ content variation and exposure days. $Ca(OH)_2$ was not found by thermal analysis after exposure for 3 days because the carbonation progress of $Ca(OH)_2$ is fast and all of Ca(OH)2 were carbonated by 3 days exposure. Since the amount of $CaCO_3$ was still increased even after 3 days exposure, however, the precipitation of $CaCO_3$ can be ascribed to the carbonation of C-S-H. Hence, the difference between molar mass of $Ca(OH)_2$ before the exposure and molar mass of $CaCO_3$ after exposure for 7 days can correspond to the amount of carbonated C-S-H and be used for the indicator to evaluate the carbonation progress on C-S-H.

Figure 10 shows the difference between molar mass of $Ca(OH)_2$ before the exposure and molar mass of $CaCO_3$ after exposure for 7 days. It is found that the difference is almost independent of fly ash replacement. Thus, it is suggested that the fly ash may not affect the C-S-H carbonation progress. In the case of polymer mixing, the carbonation progress of C-S-H are reduced when PVA was used but increased when EVA was used. It deems that the addition of polymer may affects C-S-H carbonation progress depending on the polymer type even if the dosage amount is small. In the case of cement paste with OWC, the difference between molar mass of $Ca(OH)_2$ before the exposure and molar mass of $CaCO_3$ after exposure for 7 days was 3.62mol/kg, higher than that when GWC was used. The experimental result indicates that C-S-H of cement paste using GWC may have a higher resistant to the carbonation than that with OWC.

4. Conclusions

The conclusion in this study is summarized below.

(1) The compositive replacement of silica and fly ash to the oil well cement can be more effective to improve compressive strength under moist sealed condition at 200°C than sole replacement of them. The highest compressive strength under moist sealed condition at 200°C was obtained when the replacement ratio of fly ash to GWC with silica is 30 %.

(2) Under supercritical carbon dioxide condition, the cement paste with GWC had a higher resistance to carbonation than cement paste with OWC did. The replacement of fly ash to OWC was likely to not affect the carbonation by supercritical carbon dioxide

(3) The addition of polymer may affects C-S-H carbonation progress depending on the polymer type even if the dosage amount is small.

Acknowledgement

This study was financially supported by the JSPS Grant-in-Aid for Exploratory Research No. 25630182. The authors gratefully appreciate the financial support. X ray diffraction analysis and SEM observation were conducted by UBE Industries, LTD. The authors also sincerely appreciate their technical support.

References

[1] https://www.japex.co.jp/english.html

[2] http://www3.epa.gov/climatechange/ccs/

[3] Konstantinos Kyritsis, Christopher Hall, Dale P. Bentz and Moria A. Wilson: Relationship Between Engineering Properties, Mineralogy, and Microstructure in Cement-Based Hydroceramic Materials Cured at 200-350℃”

[4] Preben Randhol, Karen Valencia, Ali Taghipour, Idar Akervoll and Inge Manfred Carlsen, Ensuring well integrity in connection with CO2 injection, SINTEF Petroleum Research, NO.936 882 331, 2007

[5] R. Hirai, H. Isozaki and S. Asamoto, Study on Carbonation and Pore Structure of Cementitous Materials Exposed to Supercritical CO2, Proceeding of 12th International symposium on new technologies for urban safety of mega cities in Asia (USMCA 2013), pp.777-786, 2013

SECM/15/074

Base Course Geocell Reinforcement Evaluation by comparing 3-D FEM and Laboratory Evaluation

S. Inti[1], M. Sharma[1], C. Tirado[1] and V. Tandon[1*]

[1]The University of Texas at El Paso, El Paso, Texas, United States of America
*E-Mail: Corresponding vivek@utep.com, TP: +19157476924

Abstract: The shortage of high-grade base material and emphasis on using recycling base material has led to use of geocells reinforced bases in the past decade. The geocells provide reinforcement by confining base material and have been used for increasing bearing capacity of supporting soil, reducing settlements, using inferior quality material, reducing thickness of base layers, etc. It can be an economical option in rehabilitation of pavements and construction of low volume roads. Various studies have been conducted to evaluate the behaviour of geocell reinforced layers using expensive and time intensive laboratory tests. The working principle of geocell reinforced layers using various pavement materials, loading types, geocell types etc., can be comprehended quickly and economically using Finite Element Modelling (FEM). In this study, various significant FEM model parameters like constitutive material models and contact models were examined. The results were compared with the laboratory test results and specific contact and constitutive material models that predict behaviour similar to the laboratory results were recommended.

Keywords: Geocell, Finite Element Modelling (FEM), Contact models, Constitutive models.

1. Introduction

Geocells are honeycomb interconnected cells that completely encase the soil and provide three-dimensional confinement geometry, which reduces the lateral movement of the soil particles [1]. Due to confinement, the geocells increase the stiffness and the load-deformation behavior of the base layers; thus, reducing the deformation of the soil. The soil-geocell layers act as a stiff mat, distributing the vertical traffic loads over a much larger area of the subgrade soil [1]; thus, increasing load bearing capacity of subgrade layer. Although, geocells have been used and studied [1, 2, 3, and 4] the mechanism for improved bearing capacity and benefits of using geocell have not been well understood. In addition, the influence of in-fill material quality on performance of geocells has not been evaluated which is a critical issue when only lower/marginal quality material is available.

Earlier research (both laboratory and finite element) on Geocell was focused more on structure foundation (mostly building foundations) and less attention was disbursed towards geocell use in pavements. Since the loading pattern differs from buildings to pavements, the research findings from structures may not be applicable to pavements. While numerical modelling, many researchers modeled the geocell and infill material as a composite material [5, 6, 7, and 8] using finite element or finite difference methods but very few have modeled them as a separate material [9, 10, 11, and 12]. In geocell reinforced base layer, the infill material (linear elastic plastic) and geocell (elastic) responds simultaneously to loading, but the working mechanism of each material is different. In order to model geocell reinforced base layer more precisely, the behavior of each material (infill and geocell) needs to be evaluated separately. In this study, the geocell and infill material were modelled separately. The focus of the study is to evaluate various parameters like constitutive material models, contact models, and various material types.

2. Methodology

Modeling of the geocells and infill material was performed using finite element software LS-Dyna. A three layered pavement structure as shown in Figure 1 was modeled with a subgrade, geocell-reinforced base layer, and a top un-reinforced base layer. Geocell panels were modeled as a shell element of rhomboidal shape that closely resembles the curve shape of the honeycomb structure. The Belytschko-Lin-Tsay Shell (BLT) formulation was selected for modeling the geocell. The BLT element formulation is suitable for four node (quad) shell elements, and offer a single point integration with hourglass control. Each element has six global degrees of freedom per node (i.e., d_x, d_y, d_z, r_x, r_y, r_z), and five (through thickness) integration points [13]. In addition, they have a bi-linear nodal interpolation.

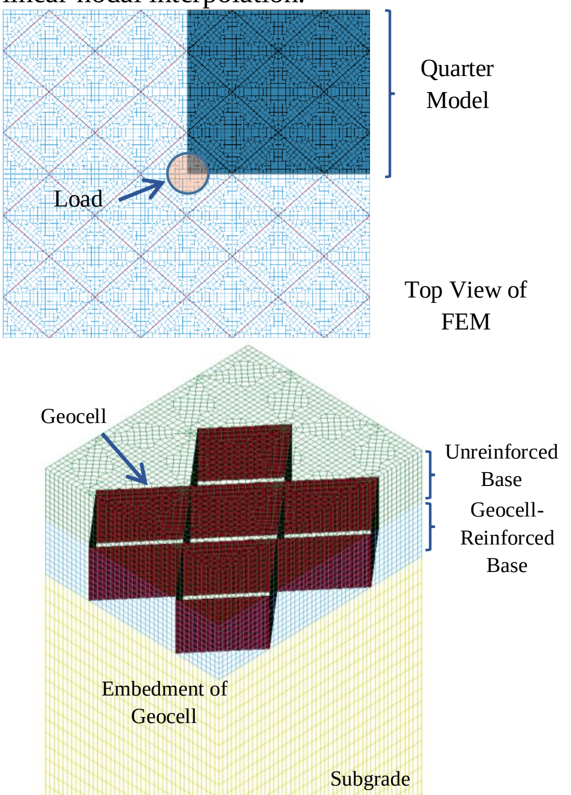

Figure 1: Finite element model of pavement structure

The 8-node constant stress solid elements were selected for the modeling of the base and subgrade structures. These solid elements use one-point integration and hourglass control. Considering the lattice pattern of geocell and its soil embedment in the base layer, proper element arrangement and nodal connectivity is required to adjust to the geocell lattice pattern and to avoid any penetration of nodes between the two different materials parts. The resulting mesh consisted of quad elements representing the geocell and a mix of solid hexahedral and prisms elements for the soil. To reduce the number of elements, and consequently the execution time, a quarter model was used.

3. Pavement Structure Dimensions and Finite Element Model Properties

Table 1 summarizes the dimension of the FEM quarter model. The applied boundary conditions restricted the displacement in the direction orthogonal to the planes. The geocell-reinforced base layer was unrestrained at the end to allow lateral movement to simulate field conditions where shoulder is not attached to the pavement.

3.1 Geocell Dimensions and Properties

Geocell dimensions and the properties used in the analyses are shown in Table 2. The properties shown correspond to a Presto GW20V geocell type, which was one of the geocells evaluated in the laboratory and modeled as linear elastic material.

Table 1: Dimensions of FEM quarter model

Pavement Structure Thickness		
Layers	Geocell Reinforced Pavement Structure	Unreinforced Pavement Structure
Top Base	100 mm	100 mm
Geocell Reinforced Base	100 mm	100 mm
Subgrade	1000 mm	1000 mm
Finite Element Model Size (Quarter Model)		
Longitudinal Dimension, *x*-axis	450 mm	
Transversal Dimension, *y*-axis	400 mm	

Table 2: Geocell dimensions and properties

Geocell Dimensions (Presto GW20V)	
Longitudinal Length	234 mm
Transversal Length	200 mm
Height	100 mm
Thickness	1 mm
Material Properties	
Density	950 kg/m^3
Transversal Length	414 MPa
Poisson's Ratio	0.45

3.2 Loading Conditions

In this study, a haversine cyclic load was applied at the center of the geocell using 150 mm diameter plate. Figure 2 shows the applied load consisting of multiple cycles each with a loading period of 0.1 sec and a rest period of 0.9 sec. The magnitude of the repeated peak load was maintained at 550 kPa, which is equivalent to tire pressure.

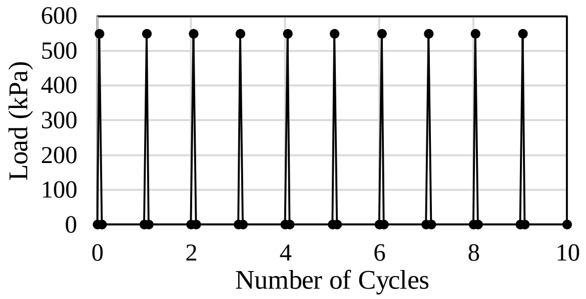

Figure 2: Loading cycle

3.3 Soil Material Model and Properties

In this study, three different constitutive material models were evaluated: linear elastic, Mohr Coulomb and FHWA soil model. FHWA soil model is a modified Mohr-Coulomb model available in LS-DYNA [14] extended to include excess pore-water effects, strain softening, strain hardening, strain-rate effects and elements deletion. These enhancements to the standard soil material models were made to increase the accuracy, robustness, and ease of use for roadside safety applications [14].

The yield surface for the FWHA soil model is given by [14]:

$$F = -P\sin\varphi + \sqrt{J_2 K(\theta)^2 + Ahyp^2 \sin^2\varphi} - c\cos\varphi = 0 \quad (1)$$

where:

P = pressure,
φ = internal friction angle,
J_2 = second invariant of the stress deviator,
c = cohesion,
$Ahyp$ = Drucker-Prager hyperbolic coefficient parameter approximated by

$$Ahyp = \frac{c}{20}\cot(\phi) \text{ , and} \quad (2)$$

$K(\theta)$ = Klisinski [15] modified Mohr-Coulomb function of angle θ in deviatoric plane, defined as

$$K(\theta) = \frac{4\left(1-e^2\right)\cos^2\theta + (2e-1)^2}{2\left(1-e^2\right)\cos\theta + (2e-1)\sqrt{4\left(1-e^2\right)\cos^2\theta + 5e^2 - 4e}} \quad (3)$$

where e is an eccentricity parameter describing the ratio of triaxial extension strength to triaxial compression strength responsible for third invariant (J_3) effects, ranging $0.5 < e \leq 1.0$, and initially modelled as $e = 0.7$, and angle θ obtained from

$$\cos 3\theta = \frac{3\sqrt{3}J_3}{2\sqrt{J_2^3}}. \quad (4)$$

The modified yield surface, as shown in Figure 3, is a hyperbola fitted to the Mohr-Coulomb surface. At the crossing of the pressure axis (zero shear strength), the modified surface is a smooth surface and it is perpendicular to the pressure axis.

4 Contact Model

One of the most important aspects for understanding the behavior of geocell-reinforced pavements comes from the interaction between the geocell and the surrounding geomaterials. In the case of composite, the modelling of geocell reinforcement becomes significantly simplified when a fully bonded model is considered. In a fully bonded model, shell nodes belonging to the geocell reinforcement are shared with solid elements representing the host infill base material. Thus, the solid elements (i.e. the base material) constrains the translational degrees of freedom of the embedded geocell. This approach has been followed by Bortz and Hossain [12] using geocell modeled as shell in an embedded region. Other authors have preferred to include an interface shear stress strain relationship based on Mohr Coulomb sliding criterion [10, 16, and 17]. The advantages offered by this type of interface consists on faster execution times and somewhat simplified meshing.

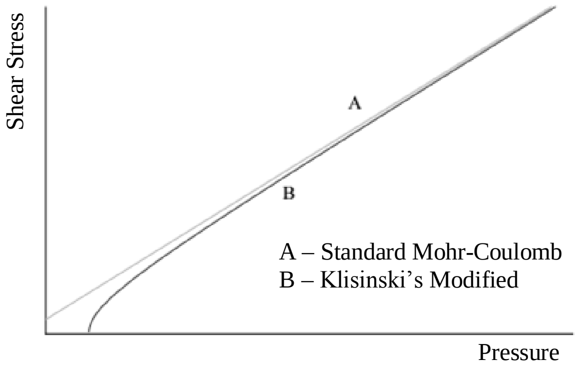

Figure 3: Comparison of Mohr-Coulomb yield surfaces in shear stress-pressure space [14].

To permit sliding between the soil and geocell, a contact models needs to be considered. Its implementation requires additional meshing and requires longer computational time. Leshchinsky and Ling studied the effects of geocell confinement on ballasted embankments by modelling the interaction of geocell and embankment with contact elements having "hard" normal contact (no penetration) and tangential contact was modeled as 2/3 of the tangent of the friction angle (45°), applied using penalty friction algorithm [18]. In this study, different contact models were evaluated and compared to a geocell-reinforced fully bonded model and to an unreinforced (continuum) model. Among the evaluated contact models, the LS-DYNA automatic single surface contact model and a discrete-beam element interface were found to be the most promising for best modelling the soil-geocell interaction.

4.1 Automatic Single Surface Contact

LS-DYNA automatic contact types determine the contact surfaces by projecting normally from the shell mid-plane a distance equal to one-half the contact thickness [13]. For single surface contacts, slave surface is typically defined as a list of parts while no master surface is defined. The automatic single surface contact makes use of a penalty method consisting in checking slave nodes penetrating the master surface. An interface force is applied between the slave node n_i and its contact point if penetration occurs, emulating the addition of an interface spring. Stiffness k_i for master segment s_i is defined as

$$k_i = \frac{f_{si} K_i A_i^2}{V_i} \text{ for brick elements, and} \quad (5)$$

$$k_i = \frac{f_{si} K_i A_i}{\max\left(l_{diag}\right)} \text{ for shell elements,} \quad (6)$$

where K_i is bulk modulus, V_i is volume, A_i is face area of the element in s_i, l_{diag} is the shell diagonal length, and f_{si} is a scale factor for the interface stiffness (normally f_{si} = 0.10) [13].

Friction is based on a Coulomb formulation. The model implements a friction algorithm that makes use of an elastic plastic spring. The algorithm is based on an iterative process that starts by calculating the yield force based on the friction and the normal force, followed by the calculation of the incremental movement of the slave node to update the interface force and check yield condition. An exponential interpolation function smooths the transition between the static and dynamic coefficients of friction based on the relative velocity between the slave node and the master, as described in the LS-DYNA theory manual [13].

4.2 Discrete Beam Element Interface

The use of discrete beam element for establishing a geocell-soil interface was also considered. Through these means, discrete beams were used to connect geocell nodes to solid nodes. A discrete beam has up to 6 degrees of freedom (DOF) whereas a spring has only one DOF. Resultant forces and moments of a discrete beam are output in the local (r, s, t) coordinate system. The length of a discrete beam may be zero or nonzero. In this study, discrete elements with linear elastic relations were used.

5. Results and Discussion

5.1 Evaluation of Material Model

For evaluating the material model, studies were carried first using fully bonded models followed by the inclusion of geocell reinforcement using LS-DYNA automatic contact model. Results shown in this section correspond to the latter model. Initially, the base and subgrade layers were modeled as linear elastic materials and soil properties used in the analysis are shown in Table 3 [19].

Only one loading cycle was attempted in the linear elastic FE analysis as other cycles would yield identical results because no plastic deformation is expected in an elastic material. The load cycle consisted of a loading period of 0.1 sec and a rest period of 0.9 sec, with a peak pressure of 550 kPa. Analysis was done for both reinforced and unreinforced pavement section and the responses were compared.

Table 2: Material properties of soil used in modelling [17]

Layer	Modulus (MPa)	Cohesion (kN/m^2)	Friction Angle, ϕ	Unit Weight (kN/m^3)
Subgrade 1 (Clay)	12	10.0	15°	15.8
Subgrade 2 (Clay)	16	10.0	15°	15.0
Base 1 (Sand)	40	0.01	34°	20.0
Base 2 (Sand)	60	1.0	29°	19.5
Base 3 (Sand)	80	0.0	29°	20.0

No significant change in responses for unreinforced and reinforced was observed using linear elastic material model. The plot shown in Figure 4, for a 35 MPa base layer and 35 MPa subgrade, and 150 mm diameter load plate applying a pressure of 550 kPa at the center of the cell, shows no significant difference in terms of deflection with respect to depth. Similar responses were obtained for all other loading scenarios and pavement distresses.

In addition to no significant effect of the geocell reinforcement, this model does not take into account plastic deformation as observed in soils subjected to repeated loading. Thus, soils models that can predict elastic as well as plastic deformation were selected for evaluating response of geocell reinforcement.

Mohr-Coulomb is the most commonly used soil material model [6, 9, 10, and 20] that is able to address the soil's elastic as well as plastic behavior. Use of this model in LS-DYNA incurred in excessive deformation at the corners farther from the loaded section forcing the analysis to terminate after 10 cycles. This model was not found suitable as deformations seemed excessive when compared to other studies. To overcome this problem, the FHWA soil model was considered instead as this model also allows to accommodate permanent deformation.

Four different types of base materials were evaluated with two distinct types of subgrades, described in Table 3. Pavements were subjected to multiple cycles with constant peak pressure of 550 kPa, as shown in Figure 2. Figure 8 shows the deflection with respect to depth under the center of load occurring at the peak load of the first cycle for both reinforced and unreinforced base layers.

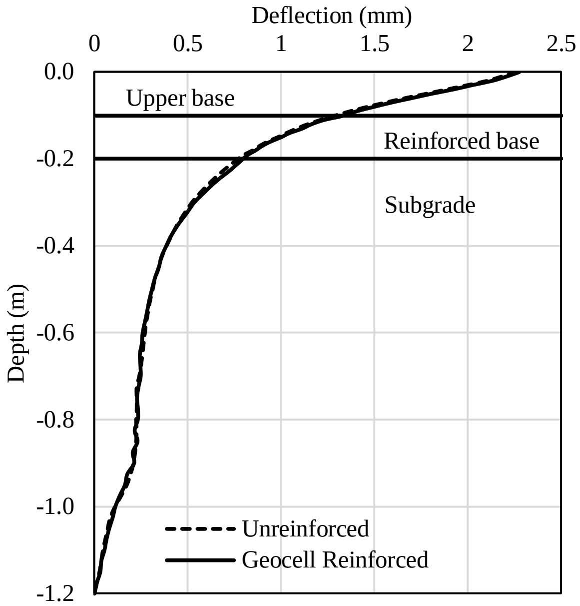

Figure 4: Change in vertical deflection with depth

The plots shown in Figure 5 correspond to the modeling of pavements consisting of Subgrade-1 (12 MPa) and Bases 1-3, ranging from 40 to 80 MPa (refer to Table 3). In these figures, it can be seen that geocell reinforcement reduces the surface deformation when compared to unreinforced sections. Yet, geocell reinforcement impact on surface deformation decreases as the base becomes more rigid. Figure 6 shows the decrease in surface deformation in terms of percent reduction between the unreinforced and reinforced sections with respect to base modulus. As the modulus of the base layer improves, the effect of geocell reinforcement diminishes. The benefit of using a geocell-reinforced base layer was not evident when a good base quality material was used.

5.2 Evaluation of Contact Model

For evaluating the contact model, the 3-D model was reduced to a one-thick element wide model as shown in Figure 7 to better focus on the behavior of the contact and expedite the analysis. Three cells are modelled, separated by the geocell material.

Both contact models were evaluated and compared with respect to the fully bonded model and to unreinforced models, using the base material with E = 120 MPa, ν = 0.33, c = 0, ϕ = 26.8° properties. Load was reduced pressure of 270 kPa, still applied to a 150 mm diameter load, and symmetry conditions were applied on left boundary to account for a half-model. Responses were evaluated the interface, at base mid-layer, on elements adjacent to both sides of the geocell, as indicated in Figure 7.

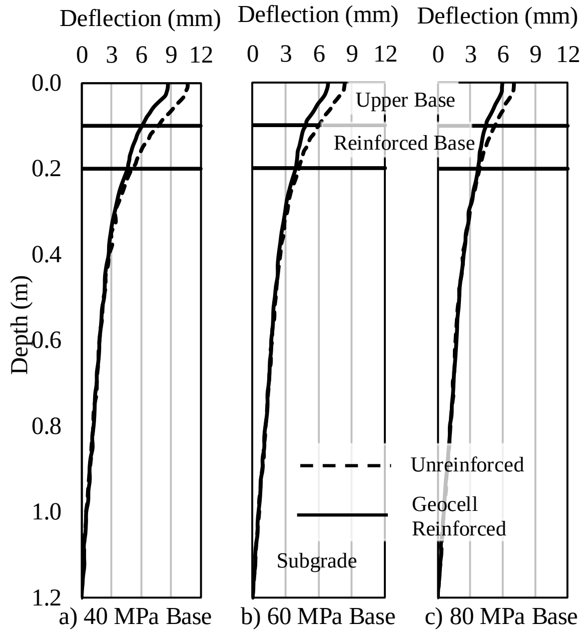

Figure 5: Vertical deflection with respect to depth at peak load of first cycle for a two-layer pavement system consisting of Subgrade-1 (E=12 MPa, ν=0.33, c=10 kN/m^2, ϕ=15°) and different base properties.

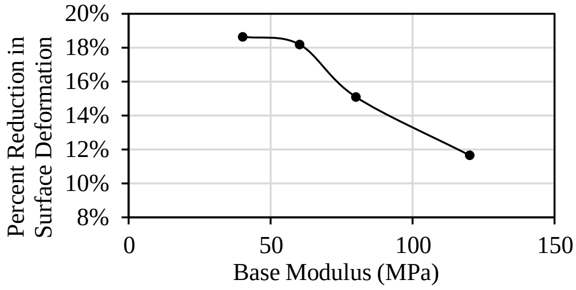

Figure 6: Percentage reduction in surface deformation with respect to base modulus for a pavement with Subgrade-1 (E=12 MPa, c=10 kN/m^2, ϕ=15°) material.

Figure 7: Reduced mesh for evaluation of contact interface.

For the automatic single contact model, it was observed that the model failed to recognize the adjacent base materials appropriately, and consequently, thin shells were replaced by thick shells, as the latter did perform satisfactorily with the contact model. All responses were evaluated, but particular emphasis was placed on the longitudinal stress to quantify reduction in stress transfer through the geocell material and the interface. In Table 3, the results from different cases are shown: (1) a linear elastic model based on the relationships developed by Boussinesq and implemented in BISAR, (2) an FE unreinforced model using FHWA soil model for the base material, (3) an unreinforced model with automatic surface to surface contact model to account for soil interaction, (4) a geocell-reinfoced model with fully bonded conditions between geocell and soil, (5) a geocell-reinforced with automatic single surface model to provide contact between geocell (thick shell) and soil, and (6) and (7) an interface defined with springs (beam discrete elements with different properties) to allow interaction between soil and geocell.

Table 3: Reinforced base responses at mid-layer, adjacent to geocell, in terms of longitudinal stress

Contact	Soil Before Geocell	Soil After Geocell
Longitudinal stress σ_x (Pa)		
1. Linear Elastic*	38.6	34.0
2. FHWA Soil*	30.3	30.6
3. Aut. Surf. Contact Soil to Soil*	34.8	33.4
4. Fully Bonded	41.8	41.0
5. Aut. Single Surface**	30.7	29.5
6. Spring: k_n=10 kN/m, k_s=1 kN/m	6.2	6.0
7. Spring: k_n=100 kN/m, k_s=1 kN/m	24.1	24.5

* Unreinforced, ** Thick Shell

Based on the base material responses, among others not included in this paper for brevity, it was found that in the fully bounded model higher stresses developed compared to other models. Though not included in Table 3, contrary to the spring-connected interface, friction values on the automatic single surface model did not have a significant effect on the responses. When connected by means of discrete beams (springs), both thin shell and thick shell elements yielded very similar results, yet when the automatic single surface contact model was used with a thin shell, the stress was not transferred from one cell to the adjacent cell through the geocell, meaning that the search algorithm failed to establish a contact. This problem is overcome by using thick shell instead of thin shell elements (results shown in Table 3). In addition, from the table it can be seen stress varies considerably in models with spring-connected interfaces depending on their normal and shear stiffness values. A drawback on the use of springs lies on the lack of standard laboratory test procedures for determining the normal and shear stiffness for these spring elements.

5.3 Laboratory evaluation of soil-geocell contact

An additional study was developed for evaluating the behavior of the soil-geocell interface. A single geocell performance was monitored during loading. A test was conducted in a 900 mm diameter cylindrical tank. A single geocell was placed on top of a 600 mm thick compacted subgrade and infill materials in the geocell pocket were compacted in three layers. A circular steel plate with 150 mm diameter and 20 mm thickness was placed at the center of the geocell pocket. The vertical load was applied through an MTS load frame and the settlement of plate was recorded. Strain gages were glued at the mid-height of the geocell, around the cell circumference, as shown in the Figure 8. A quarter bridge circuit arrangement was used to connect the strain gauges. Strain was recorded using LMS Scadas Mobile data acquisition system. A repeated load was applied in the middle of the cell as shown in the Figure 8.

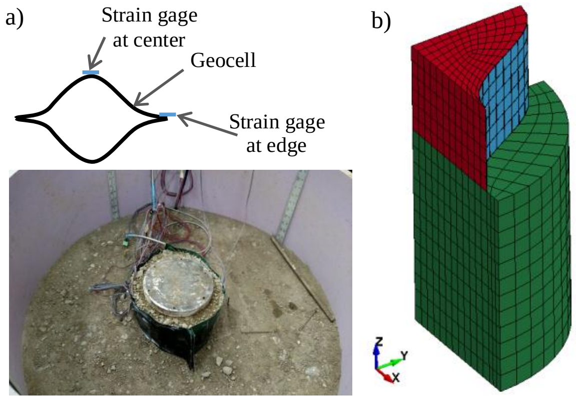

Figure 8: (a) Laboratory setup and (b) its numerical model

As per the laboratory test results, the hoop strains (circumferential strains) were maximum at the center and decreased towards the edge. Though the FEM results for both contact models provided similar results, the hoop strains at the edge of the geocell differed from the laboratory results, when an automatic single surface contact model is used. Hoop strains determined from the numerical model with a soil-geocell interface using discrete beam elements, i.e. 6-DOF spring elements, were closer to laboratory strain gage measurements, at the center and edge of the geocell, and along the perimeter of the geocell, as well. As a result, the results shown in this section are for an FE model using discrete beam elements to provide contact between soil and geocell. Figures 9 and 10 show the hoop strains observed on the edge and the center of geocell, respectively, for 100 cycles, as obtained from laboratory test and FEM. It must be noted that the FE model captured data continuously for every cycle up to the 10th cycle; afterwards, responses are only shown for every 10 cycles.

The measured strains at the edge of geocell observed were in the range of 240 με up to 90 load cycles during loading and increased up to 300 με after 90 cycles. The FEM model generated strains in the range of 100-350 με during loading and 100 με during rest period. The key difference in the results were the elastic strain in the FEM model which were higher in comparison to laboratory results. The difference in responses could be attributed impossibility of achieving zero load during unloading in the lab testing for each cycle and geocell characterized as a perfect elastic material in the FE model. Similar behavior can be observed in the responses at the center of geocell.

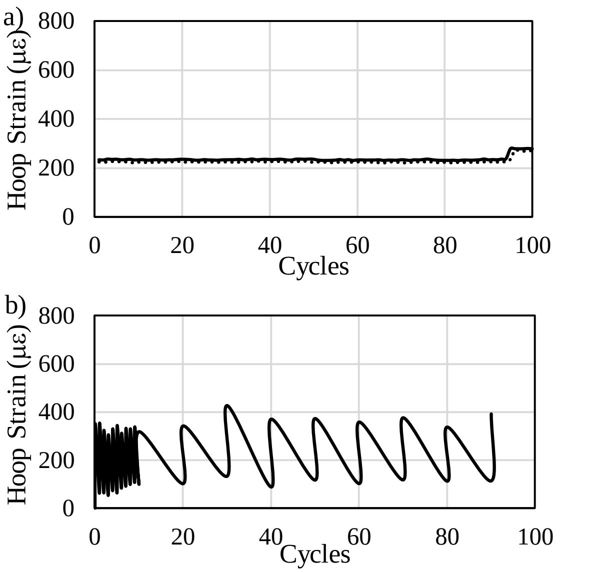

Figure 9: Strains at edge of geocell for a) laboratory b) FEM.

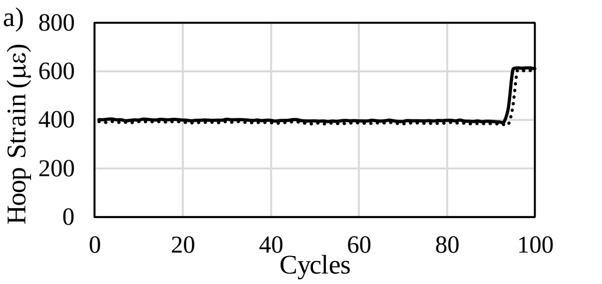

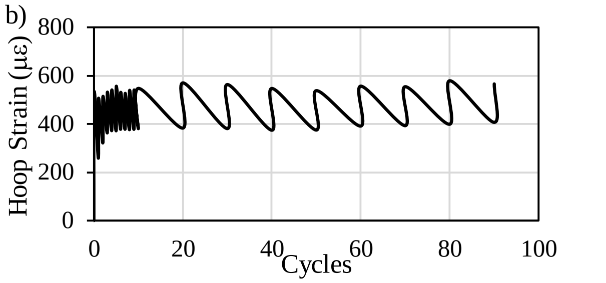

Figure 10: Strains at center of geocell for a) Laboratory, b) FEM.

6. Conclusions

Following conclusions are drawn from this study:

1. Modelling soil elements as a linear elastic shows no difference in the pavement responses for geocell reinforced pavements.
2. FHWA soil model behaves well compared to other material models and can be used for modelling soil.
3. Reinforcing the base layer with geocell reduces the permanent deformation and stresses in the pavements.
4. As the modulus of the base layer improves, the effect of geocell reinforcement diminishes.
5. The benefit of using a geocell-reinforced base layer was not evident when a good base quality material was used for FEM analysis.
6. LS-DYNA automatic contact models were found to be have issues when establishing contact when thin shell element formulations are used. Use of thick shell elements is recommended.
7. Discrete beam elements, simulating 6-DOF springs, were found to better represent the actual behavior of geocell observed in laboratory testing. However, a standard laboratory procedure for determining the normal and shear stiffness is needed.

7. Limitations

In this study, many assumptions were made in most of the FE analyses. For instance, the shape of the geocell was rhomboidal, except when compared to laboratory results, which is a close approximation to the actual shape of the geocell in the field. Additional evaluation of the contact model for modeling the interface between geocell and the infill material with the laboratory testing is still needed.

8. Acknowledgement

The authors like to gratefully acknowledge financial support for this project received from Texas Department of Transportation (TxDOT).

9. References

[1]. Emersleben, A., and Meyer, N., "The use of geocells in road constructions over soft soil: vertical stress and falling weight deflectometer measurements", Proceedings of EuroGeo4 – 4th European Geosynthetics Conference, Edinburgh, Scotland, pp. 7-10, 2008

[2]. Pokharel, S. K., Han, J., Leshchinsky, D., Parsons, R. L., and Halahmi, I., "Behavior of geocell-reinforced granular bases under static and repeated loads", International Foundation Congress & Equipment Expo, pp. 409-416, 2009.

[3]. Han, J., Pokharel, S. K., Yang, X., Manandhar, C., Leshchinsky, D., Halahmi, I., and Parsons, R. L., "Performance of geocell-reinforced RAP bases over weak subgrade under full-scale moving wheel loads", J. of Materials in Civil Eng., Vol. 23, No. 11, pp. 1525-1534, 2011.

[4]. Tanyu, B. F., Aydilek, A. H., Lau, A. W., Edil, T. B., and Benson, C. H., "Laboratory evaluation of geocell-reinforced gravel subbase over poor subgrades", Geosynthetics International, Vol. 20, No. 2, pp. 47-61, 2013.

[5]. Mhaiskar, S. Y., and Mandal, J. N., "Investigations on soft clay subgrade strengthening using geocells", Construction and Building Materials, Vol. 10, No. 4, pp. 281-286, 1996.

[6]. Bathurst, R. J., and Knight, M. A., "Analysis of geocell reinforced-soil covers over large span conduits", Computers and Geotechnics, Vol. 22, No. 3, pp. 205-219, 1998.

[7]. Latha, G. M., Dash, S. K. and Rajagopal, K., "Numerical simulation of the behavior of geocell reinforced sand in foundations." Int. J. of Geomechanics, Vol. 9, No. 4, pp. 143-152, 2009.

[8]. Latha, G. M., and Somwanshi, A, "Effect of reinforcement form on the bearing capacity of square footings on sand." Geotextiles and Geomembranes, Vol. 27, No. 6, pp. 409-422, 2009.

[9]. Han, J., Yang, X., Leshchinsky, D. and Parsons, R., "Behavior of geocell-reinforced sand under a vertical load." Transp. Res. Rec.: J. of the Transp. Res. Board, No. 2045, pp. 95-101, 2008.

[10]. Yang, X. "Numerical analyses of geocell-reinforced granular soils under static and repeated loads", Ph.D. dissertation, The University of Kansas, Lawrence, KS, 2010.

[11]. Evans, M. D., "Geocell mattress effects on embankment settlements", Vertical and Horizontal Deformations of Foundations and Embankments, ASCE, pp. 584-597, 1994.

[12]. Bortz, B., Hossain, M., Accelerated pavement testing of low-volume paved Roads with geocell reinforcement, Final Report FHWA-KS-14-14, Kansas State University Transportation Center, Manhattan, KS, 2015.

[13]. Hallquist, J. O., "LS-DYNA theory manual", Livermore Software Technology Corp., Livermore, CA, 2006.

[14]. Lewis, B. A., Manual for LS-DYNA soil material model 147, Report No. FHWA-HRT-04-095, 2004.

[15]. Klisinski, M., Degradation and plastic deformation of concrete, Ph.D. dissertation, Polish Academy of Sciences, Institute of Fundamental Technology Research (IFTR) Report 38, 1985.

[16]. Mehdipour, I., Ghazavi, M., and Moayed, R. Z., "Numerical study on stability analysis of geocell reinforced slopes by considering the bending effect", Geotextiles and Geomembranes, Vol. 37, pp. 23-34, 2013.

[17]. Hegde, A., and Sitharam, T. G., "Joint strength and wall deformation characteristics of a single-cell geocell subjected to uniaxial compression", Int. J. of Geomechanics, 04014080, 2014.

[18]. Leshchinsky, B., and Ling, H. I., "Numerical modeling of behavior of railway ballasted structure with geocell confinement",

Geotextiles and Geomembranes, Vol. 36, pp. 33-43, 2013.

[19]. Neher, H. P., and Lachler, A., “Numerical modeling of a diaphragm wall production process in Rotterdam compared to monitoring data”, 6th European Conf. on Numerical Methods in Geotechnical Eng., Graz, Austria, pp. 417-22, 2006.

[20]. Latha, G.M., and Rajagopal, K., “Parametric finite element analyses o geocell-supported embankments”, Canadian Geotechnical Journal, 44(8), pp. 917-927, 2007.

SECM/15/076

High performance concrete incorporating fly ash, nano-silica (nano-SiO2) and micro-silica (micro-SiO2)

M. S. T. Priyadarshana[1*], P. B. R. Dissanayake[2]

[1]Holcim Innovation and Application centre, Colombo 3, 00300, Sri Lanka
[2] University of Peradeniya, Peradeniya, 20400, Sri Lanka

*E-Mail: thusharaSL@gmail.com, TP: +94772990680

Abstract: High performance concrete (HPC) exceeds the properties and constructability of normal concrete. Normal and special materials such as fly ash, micro silica and nano silica are used to make these specially designed concretes that must meet a combination of performance requirements. There are many good reasons to view fly ash, micro silica and nano silica as blended materials in concrete. In many cases, concrete made with fly ash, micro silica and nano silica performs better than concrete made without them.

In this paper, an effort was made to evaluate the effect of nano-silica (nano-SiO2), micro-silica (micro-SiO2) and fly ash in improving the properties concrete. Firstly, compressive strength of concrete with different percentage of nano-silica (nano-SiO2), micro-silica (micro-SiO2) and fly ash was studied. Secondly, compressive strength of concrete with Ordinary Portland cement (OPC) and Portland fly ash cement (PPC) was studied. Thirdly, compressive strength of concrete with combination of fly ash and micro silica (micro-SiO2) was studied.

Keywords: fly ash, micro SiO2, nano SiO2, high performance concrete

1. Introduction

Concrete is the second most consumed material after water and it shapes the built environment around the world. According to U. S. geological survey, mineral commodity summaries January 2015, the cement production in the world in 2014 is 4.18 billion metric tons [1]. The concrete production was 25 billion metric tons according to Cement Sustainability Initiative (CSI) report [CSI, 2009] [2]. Fly ash and silica fume can be used as cementious materials to enhance strength and durability properties of concrete [3]. These materials can be added as a last step in cement production or when the concrete is made. In the developed world most cement is made industrially into concrete and sold as ready-mix concrete. On a smaller scale, and more commonly in developing countries, concrete is made in situ on the construction site by individual users. Concrete are defined mainly into different categories; conventional concrete, high-strength/ high-performance concrete and nano-engineered concrete etc.

High-performance concrete (HPC) exceeds the properties and constructability of normal concrete. Supplementary cementitious materials (SCM) such as fly ash and micro silica improve concrete properties mainly in two ways; first it help to generate more Calcium-Silicate-Hydrate (CSH) in the pozzolanic reaction with Ca(OH)2, and second it provide denser concrete due to better particle packing. Finally these concrete would be high strength and durable [4, 5].

American Concrete Institute (ACI) defined high-performance concrete as a concrete meeting special combinations of performance and uniformity requirements that cannot always be achieved routinely using conventional constituents and normal mixing, placing, and curing practice [6]. High performance of concrete is achieved by reducing porosity, in-homogeneity, and micro-cracks in the hydrated cement paste and the transition zone. Consequently, there is a reduction of the thickness of the interfacial transition zone in high-strength concrete. The densification of the interfacial transition zone allows for efficient load transfer between the cement mortar and the coarse aggregate, contributing to the strength of the concrete. For very high-strength concrete where the matrix is extremely dense, a weak aggregate may become the weak link in concrete strength [7, 8]

2. Experimental Program

Chemical compositions of cement and Supplementary Cementing Materials (SCM) were analysed usingX-ray fluorescence (XRF) analyser according to EN 196-2 [11] standard.
Concrete cube specimens of 150mm X 150mm X 150mm were prepared according to BS EN 12390-3standard [12]. These specimens were cast from mix designs as given in tables 1, 2 and 3, Compressive strength of concrete cubes tested at 7 days, 28 days and 60 days for compressive strength. Mix designs of world tallest building (Burj Dubai) [10] was analyzed and four mixes of C80 and C60 were done with local materials and compare performances. Apart from that, high performance concrete C70, C80 and C90 are done with ordinary Portland cement (OPC) and Portland fly ash blended cement (PPC) and compare results.

Table 01: Concrete mixture proportions for compressive strength

Concrete Test	Cement OPC (Kg)	Sand (kg)	Coarse aggregates (kg)	Water (l)	Chemical admixture (ml)*	Fly Ash (Kg)	Micro Silica (Kg)	Nano Silica (Kg)
C1 (OPC)	435.00	774	1026	174	4350			
C2 (OPC+1%mS)	430.65	774	1026	174	4350		4.35	
C3 (OPC+3%mS)	421.95	774	1026	174	4350		13.05	
C4 (OPC+5%mS)	413.25	774	1026	174	4350		21.75	
C5 (OPC+10%mS)	391.50	774	1026	174	4350		43.50	
C6 (OPC+20%mS)	348.00	774	1026	174	4350		87.00	
C7 (OPC+1%nS)	430.65	774	1026	174	4350			4.35
C8 (OPC+3%nS)	421.95	774	1026	174	4350			13.05
C9 (OPC+5%nS)	413.25	774	1026	174	4350			21.75
C10 (OPC+5%FA)	413.25	774	1026	174	4350	21.75		
C11 (OPC+10%FA)	391.50	774	1026	174	4350	43.50		
C12 (OPC+20%FA)	348.00	774	1026	174	4350	87.00		
C13 (OPC+30%FA)	304.50	774	1026	174	4350	130.50		
C14 (OPC+40%FA)	261.00	774	1026	174	4350	174.00		
C15 (OPC+50%FA)	217.50	774	1026	174	4350	217.50		

Table 02: Concrete mixture proportions – G70, G80, G90 concrete with OPC and PCC

Concrete Test	Cement OPC (Kg)	Cement PPC (25%FA) (Kg)	Sand (kg)	Coarse aggregates (kg)	Water (l)	Chemical admixture (ml)*	Fly Ash (Kg)	Micro Silica (Kg)
G70OPC	400		760	900	170	7000	125	20
G80 OPC	420		740	900	170	7500	145	30
G90 OPC	435		740	900	150	7500	145	40
G70PPC		400	760	900	170	7000	125	20
G80 PPC		420	740	900	170	7500	145	30
G90 PPC		435	740	900	150	7500	145	40

*A high range polycarboxilate type super plasticizer, Brand name: Glenium 233

Table 03: Concrete mixture proportions – trials with concrete mixes used in Burj Dubai tower

Concrete Test	Cement OPC (Kg)	Sand (kg)	Coarse aggregates (kg)	Water (l)	Chemical admixture (ml)*	Fly Ash (Kg)	Micro Silica (Kg)
C80 Burj1	380	908	910	132	4200	60	44
C80 Burj2	384	847	865	155	7500	96	48
C80 Burj3	400	830	847	160	7500	100	50
C60 Burj4	376	888	908	169	3000	82	25

*A high range polycarboxilate type super plasticizer, Brand name: Glenium 233

3. Results and discussions

3.1 Chemical composition

Chemical compositions of cement and Supplementary Cementing Materials (SCM)

Table 04: chemical analysis of materials

Material	SiO2 (%)	Al2O3 (%)	Fe2O3 (%)	CaO (%)
cement	20.38	4.79	3.26	64.40
micro silica	98.93	-	0.31	-
fly ash	52.03	32.31	7.04	5.55
Nano silica	99.59	-	0.33	-

According to chemical analysis, it showed that fly ash taken from Norochcholai power plant, can be categories as class F according to general standards. This fly ash low in lime 5.55% (under 15%), and contain a greater combination of silica, alumina and iron 84.34% (greater than 70 percent). Micro silica bought from local supplier has purity of 98.93%. Nano silica bought from Chinese supplier has purity of 99.59%.

3.2 Strength of Concrete

Strength Performance of concrete with fly ash, micro silica and nano silica are shown below.

Table 05: Compressive strength of concrete at 7 days

7Day Comp. Strength (MPa)	1%	3%	5%	10 %	20 %	30 %	40 %	50 %
Nano silica	45.3	44.6	41.4					
Micro silica	48.7	50.1	48.9	52.6	49.3			
Fly ash			46.9	53.0	46.5	40.9	35.3	32.4
Controlled	46.3	46.3	46.3	46.3	46.3	46.3	46.3	46.3

Table 06: Compressive strength of concrete at 28 days

28Day Comp. Strength (MPa)	1%	3%	5%	10 %	20 %	30 %	40 %	50 %
Nano silica	60.8	57.9	54.6					
Micro silica	57.4	62.2	62.1	57.7	54.0			
Fly ash			58.6	61.4	58.6	51.9	50.3	45.5
Controlled	57.7	57.7	57.7	57.7	57.7	57.7	57.7	57.7

Table 07: Compressive strength of concrete at 60 days

60Day Comp. Strength (MPa)	1%	3%	5%	10 %	20 %	30 %	40 %	50 %
Nano silica	61.7	60.7	59.5					
Micro silica	60.2	63.0	63.2	60.4	55.4			
Fly ash			62.7	64.1	62.4	57.8	56.2	54.0
Controlled	59.3	59.3	59.3	59.3	59.3	59.3	59.3	59.3

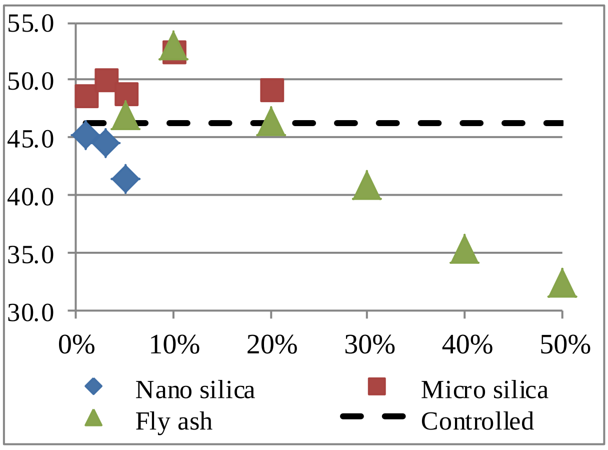

Figure 01: Compressive strength of concrete at 7 days

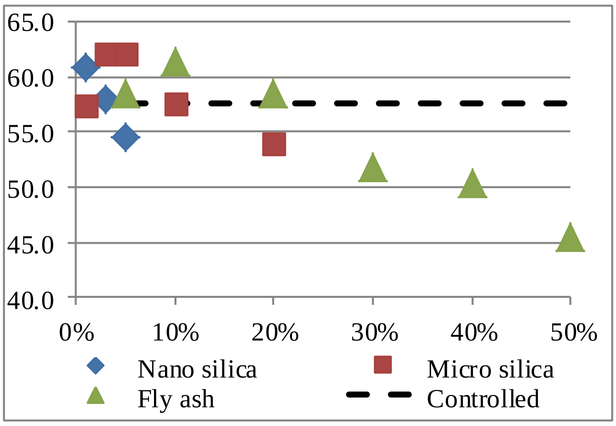

Figure 02: Compressive strength of concrete at 28 days

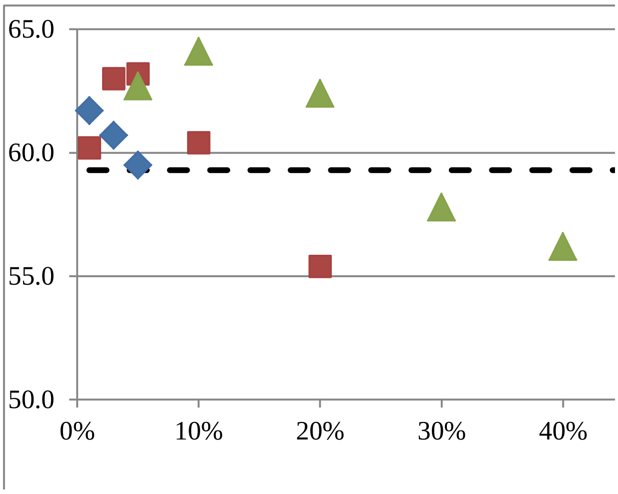

Figure 03: Compressive strength of concrete at 60 days

According to Table 5, 6, 7 and Figure 1, 2, 3, following conclusion can be made; cement can be replaced by fly ash up to 20% - 30% without losing strength of concrete at late ages (60day and 90 days). However, early strength of concrete is affected by fly ash when it uses more than 20%. The best amount of fly ash in concrete would be 10% by considering optimum benefits towards strength. Main benefits of fly ash are workability of concrete mix even at very high percentages. These are really useful for concrete which is to be pumped for longer distances, especially for high rise structures. Main issue with high volume fly ash is to get required strength when increased the amount of fly ash. As the precaution, micro silica is added into system to boost strength with fly ash.

Cement can be easily replaced by micro silica up to 10% without losing strength of concrete at all ages. The best amount of micro silica in concrete would be 3-8%. Main issue when dealing with micro silica is losing workability of concrete mix at higher percentages of micro silica. High range super plasticizers are always recommending using with micro silica.

Cement can be replaced by nano silica up to 5% without losing strength of concrete at late ages (60day and 90 days). However, early strength of concrete is badly affected by nano silica in all cases. The best amount of nano silica in concrete would be 1-3% by considering their cost and optimum benefits. It has been observed by other researchers that the compressive strength of concrete at 7 days and 28 days are maximum with 10% micro silica and 2% nano silica combination and compressive strength of concrete with 2% nano-silica is nearly same as with 5% micro silica

Table 8: Summary of cementitious material used in mix designs of the Burj Dubai Tower

Concrete Grade	Member	Level	Req. flow/ Slump	Req. E-modulus	Cement (Kg)	PFA (Kg)	GGBS (Kg)	Micro Silica (kg)	Total cementitious materials (Kg)
C80	Column & Wall	B2~L40	550±75	43,000 (@90D)	380	60 (12%)		44 (9%)	484
C80	Column & Wall	L41~ L108	600±75	41,000 (@56D)	384	96 (18%)		48 (9%)	528
C80	Column & Wall	L109~L126	650±50	41,000 (@56D)	400	100 (18%)		50 (9%)	550
C60	Column & Wall	L127~L154	650±50	37,600 (@28D)	376	94 (19%)		25 (5%)	495
C50	Beams & Slabs	B2~L108	500±75	-	328	82 (19%)		25 (6%)	435
C50	Beams & Slabs	L109~L154	600±50	-	338	112 (24%)		25 (5%)	475
C35	Blinding	-	125±25	-	300			15 (5%)	315
C50	Internal Column, Wall and Slabs	-	150±25	-	160		240 (57%)	20 (5%)	420
C50	Pile Cap Foundation, Retaining wall, Parking Slab	-	150±25	-	160		240 (57%)	20 (5%)	420
C60	Pile	-	600~750	-	315	105 (23%)		30 (7%)	450

When we analyses mix designs used in world tallest building as shown in Table 8. It can be concluded that optimum amount of cementitous materials are used in all mixes without exceeding the maximum limit defined by most of the standards [9]

This is because concrete mixes having high cement content may give rise to shrinkage, cracking and creep of concrete also increases with the cement paste content. In thick concrete sections restrained against movements, high cement content may give rise to excessive cracking caused by differential thermal stresses due to hydration of cement in young concretes [10, 11]

For high strength concretes, increasing cement content beyond a certain value, of the order of 550 kg/m^3 or so, may not increase the compressive strength.

Always, more than 21% of cement is replaced by other cementitious material (fly ash, GGBS, micro silica). Micro silica is used in all 10 mix designs, 60Kg to 112 Kg (5% to 9%) per cubic meter of concrete. Fly ash is used in 7 mix designs, 15Kg to 50 Kg (12% to 24%) per cubic meter of concrete**.** It is clear that, adding fly ash and micro silica become essential when high strength/ high performance concrete are designed.

Table 9: Results of trail mix (Burj Dubai mix designs with local materials)

Sample Ref.	Compressive Strength (MPa)		
	1D	7D	28D
C80 Burj1	27.7	62.3	81.7
C80 Burj2	39.3	68.4	83.0
C80 Burj3	38.0	72.1	93.0
C60 Burj4	22.6	47.4	62.3

As shown in the Table 9, it can be concluded that it is not difficult to achieve high strength concrete performance with local raw materials to get strength requirements for high rise building in Sri Lanka. Mix designs related to above 4 mixes can be found in Table 2. 28 days of strength of mixes C80 Burj1, 2 and 3 are above grade 80 and full fill requirements. 28 days of strength of mix C80 Burj4 is above grade 60 and full fill requirements.

Table 10 and Figure 4 witnessed that high strength concrete (G70, G80, G90) with OPC and PPC has almost similar strength at 28 days (only 1~3% different. However, early strength of concrete with fly ash blended cement tend to be considerably low as 10~13%. So, structures with early strength is not significant, it is always recommend to go for fly ash blended cement for better performance knowing that other workability and durability benefits given by the fly ash.

Table 10: Results of trail mix with G70, G80, G90 concrete with OPC and PCC

Sample Ref.	Compressive Strength (MPa)		
	1D	7D	28D
G70 (OPC)	41.2	71.2	85.6
G80 (OPC)	43.6	79.5	87.2
G90 (OPC)	46.8	84.8	105.7
G70 PPC (25% FA)	37.2	68.2	83
G80 PPC (25% FA)	38	77.2	86.2
G90 PPC (25% FA)	42.1	82.3	103.4

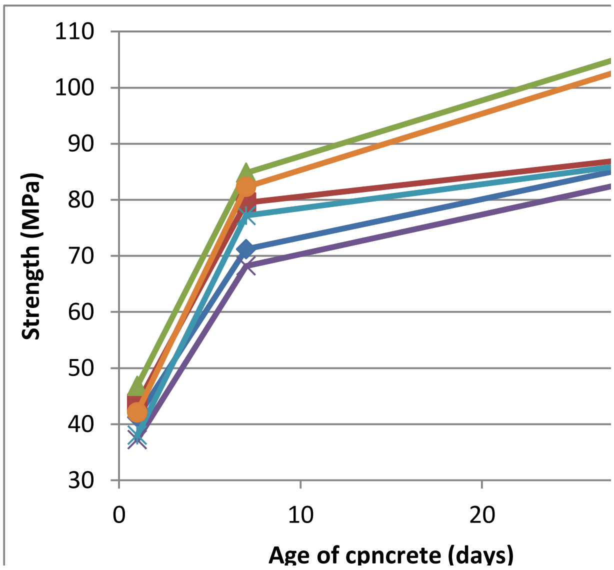

Figure 04: Compressive strength of concrete at 60 days

4. Conclusions

Test results obtained in this study indicate that up to 5% nano silica, 10% of micro silica, 20%-30% fly ash and 5% bottom ash could be advantageously blended with cement without adversely affecting the strength. However, optimum levels of these materials are 1-3% nano silica, 3-8% of micro silica, 10% fly ash and 5% of bottom ash.

Further, a higher amount of fly ash can be used in concrete if a turnery blend like nano silica or micro silica is added into the system. As an example a mix design of world tallest building (Burj Dubai), the fly ash percentage in Grade 80 concrete used for columns and walls level 109~126 were high as 100Kg (18%) with 50 Kg (9%) of micro silica, the usage of cement in this mix design was as low as 400Kg, and other materials sand 830 kg, coarse aggregates (10mm) 847 Kg, admixtures 3% and water: binder ratio was 0.3

In Sri Lanka, in most of the projects fly ash are used in the range of 20-25%. Micro silica with fly ash is used in most of the high rise building projects in the world to get higher strength and extended durability. Micro silica used in all the concrete mix designs of world tallest building, Burj Khalifa in Dubai, it is from 5% to 9% by weight. Fly ash used in all the concrete mix designs of world tallest building, Burj Khalifa in Dubai, it is from 12% to 24% by weight.

It is always recommend optimizing mix designs either with blended cement, cement replacement materials such as fly ash (with or without micro silica) to get highest performance with the concrete. There will always be a better option with blended cement or blended materials with ordinary Portland cement.

Acknowledgement

Authors acknowledge the assistance of Holcim (Lanka) Limited for its financial support, supply of materials and testing facilities at Holcim Innovation and Application Centre.

References

[1] S. Jewell, S. Kimball, Mineral commodity summaries 2015, U. S. Department of Interior, U. S. Geological survey

[2] The Cement Sustainability Initiative ACI 2009, World Business Council for Sustainable Development, E-mail: washington@wbcsd.org

[3] Chapter 3; Fly Ash, Slag, Silica Fume, and Natural Pozzolans retrieved from http://www.ce.memphis.edu/1101/notes/concrete/PCA_manual/Chap03.pdf

[4] Michael Thomas, Ph.D., P.Eng., Professor of Civil Engineering, University of New Brunswick, Optimizing the Use of Fly Ash in Concrete, Portland Cement Association (PCA)

[5] ASTM C618 - 12a, Standard Specification for Coal Fly Ash and Raw or Calcined Natural Pozzolan for Use in Concrete

[6] ACI Committee 232, Use of Fly Ash in Concrete, ACI 232.2R96, American Concrete Institute, Farmington Hills, 1996, PP 1-34.

[7] Portland cement association, Cement and Concrete Basics, Supplementary Cementing Materials, retrieved from http://www.cement.org/basics/concretebasics_supplementary.asp

[8] Mindess, Sidney; Young, J. Francis; Darwin, David., Concrete (2nd edition), 2003.

[9] Summary of concrete mix design for Burj Dubai Tower, retrieved from http://dubai-tower.blogspot.com/2008/08/summary-of-concrete-mix-design-for-burj.htm

[10] EN 196-2 2005, methods of testing Cement – Part 6: Chemical analysis of cement, European Standard, PP 1-24. March 2005.

[11] BS EN 12390-3: 2009, Testing hardened concrete. Compressive strength of test specimens

SECM/15/085

Geopolymer as well cement and its mechanical behaviour with curing temperature

S. Kajarathan[1], S. Karthikan[2] and M.C.M Nasvi [3*]
[1, 2, 3] University of Peradeniya, Peradeniya, Srilanka
*Email: nasvimcm85@gmail.com T: +94766007240

Abstract: Carbon capture and storage (CCS) technique is found as a best solution to reduce the emission of CO_2 to the atmosphere. In this technique, the CO_2 emitted from large industries is captured, and pressurized, and finally injected into deep underground reservoirs. In a geological sequestration project, integrity of injection well play an important role. It means the well cement is a key factor that affects the well integrity. In typical injection wells, Ordinary Portland cement (OPC) based cement is used as well cement and it has been found that it undergoes degradation in CO_2 rich environment. Geopolymer can be a good alternative to existing OPC based well cement as it has been found that geopolymer possess high strength and durability compared to OPC. Geopolymer is a binder produced through the process called geopolymerization of alumino- silicate materials and alkaline activators. In the sequestration wells, well cement is exposed to different curing temperatures with a geothermal gradient of 30°C/km. Therefore, it is important to study the mechanical behaviour of well cement with curing temperatures expected deep under the ground. Therefore, this research aims to study geopolymer as well cement and its mechanical behaviour at different curing temperatures (25, 40, 50, 60, 70, 80 °C). In addition, effect of ageing on the mechanical behaviour was also studied. The OPC samples were tested for the comparison of results with geopolymer. The results showed that the optimal curing temperature for higher strength of geopolymer and OPC are 60 °C and 50 °C respectively. Geopolymer possess highest strength at elevated temperatures whereas OPC possess higher strength at ambient temperatures. Moreover, at elevated temperature curing, geopolymer develops ultimate strength within short curing period and it does not gain significant strength with further ageing.

Keywords: CO_2 sequestration, geopolymer, greenhouse gases, well cement

1. Introduction

Emission of greenhouse gases is a major problem in the world. Of all greenhouse gases, CO_2 is responsible for 64% of the greenhouse gas effects [1]. There are so many ways to reduce the emission of greenhouse gases; such as minimizing fossil fuel consumption in industries and vehicles, increasing the energy conversion efficiency of fossil fuels, switching energy sources in to renewable energy sources such as wind energy, wave energy and solar radiation and capturing and storing carbon dioxide in deep under the ground [1, 2]. Of all the proposed methods, carbon capture and storage (CCS) technique is found as a good solution to reduce CO_2 emission to atmosphere [3].

The lifetime of CCS projects depends on many factors and within these well integrity plays an important role. Well cement is the major factor that affects well integrity and, in the injection wells, Ordinary Portland Cement (OPC) based cement (class G, H) is used as well cement. According to previous studies [4, 5], OPC undergoes degradation in CO_2 rich environment due to the reaction with dissolved CO_2 in brine. Kutchko et al [4], found that when OPC based well cement exposed to a CO_2 rich environment, it undergoes carbonation followed by cement degradation. Three distinct zones were identified in degraded cement, the outer most zone was fully changed as calcium bicarbonate and that is an easily solluable substance. The second zone is calcium carbonate which was the results of the reaction between $Ca(OH)_2$ and dissolved CO_2 and the third zone is unaltered cement. In addition, various other researchers [5, 6, 7] have also found that OPC based well cement experiences degradation exposed to CO_2 rich environment.

This paper examines geopolymer as well cement since, geopolymer possess high strength, excellent acid resistance characteristics and high durability [8, 9]. Davidovits, [10] proposed that an alkaline liquid could be used to react with the silicon (Si) and the aluminium (Al) in a source material of geological origin or in by-product materials such as fly ash and rice husk ash to produce binders and he termed these binders as geopolymers. Any alumino-silicate material can be used as raw material to produce geopolymer binder. When the alumino-silicate materials mixed with alkaline agent and the polymerization process will initiate. A generalized formula for geopolymer is as follows:

$$M_n [-(SiO_2)_z - AlO_2]_n .w H_2O$$

where z is 1, 2 or 3; M is an alkali cation, such as potassium or sodium, and n is the degree of polymerization [10, 11].

There are many advantages by using geopolymer in construction of injection wells compared to OPC. The manufacture of geopolymer emits 90 % less CO_2 and consumes 50 % less energy compared to OPC [12]. Furthermore the geopolymer concrete manufacture costs 10-30 % less than that of OPC concrete [13].

A typical underground well is constructed from ground level to the required depth depends on the injection reservoir level and it may vary from 800 m to 2 km. As the temperature is varying with depth with a geothermal gradient of 30 °C/ km [2], the well cement is exposed to different temperatures varying up to approximately 80 °C. Therefore variation of mechanical behaviour of geopolymer at different down-hole temperature conditions need to be studied in order to predict the behaviour of geopolymer cement during the life time in the down-hole conditions. This paper investigate geopolymer as well cement and its mechanical behaviour with curing temperature from ambient level (27 °C) to 80 °C. Testings such as X-Ray Diffraction analysis (XRD), Uniaxial Compressive Strength (UCS) and Scanning Electron Microscope (SEM) analysis were conducted to study the behaviour of well cement at different temperature conditions.

2. Materials and Methodology

To date most of the researches on geopolymer concrete was done with geopolymer paste with aggregates and also for elevated temperature curing to study fire resistance properties. In this research, geopolymer paste was used instead of concrete as the annular space in typical well is between 30- 80 mm. in addition, the sole purpose of well cement is to provide zonal isolation (low permeability) and required mechanical strength. Hence, cement paste is used in wells instead of mortar or concrete.

2.1 Materials

Geopolymer paste samples was prepared using fly ash as the alumino-silicate material and combination of NaOH and Na_2SiO_3 as alkaline activator. The ASTM class F fly ash (low calcium) which is produced at Nuraichcholai coal power plant, Puttalam, Sri Lanka, was obtained from Holcim Lanka (Pvt) ltd. 8 M NaOH solution was mixed with Na_2SiO_3 with a ratio of Na_2SiO_3 to NaOH of 2.5 to obtain higher strength [14]. The ratio of alkaline activator to fly ash used was 0.4 for all the mix design. In addition, sulphate resistant OPC samples was tested to compare the results. Sulphate resistance OPC was obtained from Holcim Lanka (Pvt) Ltd. For the mix of OPC samples, a w/c ratio of 0.44 was used as it is found to be the optimum to achieve higher strength [15].

The mix compositions of fly ash and OPC was obtained from X-Ray Diffraction (XRD) test and the results are shown in Table 1.

Table 1: Compositions of fly ash and OPC

Constituents	Percentage (%)	
	Fly ash	OPC
SiO_2	52.03	20.38
Al_2O_3	32.31	4.79
Fe_2O_3	7.04	3.26
CaO	5.55	64.4
Mgo	1.3	0.98
SO_3	0.07	2.21
K_2O	0.68	0.04
Cl	1	0.01

2.2 Sample preparation and experimental methodology

Geopolymer paste was prepared by mixing fly ash with alkaline activator in above proportions. The NaOH pellets was mixed with distilled water to prepare 8 M NaOH solution. This was mixed with Na_2SiO_3 with above proportions and the alkaline activator was prepared. PVC pipes with 50 mm diameter were cut into 100 mm height pieces to make the casting moulds. These cylindrical moulds were fixed on plywood vertically and the connections were sealed by silicon paste. Figure 1 shows the casting moulds used to cast the samples. Fly ash was mixed with alkali solution using a mechanical concrete mixture for 3 minutes and the mixture was poured in to the prepared mould in three layers. Then the samples was placed on the vibrating table for 2 minutes in order to remove

Figure 1: PVC moulds used to caste cement samples

This work includes two types of curing to study the effect of curing temperature and ageing time. To study the effect of curing temperature all the samples were cured at different curing temperatures (27- 80 °C) for 48 hours and then they were allowed to cool at room temperature (RT) for another 24 hours before testing. Based on this test, optimum temperature for high strength

any air voids present in the sample. Then the top of the mould was covered with polythene in order to avoid the moisture loss.

was observed. Effect of ageing was studied by exposing samples to two different temperatures (27 °C and the optimum temperature) for prolong curing periods of 2, 7, 14, 28 and 45 days.

After curing both side of the samples was grinded using by the mechanical grinding wheel and capped with sulphur capping. Figure 2 shows the samples prepared for testing.

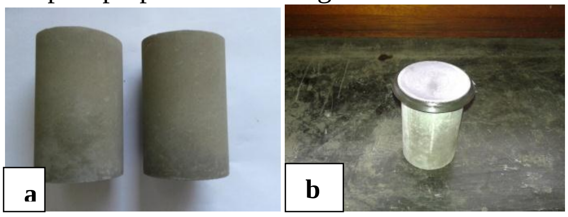

Figure 2: (a) Oven cured geopolymer samples, (b) sulphur capped sample

UCS test was conducted on the samples with a stress controlled loading rate of 0.2 MPa/ s. Schematic view of the UCS testing set-up used is shown in Figure 3. A total number of 32 samples of geopolymer cement and 32 samples of OPC were tested in this research. For each data point, two samples were tested to ensure reproducibility.

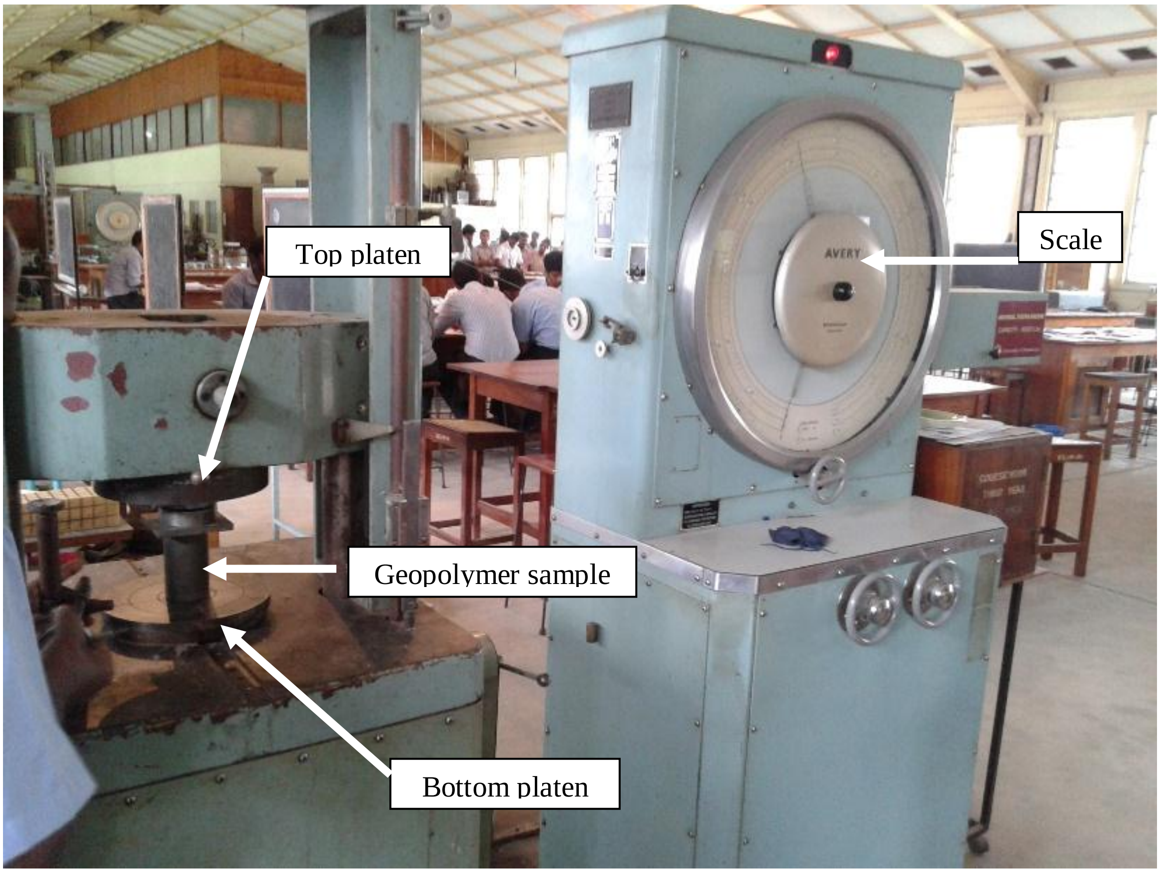

Figure 3: schematic view of UCS testing machine

To study the microstructural behaviour of geopolymer cement with temperature variations and the curing duration, SEM analysis was performed. The geopolymer samples was crushed and samples of approximately 1 mm^3 was mounted on the test plate in the machine. The samples was coated with Au (gold) to make the sample conductive. Magnification factor up to × 25000 can be used in this machine. Figure 4 shows the SEM testing machine

Figure 4: SEM testing machine used

3. Results and Discussions

3.1 Effect of curing temperature

Well cement is exposed to different temperature conditions (from ambient level to 80 ºC). Therefore, the failure stress of geopolymer paste and OPC motar was tested at different curing temperature for 48 hours of curing. Figure 5 shows the strength variation with curing temperature for both geopolymer and OPC.

According to Figure 5, at room temperature, the strength of the geopolymer is considerably low and it is because of the poor rate of geopolymerization process. The rate of geopolymerization is high at elevated temperatures [8, 9]. The optimum temperature for high strength for geopolymer and OPC are approximately 60 and 50 °C respectively. Geopolymer gains strength with curing temperature as Si and Al from the source material readily dissolves with the increase in curing temperature up to 60 ºC. After that the strength decreases with the temperature. However, some of the researches [14, 16] found that the optimum strength is between 70- 80 ºC. The optimum temperature may vary depends on the source of fly ash, type of curing, sample compositions and the mix compositions [14].

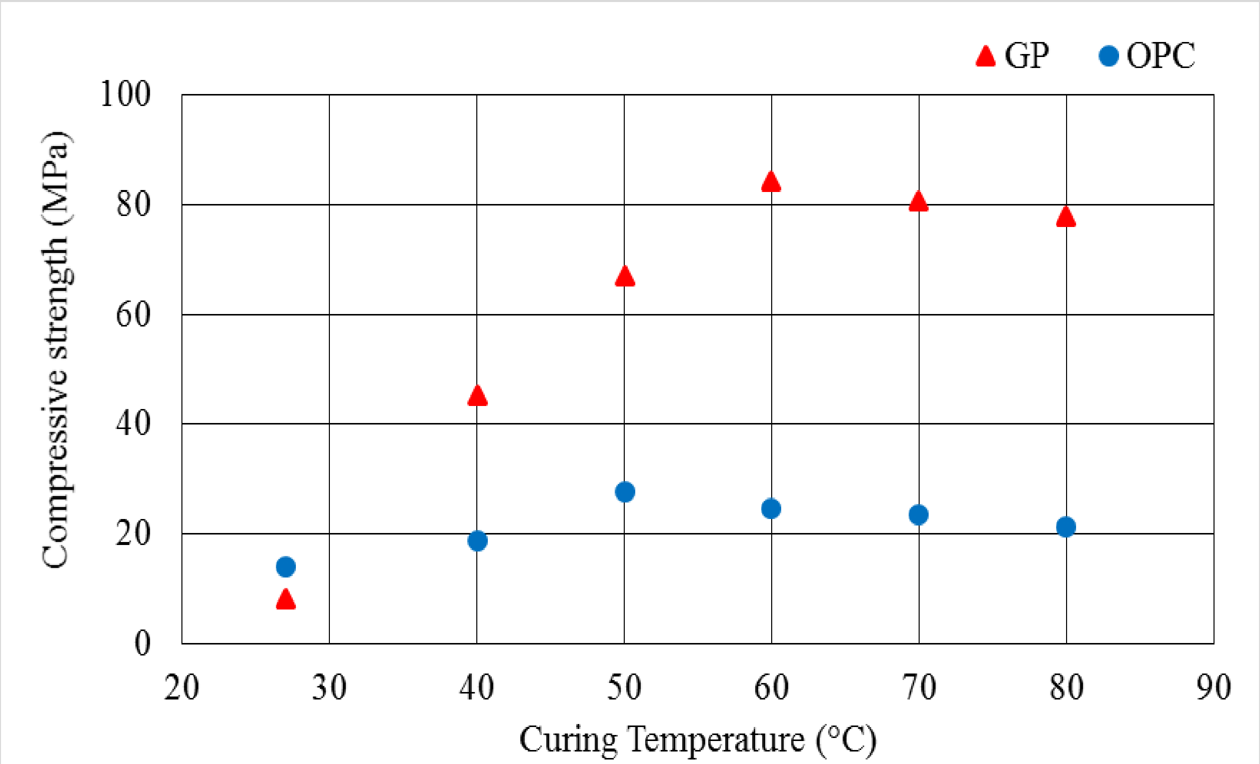

Figure 5: Variation of UCS with curing temperature for geopolymer and OPC

For geopolymer, strength is decreasing beyond 60 °C. This may be due to the weakening of microstructure at elevated temperatures or the formation of micro cracks [9]. For the geopolymerization process presence of moisture also important and at higher temperatures moisture might be vaporized and because of that strength reduction may occur. According to Figure 5, strength of the OPC is increasing with curing temperature up to 50 ºC and after that the strength decreases. The increase of strength is because of the rate of hydration increases with the temperature increment. The optimum temperature is 50 ° C, and however optimum temperature vary with the w/c ratio and the type of OPC [17].

When the behaviour of OPC and geopolymer is compared, it can be seen that at room temperature conditions, OPC has higher strength compared to geopolymer. This is because of the poor geopolymerization rate for geopolymer at room temperature. On the other hand, at elevated temperatures, geopolymer possesses high strength compared to OPC. Rate of strength increment of geopolymer from room temperature to optimum temperature (60 °C) is 90 % while the rate of increment of OPC is 49 %. The increment rate is much high for geopolymer than OPC. However, the reduction rate is low to geopolymer compared to OPC. The rate of strength reduction beyond the optimum temperature is 8 % for geopolymer while it is 23 % for OPC. Based on this, it can be concluded that the geopolymer cement is suitable for the constructions where the down-hole temperature conditions is above 40 °C.

Figure 6 shows the variation of Young's modulus with curing temperature for geopolymer and OPC. The variation of young's modulus also follow the same pattern as variation of strength. At the higher temperatures, the geopolymer is stiffer than OPC whereas at lower temperatures OPC is stiffer than geopolymer cement.

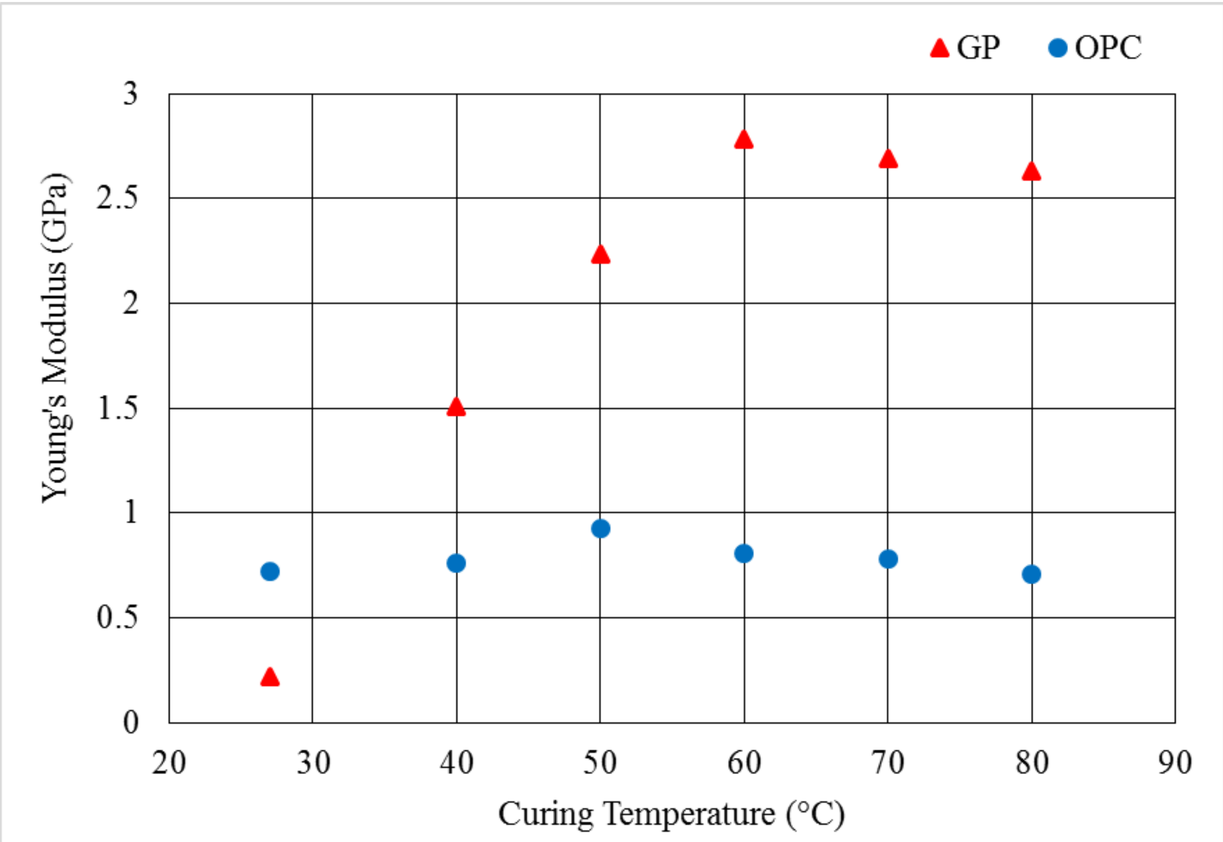

Figure 6: Variation of Young's modulus with curing temperature

3.2: Effect of ageing

To study the effect of ageing, OPC and geopolymer samples were cured at room temperature and optimum temperature (60 °C) for different curing periods. Figure 7 shows the variation of UCS of OPC and geopolymer with the ageing.

According to Figure 7, UCS of geopolymer and OPC increases with the ageing time. This is because of the geopolymerization process of geopolymer and hydration process of OPC with ageing. The strength gaining of the geopolymer cured at room temperature is higher than that of OPC cured at same conditions. At room temperature curing the rate of strength increment of geopolymer in 2- 45 days is 92 % while that for OPC is 63 %. This shows that even at low temperatures geopolymer develops higher strength compared to OPC.

For geopolymer cured at 60 °C, the rate of increment in strength is low compared to the samples cured at room temperature. For geopolymer, the geopolymerization process is almost finished within 48 hours of curing for elevated temperature. Hence, geopolymer will not develop significant strength increment with further ageing when cured at elevated temperatures**.** In OPC, the hydration process is also faster at elevated temperatures and because of that the strength is gained within short period of curing time (48 hrs) [Figure 5]. Due to that the strength increment rate is low for OPC cured at 60 °C than room temperature cured samples. At elevated temperature curing, the rate of strength increment of geopolymer is 8% while that for OPC is 22%.

3.3 SEM analysis

Micrographs of fly ash based geopolymer were obtained using a ZEISS field-emission scanning electron microscope (FESEM) operated at 20 kV. Magnification factors were changed from 500 to 3000. Figure 8 shows the SEM images of fly ash and geopolymer samples cured at different conditions. In Fig 8 (b) and (c), the grey coloured spherical particles (X) are unreacted fly ash particles and more unreacted particles can be seen at low temperature cured samples. This is due to poor rate of geopolymerization. Based on this, it can be concluded that the rate of geopolymerization is high at elevated temperature.

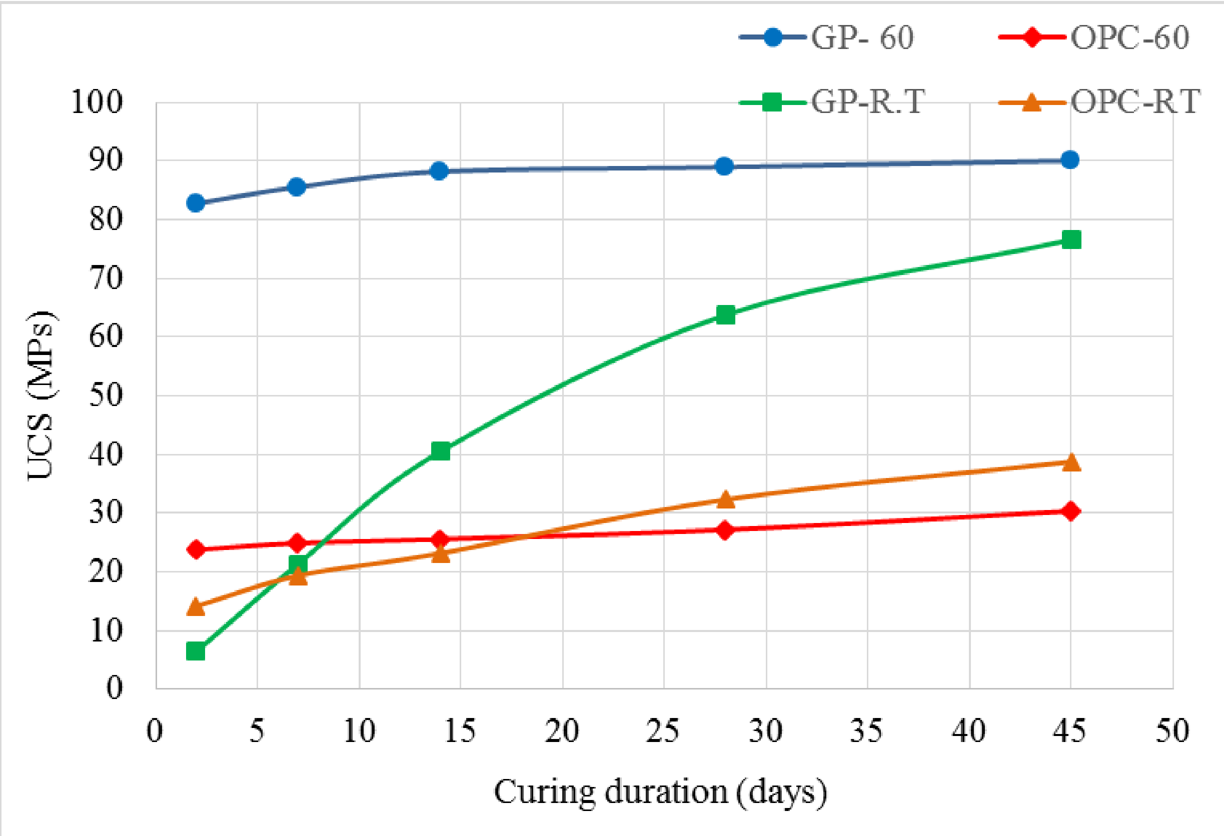

Figure 7: Variation of UCS with ageing for both geopolymer and OPC

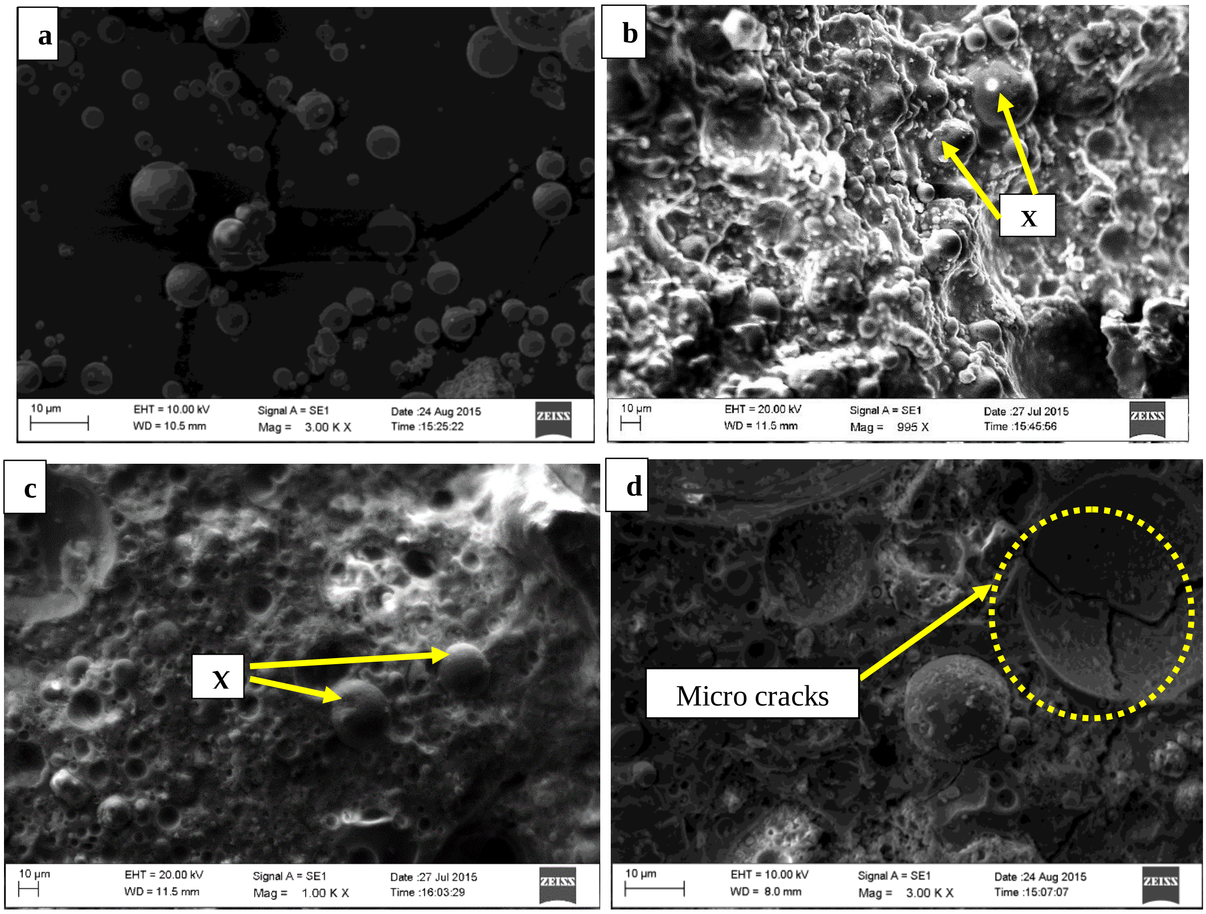

Figure 8: SEM images of (a) fly ash particles (a), geopolymer cured at (b) RT, (c) 60 ºC and (d) 80 ºC

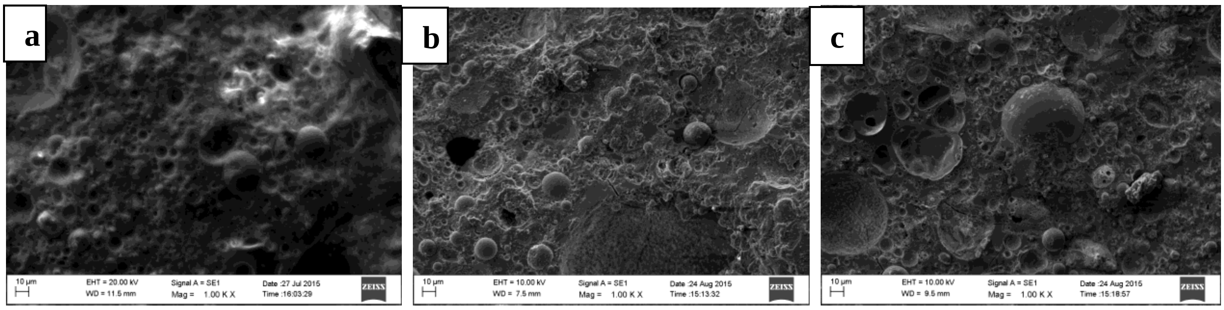

Figure 9: SEM images of geopolymer samples cured at 60 ºC for (a) 2 days, (b) 7 days, (c) 14 days

Figure 8 clearly shows that the different geopolymerization rate between samples cured at R.T and 60 ºC. But there is no significant variation of unreacted particles between samples cured at 60 ºC and 80 ºC. Based on this, it can be concluded that the strength reduction beyond 60 ºC is not due to the variation in rate of geopolymerization. In Figure 8 (d), some micro-cracks can be observed. Hence, it can be concluded that the strength reduction beyond 60 ºC is due to the formation of micro-cracks at elevated temperatures.

Figure 9 shows the SEM images of geopolymer cured at 60 ºC for different durations. There is no much difference in the unreacted particles between samples cured at 60 ºC for 2, 7, and 14 days. Based on this it is concluded that for elevated temperature curing there is no significant strength gain with ageing.

4. Conclusions

Present study focused on geopolymer as well cement and its mechanical behaviour with curing temperature as typical wellbore is subjected to a range of curing temperatures with the depth. OPC was used for the comparison of results. The following conclusions are drawn based on the outcomes of this research.

1. The optimum curing temperature for fly ash based geopolymer is 60 °C and there is no

considerable strength gain after optimum temperature.
2. UCS and Young's modulus of geopolymer increases with curing temperature up to 60 °C and beyond that it decreases.
3. The optimum curing temperature for OPC based well cement is 50 °C and beyond the optimum temperature strength decreases.
4. At lower curing temperatures (below 40 °C), OPC possess higher strength than geopolymer, whereas at elevated temperatures geopolymer possess higher strength.
5. At low temperature curing, both OPC and geopolymer develop strength with ageing and the rate of strength gaining is high for geopolymer compared to OPC.
6. At elevated temperatures, the geopolymer develop its ultimate strength within a short period of curing (48 hours) and it does not develop significant strength increment with further ageing.
7. On the whole, geopolymer is suitable for temperature of above 40 ºC, whereas OPC can be used at shallow depths where temperature is low (< 40 ºC).

Acknowledgement

The present research was funded by Tokyo cement (Pvt) Ltd and authors would like to thank them. In addition, we are indebted to Holcim Lanka (Pvt) Ltd for giving us sulphate resistant cement and fly ash. Finally, we would like to thank Department Of Civil Engineering, University Of Peradeniya for giving opportunity to perform this research work.

References

1. Bruant R, Guswa A, Celia M, Peters C, Safe storage of CO_2 in deep saline aquifers. Environmental science & technology, 2002, 36**:**240a- 245a.
2. Perera MSA, Ranjith P, Choi S, Bouazza A, Kodikara J, Airey D, A review of coal properties pertinent to carbon dioxide sequestration in coal seams: with special reference to victorian brown coals. Environmental earth sciences**,** 2011, 64: 223-235.
3. Benso S, Cook P, Anderson J, Underground geological storage. Ipcc special report on carbon dioxide capture and storage, 2005, 195-276.
4. Kutchko B, Strazisar BR, Dzombak DA, Lowry GV, and Thaulow N, Degradation of wellbore cement by CO2 under geologic sequestration conditions, Environmental science and technology, 2007, 41: 4787–4792.
5. Luke C, Deasy H, Lupton N, Integrity of Wellbore Cement in CO_2 Storage Wells State of the Art Review. Australian National Low Emissions Coal Research & Development Project, 2012, 3:1110-0084.
6. Brandvoll O, Regnault O , Munz IA, Iden IK ,Johansen H, Fluid – solid interactions related to subsurface storage of CO_2 Experimental tests of well cement. Energy Procedia, 2009, 17: 3367–3374.
7. Arina B, Sonny I, Effects of pressure and temperature on well cement degradation by supercritical CO_2. International Journal of Engineering and Technology, 2010, 10: 980-988.
8. Hardjito D, Wallah S, Sumajouw D,Rangan B, Introducing fly ash-based geopolymer concrete manufacture and engineering properties, 30th conference on our world in concrete and structures, august, Singapore, 2005, 271- 278.
9. Nasvi MCM, Ranjith PG, Sanjayan J, Geopolymer as well cement and variation of its mechanical behaviour with curing temperature, Greenhouse gases, science and technology, 2011, 1: 1-13.
10. Davidovits J, Properties of Geopolymer Cements, First International Conference on Alkaline Cements and Concretes, 1994, 131-149.
11. Van Jaarsveld J. Van Deventer J, Lorenzen L, The potential use of geopolymeric materials to immobilise toxic metals: part 1. Theory and applications Minerals engineering, 1997, 10**:** 659-669.
12. Hewayde E, Nehdi M, Allouche E and Nakhla G, Effect of geopolymer cement on microstructure, compressive strength and sulphuric acid resistance of concrete. Mag Concrete Research, 2006, 58(5):321–331.
13. Lloyd N and Rangan B, Geopolymer Concrete with Fly Ash, Second International Conference on Sustainable Construction Materials and Technologies, Ancona, Italy, 2010, 3:1493–1504.
14. Abdullah M.M.A., H. Kamarudin, H. Mohammed, I. Khairul Nizar A. R.Rafiza, and Y. Zarina, The relationship of NaOH Molarity, Na_2SiO_3/NaOH Ratio, Fly Ash/Alkaline Activator Ratio, and Curing Temperature to the Strength of Fly Ash-Based Geopolymer. Advanced Materials Research, 2011, 1475-1482.
15. Lecolier E, Rivereau A, Le Saout G, Audibert-Hayet A, Durability of hardened Portland cement paste used for oil well cementing. Oil & gas science and technology, 2007, 62**:** 335-345.
16. Thakur RN and Ghosh S, Effect of mix composition on compressive strength and microstructure of fly ash based geopolymer composites. ARPN Journal of Engineering and Applied Sciences, 2006, 4(4):68–74.
17. Runar N, Well Design and Well Integrity. Wabamun area co_2 sequestration project, 2010.

SECM/15/90

Development of a capping material for an Engineered Landfill in Wet zone of Sri Lanka

Niruthshanan P.[1]*, Loganathan F.D.[2], Premarathne H.M.W.A.P.[3], Kurukulasuriya L.C.[4]
[1,2,3,4]Department of Civil Engineering, University of Peradeniya, Sri Lanka
*E-Mail:niruth.paransothy1991@gmail.com TP: +94752858952

Abstract: Capillary Barriers (CB) which consist of coarse sand overlain by a low permeable fine soil are low cost alternatives used in capping system for controlling the infiltration in a Landfill. In wet region, the durability of capping layer is questionable as due to high precipitation, capillary effect can reduce making the layer highly permeable. A potential solution is to alter the soil grains by mixing with a Hydrophobic Agent (HA) such as Oleic Acid (OA), so that the water repellent characteristics are introduced into the sand layer.

In this study, the hydrophobicity (water repellency) of CBs containing coarse sand mixed with OA was investigated. Hydrophobicity was evaluated by measuring the time taken for a water droplet to penetrate the surface of a compacted sand sample which is identified as the Water Drop Penetration Time (WDPT). Initially, dry coarse sand particles were hydrophobized by mixing-in coating method with different OA contents. In addition, the effect of moisture content of coarse sand particles on its hydrophobicity was also studied. The results show that WDPT for dry samples increased sharply with increasing HA content and reached a peak value of 4080 s at $3gkg^{-1}$ of sand and thereafter decreased. Irrespective of the OA content, an increase in moisture content decreased the water repellency. However, this decrease is less significant for the optimum value of OA content of $3gkg^{-1}$ within the range of moisture content tested. The impact of the slope angle on the water repellancy was also investigated by increasing the slope upto 1V:3H. Results showed a decrease in water repellency when the slope angle was increased. It was observed that water drop was spreading due to the effect of weight acting along the slope and as a result the WDPT time decreased due to less surface tension.

Keywords: Capillary Barrier, Capping material, Water Repellence

1. Introduction

An engineered landfill allows final disposal of solid waste to be placed in a secure manner by minimizing the impact on the environment. Once the final capacity is attained the closure of the landfill is done by installing a cover which functions in minimizing the infiltration and assisting in gas emissions. In this respect, although the modern techniques using geosynthetics are available, the developing countries like Sri Lanka cannot afford to use them as they are an imported material. Therefore, this study investigates the effectiveness of using locally available materials.

Capillary barriers consisting of a layer of fine grains underlain by a layer of coarse grains are commonly used. Since the wet zone has a heavy precipitation, application of such capillary barriers may not be effective. To overcome this problem coarse particle are mixed with a Hydrophobic Agent (HA) to introduce water repellence properties which results in less infiltration of water into the underlying waste (Subedi et al, 2012,[1]). In this study, Oleic acid (OA) is considered as the HA and its optimum content to be mixed with the capillary barrier system is determined.

2. Materials and methods

2.1. Sample preparation

River sand was sieved using sieves of sizes ranging from 0.6 mm to 2 mm in order to separate the coarse particles. It was then washed with a low-foaming agent and rinsed thoroughly with distilled water several times, air dried and stored under 20°C climate controlled condition for two weeks.

2.2 Preparation of hydrophobized grains

OA used as the HA and the sample was prepared using mixing-in method (Subedi et al, 2012,[1]) where sand is mixed thoroughly with liquid OA in a plastic bag and stored under 20°C climate controlled condition to equilibrate. Air dried grains were mixed with different contents of Oleic Acid varying from 1 g/kg to 10 g/kg. These were called as "dry hydrophobized grains"

From the results of Water Drop Penetration Test (WDPT) on the dry hydrophobized sand, three samples with different OA contents were selected to investigate the effect of moisture content on the Hydrophobicity. For this purpose, a hydrophobized coarse sand specimen was prepared by mixing with an OA content corresponding to the peak value of WDPT and two specimens corresponding to an HA content from either side of the peak. Distilled water was added to these sand specimens to adjust the water content to predetermined values. These water added samples were mixed well and stored in plastic bags under 20°C climate controlled condition. These specimen were called as "wet Hydrophobized grains".

2.3. Water repellence measurement by WDPT test

The coated sample was packed into a 15 cm diameter, 2 cm high cylindrical ring to have a dry density of 1.6 g/cm^3 and the ring was removed carefully. A small drop of distilled water of volume 50μl was placed on the surface of the above sample using a special pipette as shown in Figure 1 and the time taken for the water drop to infiltrate (WDPT) the surface completely was recorded. For each sample three tests were carried out. This procedure was performed for both dry and wet Hydrophobized grains.

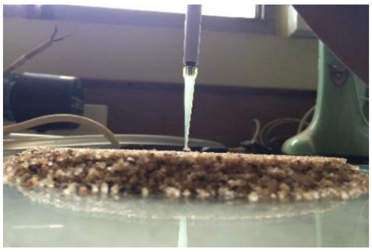

Figure 1: WDPT Test

Similar test procedure was followed to determine WDPT on the compacted dry and wet hydrophobised sand samples by varying the slope for three trial specimens of each sample.

3. Results and Discussion

The variation of WDPT with HA content is shown in Figure 2.

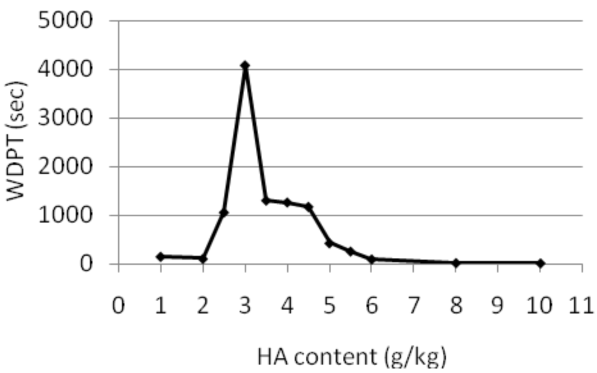

Figure 2: Variation of WDPT with HA content

Results show that the water repellency of compacted dry sand samples initially increased sharply with increasing OA content and reached a peak value and thereafter it decreased. With increasing HA content, the grain surface tends to become more hydrophobic, however, the measured WDPT values decreased after reaching the peak value of about 3g/kg, as a high amount of OA will reduce the contact angle at the grain water surface due to the multilayer coverage of the grain surface in which, a hydrophobic end may be facing the outside due to the excess OA. The peak value of 4080 seconds was obtained at a HA content of 3g/kg.

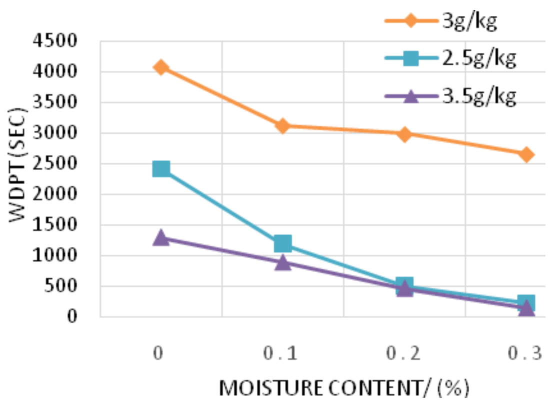

Figure 3: Variation of WDPT with moisture content

Variation of water repellence with moisture content is given in Figure 3. It shows that irrespective of the OA content an increase in moisture content has caused the water repellence to decrease. However, this decrease is less significant for the sand grains containing the optimum OA content for the range of moisture content tested.

The variation of WDPT with surface slope is shown in Figure 4.

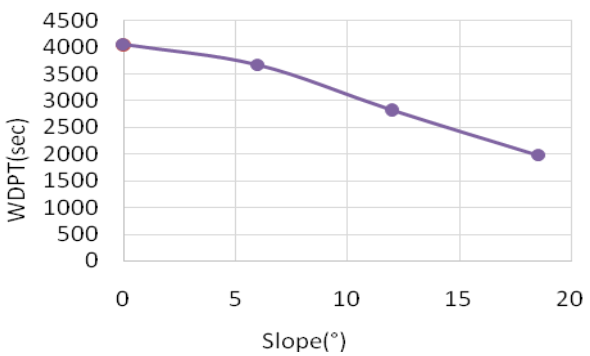

Figure 4: Variation of WDPT with surface slope

Results showed a decrease in water repellence when slope increases. It was observed that water drop was spreading, since the surface tension effect reduces, the WDPT time decreased.

5. Conclusions

It is possible to use locally available materials in a hydrophobised capillary barrier that can be developed as a low cost alternative to geosynthetics. From the results, it can be concluded that use of Oleic acid as a Hydrophobized Agent with an optimum mix ratio of 3g of HA per 1 kg of coarse sand in the capillary barrier, the water repellence is developed and it will help to minimize the water infiltration into the waste. At this optimum OA content, the influence of moisture content on the water repellency was insignificant for the range of moisture content tested.

Acknowledgements

Financial assistance granted by Tokyo Cement (Lanka) Pvt. Ltd. and the SATREPS Project is gratefully acknowledged.

References

[1]. Subedi S., Kawamoto K., Jayarathna L., Vithanage M., Moldrup P., de Jonge L.W., Komatsu T. (2012) 'Characterising time-dependent contact angle for sands hydrophobized with oleic and strearic acids', Vadose zone, Vol. 11, June 2012.

[2]. Wijewardana Y.N.S, Kawamoto K., Moldrup P., Komatsu. T, Kurukulasuriya L.C., Priyankara N.H. "Characterization of water repellency for Hydrophobized grains with different Geometrices and sizes". Journal of Environmental Earth Sciences" DOI 10.1007/512665-015-4565-6

SECM/15/099

SHEAR STRENGTH CHARACTERISTICS OF DIFFERENT GRADATIONS OF BALLAST USING PARALLEL GRADATION TECHNIQUE

V.Pakalavan[1*], B.Nirvekala[1] and L.C.Kurukulasuriya[1]

[1]University of Peradeniya, Peradeniya, Sri Lanka
*E-Mail: pakalnivi@rocketmail.com, TP: +940755634148

Abstract: Ballasted rail tracks are most commonly used rail track structure and to be designed to provide a stable, safe and economical foundation. Main components of ballasted rail track structure could be subdivided as track superstructure and track substructure. The loading from the train will be distributed from the superstructure to substructure. The main structural component of substructure is considered as track ballast which is generally crushed hard stones. Railway authorities specify gradation specifications for selection of ballast for rail tracks. Sri Lanka railways also specified a gradation limits in the selection of ballast for rail tracks. Current standard is closely resembled to the Indian rail track ballast specifications. Commonly, the ballast used in Sri Lanka is crushed gneiss rocks which are in abundance. It is well understood that granular materials derive its strength by resistance to shearing. However, there is no examination conducted to evaluate the performance of rail track ballast used in Sri Lanka considering the shear behaviour. The objective of this preliminary study is to investigate the shear strength characteristics of ballast gradation used in Sri Lanka and compare with selected other ballast gradation specifications. Parallel gradation technique was used to model the sample as it is difficult to handle large size ballast in the conventional direct shear box. Direct shear tests were conducted under three normal pressures of 15 kPa, 45 kPa and 90 kPa on different ballast gradations including current Sri Lankan specification. The results showed that the Current Sri Lankan ballast gradation specification which is the same as Indian standard gradation has the highest shear strength compared to other ballast gradations tested.

Keywords: ballast, ballast gradations, shear strength, parallel gradation technique

1. Introduction

Railway transportation plays an important role in the mass transportation sector of a country and contributes in sustaining a healthy economy. Efficiency and safety of the rail transportation is relied upon the quality of rail track structure. Ballasted rail tracks are most commonly used in rail track structures and are designed to provide a stable, safe and economic foundation. Main components of ballasted rail track structure can be divided into track superstructure and track substructure [1]. Track superstructure consists of fasteners, sleepers and substructure consists of ballast, subballast and subgrade. The loads from trains will be distributed from the superstructure to the substructure. Main functions of ballast are to resist vertical, lateral and longitudinal forces, provide sufficient resiliency, energy absorption, facilitate drainage, reduce the pressure from sleeper to an acceptable stress and distributed to the subgrade [2]. Different countries use different ballast material depending on the availability. The ballast material should be angular, crushed, uniformly graded hard rocks free of dust or dirt and shall not prone to cementing action for better performance. In Sri Lanka gneiss rock is commonly used as rail track ballast. The method of selection of ballast has been based on the physical testing of representative specimens to ensure that materials are of the suitable rock type with no inherent planes of weakness such as foliation and cleavage (Petrographic Analysis), acceptable grain shape and size distribution, adequate wearing resistance and weathering resistance (freeze-thaw, wetting and drying, and absorption) [4]. Among all, the gradation has a greater influence over the collective behavior of ballast grain as it controls the packing behavior. Therefore, different countries have specified different ballast gradations considering expected performance of ballast bed. European standard gradation, American standard gradation (AREMA), Australian standard gradation, Indian standard gradation and British standard gradation, etc. are some of these ballast specifications [3].

Sri Lankan Railway currently uses a ballast gradation specification similar to the Indian standard gradation. Due to the increased demand for a safer and quick transportation, Sri Lanka railways under the pressure to develop new rail tracks and upgrade the existing tracks to cater for increased hauling capacity and speeds yet no proper study has been conducted to evaluate the engineering behavior of ballast.

It is well understood that the shear strength of granular media is affected by the grain packing behavior. Being a granular medium, shear strength of ballast should also be affected by the particle size distribution. Previous researches [4, 5] have shown that if well graded aggregate mixtures are used, then density of granular mixture is increased and could obtain higher shear resistance [6]. Essentially, the ballast bed should have sufficient voids to sufficient hydraulic conductivity employing a very well-graded aggregate distribution as track ballast is not practical. Therefore, this study is focused to study the shear behavior of different ballast gradations and thus study the shear behavior of current Sri Lankan ballast gradation and evaluate the performance in the aspect of shear strength.

The size of the ballast grains is larger to study in conventional direct shear test apparatus available in the laboratory. Hence, it is required the ballast aggregate to be modeled to a smaller particle size distribution which could be tested in small direct shear test devices. The parallel gradation technique could be used to scale down ballast particle distribution. The modeled sample should closely duplicate the behavior of the larger prototype and could be successfully used to study the shear behavior [7].

2. Materials and Methods

European standard gradation, American standard gradation (AREMA No. 4), Indian standard gradations and British standard gradation were used for the study. It was not possible to use the prototype ballast aggregates in conventional direct shear apparatus. Hence, the parallel gradation technique was used to scale down the original gradation to a gradation with smaller particle sizes could be tested in conventional direct shear apparatus. In order to maintain the properties of rock the same with prototype ballast in rail tracks, the specimens were prepared from the material obtained from a quarry which supply ballast to Sri Lanka Railways. The lower limits of the selected standard gradations were taken for the study since it was the coarsest aggregate distribution. The Figure 1 shows the particle size distribution curves used for the study.

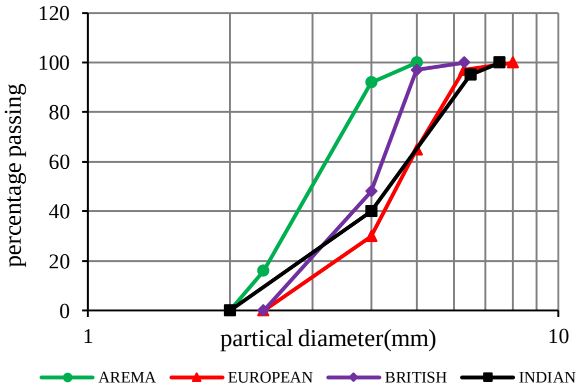

Figure 1 Different ballast gradations used for the study

The physical properties of ballast material were investigated first. The specific gravity, aggregate impact value (AIV), aggregate crushing value (ACV) and water absorption was found using relevant standards and results are tabulated in table.1. Available sieves to BS, ASTM standards were used to prepare the modeled ballast samples to follow the original prototype ballast gradations.

Table 1: Physical properties of ballast

Properties	Values
Specific Gravity	2.684
AIV	35%
ACV	28.5%
Water absorption	0.194%

The direct shear tests were conducted to investigate the shear behavior of different ballast specimens as it is the most efficient method to study the shear behavior of granular material [8, 9]. A 100 mm diameter standard direct shear device was used for the current study.

Each test sample was compacted in three layers inside the shear box applying the same compacting effort. The tamping was done using 8mm diameter steel rod with 25 blows per layer in shear box. Depending on the gradation, initial density of the specimen were not the same. The initial specimen densities are given in table 2. All the direct shear tests were conducted at the same shearing rate of 0.2mm/s under three normal pressures of 15 kPa, 30 kPa and 90 kPa.

Table 2: Density, Uniformity coefficient (C_u) and Coefficient of curvature (C_c) of tested standard gradations

Gradations	C_u	C_c	Density (kg/m^3)
European	1.68	1.14	14.52
British	1.57	1.01	14.09
AREMA	1.5	0.97	15.12
Indian	1.96	1	14.74

3. Results and Discussion

Figure 2 shows the variation of shear stress to the shear displacement under all the normal pressures for tested ballast gradations.

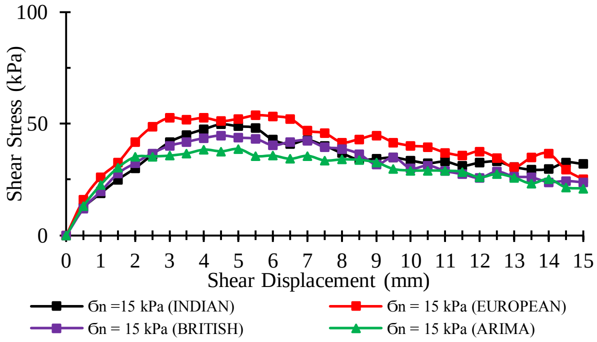

Figure 2(a)

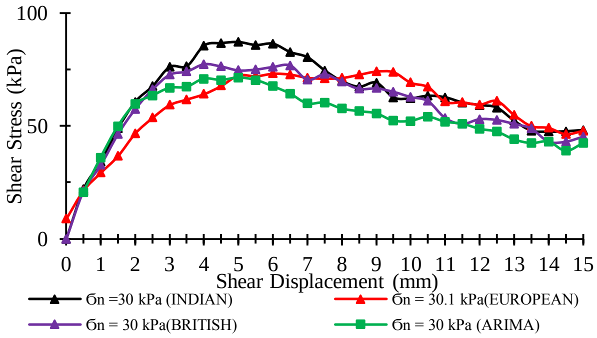

Figure 2(b)

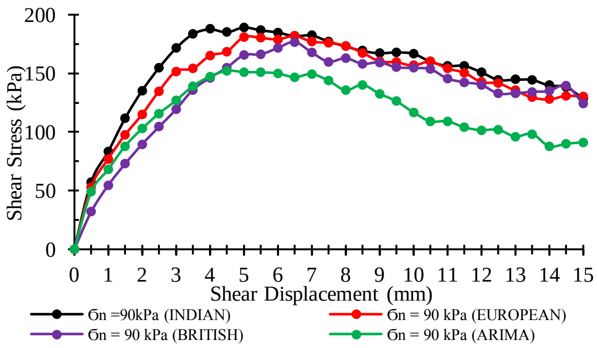

Figure 2(c)

Figure 2: Shear stress-Shear displacement relationships for normal pressures of (a)15 kPa (b) 30 kPa and (c) 90 kPa.

According to figure 2, it is seen that Indian standard gradation has the highest shear strength at high normal stress. Both Indian and European standard gradations have higher shear strength at low normal stress compared to that of other standard gradations tested.

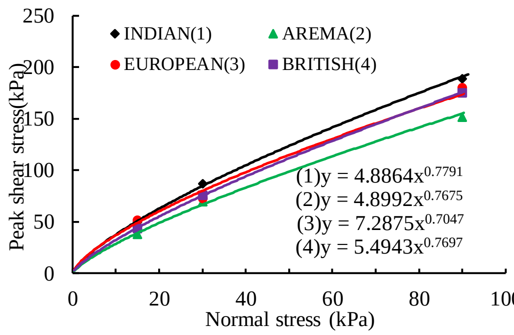

Figure 3: Relationships of peak shear strength and normal stress

Figure 3 shows the variation of peak shear strength with normal stress ballast. It was observed that for all ballast samples, the shear strength envelope at failure is better resembled to nonlinear behavior. It has been explained that this nonlinear behavior was due to particle interlocking of their highly angular nature [10]. The results of the study assuming nonlinear Mohr Coulomb failure criteria shows, Indian standard gradation has comparatively higher shear strength than the other gradations. European and British standard gradations show intermediate shear strength while AREMA No.4 ballast gradation has the lowest shear strength.

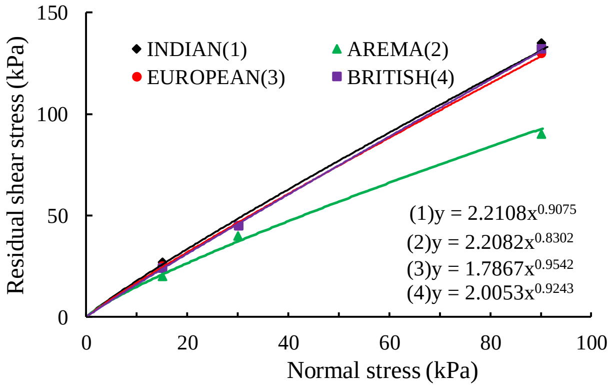

Figure 4: Variation of residual shear stress with normal stress

Figure 4 shows the variation of residual shear stress to the normal stress. It can be observed that a reduced nonlinearity of Indian, British and European ballast standards indicating a decreased interlocking and particle breakage at larger strains.

Indian, British and European ballast gradations has comparatively similar residual shear strength and American standard gradation has shown a lower residual shear strength compared to the other gradations.

It is further seen that, the friction angle is decreasing with the increase of normal stress due to the nonlinear behavior. Also it was observed an increasing trend of friction angle with the increase of uniformity coefficient for the ballast tested [12]. The observations indicate that most compacted and well graded aggregate gradations have better ability to resist loads than uniformly graded aggregates.

Table 3: Peak and residual friction angles of tested standard ballast gradations.

Gradations	Cu	peak friction angle(°)	residual friction angle(°)
European	1.68	60.0	54.6
British	1.57	59.8	55.3
AREMA	1.5	55.9	42.1
Indian	1.96	61.1	55.5

5. Conclusion

The friction angle of ballast is decreasing with the increase of normal stress.

Shear strength is increased with increase of uniformity coefficient for the ballast used in this study.

Indian standard gradation has the highest shear strength than that for European, AREMA and BS standard ballast gradations. Thus, concluded that ballast graded to Indian standard has the highest performance in load bearing characteristics and stability of track embankment.

References

[1]. Rahman, A. (2013) Permeability, Resistivity and Strength of Fouled Railroad Ballast, B.S., University of Kansas, Lawrence, Spring 2013.

[2]. John M Waters, E.T.S. (1994) Track Geotechnology and substructure management, Thomas Telford Publications.

[3]. Alemu, A.Y. (2011) Survey of Railway Ballast Selection and Aspects of Modelling Techniques, Division of Highway and Railway Engineering, Department of Transport Science,School of Architecture and the Built Environment,Royal Institute of Technology.

[4]. Kaya, M. (2004) A study on stress-strain behaviour of railroadballast material by use of parallel gradation technique, the graduate school of natural and applied sciences,the middle east technical university.

[5]. Mozhgan Asadzadeh, Abbas Soroush (n.d) 'Direct shear testing on a rockfill material', The Arabian Journal for Science and Engineering, vol. 34, Number 2B.

[6]. Indraratna, B. H.K.W.S. (1991) 'Geotechnical properties of ballast and the role of geosynthatics intrack stabilization'.

[7]. Sharma Pankaj , Mahure NV , Gupta SL , Dhanote Sandeep, Singh Devender, ‘Estimation of Shear Strength of Prototype Rock fill Materials’. 1-5 Central Soil and Materials Research Station, New Delhi, India. 424

[8]. Domenica Cambio, a.L.G. 'effects of parallel gradation on strength properties of ballast materials'.

[9]. Fityus, T.N.a.S. (n.d) 'Direct Shear Testing of a Marginal Material Using a Large Shear Box', Geotechnical Testing Journal, vol. 31, No. 5.

[10]. Methods of test for Soils for civil engineering, Part 7 (1990), authority of board of BSI.

[11]. Raymond, G. P.and Davies, J. R. (1978). Triaxial tests on dolomite railroad ballast, Journal of the Geotechnical Engineering Division, ASCE, vol. 104, No. GT6, pp. 737-751

SECM/15/100

Stability of an open dumpsite with ageing

G. Sayilacksha[1], T. Venuja[2] and L.C. Kurukulasuriya[3*]

[1,2,3]University of Peradeniya, Peradeniya, Sri Lanka
*E-Mail:chank@pdn.ac.lk, TP: +94-81-2393514

Abstract: Open dumping is the most commonly used method adopted in Sri Lanka as solid waste management. However, slope failures of open dump sites lead to environmental pollution as most of the open dumps are located near water bodies. Therefore, analysing the stability of open dumps is important in implementing mitigatory measures where required. Abandoned Udapalatha open dump site which is located near Gampola, Sri Lanka was considered as a case study to analyse the stability of its slopes consisting of old and new waste representing different degrees of decomposition. Shear strength parameters of the waste samples of the old and new waste sites were determined using box samples at different depths with particle size less than 9.5 mm. Specific gravity test, Oedometer test and Standard Proctor compaction test were performed to obtain Gs, primary and secondary consolidation parameters, maximum dry density and the optimum moisture content. In addition, direct shear test was carried out to determine the shear strength parameters of the fill. Slope stability analysis was carried out using Slope/W and Plaxis-2D software considering Mohr Coulomb and soft soil creep models respectively for waste material. Consideration of primary and secondary consolidation settlement within the landfill in the Plaxis-2D analysis resulted in an increase in the Factor of safety (FOS). Therefore, FOS values obtained from the slope stability analysis of the old site, was higher than that in the new waste site.

Keywords: Ageing, secondary consolidation, shear strength, slope stability.

1. Introduction

Municipal solid waste is a type of solid waste generated from community, commercial and agricultural operations. This includes wastes from households, offices, stores, industries and other non-manufacturing activities. Municipal solid waste removal is a major problem in all over the world. There are some methods available to remove solid wastes, such as engineering landfill, open dumping, recycle and reuse and ocean dumping. Historically, landfills have been the most common method of organized waste disposal and remain so in many places around the world. Some landfills are also used for waste management purposes, such as the temporary storage, consolidation and transfer, or processing of waste material (sorting, treatment, or recycling). An open dumping is defined as a land disposal site in which solid waste is disposed of in a manner that does not protect the environment and susceptible to open burning, exposed to the elements, scavengers, etc. There have been a number of landfill failures in the world with high loss of lives and properties. Stability of a slope is evaluated by the balance of shear stress and shear strength. A previously stable slope may be affected by many factors, making the slope unstable. Triggering factors of a slope failure can be a climatic event that can make a slope unstable leading to mass movements. Mass movements can be caused by increase in shear stress such as loading, lateral pressure and transient forces. Alternatively, shear strength may be decreased by weathering, changes in pore water pressure and organic material. In slope stability analysis, primary difficulty with analysis is locating most probable slip plane for any given situation, because most of the failure cases are analysed after the real failures. But nowadays slope monitoring using radar technology has been employed. Stability can be significantly improved by installing drainage path to reduce the destabilizing forces.

If the open dump sites undergo failures they can affect nearby water resources. There are number of landfill failures occurred in world with high loss of lives and properties such as landfill failure occurred in Ohio, USA on 9th March, 1996, Landslide at the Payatas dumpsite, Philippines on 11th July 2000 (Jafari et al.2013, [7]), Hiraya landslide in Iran on 1997. There are no slope failures in open dumpsites experienced in Sri Lanka, but most of them are located near river banks. Therefore, analysing the stability of this landfill is very important. In this research, a municipal solid waste landfill site at Udapalatha, Sri Lanka is considered as a case study. This site is adjacent to the "Mahaweli River", the longest river in Sri Lanka. It mainly consists of two distinctive areas such as new site and old site. Old site consists of MSW dumped at early stages of its operation and the new site consists of MSW dumped after the old site is filled to its capacity. After few years of operation dumping of MSW was stopped and the entire site was abandoned. These two sites consisting of MSW which have undergone different degree of decomposition are liable to undergo slope failure which could lead to severe environmental pollution mainly due to its close proximity to the river. Therefore, the research aim is to evaluate the stability of the slopes of old and new sites incorporating the spatial variation of shear strength properties within the fill.

2. Literature Review

The stability of waste mass is one of the major concerns associated with the design of landfill expansion. Past experience has shown that both vertical and lateral expansion of landfills can trigger waste mass instability. Vertical expansion generally involves a significant increase in landfill slope height (Zhan et al., 2008, [13]). For example, the postponed closure of the Payatas landfill in Philippines eventually caused a flow slide in 2000, which killed at least 278 persons (Kavazanjian and Merry, 2005).

Slope stability of a MSW landfill mainly depends on the geotechnical properties of MSW, such as unit weight and shear strength. Although it is common to perform stability analysis with uniform shear strength parameters for MSW, it should be noted that the MSW properties vary spatially due to heterogeneous nature, overburden pressure, and degradation. (Canizal et al, 2011). Thus, spatial and temporal variation in geotechnical properties of MSW should be properly considered in the landfill slope stability evaluations (Babu et al., 2014, [1]). There are various researches and tests done to obtain shear strength characteristics of municipal solid waste (Strak et al., 2000, [12]; Dixon and Jones, 2005,[5]; Zhan et al., 2008, [13]; Reddy et al., 2011, [9]; Canizal et al., 2011; Jafari et al., 2013,[7]).They are laboratory tests, field measurements and back calculation of shear strength.

In laboratory testing methods, in most of the cases direct shear test, unconfined compression test and triaxial compression test are proposed to obtain shear strength parameters. Vane shear test, standard penetration test and cone penetration test are used as field testing methods and for back calculation analysis plate load test is also used (Dixon and Jones, 2005,[5]). However, it is common to use either direct shear test or triaxial test to determine shear strength parameters (Stark et al, 2000 [12]).

3. Methodology

The MSW samples were collected from two different locations in the landfill at Udapalatha. A Hydraulically operated rotary drilling machine was used for the drilling work. Dry percussion drilling was used to collect disturbed samples in the waste at PBH locations given in Figure 1 and rotary drilling was used to advance the boreholes below the waste layer into the subgrade at BH locations. Box samples were also obtained in the landfill site at various depths.

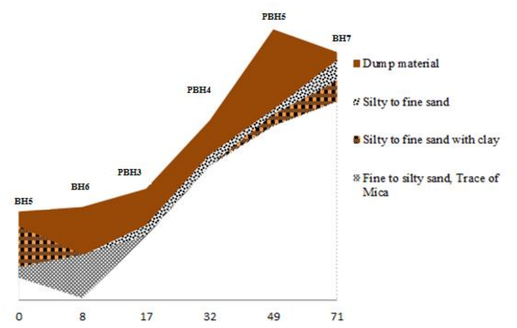

Figure 1: Cross section of old site of Udapalatha landfill

MSW is a heterogeneous material containing paper, polythene, plastic, clothes, organic matters, food particles, etc. It is difficult to analyse the geotechnical properties of MSW which contains materials such as polythene, plastic, etc. Normally fibrous materials present in the waste give additional strength to MSW in a sloped landfill. Therefore, fibrous materials were removed from box samples which were obtained at 0.5m, 1.5m, and 2.5m depths below the subgrade under the dump site. The maximum particle size selected for laboratory testing was selected as 9.5 mm as larger size particles, if present would induce a scale effect on direct shear test specimens.

In the laboratory, several parameters were measured in order to characterize its stability of slope and spatial variation of consolidation and shear strength parameters. These parameters are effective cohesion (c′), effective friction angle (ϕ′), Optimum moisture content (OMC), secondary consolidation parameters (λ*-Modified compression index, K*-Modified swelling index, μ*-Modified creep index) and unit weight (γ).

These parameters were evaluated by carrying out following tests;

1) Direct shear test-To determine c′&ϕ′

2) Consolidation test-To determine λ*, K*, μ*

3) Compaction test-To determine omc

4) Specific gravity test -To determine G_s

Slope stability analysis was done using different numerical software (Plaxis-2D and Slope/W) using different material models. Plaxis-2D with soft soil creep model and Slope/W with Mohr Coulomb model were used. Soft soil creep model is suitable for MSW materials because of its heterogeneity and the presence of more organic matters. This model tends to over predict the range of elastic soil behavior. Other material models do not take creep effects into account.

4. Results and discussion

Results were obtained from the Udapalatha old site samples. The optimum moisture content and the maximum dry density were obtained from Proctor compaction test.

Table 01: Maximum dry density and omc at different depths

Sample depth /m	0.5	1.5	2.5
Maximum dry density/ ρ_d (g/cm^3)	1.10	1.12	1.13
Optimum moisture content /w (%)	39.0	39.9	38.9

The secondary consolidation parameters were obtained from consolidation test. It was carried out in several load increments from 0.5 lbs to 64 lbs including the unloading stage. Figure 2 shows the consolidation test results of 1.5 m depth sample.

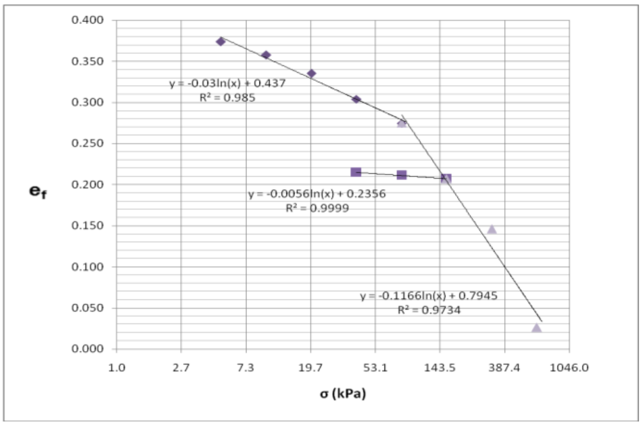

Figure 2: Variation of void ratio with σ

The modified compression index (λ* = 0.1166) was found from Figure 2 loading part and the modified swelling index (κ*=0.0056) was found from the unloading curve. Figure 3 shows the variation of void ratio with time from that graph.

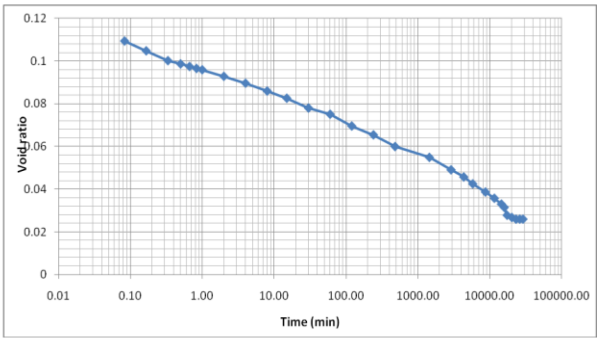

Figure 3: Variation of Void ratio with time

Secondary compression index (Cα) was obtained using the void ratio-time relationship beyond the primary consolidation. Cα was found to be 0.008 from Figure 3. Modified creep index (μ*=0.0024) was found using Cα and initial void ratio (e).

The shear strength parameters were obtained using direct shear test. Figures 4, 5 and 6 show the results of the direct shear test for samples obtained at depths of 0.5 m, 1.5m and 2.5m respectively. A displacement of 20 mm was taken as ultimate strength and corresponding shear stress and normal stress were used to draw the graphs. The shear strength parameters obtained from the direct shear test are listed below in Table 2.

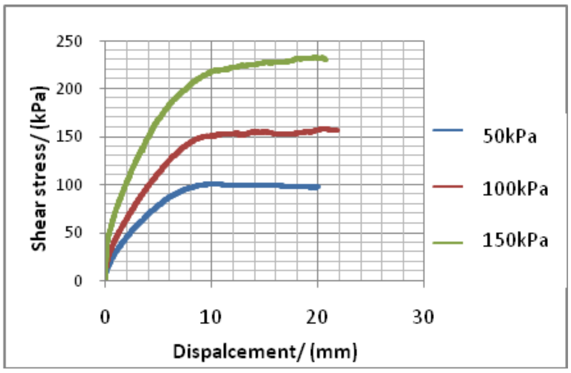

Figure 4: Variation of shear stress with shear displacement for 0.5 m depth sample

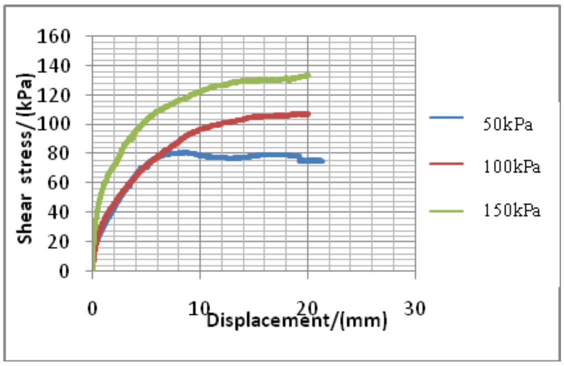

Figure 5: Variation of shear stress with shear displacement for 1.5 m depth sample

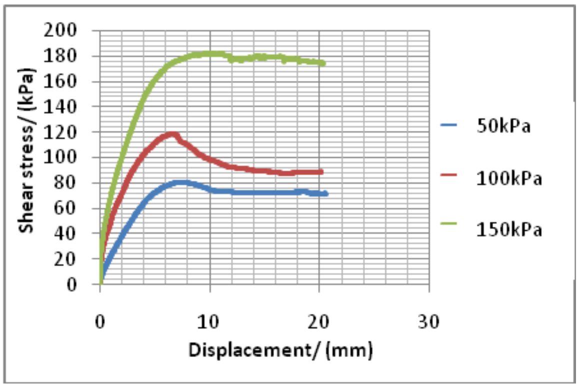

Figure 6: Variation of shear stress with shear displacement for 2.5 m depth sample

Based on the shear stress vs shear displacement curve, shear stress vs normal stress curves were prepared as shown in Fig 7 and the values for cohesion and angle of friction were found based on the graphs.

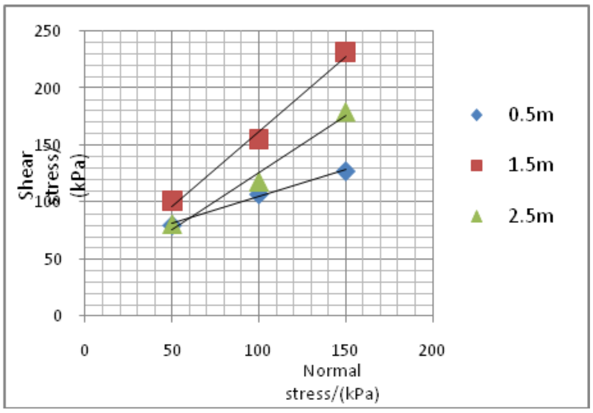

Figure 7: Variation of shear stress with normal stress

The cohesion and angle of friction values obtained for each depth from the direct shear tests are given in Table 2.

Table 2: Results of direct shear test

Depth (m)	c′ (kPa)	ϕ′ (˚)
0.5	57.9	25.1
1.5	30.9	52.8
2.5	26.9	44.7

Figures 8 and 9 show the variation of effective cohesion and the angle of friction with depth. The angle of friction obtained for the 1.5 m depth sample is higher than that of the 2.5 m depth samples. This may be obtained due to the heterogeneity and decomposition with ageing.

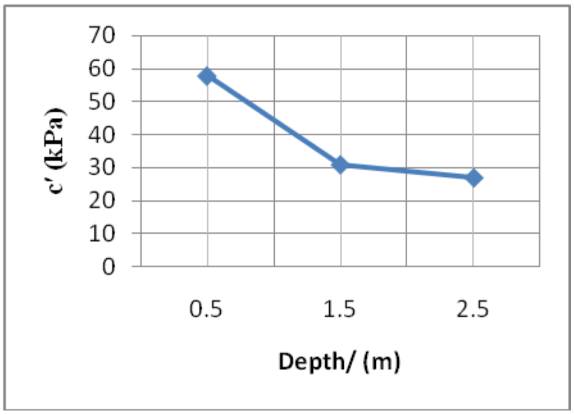

Figure 8: Variation of effective cohesion with depth

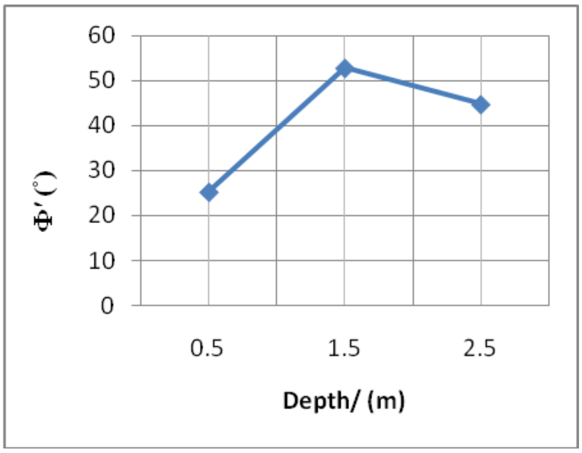

Figure 9: Variation of friction angle with depth

The stability analyses were carried out using Plaxis-2D and Slope/W software. The FOS values obtained from both software are different from each other due to the use of different material models and the results are shown in Table 3. The critical failure surfaces are shown in Figure 10. The watertable is well below the ground surface at the Udapalatha open dump site. Therefore, the stability analyses were carried out without considering the presence of watertable.

Table 3: FOS values obtained from different software (Old site)

Software	Depth (m)		
	0.5	1.5	2.5
Plaxis-2D	2.954	2.799	2.554
Slope/W	2.585	2.924	2.659

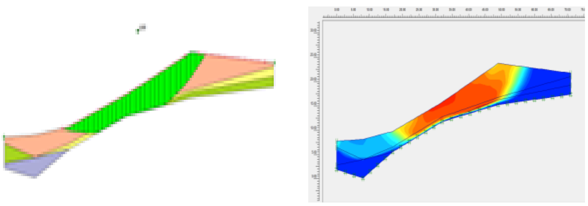

(a) (b)

Figure 10: Failure surface obtained using properties at 0.5 m depth (a) Slope/w (b) Plaxis-2D.

However, the possibility of rising of watertable to a reasonable height above the bottom level of the waste layer was also considered in the analysis. Table 4 shows the reduced FOS values obtained from Slope/W software under the above condition.

Table 4: FOS values obtained from Slope/W with watertable

Software	Depth (m)		
	0.5	1.5	2.5
Slope/W	2.384	2.698	2.452

The values of FOS given in Table 3 is compared with those given in Table 5 which gives the FOS values for the site with new waste analysed using the waste properties obtained from three different boreholes. The FOS values reported in Tables 3 and 5 reflect the effect of ageing on the stability of the slopes.

Table 5: FOS values obtained from the new site samples (after, Prathapan R. et al.(2015),[8])

Borehole	Effective Cohesion (kPa)	Effective Friction Angle (°)	FOS	
			SLOPE /W	PLAXIS -2D
PBH1	15.4	31.7	1.184	1.139
BH02	46.7	19.8	1.594	1.382
PBH2	50.2	13.9	1.722	1.428

5. Conclusions

A research study was conducted to evaluate the stability of the slope of an open dump site located in Udapalatha, Sri Lanka. Results revealed that the stability of the slope is in safer range from the obtained results using the two software and the factor of safety values obtained using Slope/W is larger than the values obtained from Plaxis-2D. Presence of ground watertable within the landfill decreases the stability of the slope as expected. Consolidation settlement inside the landfill changes the FOS which is reflected in the Plaxis-2D analysis. Stability of the landfill is increased after the secondary consolidation. Based on the comparison of FOS values of the site with old waste with that of the site with new waste, it can be concluded that the site with old waste is safer which is due to the ageing effect.

Acknowledgement

SATREPS project is gratefully acknowledged.

References

[1]. Babu, G.L.S., Reddy, K.R. and Sriva, A. (2014) 'Influence of Spatially Variable Geotechnical Properties of MSW on Stability of Landfill Slopes', *Hazardous, toxic and radioactive waste*, January, pp. 27-37.

[2]. Babu, G.L.S., Reddy, K.R. and Chouksey, S.K. (2010) 'Constitutive model for municipal solid waste incorporating mechanical creep and biodegradation-induced compression', *Waste Management*, vol. 30, pp. 11-22.

[3]. Caicedo, B., Yamin, L., Giraldo, E., Coronado, O. and Soler, N. (2002) 'Geomechanical properties of municipal solid waste in Dona Juana sanitary landfill', *Environmental Geotechnics*.

[4]. Colomer, F.J., Esteban, J. and Ferran, G. (2013) *Influence of the design on slope stability in solid waste landfills*, 2 Apirl, [Online].

[5]. Dixon, N., Russell, D. and Jones, V. (2005) 'Engineering properties of municipal soild waste', *Geotextiles and Geomembranes*, vol. 23, pp. 205-233.

[6]. Eid, H.T., Stark , T.D. and Douglas Evans, W. (2000) 'Municipal solid waste slope failure, waste and foundation soil properties', *Geotechnical and Geoenvironmental engineering*, May, pp. 397-407.

[7]. Jafari, N.H., D. Stark, T. and Merry, S. (2013) 'The July 10 2000 Payatas Landfill Slope Failure', *International Journal of Geoengineering Case histories*, vol. 2, no. 3, April, pp. 208-228.

[8]. Prathapan R., Jeyakaran T., Thakshajini L. and Kurukulasuriya L.C.(2015) 'Spatial variation of shear strength and consolidation characteristics of a municipal landfill and its implications on the stability of the fill-a case study'. *Proceedings, ACEPS conference, University of Ruhuna*

[9]. Reddy, K.R., Hettiarachchi, H., Gangathulas, J. and Bogner, J.E. (2011) 'Geotechnical properties of municipal solid waste at different phases of biodegradation', *Waste Management*, vol. 31, pp. 2275-2286.

[10]. Reddy, K.R., Gangathulasi, J., Parakalla, N.S., Hettiarachchi, H. and Jean.S (2009) 'Compressibility and shear strength of municipal solid waste under short-term leachate recirculation operations', *Waste Management & Research*, pp. 578-587.

[11]. Reddy, K.R., Hettiarachchi, H., Parakalla, N.S. and Gangathulasi, J. (2009) 'Geotechnical properties of fresh municipal solid waste at Orchard Hills Landfill, USA', *Waste Management*, vol. 29, pp. 952-959.

[12]. Stark, T.D., Huvaj-Sarihan, N. and Li, G. (2009) 'Shear strength of municipal solid waste for stability analyses', *Environ Geol*, vol. 57, pp. 1911–1923.

[13]. Zhan, T.L.T., Chen, Y.M. and Ling, W.A. (2008) 'Shear strength characterization of municipal solid waste at the Suzhou landfill, China', *Engineering geology*, vol. 97, pp. 97-111.

SECM/15/109

EFFECT OF COIR GEOTEXTILE AS REINFORCEMENT ON THE LOAD SETTLEMENT CHARACHTERISTICS OF WEAK SUBGRADE

CHETAN R BHOLE[1*], V SUNITHA[2], SAMSON MATHEW[3]

[1,2,3]Department of Civil Engineering, National Institute of Technology, Tiruchirappalli, India
[*]E-Mail: crbhole@vjti.org.in, +919967298753

Abstract: Geotextiles are permeable fabrics which, when used in association with soil, have the ability to separate, filter, reinforce and drain. It is not only allows reduction in the thickness of the pavement on a soft subgrade by the reinforcement action of geotextiles but gives less maintenance problems for long-term use. Coir geotextiles are made from coconut fibre which is a natural material composed of ligno cellulose cell obtained from the husk of coconut.

This paper presents the strength aspects of woven coir geotextiles on weak subgrade. In this paper, the results of laboratory investigation on the load-deformation behavior of the road sections are summarized. Two different varieties of coir geotextiles H2M5 and H2M6 were used as reinforcement in pavement section. The static plate load test results provide evidence that the inclusion of H2M5 coir geotextile gives higher strength at lower deformation compared to unreinforced section. Also, horizontal tensile strain and vertical compressive strain values were determined using KENPAVE software. The result of KENPAVE analysis shown that the section reinforced with H2M5 coir geotextile has lower strains as compared to unreinforced and H2M6 coir geotextile reinforced sections.

Keywords: Coir geotextiles, Pavement, Reinforcement, Soft subgrade.

1. Introduction

Over the last six decades, the State and Central Governments had drawn up several policies, programmes and implemented various schemes for the development of rural roads in India. Still there is need for further planned intervention for providing rural connectivity in an optimal way to achieve the objective of 100 percent connectivity, ensuring sustainable development. The Rural Roads Vision - 2025 aims at achieving all weather road access to all habitations by the year 2025 [1].

Road engineers are often faced with the problem of constructing roadbeds on or with soils which do not possess sufficient strength to support wheel loads imposed upon them either in construction or during the service life of the pavement. Road construction and maintenance along difficult soils have been problematic due to their inherent potential for volume change in the presence of water, which adversely impacts the performance of roads. Unless the subgrade is appropriately treated at the construction stage, the total transportation cost will increase substantially due to deteriorated pavement performance and associated road user costs.

Geosynthetics have proven to be the most versatile and cost effective ground modification material. Most of the geosynthetics are made of polymeric material. Natural geotextiles made of coir, jute, etc. are preferable to synthetic fibres on account of the fact that the material is environment friendly and ecologically compatible as it gets degraded with time. Moreover, natural fibres are less costly which make it a better choice compared to synthetic fibres. Reinforcing the sub grade using coir fabrics helps to distribute the load over a wider area and results in enhanced bearing capacity and reduced settlement. In the case of a pavement, this would result in reduced thickness of road structure and less earth work when it is used as a membrane between the subgrade and the overlying thin granular sub base layer. For unstable and wet subgrade, a coir fabric appears to provide satisfactory solution to stability and drainage problems.

2. Coir geotextile for Strengthening Subgrade

Coir is a 100% organic naturally occurring fibre, from a renewable source obtained from coconut husk. Naturally resistant to rot, moulds and moisture, it needs no chemical treatment. Hard and strong, it can be spun and woven into matting. Geotextiles made of coir are ideally suited for low cost applications because coir is available in India in abundance at very low price compared to other synthetic geotextiles. These geotextiles can be applied in the construction of unpaved roads where they can be effectively serving the purposes of reinforcement, separation, filtration and drainage.

induced by the traffic loads. At this stage, the subgrade may be strong enough to support the loads on its own without the necessity for reinforcement. For such applications, where the strength of subgrade increases with elapsed time, the natural reinforcement products are extremely suitable. After the degradation of the coir geotextiles, the organic skeleton remains in place in compressed form which will act as a filter cake keeping the moisture content of the subgrade soil constant.

3. Literature Review

Subaida et al. [2] conducted experiments to investigate the beneficial use of coir geotextiles as reinforcing material in a two layer pavement section. The effects of placement position and thickness of geotextiles on the performance of reinforced sections were investigated using two base course thickness and two types of woven coir geotextiles. The test results indicate an enhancement in the bearing capacity of thin sections.

Baruah et al. [3] studied the variation in the resistance of soil in terms of CBR value with respect to placement of coir mat in CBR mould from top surface of soil. The test results revealed that, in soaked condition the inclusion of coir mat has improved the CBR by nearly two times.

Raji et al. [4] carried out field simulation on subgrade soil with different combination of fly ash, cement and coir geotextile using a wheel tracking apparatus. It was reported that the subgrade obtained with the application of fly ash, cement and coir geotextile gives significant improvements in performance of subgrade in terms of rutting. The investigators also suggested that the rut depth and wheel repetitions obtained can be utilized for predicting the design life of unpaved roads in terms of number of load repetitions.

Nithin et al. [5] conducted model studies to investigate the beneficial use of coir geotextiles as reinforcing material on weak lateritic soil with Wet Mix Macadam (WMM) representing unpaved roads on soft subgrade. The coir geotextiles are kept at

Coir geotextiles are found to last for four to six years within the soil environment depending on the physical and chemical properties of the soil. When it is used as reinforcement, the coir layers can share the load with soil until its degradation thus increasing the load bearing capacity of the subgrade. When coir geotextiles are used, they also serve as good separators and drainage filters. In many instances, the strength of subgrade soil increases in course of time as the soil undergoes consolidation different levels in the subgrade model sections for studying the effect of position of geotextiles in upgrading the bearing capacity of soil under the monotonic loading system. It was reported that there

is a considerable amount of increment of the bearing capacity of reinforced subgrade with respect to the unreinforced subgrade at a specified settlement. The placement of coir geotextiles at base and subgrade interface shows a significant increase in the load at higher settlements due to the membrane action. Whereas, placing the coir geotextile within the base course resulted in a considerable increase in load at small as well as at large settlements.

4. Objectives of the Study

The major objectives of the study are as follows:

i. To study the feasibility of coir geotextile as a soil stabilizing material for application in road pavements.

ii. To compare the performance of H2M5 and H2M6 coir geotextile as a soil stabilizing material.

iii. To study the variation in vertical displacement and vertical stress under the static loading for coir geotextiles reinforced and unreinforced sections.

iv. To carry out the stress analysis of coir geotextiles reinforced section under loading by KENPAVE software.

5. Experimental Studies and Results

The study was conducted on the soil sample using two different coir geotextiles (H2M5 and H2M6). California Bearing Ratio (CBR) and Plate Load tests were conducted to evaluate the strength properties of the soil and to compare the influence of the different types of coir geotextile on them. The details of the testing programs are explained below:

5.1 Materials Used for Investigation

5.1.1 Subgrade Soil

The coastal area soil subgrades are predominantly composed of silt and clays. Coastal zone with poor soil subgrade was considered in this investigation. problematic soil classes. Material characterization has been made as per Indian standard specifications [6]. The values are summarized in Table 1.

Table 1: Properties of soil used

Sl No.	Properties	Value
1	Specific gravity	2.67
2	Coefficient of uniformity (Cu)	10
3	Coefficient of curvature (Cc)	0.32
4	Liquid limit (%)	27
5	Plasticity index (%)	12
6	IS Soil classification	SC
7	Optimum moisture content (%)	12
8	Maximum dry density (g/cm^3)	1.94

5.1.2 Coir Geotextiles

Two types of coir geotextiles designated as H2M5 and H2M6 were used in the experimental work. The physical properties of these coir geotextiles are reported in Table 2 [7]. Figures 1 and 2 show photographs of H2M5 and H2M6 coir geotextiles.

Table 2: Physical properties of H2M5 and H2M6 Coir geotextile

Sl.No	Parameter	H2M5	H2M6
1	Material	100% Natural coir fibre	
2	Mass/unit area (g/m^2)	740	365
3	Mesh size (mm x mm)	9 x 9	20 x 20
4	Thickness at 2kPa (mm)	9.0	7.57
5	No. of warp thread	11.0 per dm	4.6 per dm
6	No. of weft thread	7.0	4.0
7	Minimum breaking load (kN/m)		
	Warp Way	20	10.30
	Weft Way	18	9.70
8	Tensile strength (kN/m)	10.4	7.8
9	Puncture resistance (N)	920	440

Soil samples were obtained from Keelaiyur-Mattankarai Road in Kuththalam Block, Nagappattinam district, Tamil Nadu, India. The investigation conducted on the soil sample collected show that these silt and clays belong to the

Figure 1: H2M5 Coir geotextile

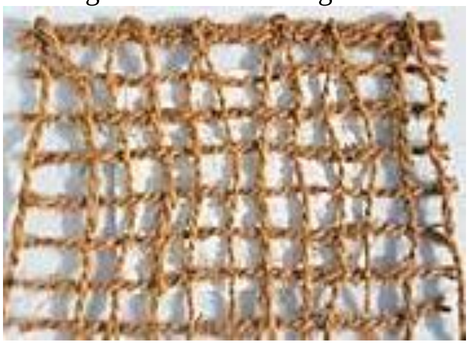

Figure 2: H2M6 Coir geotextile

5.2 California Bearing Ratio (CBR) test

The CBR value of the virgin soil sample was found to be 2%. Hence the soil was inferred to be weak in strength. CBR test was conducted for soil sample stabilized with two different varieties of coir geotextiles H2M5 and H2M6 placed at heights of h/2, h/3 and h/4 from the top of the mould, h is the height of the mould.

5.2.1 Results from CBR test

Load-penetration curves were plotted for the observations obtained from the tests. The curves for each type of coir placed at different positions were compared as shown in Figures 3 and 4. The CBR values obtained for different specimens are given in Table 3. It can be observed from the results that there is a considerable increase in the CBR value due to the presence of coir geotextile. Coir geotextile is more effective when placed near the top of the soil sub-grade due to the coir's presence come in the loading plane of the plunger.

Table 3: CBR test results

Type of Coir Geotextile	Placement of Coir Geotextile from top		
	h/4	h/3	h/2
H2M5	9.0%	7.5%	6.0%
H2M6	7 .5%	7.0%	5.0%
Unstabilized		2%	

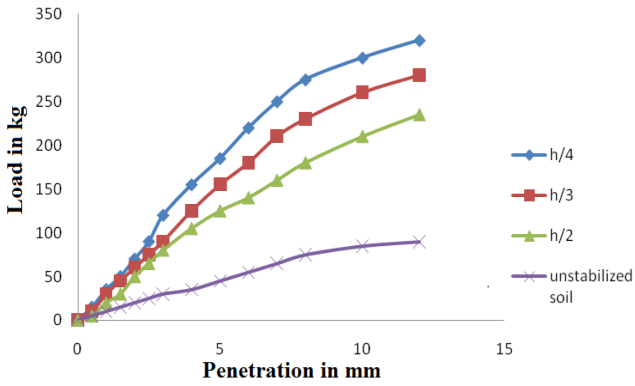

Figure 3: Load-Penetration curve for H2M5 at various positions

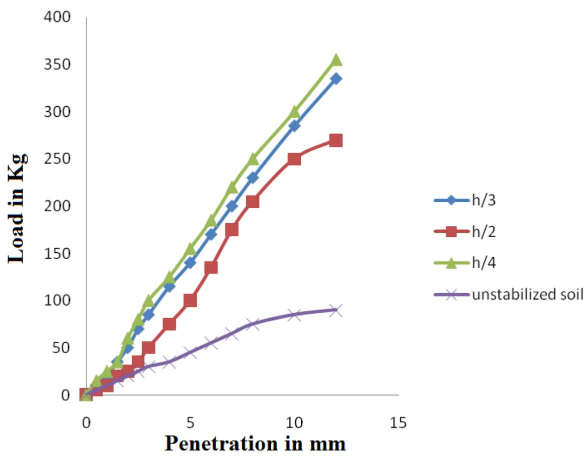

Figure 4: Load-Penetration curve for H2M6 at various positions

5.3. Plate Load Test

5.3.1 Experiment setup

Plate load tests were carried out to investigate the behaviour of soil reinforced with coir geotextile. The tests were performed in a mild steel rectangular tank of size 1.2 m x 1.2 m in section and 0.75 m deep. The loading was done with the help of 200 KN capacity hydraulic jack and reaction frame through a proving ring of capacity 50 KN.

5.3.2. Experimental procedure

The dry soil sample was thoroughly mixed with water to attain the maximum dry density and compacted in layers at required height. The water content and dry density of soil was kept constant in all the layers and equal to 12% and 1.94 g/cm^3 respectively. To achieve this, the water content of soil was determined before each layer and the water content was adjusted accordingly. Reinforced section was prepared by laying coir geotextiles at the middepth of subbase. The load was applied through a circular plate of 150 mm in diameter and 25 mm thick. The vertical deformation of the steel plate were recorded using dial gauge of the least count 0.1 mm. Load was applied at regular intervals and corresponding settlement were noted. The soil was loaded till failure. Different test sections used for testing are given in Table 4. The load setup and test process are shown in Figures 5 and 6.

Table 4: Test sections used for testing

Test Sections	Subbase thickness (mm)	Type of Coir Geotextile	Location of Coir Geotextile
Soil + Subbase	280	-	-
Soil + Subbase + Coir geotextile	280	H2M5	Mid- depth of Subbase

Figure 5: Coir geotextile at mid-depth of subbase

Figure 6: Loading arrangement for Plate load test

5.3.3 Results from Plate Load Test

The plate load test was carried on all the test sections. Figures 7 and 8 represent the relation between load and settlement for with and without coir geotextile respectively.

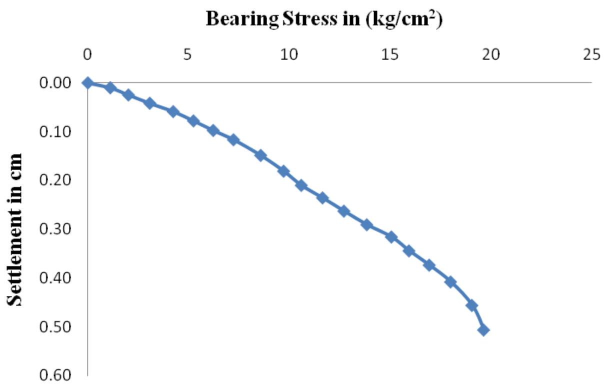

Figure 7: Load-Settlement curve for soil without Coir geotextile

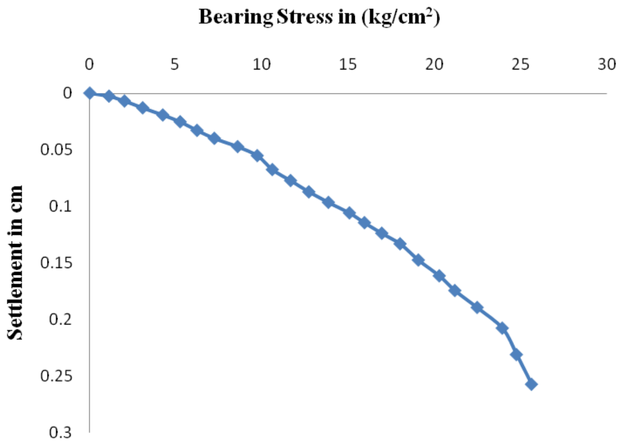

Figure 8: Load-Settlement curve for H2M5 Coir geotextile reinforced section

It is observed that the load sustained by the soil sample was 10.5 kN at a 20 mm settlement and the section reinforced with H2M5 coir geotextile can sustain a load of 23.85 kN for the same settlement. The percentage increase in load is 127% and at greater settlement the percentage increase was still higher.

6. KENPAVE Analysis

The analysis was done using the computer software KENPAVE for pavement design and analysis. The backbone of KENLAYER is the solution for an elastic multilayer system under a circular loaded area. The software does linear elastic multi-layer analysis to obtain the results including stresses, strains and deflections.

KENPAVE software was used to analyze the reinforced and unreinforced pavement sections with subgrade, sub-base, base and surface course. The sections were analyzed by using input parameters given in Table 5.

Table 5: Input parameters used for KENPAVE analysis

Sl.No	Parameter		Values
1	Material		Linear elastic layered system
2	Axle load		10.2 tonne
3	Tyre pressure		7 kg/cm^2
4	Commercial vehicle per day		200
5	Rate of growth of traffic		7.5%
6	Vehicle damage factor		0.75
7	Carraige way		Single lane
8	Subgrade thickness (mm)		500
9	Subbase thickness (mm)		450
10	Base thickness (mm)		500
11	Dense Bituminous Macadam thickness (mm)		80
12	Semi Dense Bituminous Concrete thickness (mm)		30
13	Elastic Modulus (MPa)	Subgrade	20 *
		Subbase	62.52 *
		Base	76.27 *
		DBM	1500 **
		SDBC	1700 **

*Elastic Modulus computed by using empirical formula given in IRC 37: 2012 [8].

** Assumed values of Elastic Modulus

6.1 Section Considered for KENPAVE Analysis

The pavement section designed by using above parameters was used as the primary section and various models of pavement sections were developed by varying thickness of the base and sub base course. Figures 9 and 10 show the primary section used for analysis

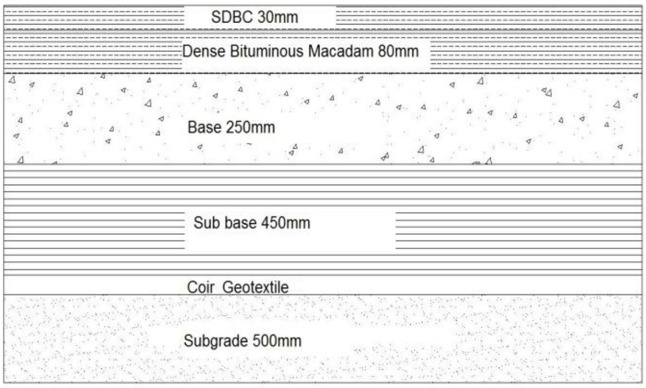

Figure 9: Pavement section with coir geotextile at interface of subgrade and subbase

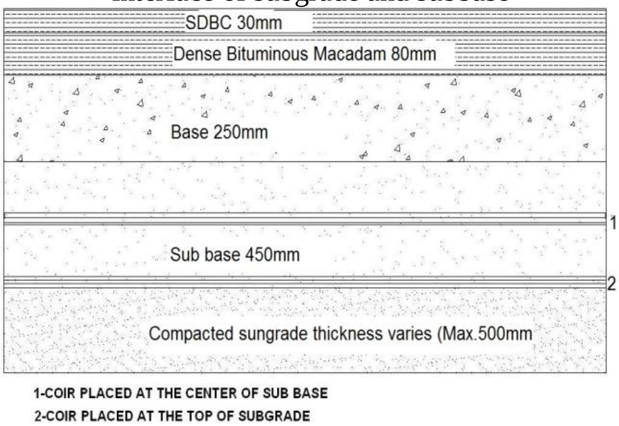

Figure10: Pavement section with coir geotextiles at interface and mid-depth of subbase

6.2 Output

The outputs of the analysis were settlement, tensile and compressive strains and shear stress. The behaviour of the pavement sections considered for analysis were studied by using coir geotextile as an intermediate layer between subbase and subgrade and by placing the coir at the top of subgrade and at the centre of subbase. Comparisons of settlement, stresses and strains at different positions of coir geotextile is shown in Figure 11 to 14.

6.3 Results and Discussion

The variation in settlement, tensile and compressive strain and shear stress for different types of coir placed at various positions, having different base and subbase course thickness are shown in Figures 11 to 14.

It is observed from Figures 11 and 12 that there is significant reduction in the settlement and the compressive strains in the pavement, as the soil is reinforced with the coir geotextile. This is due to the coir acts like a membrane, tension member which provides the necessary reaction to the applied load.

It is also observed that stiffness of coir geotextile significantly influenced the settlement and compressive strain in pavement. H2M5 coir geotextile is more effective in reducing settlement and strains than H2M6 coir geotextile, because of more stiffness. The additional layer of coir geotextile at mid-depth of sub-base further reduces the settlement and strain, but overall effect is marginal.

It has been observed from Figure 13 that reinforced pavement section with coir geotextile reduces the tensile strain in pavement. Coir geotextile has good frictional capabilities and provide tensile resistance to lateral soil movement. It is also observed that the additional layer of coir geotextile in mid-depth of sub-base significantly decreased the tensile strain over loaded area of the pavement by providing an additional lateral confinement. The reduction in tensile strain in pavement section is more for thicker sub-base course.

Figure 14 shows the variation of shear stress in pavement section for reinforced and unreinforced section. The result indicated that the shear stress increase a by minimum 2% for coir geotextile reinforced section. Also it is observed that the additional layer of coir geotextile at mid-depth of sub-base significantly increase the shear resistance of pavement section due to the hardening of lower layers. The improvement in shear stress for H2M6 two layer reinforced section is almost equal to H2M5 single layer section for thicker subbase.

7. Conclusions:

Based on the experimental results and KENPAVE analyses following conclusions were drawn:

1. Coir in the form of geotextile is advantageous for strengthening of weak soil since it reduce the settlement of soil subgrade.
2. Reinforcing the soil with coir geotextile can improve the strength characteristics of the soil.
3. The section reinforced with H2M5 coir geotextile shows significant improvement in the load carrying capacity.
4. Inclusion of a coir geotextile layer, at the interface of subgrade and subbase improves the load settlement characteristics and an additional layer of coir geotextile at mid-depth of subbase produces marginal improvement in the system.
5. Provision of a layer of geotextile at the interface between subgrade and sub base reduces the

deformation by 40%, which in turn results in the reduction of sub-base thickness required.

6. KENPAVE analysis shown that the section reinforced with coir geotextile can carry more traffic load and can be used for low volume rural roads with reduced pavement thickness in subbase course than the conventional section.

Acknowledgement

The authors gratefully acknowledge the research funding from Coir Board, Ministry of Micro, Small and Medium Enterprises (MSME), Government of India.

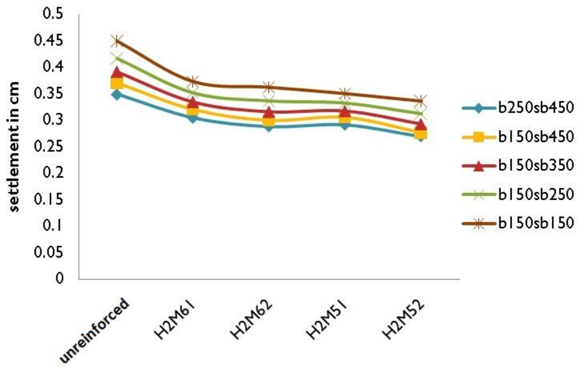

Figure 11: Settlement variation for different sections

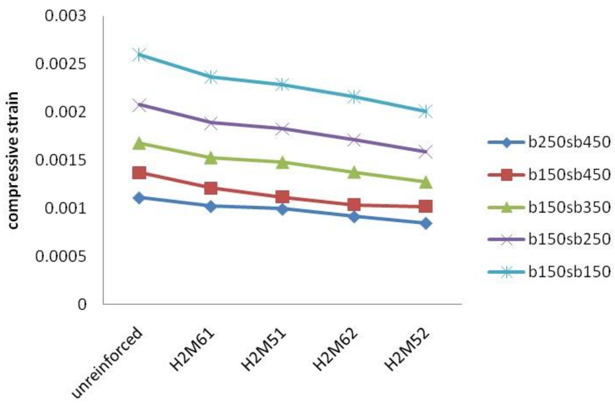

Figure 12: Compressive strain variation for different sections

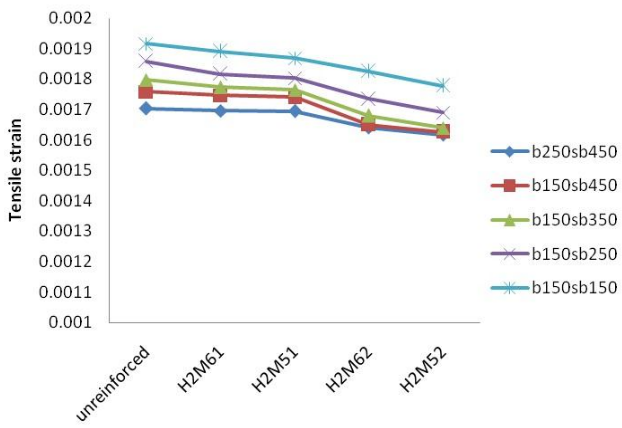

Figure 13: Tensile strain variation for different sections

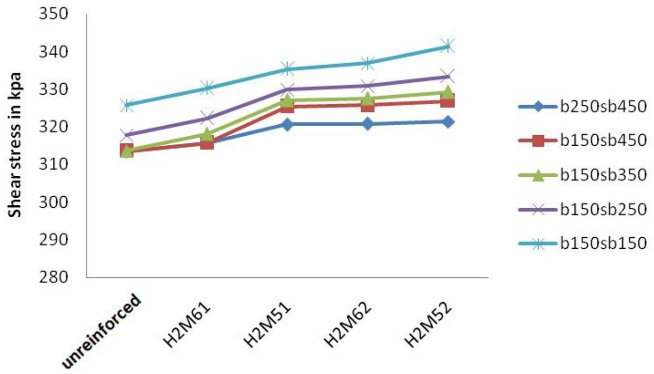

Figure 14: Shear stress variation for different sections

Note: 1) b250sb450 denotes a pavement with base thickness 250 mm and subbase thickness 450mm.
2) H2M51 and H2M61 – Coir geotextiles placed at interface of subgrade and subbase.
3) H2M52 and H2M62 – Additional coir geotextiles layer at mid-depth of subbase

References

[1]. Rural Road Development Plan: Vision 2015, Ministry of Rural Development, Government of India, 2007.

[2]. Subaida, E, A., Chandrakaran, S. and Sankar, N.,"Laboratory Performance of Unpaved Roads Reinforced Woven Coir Geotextiles", Geotextiles and Geomembranes, Vol. 27, pp. 204-210, 2009.

[3]. Baruah, U, K., Saikia, B, D. and Bora, P, K., "Road Construction in Assam by using Coir Mat", Indian Geotechnical Conference, GEOtrendz, 2010.

[4]. Raji, A, K., Amruthalekshmi, G, R., Anuj, K., Peter, M., Mohamed Sajeer., "Study of Rut Behaviour of Coir Reinforced Black Cotton Soil using Wheel Tracking Apparatus", Proceedings of Indian Geotechnical Conference, Kochi, 2011.

[5]. Nithin, S., Sayida, M, K.and Sheela Evangeline, Y., "Experimental Investigation on Coir Geotextile Reinforced Subgrade", Proceedings of Indian Geotechnical Conference, Delhi, 2012.

[6]. IS: 2720 (Part I to V) 1985, Methods of Test for Soils, Indian Standards, New Delhi.

[7]. http://www.ccriindia.org, Visited, 06th January 2015.

[8]. IRC: 37 2012, Guidelines for the Design of Flexible Pavements, Indian Road Congress, New Delhi, 2012.

SECM/15/110

Stress-Strain Behaviour of Structural Lightweight Concrete under Confinement

M.A. Senel[1], T. Tasbahji[1], L. Turanli[1] and A. Saritas[1,*]

[1] Middle East Technical University, Ankara, Turkey
[*]E-Mail: asaritas@metu.edu.tr, TP: +90 312 210 5458

Abstract: In this study, stress-strain behavior of structural lightweight concrete is studied under unconfined and confined conditions. To this end, the use of naturally occurring perlite material as lightweight aggregate and cement replacement material is considered. Although there are several studies on the confinement effects on normal weight concrete, there is lack of data on the confinement behavior attained for structural lightweight concrete by spiral or stirrup reinforcement. In order to evaluate the performances of structural lightweight concrete and normal weight concrete in a reliable manner, an experimental study is conducted. Through the experimental study on cylinder specimens that are unconfined and confined in different percentages by spiral reinforcement, the elastic and inelastic, namely post-peak behavior of structural lightweight concrete is recorded by the use of displacement-controlled testing machine. The results indicate that concrete produced from perlite as lightweight aggregate as well as through the use of cement replacement material provide significant energy absorption in the presence of spiral reinforcement.

Keywords: Structural Lightweight Concrete; Natural Perlite Aggregate; Cement Replacement Material; Confined Concrete Behavior.

1. Introduction

Concrete type or class considered in the design and construction of load carrying members of structures of civil engineering structures shall have enough strength and adequate ductility with proper reinforcement in order to ensure safety against collapse. In addition to the use of well-known normal weight concrete, the use of lightweight concrete has also been observed in structural applications, after its more popular spread into various aspects of non-structural members in construction industry. In a study conducted with the support of National Science Foundation in U.S. in 1982, the columns made of structural lightweight concrete had been proven to have lateral strength as much as columns made of normal weight concrete. Therefrom in 1983 in the United States the use of lightweight concrete was encouraged in the light of the studies with the release of ACI 318-83 (1983) [1].

Due to the light weight of aggregates used, lightweight concrete reduces the total dead weight of structures advantaging in a significant decrease in the geometrical dimensions of the structural elements, particularly foundations and columns. These reductions could provide savings in terms of structural safety, economy and ease of construction. Furthermore, lower permeability and comparatively high freeze-thaw resistance are taken into account as advantages of structural lightweight concrete.

On this subject, Turkey has a great potential of raw materials to be used as lightweight aggregate due to its geomorphologic structure; as claimed 75% of total worldwide perlite reserves are in Turkey. However the Turkish Specification TS-500 does not allow the use of lightweight concrete in structural load carrying members.

This research in this regards firstly aims to determine the stress-strain behavior of structural lightweight concrete. Although there are several studies on the confinement effects on normal weight concrete, there is lack of reliable information on the confinement behavior attained by structural lightweight concrete by spiral or stirrup reinforcement. The study of Hlaing et al. [2] is one of the remarkable ones investigating confinement effect of lightweight concrete. In their study, they have also noted that there are almost no studies that they can record on the determination of the response of lightweight concrete material's stress-strain response. In their study, different lightweight concrete samples varying between 38 MPa and 58 MPa were tested with different spiral reinforcements those having tensile stress of 1245, 1457 and 1675 MPa. Although they have performed great effort, since sample spiral spacing was comparatively low and using spiral reinforcement with comparatively high tensile capacity, minimum 1245 MPa as mentioned, they have not been able to conclude with a fair post peak response as observed in standard tests, i.e. the post-peak response of the stress-strain plots from the experiments yielded significant hardening response, which is actually not the most characteristic response that would be studied for concrete material.

While not related to lightweight concrete, the study of Leung and Burgoyne [3] can be cited as one of the remarkable studies on the determination of confinement effects on concrete. Different from their counterparts, they studied the confinement effects attained by aramid fibers. In their first set of experiments, aramid fibers were placed as single spirals with a spiral spacing of 10, 20, 35 and 50 mm, those having elasticity moduli of 90.1 GPa. In the second set, in order to visualize the confinement effect of non-circular elements, two different spirals were placed to be interlocked. The concrete in that study has been molded with design strength of 40 MPa.

In the light of experiments, they have concluded that the load versus displacement of the specimens merely differed from each other before reaching the peak load, for unconfined and confined ones. Furthermore, the ultimate strain was 4 times greater for 50 mm spaced spirals, and 7.5 times greater for 10 mm spaced spirals, than the unconfined specimens.

In order to visualize the success of the aim of the study in this research paper, the authors performed a trial testing on unconfined and confined lightweight concrete at Materials of Construction Laboratory of Middle East Technical University. As seen in Figure 1, confinement has a great effect on both maximum compressive stress and ultimate strain. In addition, the balance between the concrete and spiral reinforcement is proven to be successful to give a softening post-peak responses.

In a companion paper by Kent and Park [4], the theoretical model herein is compared with results of the experimental program carried in this research study, as well.

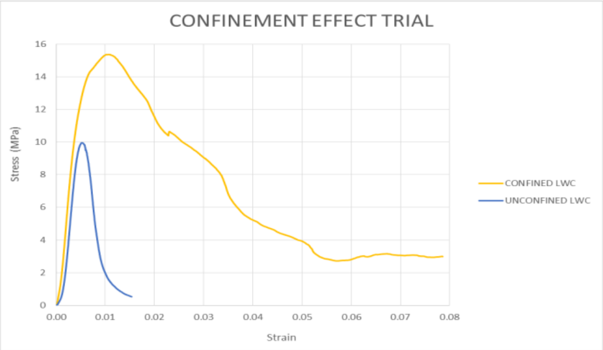

Figure 1. Early Trials on Confined LWC

2. Materials

In the experimental study, the tests are applied on three different types of concrete, naming, normal weight concrete, lightweight concrete and modified lightweight concrete. The concrete types differ from each other in some aspects. As in normal weight concrete crushed limestone aggregates are used whereas natural perlite aggregates are used for lightweight and modified lightweight concrete. To study the effect of perlite powder as a binder, in the modified lightweight concrete, 50% of the amount of cement is replaced with perlite powder.

2.1 Properties of Materials

The lightweight aggregate to be used in the scope of this paper, perlite, is found in raw form in Mollaköy, Erzincan, which is an earthquake prone region in Turkey. The Mollaköy perlite has been shown by Aşık [5] and Eser [6] to be usable as lightweight aggregate after few physical processes. The properties of the aggregate and its powder are presented in Table 1 and Table 2 as obtained from the studies of Asik and Eser.

Furthermore, Table 3 below lists the properties of limestone aggregates used in normal weight concrete.

Apart from aggregates types, in all the concrete mixtures, the same Portland cement of type CEM I 42.5 R is used. The chemical and physical properties of which are cited in Table 4 below.

Furthermore, BASF Gilenium 51 is used as superplasticizer in a ratio of 1% by mass. The properties of BASF Gilenium 51 are cited in Table 5.

Table 1. Physical Properties of Perlite Aggregate

Aggregate Size (mm)	0-3	8-12
Dry-Loose Unit Weight (kg/m3)	1288	1002
Oven Dry Specific Gravity	2.06	1.93
Saturated-Surface Dry Specific Gravity	2.18	2.04
Water Absorption Capacity (%) – 72 hr	5.64	5.59
No.200 Sieve % Passing	11.64	-
Los Angeles Abrasion (%)	-	49.7

Table 2. Chemical and Physical Properties of Perlite Powder

Chemical Composition of Perlite Powder	
SiO2	70.96
Al2O3	13.40
Fe2O3	1.16
MgO	0.28
CaO	1.72
Na2O	3.20
K2O	4.65
Loss on ignition	3.27
Physical Properties of Perlite Powder	
Specific Gravity	2.38
Fineness	
Passing 45-µm (%)	80
Specific Surface, Blaine(m2/kg)	413
Median Particle Size (µm)	19.1
Strength Activity Index (%) *	
7 Days	78
28 Days	80

Table 3. Physical Properties of Limestone Aggregate

Aggregate Type (mm)	0-4	4-12	12-25
Saturated-Surface Dry Specific Gravity	2.62	2.71	2.71
Oven Dry Specific Gravity	2.59	2.70	2.70
Water Absorption Capacity (%)	1.4	0.29	0.22

Table 4. Chemical and Physical Properties of Portland Cement

CEM I 42.5 R	
Chemical Composition, %	
CaO	62.54
SiO2	19.32
Al2O3	4.76
Fe2O3	4.36
MgO	2.04
SO3	3.49
K2O	0.67
Na2O	0.21
Cl-	0.0219
LOI	2.26
IR	0.63
Physical Properties	
Specific Gravity	3.17
Blaine Fineness, cm2/g	4534
Initial Set, min	115
Final Set, min	160

Table 5. Properties of Superplasticizer

Structure of Material	Polycarboxylic ether based
Density	1.082 - 1.142 kg/lt
Chlorine Content	< 0.1%
Alkaline Content	< 3%

The reinforcing steel used as spiral confining reinforcement has a diameter of 4 mm that will help in demonstrating the confinement properties properly. The steel wires were tested in universal testing machine, and its stress-strain performance is presented in Figure 2. The tension test resulted in a yield strength of 226 MPa and ultimate strength of 351 MPa.

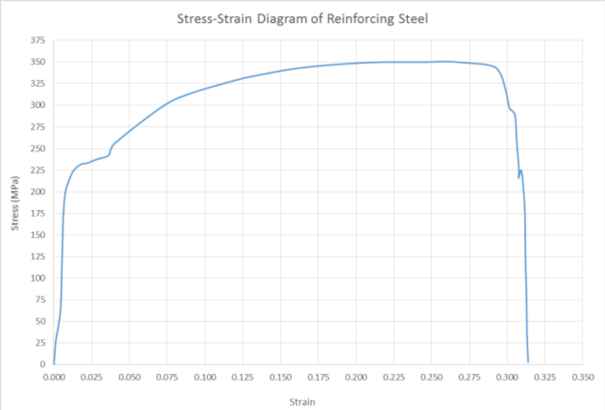

Figure 2. Stress-Strain Diagram of Reinforcing Steel

2.2 Specimens and mix proportions.

The samples prepared for the tests are molded in 10×20 cm cylindrical specimens. The tests will be applied on unreinforced and two types of reinforced samples; with 30 mm spaced spiral reinforcement and 50 mm spaced spiral reinforcement. To not violate the clear cover of specimens, all the reinforced samples are provided with 1 cm clear cover. With the help of wooden sticks the clear cover is provided for both the top and the bottom of each specimen.

To reduce the error of experiments, for each type of specimens the results will be evaluated as the average of 3 tested samples.

The concrete mixture composition is designed to obtain 20 MPa compressive strength at the time of testing. In order to monitor the progress in a successful manner, the specimens are tested in seven days intervals. For the unconfined concrete samples that reach a compressive strength close to 20 MPa, their successor spirally confined samples start to be tested. The composition of concrete mixture is presented in Table 6

Table 6. Mixture Proportions of Concretes

Mix Proportions (kg/m3)			
Concrete Type	NWC	LWC	MLWC
Cement	250	250	125
Perlite Powder	0	0	125
Water	133	202	202
0-3 mm Perlite Aggregate	0	883	883
8-12 mm Perlite Aggregate	0	657	657
0-4 mm Limestone Aggregate	1111	0	0
4-12 mm Limestone Aggregate	421	0	0
12-25 mm Limestone Aggregate	526	0	0
Superplasticizer	2.5	2.5	2.5

Table 7. Properties of Fresh Concrete

Concrete Type	W/C	Slump (mm)	Air-Content (%)	Density (kg/m^3)
NWC	55	85	2	2410
LWC	80	100	2.5	1913
MLWC	80	90	2.2	1910

After the preparation of the concrete mixtures, various fresh concrete tests are performed to measure and evaluate the workability, durability and integrity of the mixtures. The results obtained from the tests are presented in Table 7.

In the light of results obtained from fresh concrete samples, the removal time of cases of normal weight concrete is 24 hours after pouring of concrete while for lightweight concrete and modified lightweight concrete is 48 hours after pouring. In order to prevent the dehydration of fresh concrete, humid blankets are used. After removing the molds, the specimens are left for curing in the curing pool of 21 °C in the Construction Materials Laboratory.

3. Tests and Results

3.1 Normal Weight Concrete

In the experimentation of normal weight concrete specimens, concrete gained early strength in a couple of days as expected due to the use of rapid setting cement type. Accordingly, the unconfined specimens tests started in the 3rd day, after which, the confined specimens were tested a day later, both at a loading rate of 1mm/min.

The peak strength observed in unconfined samples is about 16 MPa, this value was considered to be an acceptable level of peak strength gained, where the strain at peak strength is observed as 0.0038. On the other hand, the confined samples with 30 mm spiral spacing had a peak strength value of 17.7 MPa, with a strain of 0.006. The energy absorbed at the ultimate strain is calculated as 1709 kN.mm. Next, 50 mm spiral spaced confined normal weight concrete samples are tested. The maximum strength is recorded as 16.7 MPa with a strain of 0.0055 at this point. The energy absorbed at the ultimate strain, εc20, is calculated as 802 kN.mm. The stress-strain diagrams, regarding the average of three samples, for unconfined and confined with 30 mm and 50 mm spiral spaced concrete samples are presented in Figure 3.

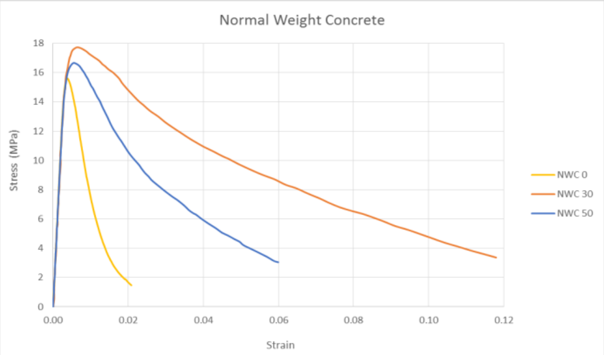

Figure 0. Stress-Strain diagram of Normal Weight Concrete

The results obtained from the series of experiments are compared with the theoretical calculations, those obtained in the light of Kent and Park Model [4]. The theoretical and experimental results differed from each other in some respects. In the experimentation of 30 mm spiral spaced concrete, maximum stress achieved is 6% smaller than the theoretical results, whereas the strain at the ultimate stress is 30% greater than the theoretical calculations. Similarly, the maximum stress for the 50 mm spiral spaced concrete is 5% smaller than the theoretical calculations, with a 28% smaller strain at the point of maximum stress.

Additional samples are tested 180 days later in order to observe the strength gain behavior of unconfined and confined normal weight concrete. Unconfined specimens gained strength to reach an average peak stress of 41.53 MPa, confined specimens with 30 mm and 50 mm spiral spacing showed near results of 41.88 and 41.39 MPa peak stresses, respectively.

3.2 Light Weight Concrete

In the case of lightweight concrete, the concrete specimens were tested starting from the 7th day as anticipated to reach the expected results. The maximum load carrying capacity is recorded as 133.5 kN and 17 MPa with a strain of 0.0042. The strain and stress experienced are in line with the predicted results.

As unconfined samples reach strength of 19 MPa, confined samples tests started. In Figure 4, relevant stress-strain diagrams are presented for unconfined and confined concrete with spiral spacing of 30 mm and 50 mm. The test set up and experimentation is presented in Figure 5. The peak strength of unconfined lightweight concrete samples is recorded as 19 MPa with a strain of 0.0046. Successively, the confined concrete samples are being tested under compression with a loading rate of 1 mm/min. The peak strength observed in the test of 30 mm spiral spaced samples is recorded as 20.6 MPa with a strain of 0.006. The energy absorbed at the ultimate strain is calculated as 776 kN.mm. Following the 30 mm spiral spaced samples, 50 mm spiral spaced concrete samples are tested. The maximum stress is recorded as 19.88 MPa with a strain of 0.0054. The energy absorbed, according to the results mentioned, is observed as 498 kN.mm.

The results obtained from the experimentation are compared with the theoretical calculations based on Kent and Park Model. For 30 mm spiral spaced samples, the ultimate stress experienced is 9% smaller than the theoretic calculations, whereas the strain at ultimate load is 20 % greater than the theoretic calculations. The results observed for 50 mm spacing do differ from the results of 30 mm spiral spaced samples. The ultimate stress is 6 % smaller than the theoretical calculations. While, the strain at the ultimate load for 50 mm spiral spaced is 8% greater than the theoretical calculations.

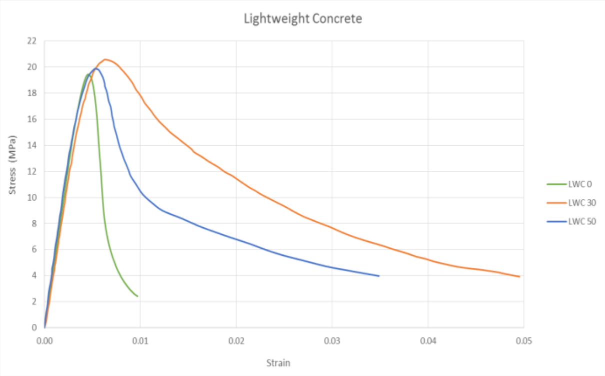

Figure 4. Stress-Strain diagram of Lightweight Concrete, 11 Days

Figure 5. Test Set up and Experimentation

As a later step, similar specimens in this group are tested 180 days later. Unconfined specimens showed an average maximum compressive strength of 32.95 MPa. Yet, while confined specimens with 30 mm spacing showed higher results, 35.40 MPa compressive strength, samples with 50 mm spaced confinement showed relatively close average result of 31.87 MPa.

3.3 Modified Light Weight Concrete

The compressive strength of modified lightweight concrete samples is tested in several days. These experiments were conducted on the 7th, 14th, 21st, 28th and 42th days. Being close to the results expected, the final tests are conducted on 42nd day.

The compressive strength of modified lightweight concrete has increased day by day after moulding. As seen in the Figure 6, the compressive strength has increased from 7 MPa to 15 MPa between 7th and 42nd days. Similarly, its elasticity modulus increased approximately double of its value from 7th day to 42nd day. As seen in Figure 7, the unconfined sample of modified lightweight concrete reached a compressive strength of 15.37 MPa with a strain of 0.005 relatively. The ultimate strain reached demonstrates the great energy absorption capacity of modified lightweight concrete.

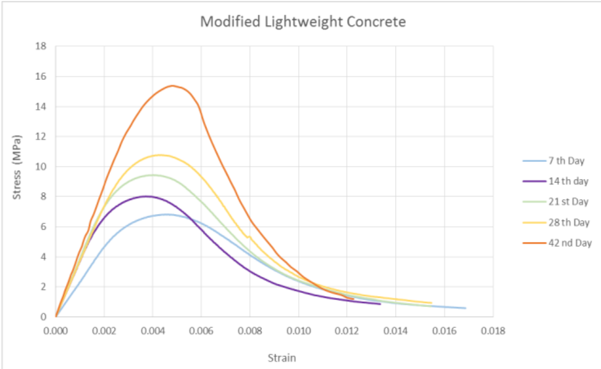

Figure 6. Stress-Strain diagram of Unconfined Modified Lightweight Concrete

In the next step, confined samples of modified lightweight concrete are tested. Initially, the samples with 30 mm spiral spacing are tested. The samples tested have reached an average value of 17.6 MPa with a strain of 0.008. The energy absorption capacity of the sample is calculated as 1159.55 kN.mm. Then, the confined samples of 50 mm spiral spacing are tested. The samples have an average compressive strength of 16.23 MPa with a strain of 0.006. The energy absorption capacity is calculated as 499.93 kN.mm. The overall results of tests performed on modified lightweight concrete are presented in Figure 7. The results of modified lightweight concrete are compared with the Kent and Park Model, as well.

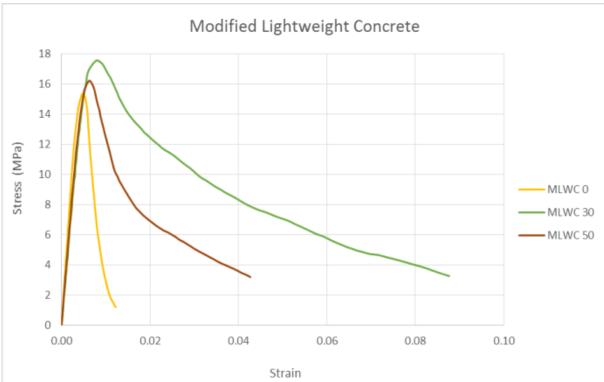

Figure 7. Stress-Strain diagram of Modified Lightweight Concrete

In the case of samples with 30 mm spiral spacing, the experienced ultimate stress is 6% smaller than the theoretical calculations. On the other hand, the samples experienced a strain of 26% greater than the theoretical calculations. Similarly, the 50 mm spiral spaced specimens have 6% smaller ultimate stress with 12% greater strain, when compared with the theoretical calculations.

To study the behaviour of confined perlite modified light weight concrete in long periods; additional specimens are tested in deformation controlled machine at 180 days. The samples with both spiral spacing showed a significant increase in the peak compressive strength. As can be seen in Figures 8 and 9, 30 mm spaced specimens showed peak strength of 21.53 MPa and 50 mm spaced specimens resulted with 20.51 MPa.

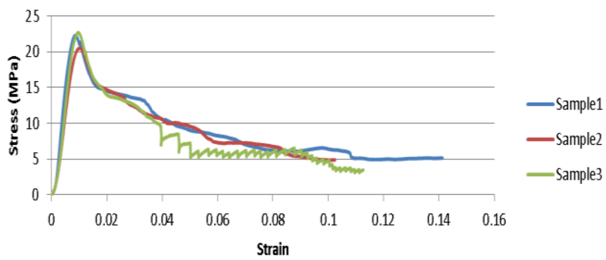

Figure 8. Stress-Strain diagram of Modified Lightweight Concrete with 30 mm spaced spirals.

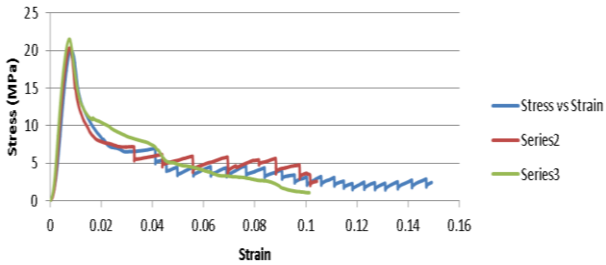

Figure 9. Stress-Strain diagram of Modified Lightweight Concrete with 50 mm spaced spirals.

4. Conclusion

In the light of experimental studies on cylinder specimens, it is concluded that lightweight concrete and modified lightweight concrete have comparatively weaker performance in terms of ultimate strain and energy absorption capacities, but with the presence of spiral confinement provides significant increase in energy absorption for these materials. The performance of lightweight concrete as a structural material cannot be disregarded in terms of its ultimate strength and relative strain values. Although use of lightweight concrete is prevented in some structural codes, through the experiments performed, it is conspicuous that lightweight concrete can reach the required mechanical and physical properties easily. In this respects, limitations on the use of lightweight concrete does only prevent the advances in the area and discourage the attention of both researchers and designers. Through further studies and advances in lightweight concrete, it will be fair to realize that lightweight concrete is a reliable construction material even for structural purposes as normal weight concrete is.

5. References

[1] American Concrete Institute (ACI), 1983, Standard Building Code Requirements for Reinforced Concrete, ACI 318-63

[2] Hlaing, M.M., Huan, W.T., Thangayah, T., 2010, Response of Spiral-Reinforced Lightweight Concrete to Short-Term Compression, Journal of Materials in Civil Engineering, ASCE, Vol. 22 Issue 12

[3] Leung, H.Y. and Burgoyne, C.J., 2001, Compressive Behaviour of Concrete Confined by Aramid Fibre Spirals, The International Conference on Structural Engineering Mechanics and Computation, Cape Town, pp. 1357-1346.

[4] Kent D.C. and Park R., 1971, Flexural Members with Confined Concrete, Journal the Structural Division, American Society of Civil Engineers, New York, Vol. 97, ST7.

[5] Aşık, M., 2006, Structural Lightweight Concrete with Natural Perlite Aggregate and Perlite Powder, MSc Thesis, Middle East Technical University, Department of Civil Engineering, Ankara.

[6] Eser, H., 2014, High Performance Structural Lightweight Concrete Utilizing Natural Perlite Aggregate and Perlite Powder, MSc Thesis, Middle East Technical University, Department of Civil Engineering, Ankara.

SECM/15/114

Planning & Mitigation Methods to Reduce the Project Delays in Sri Lankan Civil Engineering Construction Industries

M. Kesavan[1*], N. N. Gobidan[2] and P. B. G. Dissanayake[3]

[1]University of Peradeniya, Peradeniya, Sri Lanka
[2]University of Peradeniya, Peradeniya, Sri Lanka
[3]University of Peradeniya, Peradeniya, Sri Lanka
*E-Mail: k7efac@gmail.com, TP: +94772980321

Abstract: A construction project is commonly acknowledged as a successful project when the aim of the project is achieved in terms of predetermined objectives of completing the project on time, within budget and to the required quality standard. Delay in the completion of a construction project can be a major problem for contractors, consultants as well as for clients. These delays lead to costly disputes and adverse relationships amongst project participants. Projects can be delayed due to large number of reasons. The reasons are related to various types of uncertainties associated with activities during the construction process or during the planning and design stages. Project delays in general are due to delays caused by the client, delays caused by the contractors/consultants and delays due to equipment/materials & environmental factors. The objective of this research was to identify the major causes of construction project delays in the construction industries in Sri Lanka and find out how planning and mitigation methods would minimize their impacts. This study was carried out through questionnaire surveys and interviews conducted within the construction industry professionals in Sri Lanka. It is expected that this study would identify project planning deficiencies in the construction industry and propose recommendations to rectify identified issues and thereby reduce project delays which would contribute towards sustainable construction.

Keywords: Construction Delays, Construction Planning, Project Delays, Project Planning

1. Introduction

A construction project is a high risk activity which must be managed effectively in all stages.

A project represents a unique set of activities that need to be completed to produce a unique product. The success of a product is judged by meeting the criteria of cost, time, quality, safety.

One of the most important problems that may occur in a construction project is delays and the significance of these delays vary considerably from project to project. Any disruption to a project's objectives will certainly contribute to project delays with its specified adverse effects on project objectives.

The causes for construction project delays are client related causes, contractor related causes, consultant related causes, material related causes, labour related causes, and equipment related causes and external causes. The effects of construction delays are acceleration of work, schedule change, delayed project completion, increased cost, liquidated damages etc.

Planning is the heart of construction project management. The planner must weigh the cost and the reliability of different options, at the same time ensuring technical feasibility. Construction planning is more difficult in same ways since the construction process is dynamic as the site and the physical facility change over time as construction proceed.

2. Literature Review

Several researchers have studied about the causes of the construction project delays in different countries. The findings of such studies have been reviewed for this research.

Frimpong et al (2001) had carried out the research on finding out delay causes in ground water construction projects in 2001 in Ghana as a case study. The objective was to study and evaluate the factors that contribute to delay and cost overrun in ground water constructions.

There were 26 factors affecting construction delays identified from the previous observations their relative importance index were determined.

Monthly payment difficulties from agencies, poor contractor management, planning and scheduling deficiencies, material procurement and poor technical performance were identified as major causes of delays. Identifying appropriate funding levels of the projects at planning stage, introducing training programmes to improve managerial skills of the contractors and introducing effective material procurement systems were suggested as mitigation activities.

Chan and Kumaraswamy (1997) did a survey to assess the relative importance of 20 potential delay factors in Hong Kong construction projects and five key factors were found, such as poor risk management and supervision, unforeseen site conditions, slow decision making, client-initiated variations, and work variations. However, Al-Momani (2000) in a research on construction delays in 130 public projects in Jordan found that weather, site conditions, late deliveries, economic conditions and increase in quantity are the critical factors which cause construction delays in Jordan construction industry.

Assaf *et al.* (1995) identified 56 main causes of delay in large building construction projects in Saudi Arabia and calculated their relative importance. Based on the contractors surveyed the most important delay factors were preparation and approval of shop drawings, delays in contractor's progress, payment by owners and design changes.

3. Objective and Scope

3.1 Objective of the study

i. Study the causes of construction project delays
ii. Identify methods to minimize construction project delays
iii. Propose proper project planning methods to avoid construction project delays

3.2 Scope of the study

The scope of the study was limited to Sri Lankan civil engineering projects such as Building, Roads/Highway, Irrigation, Water supply etc.

4. Methodology

To understand the current status of project delays and planning solutions in construction industry, the data collection was carried out through a questionnaire survey and a series of interviews. Preliminary survey was carried out through interviews and discussions to finalize the questionnaire.

The questionnaire survey included 107 nos. Sri Lankan construction projects. The questionnaire was divided into three main parts. Part one includes the details of the respondents and organizations in order to get the information about the respondent's details and organization as well. Part two included factors that cause construction project delays in Sri Lankan construction industry. This part is comprised of seven categories such as client, contractor, consultant, materials, equipment, labour and external factors.

Causes of delays by Client

- Delay in progress payments
- Delay to furnish and deliver the site
- Change orders by owner during construction
- Delay in revising and approving design
- Delay in approving shop drawing and sample
- Poor communication and coordination
- Slowness in decision making process
- Conflicts between joint-ownership of the project
- Suspension of work by client

Causes of delays by Contractor

- Difficulties in financing project
- Conflicts in sub-contractors schedule
- Rework due to errors during construction
- Conflicts between contractor and other parties
- Poor communication and coordination
- Ineffective planning and scheduling of project
- Implementation of improper construction
- Delays in sub-contractors work
- Inadequate contractor's work
- Frequent change of sub-contractors
- Poor qualification of the contractor's technical staff
- Delays in site mobilization

Causes of delays by Consultant

- Poor communication and coordination
- Delay in approving major changes in the scope of work
- Inadequate experience of consultant
- Mistakes and discrepancies in design documents
- Delays in producing design documents
- Unclear and inadequate details in drawings
- Insufficient data collection and survey before design
- Non-use of advanced engineering design software

Causes of delays by Material

- Shortage of construction materials in market
- Changes in material types during construction
- Delay in material delivery
- Damage of sorted material while they are urgently needed
- Delay in manufacturing special building materials
- Late procurement of materials

Causes of delays by Labour

- Shortage of labours
- Work permit of labours
- Low productivity level of labours
- Personal conflicts among labours

Causes of delays by Equipment

- Equipment breakdowns
- Shortage of equipment
- Low level of equipment operator's skill
- Low productivity and efficiency of equipment
- Lack of high-technology mechanical equipment

External causes of delays

- Effects of subsurface and ground conditions
- Delay in obtaining permits from municipality
- Weather effect on construction activities
- Traffic control and restriction at job site
- Accident during construction
- Changes in government regulations and laws
- Delay in providing services from utilities
- Delay in performing final inspection and certification

Part three included identified mitigation methods to reduce the impact of project delays.

- Proper project planning and scheduling
- Effective strategic planning
- Site management and supervision
- Collaborative working in construction
- Frequent coordination between the parties involved
- Frequent progress meeting
- Accurate initial cost estimates

The questions were based on the Liker's scale of five ordinal measures from 1 to 5 (very low effect to very high effect) according to level of contributing.

- Relative Importance Index (RII) was calculated.

$$RII = \frac{\sum w_i x_i}{\sum x_i}$$

Where:
i - Response category index
w_i - Weight assigned to i^{th} response (1, 2, 3, 4, 5 respectively)
x_i - Frequency of the i^{th} response given as percentage of the total responses for each factor

- The factors were ranked in each category based on the Relative Importance Index (RII)

5. Analysis and Results

5.1 Factors that contribute to construction project delays

All the causes of delays were ranked based on their Relative Importance Index as shown below.

Table 4.1: Ranking of Causes of Delay in Sri Lankan Construction Projects

Causes of delay	**RII**	**Rank**
Conflicts in sub-contractor's schedule during execution of project	3.27	1
Delay in progress payments	3.27	1

Weather effect on construction activities	3.22	3
Difficulties in financing project	3.21	4
Shortage of labour	3.20	5
Frequent change of sub-contractors	3.18	6
Low productivity level of labour	3.14	7
Delays in sub-contractor's work	3.13	8
Rework due to errors during construction	3.13	8
Effects of subsurface and ground conditions.	3.08	10
Poor communication and coordination	3.08	10
Delay in material delivery	3.07	12
Delay in approving major changes in the scope of work	3.03	13
Personal conflicts among labour	3.02	14
Ineffective planning and scheduling of project	3.01	15
Change orders by owner during construction	3.01	15
Insufficient data collection and surveying before design	3.00	17
Slowness in the decision making process	3.00	17
Suspension of work by owner	2.98	19
Lack of high-technology	2.97	20
Inadequate contractor's work	2.94	21
Traffic control and restriction at job site	2.94	21
Delay to furnish and deliver the site	2.93	23
Shortage of equipment	2.92	24
Delays in producing design documents	2.92	24
Non use of advanced engineering design software	2.92	24
Equipment breakdowns	2.91	27
Delay in obtaining permits from municipality	2.91	27
Poor communication and coordination	2.91	27
Improper construction methods implement	2.90	30
Delay in approving shop drawing and sample materials	2.90	30
Late procurement of materials	2.89	32
Delay in manufacturing special building materials	2.88	33
Conflicts between contractor and other parties	2.87	34
Unclear and inadequate details in drawings	2.83	35
Delay in revising and approving design documents	2.83	35
Shortage of construction materials in market	2.82	37
Low productivity and efficiency of equipment	2.81	38
Work permit of labours	2.79	39
Poor communication and coordination	2.78	40
Changes in material types during construction	2.77	41
Poor qualification of the contractor's technical staff	2.75	42
Delay in providing services from utilities	2.73	43
Damage of sorted material while they are needed urgently	2.73	43
Mistakes and discrepancies in design documents	2.73	43
Delay in performing final inspection and certification	2.72	46
Inadequate experience of consultant	2.71	47
Low level of equipment-operator's skill	2.71	47
Changes in government regulations and laws	2.64	49
Conflicts between joint-ownership of the project	2.59	50
Delays in site mobilization	2.59	50
Accident during construction	2.40	52

5.2 Factors affecting construction project delays

Delay affecting factors were ranked based on their Relative Importance Index shown below.

Table 2: Ranking of delay affecting factors

Related Factors	RII	Rank
Labour	3.04	1
Contractor	2.99	2
Client	2.92	3
Consultant	2.90	4
Equipment	2.86	5
Material	2.86	6
External	2.83	7

5.3 Mitigation methods to reduce delays in Sri Lankan construction projects

Methods of minimizing delays are ranked based on their Relative Importance Index shown below.

Table 3: Ranking of mitigation methods to reduce delays in Sri Lankan construction projects

Minimizing methods	**RII**	**Rank**
Proper project planning and scheduling	3.97	1
Effective strategic planning	3.93	2
Collaborative working in construction	3.77	3
Site management and supervision	3.75	4
Frequent coordination between the parties involved	3.71	5
Accurate initial cost estimates	3.70	6
Frequent progress meetings	3.68	7

6. Conclusion

Delay in Sri Lankan construction projects is mostly originated by labour, followed by contractor and client, while external related causes are less important. Client and contractor specified that labour related causes as sources of delay. Conflicts in sub-contractors schedule, delay in progress payments, weather effects on construction activities, difficulties in financing project, shortage of labour, frequent change of subcontractors, low productivity level of labour, delays in sub-contractor's work, rework due to errors during construction and effects of subsurface and ground conditions are the top 10 major causes of delay in Sri Lankan construction projects. Proper project planning and scheduling and Effective strategic planning are the major mitigation methods to reduce construction project delays in Sri Lanka.

7. Recommendation

Continuous monitoring, financial controlling, labour management, revising schedule, material/ Equipment controlling and usage of planning softwares are the planning activities proposed to minimize and control delays in Sri Lankan construction projects.

The clients should pay special attention to minimize changes in order during construction so as to avoid delays, pay progress payment to the contractors on time as it weakens the contractor's ability to finance the work and speed up reviewing and approving of design documents. Consultants should focus on avoid delays in reviewing and approving design documents, build up the knowledge and skills of technical staff and improve coordination between parties. The contractors should give more attention to improve the knowledge and skills of technical staff and manage the financial resources and plan cash flow by utilizing progress payment.

More research on construction delays should be done in order to develop guidelines and planning activities.

Acknowledgement

The authors express gratitude to the Faculty of Engineering, University of Peradeniya for providing an opportunity to contribute towards the research project funded by the University Research Grant RG/AF/2013/25/E. The authors would also like to express sincere and heartfelt gratitude to the Department of Civil Engineering, Faculty of Engineering, University of Peradeniya for the support provided during the study.

References

[1]. Al-Momani A.H. (2000).' Construction delays: a quantitative analysis', International Journal of Project Management, 18(1), 5–9.

[2]. Assaf S.A., Al-Khalil M. and Al-Hazmi M. (1995). 'Causes of Delay in Large Building Construction Projects', Journal of Project Management in Engineering ASCE, 2; 45-50.

[3]. Bon G. Hwang & Lay P. Leong (2013). 'Comparison of schedule delay and causal factors between traditional and green construction projects', Technological and Economic Development of Economy, Vol.19, pp.310-330.

[5]. Thomas Ng, Cheung Sai On and Mohan M Kumaraswamy(2004). 'Selection of Activities to be crashed for Mitigating Construction Delays'. HKIE Transactions, Vol.11, pp.42-47.

[6]. Assaf S.A. and Al Hejji S. (2006). 'Causes of delay in large construction projects', International Journal of Project Management, 24, 349-357.

[7]. Chan D.W.M. and Kumaraswamy M.M. (1997). 'An evaluation of construction time performance in the building industry', Journal of Building and Environment, 31(6), 569-578.

[8]. Mohan M. Kumaraswamy & Daniel W. M. Chan (1998). 'Contributors to construction delays', Construction Management and Economics, 16, 17-29.

[9]. Murali Sambasivan & Yau Wen Soon (2007). 'Causes and effects of delays in Malaysian construction industry', International Journal of Project Management. 25, 517–526.

[10]. Odeh A.M. and Battaineh H.T.(2002). 'Causes of construction delay: Traditional contracts'. International Journal of Project Management, 220, 67-73.

[11]. Frimpong Y., Oluwoye J. and Crawford L.(2003). 'Causes of delay and cost overruns in construction of ground water projects in developing countries; Ghana as a case study', International Journal of Project Management. Vol.21, pp.321-326.

SECM/15/125

Atterberg Limits Estimation of Pilani Soil Using Ultrasonics

K. Kumar[1*]

[1]Birla Institute of Technology & Science, Pilani, Jhunujhunu, India
[*]E-Mail: kamalesh@pilani.bits-pilani.ac.in

Abstract: Depending on water content, four physical states of soil consistency are used. The water contents at which soil undergoes physical state change are called Atterberg limits. Liquid as well as plastic limit are two commonly used Atterberg limits and are used extensively, either individually or together, with other soil properties to correlate with engineering behavior such as compressibility, compactibility, shrink-swell and shear strength. Conventional method of liquid limit determination requires test to be conducted at 5 (at least) different water contents for accurate estimation. Even liquid limit estimation using cone penetrometer requires experiment to be carried out at more than one water content. Same is applicable for plastic limit estimation. Sand content has effect on its liquid and plastic limit, as well as pulse velocity through it. Consequently, it should be possible to estimate liquid and plastic limit by knowing pulse velocity through it. Pulse velocity using through transmission technique (at constant water content and density); as well as their liquid and plastic limits using conventional techniques at varying sand content were determined and plotted for Pilani soil. This plot can be used as calibration curve for aforementioned estimation purposes and can be developed for other region soils as well.

Keywords: Atterberg limits, Calibration curve, Soil behavior, Through transmission technique, Ultrasonic pulse velocity.

1. Introduction

The Atterberg limits are basic measure of the critical water contents of a fine-grained soil, such as its shrinkage limit, plastic limit, and liquid limit. As a dry, clayey soil takes on increasing amounts of water, it undergoes dramatic and distinct changes in behavior and consistency. Depending on the water content of the soil, it may appear in four states: solid, semi-solid, plastic and liquid. In each state, the consistency and behavior of a soil is different. Consequently so are its engineering properties. Thus, the boundary between each state can be defined based on a change in the soil's behavior. The Atterberg limits can be used to distinguish between silt and clay. It can distinguish between different types of silts and clays. These limits were created by Albert Atterberg, a Swedish chemist. They were later refined by Arthur Casagrande. These distinctions in soil are used in assessing the soils that are to have structures built on it. Soils when wet retain water and expand in volume. The amount of expansion is related to the ability of the soil to take in water and its structural make-up. These tests are mainly used on clayey or silty soils since these are the soils that expand and shrink due to moisture content. Clays and silts react with water, thus size changes and they have varying shear strengths. Thus these tests are used widely in the preliminary stages of designing. It ensures that the soil will have correct amount of shear strength and not too much change in volume as it expands and shrinks with moisture content.

As a hard, rigid solid in dry state, the soil becomes a crumbly semisolid when a certain water content, termed the shrinkage limit, is reached. If it is an expansive soil, this soil will also begin to swell in volume as this water content is exceeded. Increasing the water content beyond the soil's plastic limit transforms it into a malleable, plastic mass, causing additional swelling. The soil will remain in plastic state until its liquid limit is exceeded with increase in water content. This causes it to transform into a viscous liquid that flows when jarred [1].

If silty clay content in sand changes, its liquid limit and plastic limit also changes. This change in liquid limit & plastic limit is due to change in soil micro-structure as well as due to change in inter-particle interaction between soil particles in the presence of pore water when silty clay content changes. These two limits are determined using standard experiments in the soil mechanics laboratory.

The original liquid limit test of Atterberg involved patting a mixture of soil and water in a round-bottomed porcelain bowl of 10–12 cm diameter. A groove was cut through the soil-water mixture with spatula, and the bowl was then struck many times against the palm of one hand. Casagrande subsequently standardized the apparatus and the procedures to make the measurement more repeatable. Soil is placed into the metal cup portion of the device and a groove is made down its center with a standardized tool of 13.5 millimetres width. The cup is repeatedly dropped 10 mm onto a hard rubber base at a rate of 120 blows per minute, during which the groove closes up gradually as a result of impact. The number of blows for the groove to close is recorded. The water content at which it takes 25 drops of the cup to cause the groove to close over a distance of 13.5 millimetres is defined as liquid limit. The test is normally run at several water contents, and the water content which requires 25 blows to close the groove is interpolated from the test results.

Another method for measuring the liquid limit is fall cone test, also called cone penetrometer test. It is based on the measurement of penetration into the soil of a standardized cone of specific mass. Although the Casagrande test is widely used across North America, the fall cone test is much more prevalent in Europe due to being less dependent on the operator in determining the Liquid Limit. In this method also, several water contents have to be tested.

The plastic limit is determined by rolling out a thread of fine portion of a soil on a flat, non-porous surface. If the soil is at water content where its behavior is plastic, this thread will retain its shape down to a very narrow diameter. The sample can then be remoulded and the test repeated. As the moisture content falls due to evaporation, the thread will begin to break apart at larger diameters [2]. The plastic limit is defined as the water content where the thread breaks apart at a diameter of 3.2 mm. A soil is considered non-plastic if a thread cannot be rolled out down to 3.2 mm at any water content.

It is clear from aforementioned discussion, that experiments involved in determining liquid & plastic limits are quite complicated and time consuming. There should be alternative technique of estimating it. In the present study, it has been achieved using ultrasonics.

Ultrasonic testing is a family of non-destructive testing techniques based on the propagation of ultrasonic waves in the object or material tested. In most common applications, very short ultrasonic pulse-waves with center frequencies ranging from 0.1-15 MHz, and occasionally up to 50 MHz, are transmitted into materials [3]. Ultrasonic testing is often performed on steel and other metals and alloys, though it can also be used on concrete, wood, soil and composites, albeit with less resolution. Obtained ultrasonic pulse velocity changes with change in material micro-structure, soil particle size composition for example.

When ultrasonic pulses travel through soil samples, the pulse velocity changes with changes in properties of the soil such as density, moisture content, void ratio, porosity, degree of saturation and particle size composition [4]. Hence variation in any one of these parameters can be correlated with the changes in the ultrasonic pulse velocity, provided other parameters remain unaltered. In the present study, variation in ultrasonic pulse velocity with soil particle size composition has been studied. Frequency of ultrasonic pulses used in the present study was 0.15 MHz. Study has been conducted at 10% water content and at constant density of soil compact at 1.45 gm/cm^3.

Ultrasonic pulse velocity testing is a long established non-destructive testing method. It involves determination of velocity of ultrasonic pulses through the sample. This can be achieved by measuring time taken by ultrasonic pulse to travel a measured distance in the soil sample. Transducers are placed in contact with the sample and low frequency transducers are used for this purpose. Measurement can be done using through transmission technique. In this method transmitting and receiving transducers are placed on the opposite faces of the soil sample. The axes of the transducers are aligned. The pulse velocity is determined by using the single equation:

Pulse velocity = path length/transit time (1)

This single equation can be applied to transmission of pulses through material of any shape or size. Only restriction being that the least lateral dimension (dimension measured perpendicular to the path of pulses) should not be less than the pulse amplitude. Plan area of soil samples used in present study in ultrasonic testing was 6 cm x 6 cm. Sample thickness was 1.7 cm.

The pulse velocity is not affected by the frequency of the pulse. As a result the wavelength of the pulse vibrations is inversely proportional to its frequency. Thus pulse velocity will generally depend only on the properties of materials. For assessing quality of materials from ultrasonic pulse velocity measurement, measurement should be of high accuracy. Path length and transit time should each be measured to an accuracy of about $\pm$ 1% [5]. Velocity of ultrasonic pulses in present study in which soil particle composition was changing was found to range from 340 m/s to 510.5 m/s.

Liquid limit, plastic limit as well as ultrasonic pulse velocity (at constant water content & bulk density) strongly depend on soil particle size composition. This fact has been used to develop calibration curves to estimate liquid as well as plastic limit by knowing ultrasonic pulse velocity through it for Pilani soil in the present study.

2. Experimental details and discussion

Experimental work required coarse-grained as well as fine-grained soil. Coarse-grained soil was collected from desert stretch located some distance from Institute campus. Soil from this location was predominantly coarse grained. Soil sample had an in-situ moisture content of 4 to 5%. Experimental work also required fine grained soil. This soil was available locally close to the Institute campus at a depth of 12 to 15 meters. It was collected in the month of April from a deep ditch excavated at that location and the in-situ water content of the soil was 6%. Both soils were oven dried for 24 hours before using it for experiments.

Coarse grained soil retained on 150 μ sieve has been classified as sandy. Similalrly fine grained soil retained on 75 μ sieve as well as on pan have been classified as silty clay. This classification is based on dispersion test.

Five different particle size composition of soil were used in the present study, S_{150} = 90% by weight, C_{75} = 5% by weight, C_p = 5% by weight; S_{150} = 70% by weight, C_{75} = 15% by weight, C_p = 15% by weight; S_{150} = 50% by weight, C_{75} = 25% by weight, C_p = 25% by weight; S_{150} = 30% by weight, C_{75} = 35% by weight, C_p = 35% by weight; S_{150} = 10% by weight, C_{75} = 45% by weight, C_p = 45% by weight. S_{150} refers to sand retained on 150μ sieve, C_{75} refers to silty clay retained on 75μ sieve and C_p refers to silty clay retained on pan.

Liquid and plastic limit of aforementioned five soil samples were determined as per specifications [6]. Ultrasonic pulse velocity of same these samples were determined by using ultrasonic materials tester (Model : Emefco type UCT3). This ultrasonic materials tester is a low ultrasonic frequency (150 kHz) tester for civil engineering applications. Coarse grained samples like soils can conveniently be tested with this ultrasonic materials tester. Transmission time of the ultrasonic wave was measured through a given soil sample of known thickness. Testing was done using through transmission technique.

Transmitting and receiving transducers having diameter of 36 mm each were placed on the opposite faces of the soil sample so that their axes remain collinear. Grease was used as coupling agent between transducer face and soil sample. Ultrasonic wave passes through the soil sample from transmitting to receiving transducer. Transmission time of ultrasonic pulse was measured using this ultrasonic materials tester and pulse velocity was determined from Equation (1). Results of the experiments are summarized in Table 1 and plotted in Figure 1.

Table 1: Liquid limit, plastic limit and ultrasonic pulse velocity variation with sand content

Sand content (%)	Liquid limit (%)	Plastic limit (%)	Ultrasonic pulse velocity (m/s)
10	29	19.4	459.4
30	28	18.2	510.5
50	24.4	14.1	448.5
70	23.7	13.8	376.1
90	24.5	14.3	340

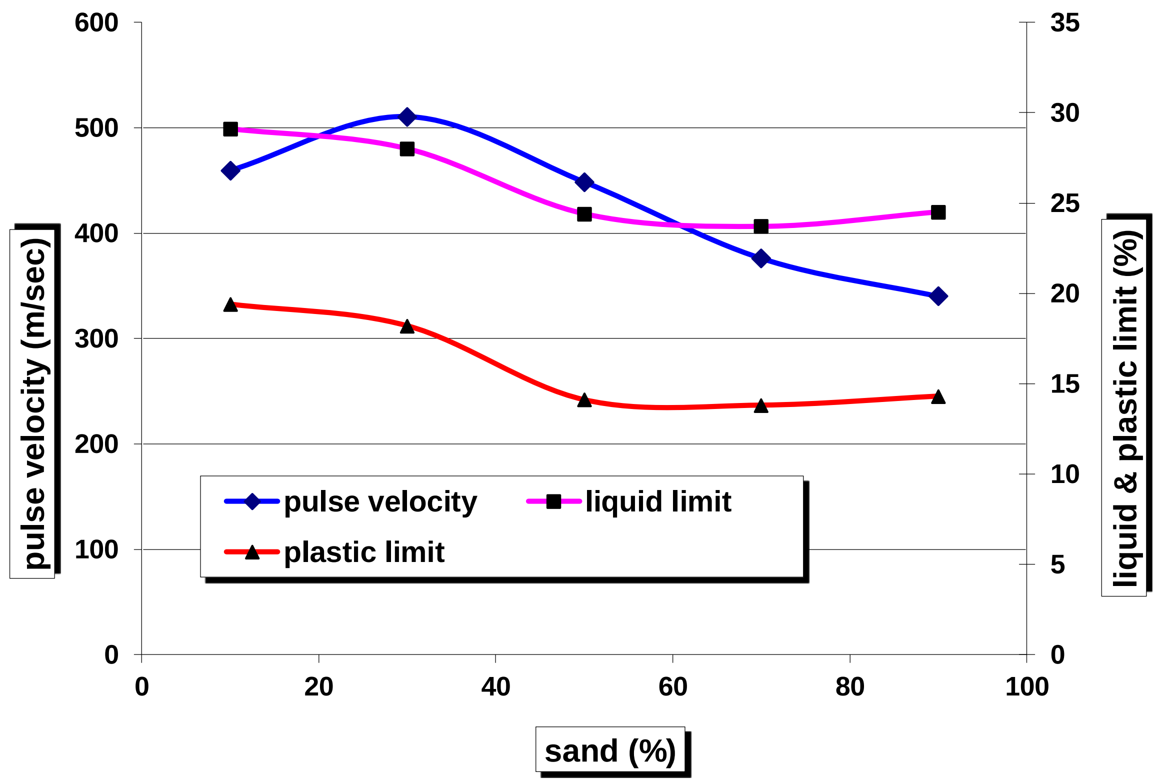

Figure 1: Liquid limit, plastic limit and ultrasonic pulse velocity variation with sand content

There is attraction as well as repulsion between soil particles in the presence of water [7]. From Figure 1 & Table 1 it is clear that as sand content increases from 10% to 70%, attraction effect decreases (in plastic as well as in semi-solid state) resulting in decrease in liquid as well as in plastic limit. For sand content increase from 70% to 90%, there is attraction effect increase (in plastic as well as in semi-solid state) resulting in increase in liquid as well as in plastic limit.

When an ultrasonic pulse propagates through soil, attenuation of the ultrasonic pulse takes place along the travel path. Scattering of ultrasonic pulse at the microscopic interface of soil particles is an important mechanism for attenuation of ultrasonic pulse. When particle size of soil increases, scattering of ultrasonic pulses also increases. Consequently an increase in soil particle size results in increased attenuation. An increase in attenuation of ultrasonic pulses through soil, in turn leads to higher transmission time of ultrasonic pulses through soil. Consequently ultrasonic pulse velocity decreases [8].

In the present study, sand content of soil was reduced from 90% to 30%, i.e. silty clay content of soil increased from 10% to 70%. This resulted in the decrease of ultrasonic attenuation leading to higher ultrasonic pulse velocity. The observed increase in ultrasonic pulse velocity was from 340 ms^{-1} to 510.5 ms^{-1} corresponding to the said decrease in sand content of soil from 90% to 30%.

If one goes for further reduction in sand content of soil from 30% to 10% i.e. increase in silty clay content from 70% to 90%, it leads to aggregation of silty clay soil particles in the presence of water resulting in floc formation. The flocculated silty clay soil particles behave like coarse grained particles. Consequently attenuation also increases under such conditions. This results in reduction of ultrasonic pulse velocity through soil. In the present study, ultrasonic pulse velocity through soil was found to decrease when sand content of soil was reduced from 30% to 10%.

3. Development of calibration curves

Figure 1 can be used as calibration curve. One can take soil sample from required location in Institute campus as well as from the vicinity, oven dry it, sieve it through 300 micron sieve (standard sieves used in soil sieving are 2.36 mm, 1.18 mm, 600 micron, 300 micron, 150 micron, 75 micron and pan in that sequence) and find out ultrasonic pulse velocity through it using the technique described in previous two sections. Estimated values of liquid and plastic limit then can be directly read from Figure 1 as long as pulse velocity is less than 459.4 m/sec for the obtained pulse velocity. For pulse velocity more than 459.4 m/sec, aforementioned soil passing through 300 micron sieve can be sieved through 150 micron sieve also to get exact silty clay content. Figure 1 then can be used to read estimated values of liquid & plastic limit for the obtained pulse velocity. It is clear from Table 1 as well as from Figure 1 that a wide range of particle size composition has been covered. Similar calibration curve can be developed for other reigon soil also.

4. Conclusions

Liquid as well as plastic limit are two commonly used Atterberg limits and are used extensively, either individually or together, with other soil properties to correlate with engineering behavior such as compressibility, compactibility, shrink-swell and shear strength. Experiments involved in determining liquid & plastic limits are quite complicated and time consuming. There should be alternative technique of estimating it.

Technique suggested in present study involves determination of ultrasonic pulse velocity through soil sample for the development and use of the calibration curve. Use of non-destructive testing (NDT) techniques is finding increasing applications for assessing the quality of materials including quality of soils. These testing techniques are very useful because they provide the desired information about the properties of the material. Ultrasonic testing is one such non-destructive testing (NDT) technique and is used for testing materials of civil engineering importance (e.g. concrete, wood, brick etc.). Measuring ultrasonic pulse velocity through soil samples requires only a simple set-up and is welcome alternative for assessing liquid and plastic limit of soils. Similar calibration curves can be developed for other reigon soil also, and hence developed calibration curves in present study involving the determination of ultrasonic pulse velocity through soil is of great significance.

References

[1]. https://en.wikipedia.org/wiki/Atterberg_limits, Visited, 13th October, 2015.

[2]. Seed H.B. "Fundamental Aspects of the Atterberg Limits", J. of Soil Mechanics and Foundations Div., 92(SM4), 1967.

[3]. Brandt H., "A Study of Speed of Sound in the Granular Media", J. of Applied Mechanics, Vol.22, pp 479 – 486, 1955.

[4]. Blangy J.P., Strandenest S., Moos D. and Nur A., "Ultrasonic Velocity in Sands-Revisited", Geophysics, Vol. 58, No. 3, pp 344 – 356, 1993.

[5]. Krautkramer J. and Krautkramer H., Ultrasonic Testing of Materials, Springer-Verlag, Berlin, 1969.

[6]. IS:2720, Test for soils: Part 5 – 1985, Determination of liquid and plastic limit, 1995.

[7]. Lambe T.W., "The Structure of Compacted Clay", Proceedings, ASCE, Soil Mechanics and Foundations Division, Vol. 84, No. SM2, Paper No. 1654, 1958.

[8]. Koerner R.M., Lord A.E., McCabe W.M. and Curran J.W., "Acoustic Emission Behavior of Granular Soils", J. of the Geotechnical Engineering Division, ASCE, Vol. 102, No. GT7, pp 761-773, 1976.

SECM/15/135

Incorporating recycled PET fibres for concrete Cylindrical Culverts

Rathnayaka R.M.M.P, Malshan W.V.D, De Silva Sudhira and De Silva Subashi

Department of Civil and Environmental Engineering, Faculty of Engineering, University of Ruhuna, Galle, Sri Lanka
E-Mail: madushanpri@gmail.com, TP: +94779991335

Abstract: Fiber reinforced concrete is one of the prominent solutions for many problems that concrete had from its early stage. Polyethylene terephthalate (PET) fiber is a sustainable solution for fiber reinforced concrete since it makes fiber material an eco-friendly material. It's a well-known fact that steel reinforced concrete is vulnerable to corrosion. It is accelerated in the water conveying elements such as concrete pipes. So usage of PET fibers as a replacement material for steel reinforcement cage in reinforced concrete pipe element would definitely have a long life. At the initial stage concrete cubes were casted with different fiber compositions for water cement ratio of 0.3 and 0.45.From that it has observed that 2% of PET fiber would give the optimum result for concrete having 0.3 water cement ratio. Three sets of specimens (plain concrete, Reinforced concrete and PET fiber concrete) were subjected to three-edge-bearing test. It was identified that PET fiber reinforced concrete is the most applicable method for production of concrete pipes. Because manufacturing of the cage form of the conventional reinforcement bars adjusted for concrete pipes requires special bending, welding, and placement machinery, and also it is time-consuming. PET fibres of standard sizes, on the other hand, can be added to the pan-mixer of any concrete plant as if they were another aggregate or mineral admixture. Without any extra process modification, PET-fibre concrete can be produced and cast in the moulds similar to the ordinary plain concrete. Therefore it can be declared that PET-fibre concrete pipes seem to be an economical alternative to the classically-reinforced-concrete pipes.
.

Keywords: Recycled PET, PET Fiber reinforced concrete, cylindrical culverts, three edge bearing test

1. Introduction

Fiber reinforced concrete has become a prominent solution for the drawbacks of ordinary concrete. Pavement laying, shotcrete tunnel linings, blast resistant concrete, overlays, and application to mine construction have proven the above statement (Ochi T, Okubo S & Fukui K, 2007).

Polyethylene terephthalate (PET) analysed in present study belongs to the polyester group. Due to rapid development in the technology the use of PET materials has been increased. Among that PET bottles used for beverage containers has become a major issue. This will eventually become an environmental pollutant (Kim et al, 2010).Use of recycled PET fiber in fiber reinforced concrete would provide a sustainable solution for the environment pollution.

One of the application of fiber reinforced concrete can be identified as the casting of cylindrical pipes. Casting of the pipes using reinforced cage with concrete is the current practise. There are many advantages of using steel fiber reinforced concrete over the ordinary steel reinforcement pipe. Manufacturing of the cage form of the conventional reinforcement bars adjusted for concrete pipes requires special bending, welding, and placement machinery, and it is time consuming. Steel fibres of standard sizes, on the other hand, can be added to the pan-mixer of any concrete plant as if they were another aggregate or mineral admixture. Without any extra process modification, steel-fibre concrete can be produced and cast in the moulds similar to the ordinary plain concrete. Therefore, steel-fibre concrete pipes seem to be an economical alternative to the classically-reinforced-concrete pipes. But there is a significant drawback in steel fiber reinforced concrete cylindrical pipes. These pipes are used to convey liquid such as water and waste water. Therefore in the process of conveying liquid through these pipes steel or fiber could be exposed to the moisture. As a result of that steel fiber will be corroded and durability of the pipe would reduce. To overcome that problem PET fiber reinforced concrete is used in this study. As the first stage of the study different mix proportions were checked in order to identify the best mix proportion for the application.

Fraternali (2011) conducted an experiment in order to determine the compressive strength of FRC and identified that it has an improvement in the compressive strength over the normal concrete. And also it has been identified that compressive strength was increased with the increment of PET fiber diameter. Short PET fibers give more compressive strength than the long PET fibers. Despite of Fraternalis findings, Kim (2010) observed that there was a reduction of compressive strength by 1~10% as the volumetric fiber percentage increase form 0% to 1% with 0.25 increments. Marthong (2015) also identified that there is a reduction of compressive strength as the volumetric fiber percentage increases beyond 0.5%. Additionally, it was declared that compressive strength also varies with the geometry and the dimensions of fibers. Ochi (2006) conducted uniaxial compression test and identified that compressive strength of PET FRC was increased with the fiber content and this was valid up to 1% of fiber. While compressive strength was decreased with the increment of fiber content. Similar to the Ochi's findings Sandaruwani (2012) identified that compressive strength of PET FRC is increasing with the fiber content and this is valid up to 1% of fiber then the compressive strength is decreasing with the increment of fiber content.

According to the Marthong's (2015) findings, it was found that that the inclusion of PET fiber above 1.0% decreases the tensile strength. The inclusion of PET fiber improved the tensile property and showed the ability in absorbing energy in the post-cracking state due to the bridging action imparted by the fibers during cracking. But Sandaruwani (2012) identified that fiber content can be increased up to 2% with an improvement in the tensile strength. After that the tensile strength will reduce as the fiber content increase beyond 2%.

Haktanir (2007) conducted a research to identify the performance of fiber reinforced concrete as a material for concrete pipes. Steel fibers were used at dosages of 25kg/m^3 and 40 kg/m^3. In this study, three concrete pipes were casted using plain concrete, reinforced concrete and fiber reinforced concrete. The common type of Dramix RC80/60-BN steel fibres were used for one set of samples. Smaller type of steel fibres, ZP-308 was also used for another set of samples. The total length and cross-sectional diameter of RC80/60-BN and ZP-308 are 60 mm and 0.75 mm, and 30 mm and 0.75 mm, respectively.

Concrete pipes of 500mm inner diameter were casted. Concrete were poured in to steel mould which rests on a strongly vibrating platform. Three cylindrical samples of 150x300 mm were used to determine the compressive strength of the concrete.

Plain concrete pipes were casted using grade 35 concrete. Wall thickness of the pipe was 65 mm.For the reinforced concrete pipes, 7 mm reinforcement bars were used at 75 mm intervals.

Table 01: Test results (Haktanir (2007))

Pipe	Average ultimate load(KN)	Crack length (mm)	Crack width (mm)
Plain concrete	64.5	550	1.5
Reinforced concrete	110.6	217	0.22
ZP-308 25kg/m3	105.3	117	0.1
ZP-308 40kg/m3	112.3	93	0.03
RC80/60-BN 25kg/m3	117.4	85	0.02
RC80/60-BN 40kg/m3	120.8	53	0.02

Three edge bearing test was perfumed to each cylinder and results are shown in the Table 01.It can be identify that there is an improvement in fiber reinforced concrete over plain concrete and steel reinforced concrete.

The objectives of this present study were : to investigate the appropriate mix proportions and resultant variations in strength characteristics of fiber reinforced concrete made with re-cycled PET fibers and to investigate the mechanical and durability characteristics of fiber reinforced concrete made with shorter-cycled PET fibres and study its practical application in construction industry.

2. Methodology

2.1 Specimens for mix proportion identification

Re-cycled PET fibers obtained from Beira Group, Horana, Sri Lanka was introduced in to the concrete mix. PET fibber was added on the volume basis, and it would not replace any material in the concrete. Each PET fiber addition was done for two water cement ratios of 0.3 and 0.45 samples preparation as shown in Table 2. Fibers were added in 0%, 1%, 2%, and 3% of total volume to check the performance of the concrete mix.

Table 02: PET sample preparation

Sample	PET fiber diameter (mm)	PET fiber length (mm)	Water cement ratio	PET fiber percentage (%)
C0				0
C1	0.7	50±0.5	0.3	1
C2				2
C3				3
D1				0
D2	0.7	50±0.5	0.45	1
D3				2
D4				3

2.1.1 Experimental procedure

Compressive strength of concrete was tested using 150x150x150 mm. Cubes were casted according to BS 1881 -108 (1988) and cured until the test day as described in BS1881-111(1988). Concrete is mixed based on the mix design in accordance with BS 5328. In order to achieve a workable mix admixture Rheobuild 1000 is added to the concrete mix as a high-range water-reducing admixture

Slump was evaluated for each set of specimen on the day of mixing before casting the cubes (BS 1881 102). These test specimens were crushed on 3rd. 7th 14th 21st and 28th day form they are casted as shown in Figure 2.1. Compressive strength was measured in accordance with BS 1881 115(1988) and BS 1881 116(1988)

(a) (b)

Figure 2.1: Testing of specimens; (a) Compressive strength test, (b) Split tensile strength test.

Cylindrical specimens of 150x300 mm were casted to test tensile strength of concrete. Tensile strength was evaluated by split tensile test as shown in the Figure 2.1 (a).

2.2 Cylindrical specimen casting

Using the results of the above study it was identified that for water cement ratio of 0.3 and 2% of PET fiber would give the optimum results for both compressive strength, slump and tensile strength.

Table 03: Composition of cylindrical culvert

Specimen	Steel reinforcement	PET fibers (Total volume)
Plain concrete	non	non
Reinforced concrete	6mm mild steel at 120mm c/c spacing	non
Fiber reinforced concrete	non	2% PET

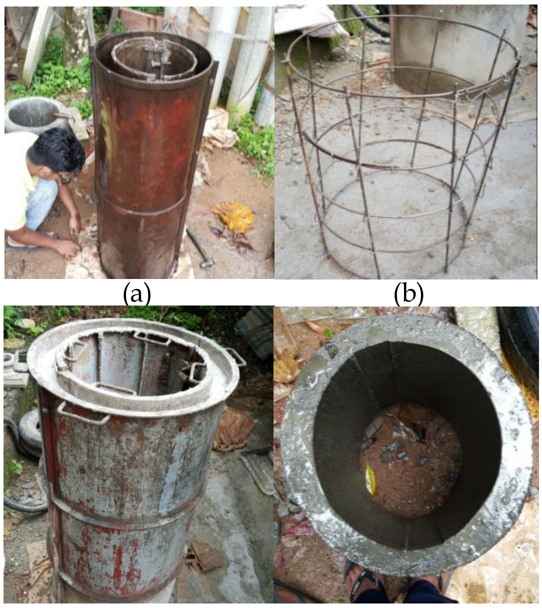

(a) (b)

(c) (d)

Figure 2.2: Casting procedure of cylindrical culverts; (a) Assembling of the mould. (b) Steel reinforcement cage, (c) Concreting, (d) Curing

Testing of Cylindrical culverts was performed in accordance with concrete pipe and portal culvert handbook. According to the standard specified in the manual, three edge bearing test was performed as shown in the Figure 2.3. Then the proof load was obtained and then ultimate load that the pipe can sustain was calculated. According to the handbook proof load is the line load that a pipe can sustain without the development of cracks of width exceeding 0.25 mm or more over a distance exceeding 300 mm in a two or three edge beading test. Then the ultimate load obtained by multiplying the proof load by 1.5.

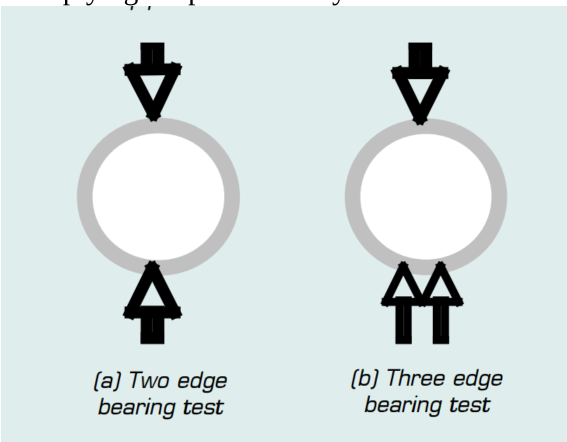

Figure 2.3: Two edge and three edge bearing tests

4. Results and Discussion

4.1 Variation of compressive strength with PET fiber content

For water cement ratio of 0.45 there is a significant reduction in the compressive strength compared to the control specimen as shown in the Table 4.1. Variation of 28 days compressive strength with the fiber percentage is shown in the Figure 4.1(a).

Table 4.1: Reduction of compressive strength with PET fiber percentage for w/c ratio of 0.45

PET fiber percentage (%)	Compressive strength reduction (%)
1	42.35
2	42.14
3	37.61

But for a water comet ratio of 0.3 the variation of compressive strength with the PET fiber percentage is less significant compared to the water cement ratio of 0.45. The variation of strength is shown in the Table 4.2. Variation of 28 days compressive strength with the PET fiber content is shown in the Figure 4.1(b).

Table 4.2: Reduction of compressive strength with fiber percentage for 0.3 W/C ratio

PET fiber percentage (%)	Compressive Strength reduction (%)
1	11.29
2	8.92
3	11.12

4.2 Variation of tensile strength with PET fiber content

Even though there is a reduction in the compressive strength, it can be observed that there is an improvement in the tensile strength of PET fiber concrete for both water cement ratios of 0.3 and 0.45. In the Figure 4.2 it indicates how the improvement of tensile strength compared to the control specimen.

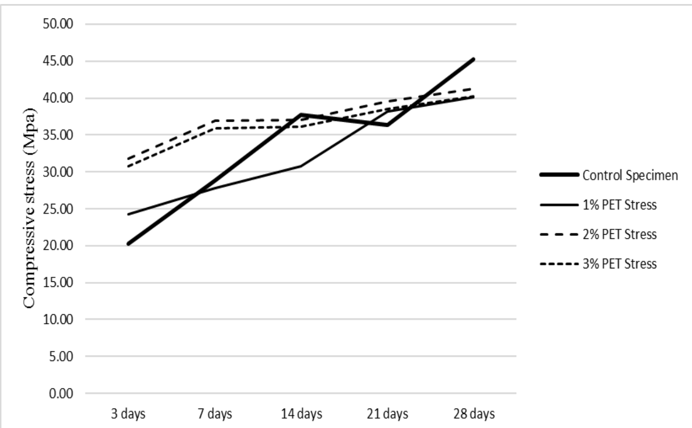

(a)

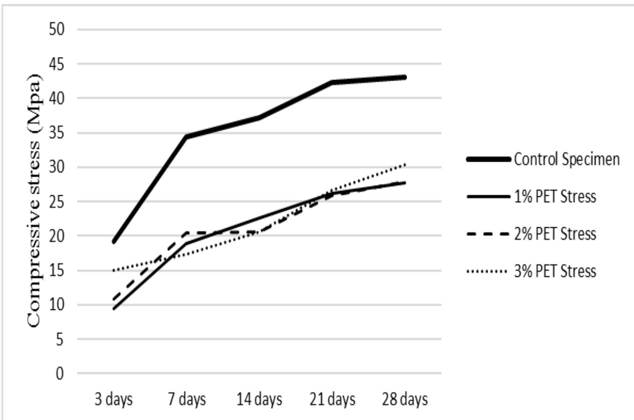

(b)

Figure 4.1 Variation of compressive strength; (a) Water cement ratio 0.45, (b) Water cement ratio 0.3

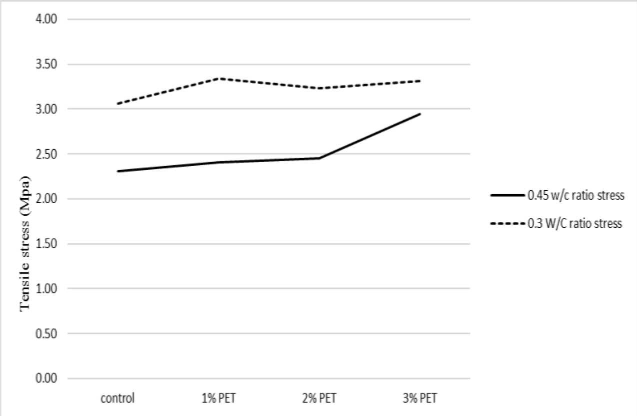

Figure 4.2: Variation of tensile strength for water cement ratio of 0.3 and 0.45 of 0.45 and 0.3
Variation of tensile strength

4.3 Variation of slump of concrete with PET fiber content

Slump value of the concrete with a water cement ratio of 0.45 is higher than the concrete with water cement ratio 0.3. As the fiber is added to the concrete, slump value of the concrete starts to reduce. The variation of the slump values with the PET fiber content is shown in the Figure 4.3.

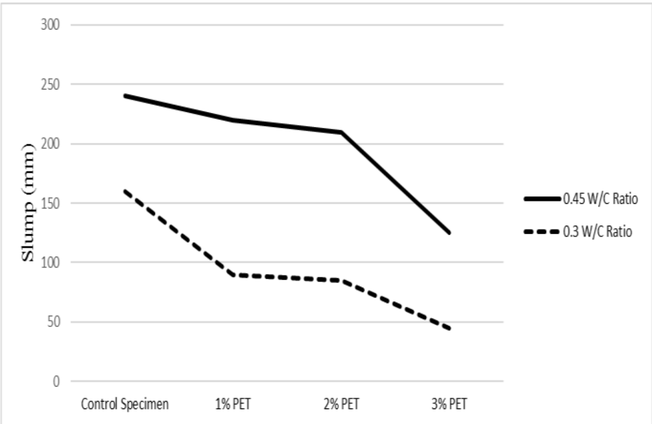

Figure 4.3: Variation of slump for water cement ratio of 0.45 and 0.3

4.3 Bearing load test results for concrete culverts

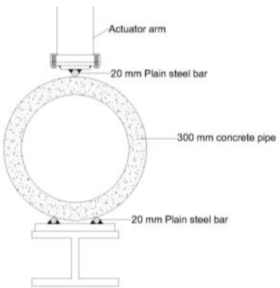

Reinforced concrete cylinder shows an improvement in ultimate load over the plain concrete. But it was identified PET fiber concrete performs well in bearing test comparing to the steel reinforced concrete and plain concrete. Also a significant reduction in the crack length and width was observed in the PET fiber reinforced cylinder.

Table 4.4 Test results of cylindrical specimens

	Plain concrete	Reinforced concrete	Fiber reinforced concrete
Ultimate load (kN/m)	15.1	32.00	30.04
Crest displacement(mm)	1.54	5.74	3.72
Lateral displacement(mm)	1.44	2.19	1.76
Crack width (W) (mm)	0.25<W	0.12<W<0.15	W<0.05

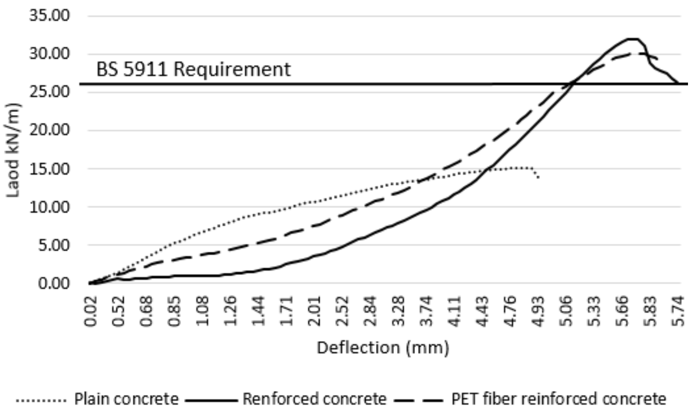

Figure 4.4: Three edge bearing test

Figure 4.4 Comparison of test results with BS 5911 part 100 standards

5. Conclusions

For water cement ratio of 0.3 and 0.45, the workability of fresh concrete decreases with the addition of PET fiber. However, geometry of PET fibers has a small effect on the workability of concrete. But in the case of 3% of PET with water cement ratio of 0.3 achieved a less workable mix.

Significant reduction of compressive strength in PET fiber reinforced concrete was observed for water cement ratio of 0.45. But in the case of 0.3 water cement ratio there is a slight reduction in 28 day compressive strength, but increases in the tensile strength clearly observed. The inclusion of PET fiber improved the tensile property and showed the ability in absorbing energy in the post-cracking state due to the bridging action imparted by the fibers during cracking. Therefore, use of PET fiber concrete in the production of cylindrical culvert is one of the good applications. Further studies will continue to check whether quality of these applications and other mechanical properties in re-cycled PET fibers.

Acknowledgement

The authors would like to express their gratitude to Faculty of Engineering Research Grant 2015 for providing necessary financial support and Department of Civil and Environmental Engineering, Faculty of Engineering, University of Ruhuna for the supports to carry out the research work successfully. The authors also wish to thank Lal Construction for support extended in preparation of specimens.

Reference

[1]. Kim Sung Bae,Yi Na Hyun,Kim Hyun Young,Kim Jang-Ho Jay,Song Young-Chul, 2010. Material and structural performance evaluation of recycled PET fiber reinforced concrete. *Cement and concrete composites,* 32(3), pp. 232-240.

[2]. Ochi T, Okubo S,Fukui K, 2007. Development of recycled PET fiber and its application as concrete-reinforcing fiber. *Cement and Concrete Composites,* 29(6), pp. 448-455.

[3]. Tefarul Haktanir, Kamuran Ari, Fatih Altun,Okan Karahan, 2007. A comparative experimental investigation of concrete reinforced-concrete and steel-fibre concrete pipes under three-edge-bea ring test. *Construction and Building Materials,* Volume 21, pp. 1702-1708.

[4]. Fernando Fraternali a, Vincenzo Ciancia , Rosaria Chechile, Gianvittorio Rizzano, Luciano Feo, 2011. Experimental study of the thermo-mechanical properties of recycled PET fiber-reinforced concrete. *Composite Structures,* 93(9), pp. 2368-2374.

[5]. Arful, M. C., 2015. Effects of PET f 120 arrangement and dimensions on mechar 120 properties of concrete. *The IES Journal A: Civil & Structural Engineering,* Issue ahead-of-print, pp. 1-10.

[6]. Sandaruwani A.H.W.E,and Bandara K.A.J.M, 2012. *Use of recycled short fibers in structural concrete to enhance mechanical properties,* Galle: Faculty of Engineering,University of Ruhuna, Undergraduate Research Thesis, 125 pp.

[7]. Sandaruwini A.H.W.E, Bandara K.A.J.M and De Silva G.S.Y., *Investigation on Mechanical Behavior of Concrete with Fibers Made of Recycled Materials,* Proceedings of International Conference on Sustainable Built Environment (ICSBE-2012), 14-15 December 2012, paper no. SBE/12/81.

SECM/15/137

Enhanced Performances for Marshall Properties of Hot Mix Asphalt (HMA) by Incorporated 60/70 Grade of Bitumen

P. Wickramarachchi[1*], H.L.D.M.A. Judith[2], D. Perera[1], and K. Priyashantha[3]

[1]Access Engineering PLC, Colombo, Sri Lanka
[2]Research & Development Division, Rathmalana, Sri Lanka
[3]Bitumix (Private) Limited, Homagama, Sri Lanka

*E-Mail: praneeth@accessengsl.com, TP: +94(0)777444293

Abstract: During the last decade, the rehabilitation and improvements of road networks in Sri Lanka exhibited a rapid development. As a result many of roads were undergone for new asphalt surfacing with hot mix asphalt, at least a wearing course, and the black top. However, with this rapid development, few premature failures were also observed in many of these newly constructed asphalt roads covering all part of Sri Lanka. Pre-mature cracking, removal of top thin film of wearing layer, bleeding and localized failures were among them. Bitumen played a very important role in hot mix asphalt and improvement for bitumen can enhanced the improved properties of HMA significantly. In this research, instead neat 60/70 grade of bitumen, it was used modified 60/70 grade, with Nano silane, enhancing anti-stripping and bonding capabilities. Research was comprised three stages of testing, lab trials, plant trials and filed trial in Colombo- Kandy road section. Results showed significant improvement for marshal properties. The stability and flow increased by 24% and 35 %, respectively. The anti-stripping property was also increased significantly, even after 6 hr, boiling test, it showed elevated no of coated aggregates. In addition, the mix was very well after few weeks, and very sticky condition proved that the strong bonding ability. All enhanced characteristics can be caused to exhibit improved performance and can be lead to extended life period of road construction.

Keywords: Anti-Stripping, Hot Mix Asphalt, 60/70 grade Bitumen, Marshal Properties.

1. Introduction

Rehabilitation and improvement of road network is a main strategic movement of any government in order to provide a better infrastructure facilities which can be heavily affect for rapid development. The same phenomena were applied during the last two decades in Sri Lanka and as a result many of roads were gotten new shape and ultimately facilitating the commuters. The new shape basically consisted the widening and having the black top. In other words, hot mix asphalt (HMA) layer was applied all most all road networks.

Though, the government and the client of these road network, the road development authority (RDA) anticipated the significant life time of such rehabilited roads, the unsatisfactory conditions or pre-mature failures were observed in many of roads covering all over the Sri Lanka. The pre-mature failures were, surface cracking, ravelling, stripping the top layer of bitumen, corrugations and so on. Development of surface cracking was a significant problem of newly laid asphalt wearing course. On the other hand, removal of very top thin layer of bitumen was also observed in all most all cases with the traffic. All key stakeholders were alarmed and focused to investigate the possible causes, basically attention was directed in three ways, quality of aggregates, and quality of bitumen and construction process. However, having solid and comprehensive experience of construction process by main contractors, the investigate area was further narrow to quality of aggregates and bitumen. It is well known fact that the quality of aggregates in Sri Lanka is in high quality all over the country and careful selection has been well established. Therefore, finally, concentrate attention was directed for the bitumen used to produce the asphalt and its characteristics.

The bitumen plays a very vital role in hot mix asphalt and improvement of its characteristics can be greatly attribute to the enhance performance of mot mix asphalt. The quality of bitumen and its strong relationship with aggregates are essential characteristics for quality asphalt in the field to meet the desired results in long run. Basically, the bitumen act as a bonding agent in mot mix asphalt mixture. It is a durable adhesive that binds together a variety of paving materials without affecting their properties. Its durability is essential to prolong the life of pavement/roads and bitumen gives controlled flexibility to mixture of mineral aggregates and is used for paving roads. The deduction of the adhesion between bitumen and aggregates specially in the presence of water and the deterioration of the asphalt due to cohesive failure with in the binder itself has been known as two primary mechanism that may results in pre-mature distress in asphalt (Terrel and Al Swailnri, 1994).

Further, moisture damage is one of the primary modes of distress in HMA, commonly known as stripping, this damage accelerates the structural degradation of the mixture in conjunction with cracking and plastic deformation. Physio-chemical surface properties of mineral aggregates are more important for moisture induced stripping of the HMA compared to the properties of binder. Recently, with the advent of new liquid adhesive promoters in the market, and the ease of application, liquid adhesive promoters are gaining rapid popularity. The function of these promoters is to alter the relative surface properties and polarity, thus facilitating a strong bond between the bitumen and aggregates which also resists to water displacing effect for the service life of the pavement.

2. Problem statement

Non formation of stable bond (weak bonding) in hot mix asphalt which was used in road construction was observed. In addition, the pre-mature surface cracking and stripping were developed in many pavements in Sri Lanka.

3. Research Objectives

(i). To enhance the Marshall properties of HMA
(ii). To improve the bonding capabilities in HMA
(iii).To increase the resistance to moisture damage

4. Scope of the study

To achieve the above objectives, the only parameter alter was the type of bitumen. Same mix design and same type of aggregates were used. Neat 60/70 bitumen and silane based incorporated bitumen 60/70 were used to compare the performance. Lab evaluation and filed laying were performed in a section of Colombo – Kandy (A1) road. Hydrated Lime ($Ca[OH]_2$) was also added as 1 % from the total volume.

5. Materials and Methods

5.1. Laboratory analysis

All lab works were carried out at the laboratory located at Kotadeniyawa asphalt plant which is managed by Access Engineering PLC. The approved mix design for wearing course for the project of Kadawatha _ Nittabuwa road (KNRP) was used. The hot bin samples were collected at Kotadeniyawa plant premises. Bitumen 60/70 and Nano grip 60/70 3 E were supplied by Bitumix Pvt. Ltd for this research.

Table 1: Mix proportion used in this study

Mix Proportions	Bitumen (%)	Hot Bin 4 (0-5 mm)	Hot Bin 3 (5-11 mm)	Hot Bin 2 (11-16 mm)	Hot Bin 1 (16-22 mm)	Filler	Total
Wearing Course	0	12%	14%	28%	45%	1%	100
Wearing Course	4.7	11.4	13.3	26.7	42.9	0.95	100.0

HMA design complying with type 3 grading band was carried out according to the Marshall method to evaluate the adhesion promoter. Marshall samples were prepared at the optimum bitumen content (4.7 %) using neat bitumen 60/70 and Nano grip 3 E.

Nano grip 60/70 3 E is the trade name of incorporated bitumen which was supplied by Bitumix Pvt Ltd. It is modified 60/70 bitumen with nano silane the product of UK. The 3 E denotes the Extra strong bonding, Excellent coating and Easy compaction. Through it is modified, the incorporated bitumen matches with conventional properties of 60/70 grade.

Table 2: Test Results of Nano grip 60/70 3 E

Property	Test Method	Specification Limit Min	Specification Limit Max	Test Results
Penetration 77^0F (25^0C) 100g, 5s	ASTM D 5 - 86	60	70	63
Flash Point ^{0}C	ASTM D 92 - 78	232		315
Softning Point ^{0}C	ASTM D 36 - 86	48	56	49
Loss on Heating for 5 hrs at 163 ^{0}C (i) Loss by weight percent (ii) Penetration after loss on heating test percent of its original value	ASTM D6 - 80 ASTM D5 - 86	75	1.0	95
Solubility in trichloroethyne %	ASTM D 2042 - 81	99		99.6
Specific gravity at 25/25 ^{0}C	ASTM D 70 - 82	1.01	1.06	1.021
Ductility (25 ^{0}C) 5 cm/min., cm	ASTM D 113 - 86	100		121
Effect on water on bituminuos coated aggegates using boiling water	ASTM D 3625 - 96	95		above 95

Boiling water test (ASTM D 3625) and coating and stripping test (ASTM D 1664) were carried out for samples. The boiling water test was extended up to 30 min, 1 and 6 hrs in addition to the standard values of 10 min to evaluate the enhanced performances.

5.2. Field trial laying

Once convinced the results, all stakeholders agreed to lay the wearing course which has incorporated bitumen 60/70 3 E at site. A 300 m length and 3.7 m width stretch was selected at Colombo – Kandy road, the improvement was done by Access Engineering PLC. The all required tests were performed and extraction test was also jointly carried out at site laboratory. All personnel representing client/consultant and main contractor participated to witness the activity.

6. Results and Discussion

6.1. Marshall properties

Table 3: Comparison of Marshall Properties

Strength & Flow Improvement	Marshall Stability (kN)	Flow (0.25 mm)
Control Sample	15.6	10.4
Nano grip 60/70 3 E	19.5	13.9

.

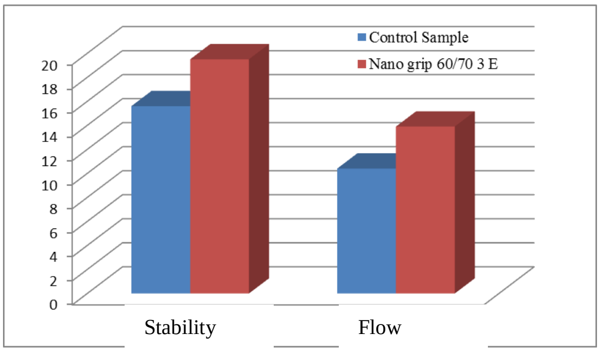

Figure 1: Comparison of Marshall Properties

The above table 2 depicts the comparison of Marshall properties of neat bitumen and Nano grip samples. The shown values are average values of duplicate samples. The Marshall stability values have been increased to 19.5 from 15.6 kN whereas the flow values has been elevated to 13.9 from 10.4. The figure 2 also illustrates the graphical view of above mentioned parameters. These two properties are very important in practical sense in the field for HMA. Generally, when stability increases the flow will reduces, but the given range of bitumen content both parameters tend to increase. Increment of stability is important to bear the traffic load without breaking, but too much stability can create the solid surface and less comfort to drive, but in this case the flow was also increased. It makes the better flexibility with hot temperature and will not allow breaking the surface. When both elevated properties arise together it can cause to keep good HMA surface in long run.

6.2. Extended boiled water tests (% coating ability)

Table 4: Extended boiled water tests **Error! Not a valid link.**

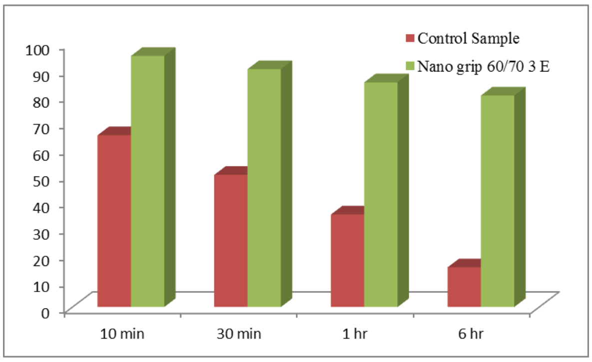

Figure 2: Graphical representation of extended boiled water test

The boiling water (ASTM D 3625) test is to quantify the coating ability (%). The standard is 10 min boiling and visually observes the coating retention. However, to further convince the ability the extended boiling water test up to 6 hr was carried out. The table 3 showed the values and figure 2 illustrates the graphical representation. It is clearly observed that even after 6 hr, the Nano grip samples showed higher coating ability, in other words, the very low stripping values. Interestingly, the neat bitumen showed very low coating ability values with the time, highlighting the elevated stripping values. Even rate of stripping is very rapid in neat bitumen samples. This result highlights the weak bonding the ease to de-bonding with the presence of moisture in neat bitumen.

When carrying out the experiments, it was shown that very strong bonding of aggregates and Nano grip 3 E compared to the neat bitumen samples. The state of very stickiness was very high and even the coated aggregates were strongly stick to the hand and was not fall apart freely. In addition, the whole surface of aggregates was covered by incorporate bitumen with relatively thicker layer. The samples which were broken after even 2-3 weeks later, showed very fresh state compared to neat bitumen.

6.3. Observations at field laying

The filed trial were carried out at a section of Kadawatha – Nittabuwa road project (KNRP), the main contractor was the Access Engineering PLC. With the proper approval of client (RDA), Quality consultant (R & DA) the both binder and wearing courses were laid. The length and width of the sections were 300 m and 3.75 m, respectively. The thickness of the wearing course was 50 mm. The following special observations were made during the filed application.

- Samples which casted using Nano Grip 60/70 3 E, exhibited very fresh/live conditions compared to the samples prepared with neat 60/70 bitumen.

- Once mixed, Nano Grip showed very sticky state and all aggregates were well coated

- Even after several days later, the broken samples showed same bonding/stickiness, and neat bitumen samples were looked like little ageing.

- Nano Grip samples exhibited fresh/live condition after several weeks later while neat bitumen samples showed little ageing conditions.

- Once tested for Marshal properties both stability and flow had increased significantly in Nano Grip samples compared to neat bitumen.

In addition to the above, the self-compaction ability has also shown increment while lying.

Figure 3: Asphalt laying using paver

Figure 4: Initial compaction by steel roller

Figure 5: Final compaction by pneumatic roller

7.0 Conclusions

All three experimental conditions (Lab, Plant and Field) exhibited enhanced performance of asphalt specially Marshal properties. The stability and flow has improved averagely 25 % and 35 %, respectively with compared to the neat bitumen asphalt.

Bonding abilities have been also improved, resulting higher no of coated aggregates, which shows the low stripping abilities with the present of moisture.

Asphalt mixture showed very fresh and lively conditions and higher workability.

8.0 Special notes and recommendations

- Even through, the lab, plant trials exhibited enhanced properties; it is a must to confirm those at site in longer run. So that some realistic mechanism must be in place to confirm the advantages of adding this modified/improved bitumen.
- It is advisable to set up a team comprising a member from main contractor, RDA, R & D and one from independent body such as university.
- The team first has to outline the mechanism and activities to be carried out at particular time intervals
- If within reasonable time frame, the enhance properties are existing, then concrete decision can be taken to move forward in large scale or can be produced to policy makers.

Acknowledgement

The authors wish to express their appreciation to the higher management of Access Engineering PLC for their vision and approval to proceed the experiments. In addition the support given by research and development division of RDA was highly commendable. The assistance from Bitumix (Pvt) ltd was also highly appreciated. Finally, authors would thank all technical staff of asphalt plant and lab of AEPLC for their unconditional supports.

References

[1]. ASTM Standards, ASTM International, West Conshohocken, PA, 2003.

[2]. Bitumix Private Limited, Technical Bulletin, NanoGrip 60/70 3 E, Homagama, 2015.

[3]. Terrel, L., R., and Al-Swailmi, S., “Water sensitivity of asphalt-aggregates mixes: Test selection”, Oregon State University, 1994.

SECM/15/138

Investigation of Strength Parameters and Physical Properties of non-class Timber Species in Sri Lanka

[1]Ruwanpathirana B.S, [2]Rathnayaka R.M.C.P, [3]De Silva Sudhira and [4]De Silva Subashi

Department of Civil and Environmental Engineering, Faculty of Engineering,
University of Ruhuna, Galle, Sri Lanka
[1]E-Mail: bishansampath@gmail.com, TP: +94712229965

ABSTRACT: Timber is a commonly used construction material in Sri Lanka. But the strength parameters of locally available non-class timber are not available. In this study main objectives are to determine strength parameters and physical properties of selected local timber materials and to develop a strength class classification with their possible applications in the construction field. Different strength parameter tests are conducted in bending, compression (grain parallel and perpendicular), tension (parallel to grains), and shear perpendicular to grain. In addition, durability, fire resistance tests and physical properties such as dry density, bulk density, and water absorption were carried out. For those tests BS 373 (1957) and EURO CODE 5 were used as references. Average moisture contents of non-class timber specimens were around 12%, modulus of elasticity varies 3200 MPa - 13,000 MPa, modulus of rupture varies 37 MPa – 85 MPa, dry density varies 600 kg/m^3 - 900 kg/m^3. Strength parameters at serviceability limit, mainly compressive strength at parallel to grains varies 13 MPa - 45 MPa, and compressive strength perpendicular to grains varies 3 MPa – 22 MPa in most of the non-class timber species. Shear capacity of perpendicular to graons of non-class timber materials varies 0.9 MPa - 5 MPa at serviceability limit. Tension capacities of timber materials vary 35 MPa - 100 MPa and charring rate of timber species varies 0.25 mm/min - 0.8 mm/min. Similarly other test parameters were investigated and presented in the paper. Finally identified non-class timber species were classified according to available strength classes and proposed suitable applications for each type.

Keywords: non-class timber, strength classes, compression, tension, durability, fire resistance

1. Introduction

Timber is one of the oldest building materials in Sri Lanka. According to Sri Lankan history, “Lovamahapaya ", which was built by King Dutugemunu in the second century BC, had a full wooden structure originally consisting of nine floors with a height of over 20 meters. Timber used as a construction material of several hundreds of different types of wood species, some of which are less well known but each species has various wood properties.

According to State Timber Cooperation (STC) Sri Lanka, there are about 400 timber species are available in Sri Lanka. STC studied about 227 type timber specimens. But that studies were limited only to visual grading and past experience of timber. So that engineering techniques unable to use due to lack of data. This research was conducted to obtain structural and resistivity parameters of local timber species which necessary for the timber classification. Kempus (*Koompassia malaccensis)* is used to validate the test results. This research tests were based on BS373:1957 and EURO CODE 5. Timber species were used in the research are shown in Table 1.

Table 1: Tested Timber Species

No	Local Name	Scientific Name
1	Pare Mara	Samanea saman
2	Lunumidella	Melia dubia
3	Ketakala	Bridelia retusa
4	Mango	Mangifera indica
5	Nikadaula	Neolitsea cassia
6	Kon	Schleichera oleosa

7	Jak	Artocarpus heterophyllus
8	Damaniya	Grewia tilliafolia
9	Madan	Syzgium cumini
10	Liyan	Homalium zeylanicum
11	Havarinuga	Alastonia macrophyla
12	Bata Domba	Syzygium operculatum
13	Mahogani	Swietenia macrophylla
14	Dawata	Carallia branchiate
15	Donga	Sandoricum indicum
16	Gini Sapu	Michelia champaca
17	Saukku	Grevillea robusta
18	Karpantine	Eucaliptus microcorys
19	Karpantine	Eucaliptus grandis

2. Methodology

Compression, Tension, Flexural and Shear tests were done to determine structural properties of Timber materials. Durability and Thermal resistivity of timber materials were also tested. Testing methodology was done according to the international standards. This experiment procedures have been referred international codes BS 373:1957 and EURO CODE 5 for the testing of above parameters. Test results were verified by using known timber parameters in species like Kempus.
All the samples for Compression, Tension and Flexural experiments were taken with the moisture content around 12%.

2.1 Dry Density

Dry weigh of the samples were taken by placing in 105C° oven for 48 hours. (BS373, 1957 [1])

$S_0 = W_0/(l \times b \times h)$ (1)

W_0 = Weight of sample, oven-dry
l = Length
b = Breadth
h = Height

2.2 Compression Test

Compression test was conducted for specimen with 12% moisture content by parallel to grain and perpendicular to grain. Axial compression was given at the rate of 2 mm per minute up to ultimate failure by using Universal Testing Machine. (BS373, 1957 [1])

$$\text{Compressive strength} = \frac{\text{Servieability Load}}{\text{Average area}} \quad (2)$$

2.2.1 Compression parallel to Grains

Standard size of compression capacity parallel to grain test specimen is 50mm×50mm×400mm timber section as shown in Figure 1.

Figure 1: Compression parallel to Grains

2.2.2 Compression perpendicular to Grains

Compression test perpendicular to the grains was conduct by using 50mm×50mm×50mm timber sections. Same procedure was conducted for the compression in grains parallel.

2.3 Flexural Test

Specimens were subjected to centre point loading at the mid span. During the test applied load and mid span deflection was measured.
Timber specimens 50mm×50mm×750mm were used for the above test. Load was given at the rate of 2mm per minute up to ultimate failure by using Universal Testing Machine (UTM) with simply supported condition at the ends as shown in Figure 2. This test was carried out according to the BS373, 1957 [1]. Test results were used to calculate Modulus of Elasticity (MOE) and Modulus of Rufture (MOR).

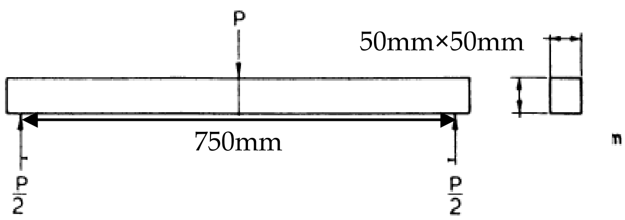

Figure 2: Flexural test

Figure 3: Flexural test apparatus

$$\mathrm{MOR} = \frac{\mathrm{M} \times \mathrm{y}}{\mathrm{I}} \qquad (3)$$

M – Maximum Bending moment
y – Maximum distance from neutral axis to edge of the section
I – Second moment of area

$$\mathrm{MOE} = \frac{\mathrm{WL}^3}{48\delta \mathrm{I}} \qquad (4)$$

L – Length of timber specimen

W – Maximum Load act in centre of specimen

δ – Maximum deflection of timber beam

I – Modulus of elasticity

2.4 Tension Test

50mm×50mm×300mm timber specimens with 12% moisture content used for the test. Test was conducted to grains parallel of the samples. This test was carried out by using Universal Testing Machines with 2mm per minute loading rate as shown in the Figure 3. (BS373, 1957 [1]).Tension capacity of the specimens were calculated using maximum load and average area of the the specimens using Eq. (5).

$$\text{Tension strength} = \frac{\text{Servieability Load}}{\text{Average area}} \quad (5)$$

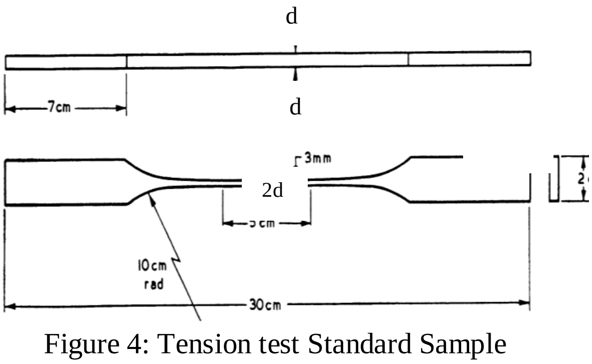

Figure 4: Tension test Standard Sample

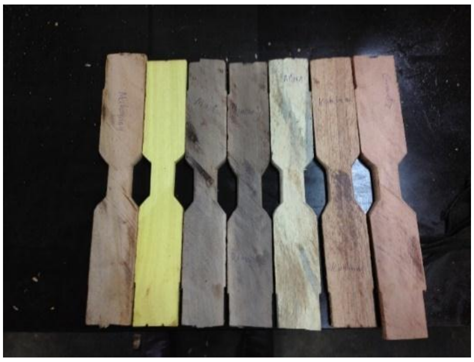

Figure 5: Sample preparation of Tension test

Figure 6: Tension test apparatus

2.6 Durability Test

This study has been done according to previous study by Breyer and Banks (1957). 50mm×50mm×400mm timber samples were oven dried and placed in 3% sulfuric acid solvent. Three specimens were soaked for a period of four weeks and dried in oven for 24 hours. Then weight loss was considered by using initial and final weight of specimens. Main parameters were considered in this test are; Compression capacity change and Weight loss.

Figure 7: Specimens Soaked in Acid bath

2.7 Thermal Resistivity

Burning length was measured of 50mm×50mm×250mm inch timber samples after 30min of burning with $250C^0$ flame and charring rate was calculated. (EUROCODE5, 1995 [3])

$$\beta = \frac{D}{t} \qquad (6)$$

D – Burning length
t – Time (30min)
β – charring rate

Figure 8: Fire Resistivity test

2.8 Water Absorption

50mm×50mm×50mm timber cubes were used for the test. First samples were oven dried at the $105C^0$ temperature for 48hrs and weighted. Then samples were placed in a water bath and measure the weight in every week.

After that weight gain vs. time relationship were plotted.

Figure 9: Water absorption Test

3. Results and Discussion

All results were compared and validated by using properties of known timber specie of Kempus. Test result of compression, tension, flexural, durability, thermal resistivity and water absorption are shown in the Tables from 2 to 5.

3.1 Dry Density

Table 2: Dry density of Timber Species

Timber Type	Avg. Dry density
Grandiz	680.32
Jak	645.82
Kempus	829.99
Kon	883.00
Micro	791.21
Havarinuga	680.03

Dry density of timber specimens shows relationship with compression capacity. Kon, Grandiz and Micro has highest compression capacity while they are having high dry density values.

3.2 Durability

Jak and Subukku timber specimens are more resistive for acids while Ketakala has low resistivity for acids.

Table 3: Weight loss after 28 days

Timber Type	Weight Loss % after 28 days
Grandiz	6.52
Havarinuga	0.70
Jak	0.50
Kempus	4.62
Ketakala	13.93
Micro	9.19
Subukku	0.34

These results are very essential to select timber materials for different structural applications. It was revealed that members with high moisture content caused high insect & fungi attacks. Therefore selection timber species with less moisture content and high dry density is most desirable selection.

3.3 Structural Properties

Structure properties of Timber species are very important to design timber element and structures. Table 4 summarized parameters of tension, MOR, MOE and compressive strength obtain from above test mentioned.

Tension capacity of specimens of same species has high deviation due to their grain pattern. Kon, Grandiz and Micro have high tension capacity while they are having highest compression capacity. Kon, Grandiz and Micro also have high MOR.

Table 4: Structural properties of Timber Species

Timber Type	Compression strength (MPa)		Tension capacity (Mpa)	Shear capacity (MPa)	MOR (MPa)	MOE (MPa)
	Parallel to grains	Perpendicular to grains				
Grandiz	28.96	3.17	70.39	0.95	80.14	12912.89
Paremara	22.90	9.79	59.30	2.42	57.85	6624.91
Kempus	47.31	26.54	64.40	1.40	63.31	17404.76
Kon	44.75	21.31	88.59	4.12	71.56	6026.51
Micro	23.97	8.38	117.55	2.18	66.07	5340.50
Havarinuga	27.98	6.46	86.33	1.56	84.51	5574.57

MOR value is indicate ultimate flexural strength of timber species. This parameters is very important to designing beams elements. Grandiz, Kon and Havarinuga have high MOR value regarding the other non-class timber materials. Stiffness of timber materials indicate by MOE value. It's very essential parameter to determine deflection of timber beams. Grandiz has highest MOE value compare to other timber species. Kon has highest shear capacity perpendicular to grain while Grandiz has lowest.

3.4 Water Absorption

Table 5: Water Absorption after 5th week

Timber Type	Water absorption % after 5th week	Ult. Compressive strength N/mm2
Kempus	24.09	55.36
Kon	49.60	55.04
Grandiz	73.10	40.48
Sabukku	104.00	36.17
Lunumidella	134.01	25.61

High strength timber materials have less water absorption. Subukku and Lunumidella has high water absorption. These timber specimens have low strength capacity.

Figures 10 and 11 show variation of water absorption of Kon and Lunumidella timber species. Absorb water content was tend to constant after 3rd weeks.

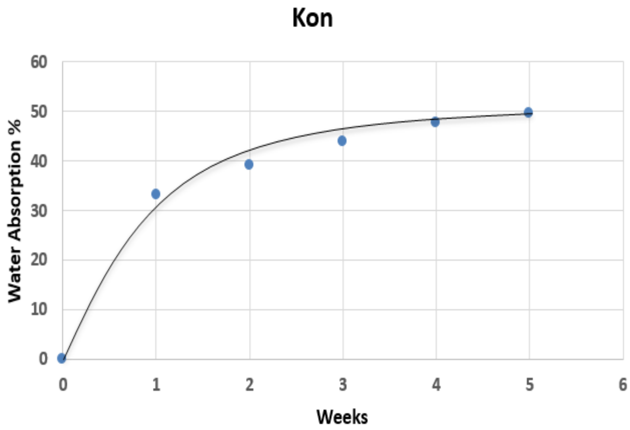

Figure 10: Water absorption results of Kon

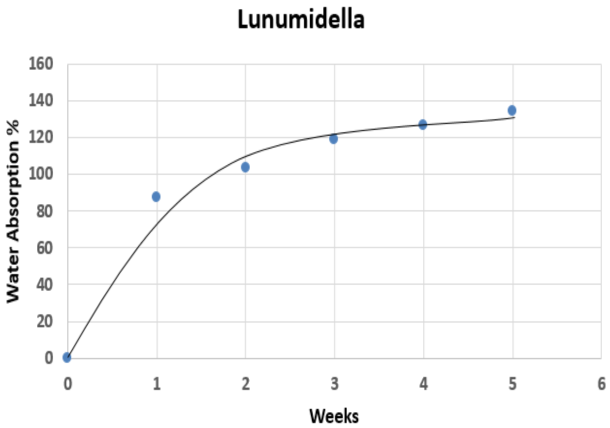

Figure 11: Water absorption results of Lunumidella

Lunumidella has much higher water absorption capacity compare to Kon but shows less compressive strength relative to Kon.
Therefore water absorption indicate porosity of timber material which effect to timber strength characteristics.

3.5 Thermal Resistivity

Table 6: Charring rate values

Timber Type	Charring rate (β value) mm/min
Lunumidella	0.27
Sabukku	0.37
Kempus	0.43
Grandiz	0.43
Havarinuga	0.47
Paremara	0.57
Jak	0.77

Subbukku and Lunumidella have low charring rate while timber species which have high density have high charring value. Voids are effect to charring value.

4. Conclusions

According to the test results, strength parameters of Kempus lies between standard values. Therefore test results values of other timber species were validated.
From this study following conclusion were derived; Average dry density of selected timber materials lies between 600-900 kg/m^3. Strength parameters at serviceability limit, mainly compressive strength at parallel to grains varies from 13 MPa to 45 MPa and compressive strength perpendicular to grains varies from 3 MPa to 22 MPa in most of the non-class timber species. “Kon” has highest strength values in compression (parallel to grains and perpendicular to grains) compare to others. Modulus of Rupture and Modulus of Elasticity values varies 3200 MPa - 13,000 MPa, and 37 MPa – 85 MPa which have highest values in “Grandiz”. “Micro” has the highest tension capacity compare to other non-class timber materials where tension capacity varies 35 Mpa - 110 Mpa. Compressive strength of timber materials are decreased with increment of water absorption. Shear strength perpendicular to grain varies 0.9 MPa - 5 MPa. Highest acidic resistivity timber materials are “Jak” and “Subukku”. Charring rate of timber species varies 0.25 mm/min - 0.8 mm/min. Lunnumidella and Subukku have low charring value thus they are more fire resistive while they are having high porosity.

Acknowledgement

First and foremost authors would like to acknowledge Faculty of Engineering, University of Ruhuna Research Grant 2015, which provided financial support to succeed this research. Special thanks for Mr. V.S.C. Weragoda, Technical Officer, Department of Material Science and Engineering, University of Moratuwa who dedicated his valuable time and facilitate to testing of specimens. We are grateful Dr. N. Ruwanpathirana, Deputy General Manager, State Timber Cooperation and Staff of the State Timber Cooperation, Galle Branch who have given existing details of timber species in Sri Lanka.

References

[1]. BS373, 1957. *Methods of testing small clear specimens of timber*

[2]. Civilengineering, 2012. *Civil Engineering.* [Online]
Available at:
http://www.civilengineeringx.com/traditional-materials/classification-of-timber
[Accessed 1 6 2015].

[3]. EUROCODE5, 1995. *Structural Timber Design.*

[4]. G.Breyer, M. & :C.H.Banks, 1957. Comparison of resistance of six timbers to sulpuric acid. *South african furestry association*, 30(1), pp. 7-29.

[5]. Ruwanpathirana, N., 2008. [Online]
Available at:
http://timber.lk/timberindustry/publish/Timber%20Utilization%20in%20Sri%20Lank%20-presentation.pdf

[6]. Ruwanpathirana, N., 2011. 2011 World Forest Day. *Vidusara.*

[7]. Ruwanpathirana,N., 2005. *State Timber Corporation.* [Online]
Available at:
http://www.timco.lk/statetimco/
[Accessed 03 06 2015].

SECM/15/139

Effect of Rice Husk Ash (RHA) on structural properties of fired clay bricks

B.V.A. Perera[1], K.G.S. Madhushanka[2], G.H.M.J. Subashi De Silva and G.S.Y.De Silva

Department of Civil and Environmental Engineering, University of Ruhuna, Sri Lanka.
[1)]vikumperera7@gmail.com [2)] sajith.madhu@gmail.com

Abstract: In Sri Lanka, some amount of rice husk has been used as a fuel to fire bricks. However, rice husk ash (RHA) produced from the brick firing process has not yet been utilized effectively. Objective of this study is to utilize the rice husk ash wasted from the brick kiln to enhance structural properties of fired clay bricks.

Rice husk ash was collected from the brick kiln, located in Embilipitiya area, while the clay was collected from Dankotuwa area, where a brick manufacturing has been well established. Sieve analysis was performed for the collected RHA to identify the particle size distribution. The clay was mixed manually with different percentage of RHA: 0%, 2%, 4%, 6%, 8% and 10%. Atterberg limit of the mixture was investigated in order to identify suitability of the mixture for brick production. Bricks having a size of 195mm x 95mm x 50mm were cast manually and kept for drying. All the bricks were fired in a brick kiln. The burning temperature was within the range of 600 ^{o}C to 850 ^{o}C. Compressive strength and water absorption of fired bricks were investigated.

All percentages of addition of RHA improve the mixture for brick manufacturing. The optimum compressive strength of 3.55 N/mm^2 was found at 4% of addition of RHA. It was found that 32.7% improvement in the compressive strength of the bricks with 4% RHA addition compared to the control bricks (i.e., fired clay bricks with 0% of RHA), implying that RHA wasted from the brick kiln can be effectively used to improve the structural properties of the fired clay bricks.

Keywords: Rice Husk Ash (RHA), burnt clay bricks, compressive strength, water absorption, silicon aluminium ratio

1. Introduction

At present the generation of solid waste is enormously high. Hence large amount of environment impacts occur. Most of the solid waste has appreciable properties. Therefore waste materials can be used for various purposes as building materials. The major quantities of wastes generated from agricultural sources are rice husk, sugarcane bagasse, jute fibre, coconut husk, cotton stalk, etc. (Raut, et al. [1]).

Sri Lankans have been engaged in agricultural tasks since ancient time. Sri Lankan farmers produce large amount of rice, as a result, large amount of rice husk is disposed as waste. Rice husk ash (RHA) is obtained from burning of Rice husk. The husk is a by-product of the rice-milling industry. By weight, 10 % of the rice grain is rice husk. On burning the rice husk about 20 % becomes RHA. (Agus [2])

In Sri Lanka, rice husk is often used as a fuel. For example, in Embilipitiya area the handmade brick producers used rice husk to fire clay bricks and the resulting RHA is open dumped. The use of rice husk on energy production is a good practice. However, the wasting of RHA, which has high percentage of silica, is not appreciable. In some areas of Sri Lanka, the Rice husk is open burning. This practice causes a lot of environmental issues.

Izwan et al. [3] concluded that the risk husk ash burnt in a controlled manner with high temperature have high percentage of SiO_2 .According to the investigation of the De Silva and Uduweriya [4], ideal temperature for producing RHA with high pozzalonic activities is control buring at 600 ^{o}C for

2-3 hrs. In addition, they found that in the brick kiln, where the rice husks were burnt, the temperature varies from 600°C to 850°C. Chemical composition of RHA that are available in different countries has been investigated in previous studies (Agus [2], Ghassan et al. [5]. and Nilantha et al [6]) Nilantha et al. [6] have investigated the properties of the Sri Lankan RHA, which was collected from brick kiln. Agus [2] and Ghassan et al. [5] have investigated the properties of RHA obtained from control burning process. Chemical composition of RHA reported in above mentioned studies are compared in Table 1. It can be observed that the RHA collected from brick burning process contains high amount of SiO_2; similar to SiO_2 in RHA obtained from control burning process.

The fired clay bricks are very popular among public due to its low cost and thermal performance. The demand for the graded clay bricks is comparatively high. As mention in the Sri Lankan standards for handmade fired clay bricks the average compressive strength of bricks should be more than 2.8 N/mm^2 and the water absorption should be less than 28%. At present, bricks produced in most of the areas, was not able to reach these standards: the compressive strength and water absorption properties have a considerable deviation. However, if the brick has low compressive strength properties it directly influences on propagation of cracks. The wall should be capable of withstand humid weather conditions; if the walls have less water résistance, the water will penetrate into the building. When constructing a wall, burnt brick should be immersed in water to absorb water, otherwise the water, which is in the mortar will be absorbed by the blocks and then the mortar will not be properly strengthen. Hence the water absorption should be balanced. Major properties (i.e., compressive strength and water absorption) of the bricks should be satisfied in order to use bricks for constructing buildings.

To improve properties of the bricks, chemical behaviour of clay materials plays a major role. De Silva and Crenstil [7] have investigated the chemical behaviour of clay materials under different ratio of SiO_2/Al_2O_3 and found that the proper SiO_2/Al_2O_3 can improve the strength characteristics of clay. Adding RHA which contains high amount of silica to clay can be used as a method to increase the silicon/aluminium ratio.

Table 1**:** Chemical Compositions Rice Husk Ash

	Nilantha et al. [6]	Ghassan et al. [5]	Agus [2]
SiO_2	91.75	88.32	89.08
Al_2O_3	2.07	0.46	1.75
Fe_2O_3	1.56	0.67	0.88
CaO	1.3	0.67	1.29
MgO	1	0.44	0.64
Na_2O	0	-	0.85
K_2O	2.32	2.91	1.38
Loss in ignition	-	5.81	2.05

When constructing buildings the bricks play a key role by satisfying major properties such as compressive strength and water absorption.In addition, the properties of the material that used in burnt clay brick production should have liquid limit, plastic limit and plasticity index of 38.09%, 20.21%, and 17.78%, respectively (Lin et al.[9]), in order to mold a brick.

Objectives of the present study are,

- to investigate the effect of the Rice Husk Ash on compressive strength and water absorption of fired clay bricks in industrial scale brick manufacturing process.
- to investigate optimum mix proportion of RHA that can be used to manufactured fired clay bricks.

2. Methodology

Methodology includes selection of materials, manufacturing of fired brick with RHA in industrial scale and conducting experiments in the laboratory.

2.1 Materials

Clay: The clay for this study is collected from Dankotuwa (located in Puttlam District, North Western Province). It was collected from a pit about 1m deep near the bank of the river (Maa Oya, Sri-Lanka). The pit was dug and excavated with the aid of an excavator.

Rice Husk Ash: The rice husk ash was collected from the output of the brick kiln (Figure 1), located in Embilipitiya.

Figure 1: RHA collected from brick kiln

2.2 Manufacturing of Bricks

Different amount of rice husk were mixed with clay according to different weight percentages: 0% (control sample), 2%, 4%, 6%, 8% and 10%. The rice husk ash was used as silica (SiO_2) containing additive. The handmade bricks of dimensions 195mm x 95mm x 50mm were prepared using the moulds under local brick production workmanships. The materials were measured using weighing balance. The clay bricks were dried under the warm weather condition prevailing in dry zone in Sri Lanka. The clay bricks were fired in a brick kiln, which is the industrial scale manufacturing process of fired bricks in Sri Lanka.

When preparing the clay for the brick casting, first the collected clay was mixed with water and prepared it to a suitable with correct plasticity and the workability. This prepared clay was weighed and approximately 2.5kg clay samples were prepared. Then RHA was mixed with clay as weights shown in Table 2.

Table 2: RHA Sampling

Weight of RHA (g)	Percentage of RHA (%)
50	2
100	4
150	6
200	8
250	10

The RHA was mixed with clay manually while adding water until proper mixing reached The mix was placed in the mould and the clay brick was prepared. The prepared clay bricks were covered by saw dust to avoid engaging with other newly prepared clay bricks. The prepared clay bricks were kept one week for the drying. When the required drying condition of the clay bricks was achieved they were placed in the kiln for the burning process. The burning was done for two days continuously and kept about one week. Fired clay bricks were transported to the laboratories after two weeks and subjected to require experiments. Figure 2 shows the prepared clay bricks (a) before burning (b)after burning.

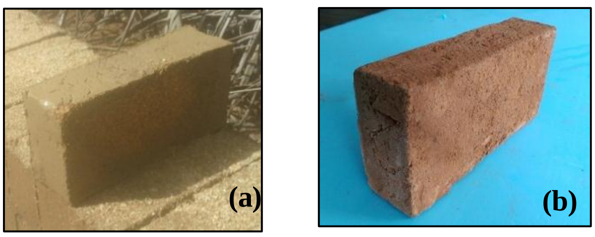

Figure 2: Manufactured Clay Bricks
(a) Before burning (b) After burning

2.3 Laboratory Experiments

Laboratory experiments were conducted to measure the probable property variation. The Atterberg test and the hydrometer analysis test were conducted to determine the suitability of the clay for brick manufacturing. The compressive strength test and water absorption test were conducted to measure the property variation due to addition of RHA.

2.3.1 Atterberg limit test

Atterberg limit test was performed to determine the liquid limit, plastic limit and plasticity index of the soil that was used to cast clay bricks and also the test was performed for clay soil with relevant mix proportions (0, 2, 4, 6, 8, and 10% RHA contents). Atterberg limit test was conducted in accordance with the British standard specification BS1377 (1990).

2.3.2 Sieve analysis for the RHA

The RHA was dried and large broken brick particles were removed. The weights of the sample and the weight of each sieve were measured. The set of sieves (2.36mm, 1.70mm, 1.18mm, 0.85mm, 0.60mm, 0.425mm, 0.25mm and 0.075mm)were arranged as the largest mesh opening was at the top and the smallest was at the bottom. The pan was attached at the bottom of the stake of sieves. The sample of RHA was poured on the top sieve and the cover plate was added to avoid dust and loss of particles while shaking. The stacks of sieves were placed on the mechanical shaker and horizontal shaking was applied for a time of 10 minutes. Then the weight of the sieve with remaining RHA was measured and the percentage of soil passing was determined.

2.3.3 Wet Sieve Analysis

The clay samples collected from Dankotuwa was subjected to the wet sieve analysis. The collected clay samples were put into a 1000ml measuring cylinder and water and sodium hexa sulphate were added and mixed thoughrouly. The cylinder was kept for 24 hours without any disturbance. The sample was mixed again and passed through the 0.075mm sieve. The remaining on the sieve was washed from water until the entire fine particles passed. The retained particles on the sieve and the pan were collected to the weighed pans separately. Then the samples were oven dried for 24 hours and the dry weights were measured. The retaining on the 0.075mm sieve was analysed using general method of sieve analysis descried in a preceding section.

2.3.4 Compressive Strength

The compressive strength was investigated by using the compressive strength machine available in the Construction and Building Materials laboratory. Six bricks from each level of RHA addition were tested (Figure 3) and average compressive strength was calculated. The strength characteristics were compared with the brick standards.

Figure 3: Testing of Bricks using Concrete Crushing Machine

2.3.5 Water Absorption

Water absorption test was performed to determine the water absorption property of the rice husk ash mixed fired clay bricks. Three bricks from each level of RHA addition were selected and the water absorption test was performed. First the samples were kept under the temperature of 100-105 ^{o}C for a period of 24 hours and the dry weight of the samples was measured. The same bricks that were dried in an oven were immersed in the water for a period of 24 hours and the wet weight of each brick was measured. Water absorption is defined as the ratio of the reduction of weight to dry weight of the brick and presented as a percentage. An average value of water absorption was calculated for each proportion of additive added bricks.

3. Results and Discussion

3.1 Suitability of the clay for brick production

Figure 4 shows the variation of the liquid limit with each RHA proportions. The addition of RHA up to 4% lead to decrease the liquid limit to a value of 37.2% and after that the liquid limit is gradually increased up to 40.1% with further addition of RHA. Reducing the liquid limit lead to less shrinkage and when it increases the dry strength permeability and the shrinkage are increasing (Lin and Weng [8]). Lin and Weng [8] have found a liquid limit of 38.09% as the clay soil. In the current study, 4% addition of RHA resulted a mixture with the liquid limit to be 37.2% and is a similar value compared with the findings of the Lin and Weng [8].

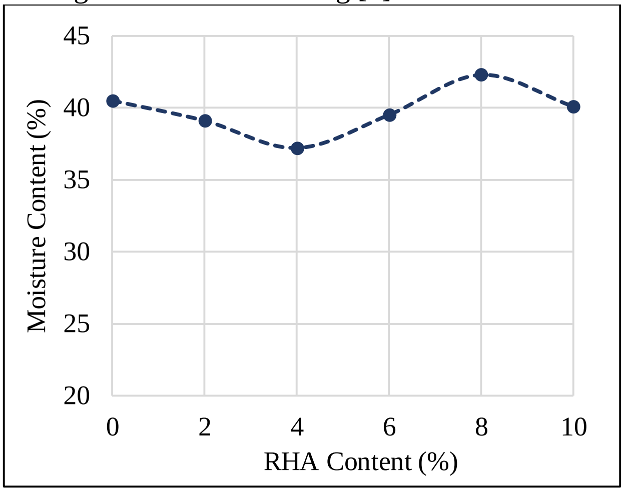

Figure 4: Liquid limit variation with RHA content

3.2 Particle size distribution of RHA

Particle size distribution of the RHA is presented in Figure 5. It can be observed that (250□m) sieve passing RHA particle percentage is 58.15%, indicating that the collected RHA samples consist with more fine particles. When the RHA particles are much finer the particles move much easier between clay particles. Consequently, the achievable degree of mixing of RHA to clay is significantly high and the expected reaction between clay and RHA at high temperature may have much efficiency.

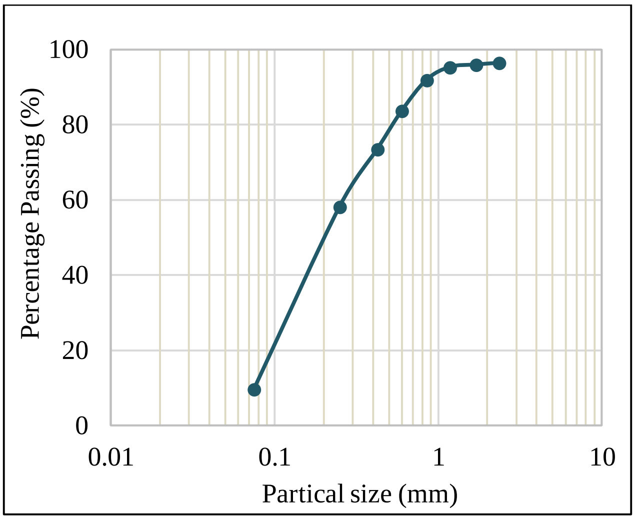

Figure 5: Particle Size Distribution Curve of RHA Sample

3.3 Particle size distribution of clay

Particle size distribution of the Dankotuwa clay is presented in Figure 6. It can be observed that the percentage of silt and clay (less than 0.□□□m) is more than 95% and the sand percentage is about 4%. It seems that Dankotuwa clay has high amount of micro particles which will contribute efficiently to the effective interaction with RHA particles.

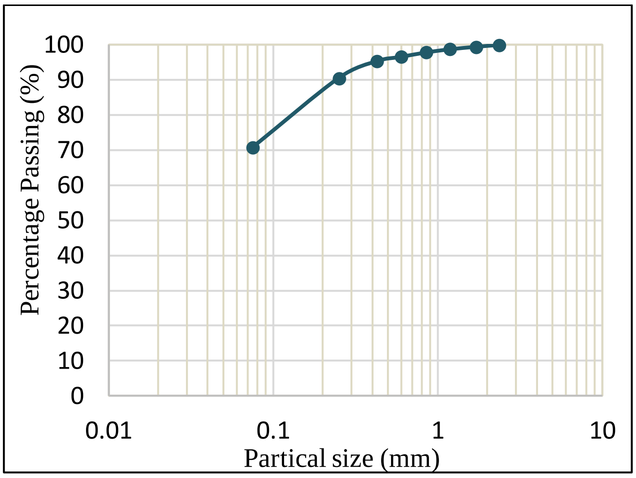

Figure 6: Particle Size Distribution Curve of Clay Sample

3.4 Compressive Strength

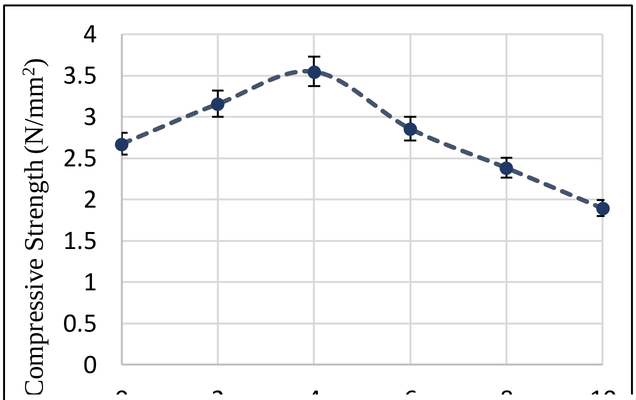

Figure 7: Compressive Strength variation of fired Clay Brick with different RHA content

The optimum compressive strength was found as 3.55N/mm^2 at the 4% addition of RHA (32.7% improvement) (Figure 7). Compressive strength of 2.675 and 1.813N/mm^2 were found at 0% and 10 % RHA respectively. When heating clay bricks a chemical recrystallization occurs. Amount of SiO_2 affects the strength gaining in the latest stage and also efficiency of the reaction and the amount of recrystallized material developed decide the latest strength (De Silva and Crenstil [7]). The strength increase up to 4% addition of the RHA can be explained through the amount of available RHA affects the latest stage strength gaining.
The recrystallization after dehydroxylation of water molecules, hence other parameters affect the process of dehydroxylation may cause to strength reduction after 4% addition of the RHA. The increase of water pressure increases the dehydroxylation temperature (De Silva [7]). Plasticity limit variation 19.3-33.7 indicates that the addition of RHA increase the amount of water content in the clay. Hence these conditions may cause the strength reduction after 4% addition of the RHA.

3.5 Water Absorption

It was found that until 0% to 4% addition of RHA, the water absorption does not have much variation, although it decreases (Figure 8). The addition of the RHA to 2% to 4% produce a good stable structure and it is explained that under the availability of the silica, later strength can be achieved hence the pores of the clay brick reduced and the water absorption reduced due to the activeness of better recrystallization. According to the plastic limits the increase of the water content increase with the addition of the RHA content. Hence the peak reaction temperature increase and it may occur a reduction in stable structure development or recrystallization. The increase of water absorption capacity indicates that the less recrystallization and less strength. According to Figures 7 and 8, it is indicated that when the water absorption increases the compressive strength decreases. Also this relationship defines that there may be an effect on water absorption to strength gain of fired clay bricks as explained in a preceding section

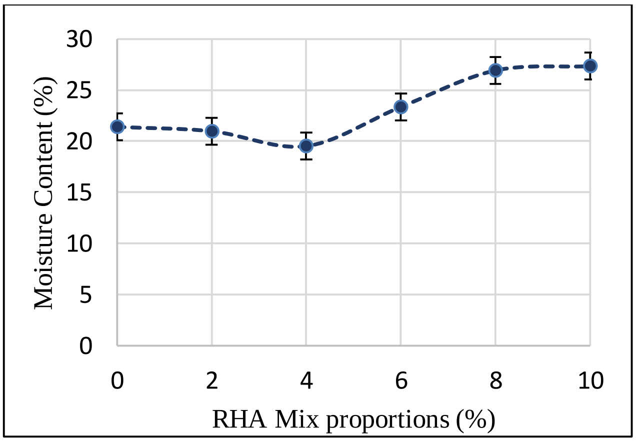

Figure 8: Water absorption variation of fired clay brick with different RHA content

4. Conclusions

The Rice Husk Ash (RHA) wasted from the brick kiln contains high amount of silica and can be used as SiO_2 provider for clay materials to increase SiO_2/Al_2O_3 ratio. The water absorption and compressive strength characteristics showed a great improvement with 4% RHA addition. The compressive strength of the fired clay brick was optimized with a value of 3.55N/mm^2 which is greater than Sri Lankan standards. At this level of RHA addition, brick strength had an improvement of 32.7% (compared with 0% RHA addition) indicates that bricks are suitable for load bearing walls. At 4% RHA addition, the lowest water absorption was obtained with a value of 19.51%. A waste of RHA from a brick firing process can be utilised as an additive for manufacturing of the fired clay bricks which increase the strength characteristics. Utilization of RHA for clay brick manufacturing prevents environmental pollution caused by open dumping of rice husk and this will contribute to use the rice plant with a maximum efficiency.

References

[1] Raut S., Ralegaonkar R. and Mandavgane S., 2011. 'Development of sustainable construction material using industrial and agricultural solid waste. *Construction and Build Masterials*, 25.

[2] Agus S, M., 2002. 'Utilization of Uncontrolled Burnt Rice Husk Ash in Soil Improvement'. *Dimensi Teknik Sipil*, 4(2), pp.100-05.

[3] Izwan J. et al., 2011. 'Chemical and Physical Properties of fired-Clay Brick at Different type of Rice Husk Ash'. *Proceedings of International Conference on Environment Science and Engineering*. Singapore, 2011. IACSIT Press.

[4] De Silva S. and Uduweriya R., 2011. Investigation of the Properties of Concrete containing Rice Husk Ash. *Transactions of the Institution of Engineers, Sri Lanka (IESL)*, 71-79

[5] Ghassan A. and Mahmud H., 2010. 'Study on Properties of Rice Husk Ash and Its Use as Cement Replacement Material'. *Materials Research*, 13(2), 185-90.

[6] Nilantha B, G., Jiffry I., Kumara Y. and Subashi G.H.M.J.., 2010. 'Structural and Thermal Performances of Rice Husk Ash (RHA) Based Sand Cement Block'. *Proceeding of the International Conference on Sustainable Built Environments*, 138-44.

[7] De Silva P. and Crenstil K.S., 2008. 'The Effect of Al_2O_3 and SiO_2 On Setting and Hardening of Na_2O-Al_2O_3-SiO_2- H_2O Geopolymer Systems', *J. Aust. Ceram. Soc. 44 [1] , 39-46*

[8] Lin D. and Weng C., 2011. 'Use of sewage sludge ash as brick material'. *Journal of Environmental Engineering*, 127, 215-20.

SECM/15/141

Evaluating Subcontractor Performance in Construction Industry

H.W.L. Chamara[1], K.G.A.S. Waidyasekara[2] and Harshini Mallawaarachchi[3*]

[123]University of Moratuwa, Colombo, Sri Lanka
*E-Mail: hmallawarachchi@gmail.com, TP: +9471-2201158

Abstract: Most of the construction projects undertaken are more complex in nature, demanding greater skills and technologies. In the past two decades, subcontracting has been utilized extensively in construction industry. Hence, subcontractor is a key person to assure the success of a construction project although many issues involved in subcontracting practice and rarely acknowledged. The reliance of main contractors on subcontractors to execute major portions of construction work makes the success of construction projects highly susceptible to the performance of subcontractor organizations. Early researches picked out those subcontractors are not being fully utilized due to various issues. As a result, subcontractors are subjected to put tremendous pressures on project performance in terms of quality, time and cost in construction industry. Therefore, in construction industry, there is a gap between the required performance level and the current performance of subcontractors. Thus, this study attempts to fulfill the gap between required and current performance of subcontractors by investigating subcontractors' issues on the project performance in terms of time, cost and quality. Literature review indicated number of issues with subcontractors that had adversely influenced the performance of a construction project. The study was adopted survey approach to fulfill the research objective. The structured questionnaire which was developed by supporting literature findings was distributed among main contractors and sub-contractors. Relative Important Index was adopted to analyse and evaluate the collected data. The results revealed that, selection method, critical site coordination, labour migration, delay payment and site safety were respectively significant on subcontractor performance. Further, it was identified there is a positive relationship between attitudes of main contractor and subcontractor. The paper describes the mitigation measures that could be used to maximize the performance of construction projects in terms of time, cost and quality, while enhancing the performance of subcontractors.

Keywords: Construction Industry, Subcontractor Performance, Project Performance, Issues

1. Introduction

The modern constructions are tending to be more specific and complex in nature of its technology, size and scale. As a result, main contractor prefers to subcontract the work because of insufficient resources or lack of expertise in a specific area. The specialized works make construction process more complex and specialized knowledge and experience are needed to execute some works. In such situations, the main contractor is not in a position to fulfill clients' whole requirements. Further, the contractor tends to sublet part or parts of the contract to other contractor or several contractors. In the past two decades, subcontracting has been utilized extensively in the construction industry. It is common to subcontract 80% to 90% of the construction work to subcontractors [1].

A study by [2] stated that the above situation is similarly applied in the Sri Lankan context as it had found that more than 80% of specialized works were done by the subcontractors in Sri Lanka. As [3] Indicated, subcontractors continue to play a vital role in executing significant portions of construction work. The qualified subcontractors are usually able to perform their work specialty more quickly and at a lesser cost than the main contractor (Arditi and Chotibhong, 2005 cited [1]). [4] postulated that, in practice the main contractor cannot provide the construction site with necessary resources. As [5] showed, the subcontractor is a key characteristic of a construction project which delivers labour up to 90% of the total project. However, [6] argued that, subcontractors are subjected to tremendous pressure in terms of quality, service and cost. Moreover, [7] pointed out that the performance of construction projects, in terms of time, cost and quality, continues to be less than the expected.

Therefore, in the construction industry, there is a gap between the required performance level and the current performance of the subcontractors. Early researches focused to bridge this gap, by only considering selection process of subcontractors where a considerable amount of researches aimed at identifying the drawbacks of selection process of subcontractors. A study by [9] showed that subcontractors are very important to the successful completion of most construction projects, yet many issues involved in subcontracting practice are seldom acknowledged. Similar phenomenon can be identified in Sri Lankan context.

Hence, the aim of this study is to fulfill the gap between required and current performance levels of the subcontractors by investigating subcontractors' issues on the project performance through three objectives as (i) to identify the current status and performance of subcontractors, (ii) to identify the issues faced by subcontractors, (iii) to analyse the most significant issues of the subcontractors on performance of the project in terms of time, cost and quality.

2. Literature Review

2.1 Subcontractors practice in construction industry

- **Subcontractors**

As [9] indicated that a subcontractor is a construction firm that contracts with a main contractor to perform some aspects or special aspect of the main contractors' work. [10] stated that subcontracting system is usually described as the contractual process in which a main contractor subcontracts parts of the job to another contractor who may also subcontract it to another firm or further subcontract. Further, [11] identified three main categories of subcontractors in the construction industry as trade contractors, specialist, and the labour only subcontractors.

However, according to the contractual point of view, [12] pointed out that, subcontractors could be categorized as domestic subcontractors and nominated subcontractors. In addition to above two categories, which was identified by [12] and [13] as named subcontractors those who contracts with the main contractor to supply or fix any materials or goods or execute work forming part of the main contractor.

In contemporary construction market, subcontractors execute significant portions of construction work. Subcontractors minimize resource requirements faced by main contractors and provide specialized expertise to construction projects [14]. As an example, [5] commented that up to 90% of the total value of a construction project, subcontractors supply labour and material facility in Netherland context. Subcontractors helped main contractors to overcome problems related to the need for special expertise, shortage in resources and limitation in finances [15]. [10] showed that the proportion of subcontracted works increased steadily all through the 21 years between 1983 and 2003 in world wide. In 1983, about 47% of the total value of building contracts was subcontracted out. In 2003, the proportion increased to almost 60% in Hong Kong context. As a developing country, in Brazil, the practice of employing labour through subcontractors has increased in the 1990s. Further, the proportion of construction employees employed by subcontractors in United Kingdom enlarged from 25% in 1983 to 45% in 1998 [16]. However, [10] said that technology requirements in typical civil engineering construction are less demanding than building construction. Consequently, a civil engineering or infrastructure contractor could not subcontract out as much as a building contractor, given the usual technologically complex nature of civil engineering works. As [10] further discussed, it is commented that, there are no subcontracted works in the "preliminaries" and 90% and 80% of the works are subcontracted out in the cases of sub-structure and building services installation. Hence, many researches revealed that the proportion of subcontracting is remaining for major building elements as (i) structural works, (ii) walls/doors and windows, (iii) finishes and (iv) fittings and fixtures.

- **Issues of subcontractors**

[8] made it clears that today, in many cases, it is considered a matter of fact that the construction industry is unable to perform in terms of delivering projects of the right quality at the right price and at the right time. The several set of circumstances have contributed to the construction industry having a poor reputation in society. As a result, construction output is not in required level. It is clear that the performance of subcontractors was at deprived level. Many researches stated that the performance of subcontractors may affect on project in many aspects.

According to the study by [9] and [17], payment and profit is a main concern for subcontractors. [9] further showed that the most subcontractors, main contractors, and owners regard the issue of retention to be a major problem. [18] observed that subcontractor bonds are another issue. The main contractor is responsible for the job performance of the subcontractors and the contractor becomes liable if a subcontractor fails to pay for works. Subcontractor bonds are sometimes required by main contractors because such bonds are normally required only on large construction projects or projects that involve high risks, particularly with subcontractor default.

Further, insurance procedure contains several issues which can be negatively affected on the subcontractors [19]. Mendes (2000 cited [9]) found that insurance responsibility is commonly shifted to subcontractors and those subcontractors often share losses even though they are not directly involved with the defective work. The discrepancy on the part of the owners can be attributed to the fact that owners are far removed from the insurance agreements between main contractors and subcontractors. In addition, site safety creates high influence on subcontractors according to a study by Quinlan (2003 cited [20]). As [9] stated that, construction is a high risk industry with a high incidence of workplace deaths, injuries and diseases and a poor safety record. There are evidences that the shift to subcontracting is having negative health and safety effects on workers. Further, back charging can lead to claims and disputes if the subcontractor is not properly notified or if the subcontractor does not agree with the charges. Less capabilities, experience and knowledge of main contractors' superintendents can be negatively impacted on the productivity of subcontractors [17]. James further verified that the administrative skills and people management skills of the project manager have a direct effect on the success of every project. As [21], [22] and [23] phrased the success level of projects may depend on the philosophy of selecting the right person for the right job. Subcontractor selection is largely on the basis of the lowest tender. [24] argued that it may result in problems in quality of work, delay in project duration, create additional costs in construction projects and lead to serious money losses for construction companies in the long run. Hence, it can be negatively affected on productivity of subcontractors which, in turn, reduces their profit margins.

Furthermore, labour migration is a widespread major problem in construction industry faced by many countries [25]. Most subcontractors complained that they are unable to efficiently and effectively perform their site works due to main contractors' poor site coordination. Many of the subcontractors complain that they are not being fully utilized due to main contractors' poor site coordination [26]. Many studies revealed that those issues can be identified in relation with seven types as construction information, working programme, preparation for work place, interfacing work to be completed by others, access to work place, plant support and material support.

2.2 Subcontractor practice in Sri Lanka

Similarly in Sri Lanka, subcontracting has been utilized extensively in the construction industry. As [27] mentioned, labour only subcontract is taken as the most significant feature in the Sri Lankan industry as well as worldwide which is given labours for construction works. Further, subcontractors undertake significant portion of construction works however, when compared to other countries this trend has not been escaped in the Sri Lankan context. Interviews with 3,300 construction workers on building sites in Sri Lanka revealed that 82% of the skilled workforce and 93% of the unskilled workforce are employed on a temporary basis, either as casual workers or through labour subcontractors [27]. Hence, subcontractors carried out different work activities as finishes (22%), door & windows (17%), plumbing (15%), air condition (12%), electrical (l18%) and pilling works (6%).

As a result, at the last two to three decades the subcontractor practice has increased in rapidly in Sri Lankan construction industry. Further, the involvement of subcontracting is more than half of the total cost of the project, according to preceding studies. At present, it is an essential factor to the construction industry and helps to successful project completion. However, the reliance of main contractors on subcontractors to execute major portions of construction work makes the success of construction projects highly susceptible to the performance of subcontracting organizations. As a result, subcontractors are subject to tremendous pressures on project performance in terms of quality, time and cost in construction industry.

Thus, many researches revealed that the performance of subcontractors was at ineffective level thus, there is a gap between actual and required performance. Accordingly, literature findings establish necessity to study about the subcontractor performance in construction industry in order to fulfill gap between actual and required performance. Next explains the research methodology adopted in this study.

3. Research Methodology

Literature review was conducted on the major areas of subcontracting including subcontractor practice and issues of subcontractors which was globally significant in building projects. The data were mainly collected through questionnaire survey under the survey approach. The target population was the prominent professionals who had already engaged in construction work within Sri Lanka. Professionals like Project Managers, Civil Engineers and Quantity Surveyors etc. were targeted mainly in main contractors' perspective while owner of the subcontracting organization was targeted in subcontractors' perspective. The sample of 30 professionals was decided to be a reasonable sample and a random sample of 40 prominent professionals in the construction industry was selected with the purpose of receiving targeted 30.

Table1: Profile of sample

Category	Number of Distributed	Response (%)
Main Contractor	40	77.50
Subcontractor	40	82.50

Collected data was subjected to statistical analysis. Relative Importance Index (RII) was used to analyse collected data through questionnaire survey. Each issue of subcontractors was ranked on the relative importance index. Further, Hypothesis Testing and Rank Correlation Coefficient statistical techniques were used to evaluate relationships of the views of both main contractor and subcontractor.

4. Research Findings and Discussion

4.1 Current status and performance of subcontractors

- **Types of works carried out**

While working in construction industry, subcontractors were preferred to undertake different projects. Electrical, fire, plumbing, air conditioning, structural works and finishes were the types of work carried out by the subcontractors generally in building construction. The survey findings proved that the subcontractors carried out finishing works and services (electrical, plumbing, air conditioning, fire) rather than the structural works.

In the industry, subcontractors carried out finishing works more than 50% while undertook electrical and plumbing works 33% and 30% sequentially. Most of the main contractors also preferred to subcontract finishes, plumbing and electrical works. Hence, the main contractors sublet 47% of finishes, 37% of electrical works and 30% of plumbing works.

- **Performance of subcontractors**

In the current construction industry practices, both main contractors and subcontractors have different perceptions towards subcontractor's performance (refer Figure 1). Survey findings revealed that most of the main contractors were not pleased with current performance of subcontractors. According to the analysis, 13% of main contractors are satisfied with subcontractors' performance very often, while more than 50% are satisfied sometimes. However, 30% of subcontractors are always satisfied with their performance while majority of subcontractors (70%) are satisfied very often. However, the current performance of subcontractors was at unsatisfactory level as verified by survey findings. It further proved that several factors can be affected on poor performance of subcontractors.

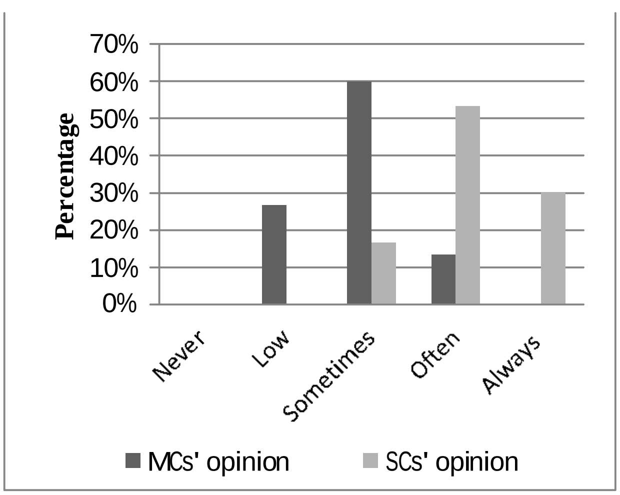

Figure 1: Perceptions on subcontractor performance

4.2 Issues with subcontractors

As revealed by survey findings, several issues were identified which can be affected on the performance of subcontractors (refer Table 1).

- **Selection process**

There are various performance evaluation methods were adapted for selecting suitable subcontractors for construction projects. Survey data showed that there was a huge disagreement between main contractors' and subcontractors' opinion towards the selection of subcontractors. As evidenced by survey findings, more than 75% of both parties recommended that the selection method of subcontractor must be changed to overcome issues in existing selection process.

- **Bonds and insurance**

Survey findings revealed that main contractors and subcontractors have different views on bonding and insurance. More than 70% of main contractors said that the current bonds and insurance practice is good enough, probably because main contractors are well protected within the current practice. However, only11% of subcontractors accepted the current practice, because most of the risks were easily shifted to subcontractors according to the subcontractors' point of view.

- **Delay Payment**

Main contractors are well-known for being slow to pay their subcontractors for completed work. Indeed, more than 40% of subcontractors verified that the payments received from main contractors were delayed by more than 45 days after the completion of the work, while only 18% of main contractors agreed on that. Hence, late payment is major issue in construction industry as perceived by many subcontractors. Therefore, almost all subcontractors and main contractors (more than 80%) indicated that the present payment practice needs to be improved.

- **Retention withheld by main contractor**

The findings suggested that over 60% of subcontractors regard that the retainage issues were created cash flow problems to subcontractors, even though most of the main contractors (88%) did not regard likewise. More than half of the subcontractors (62%), and main contractors (53%) indicated that the magnitude of the retainage was an important factor to be considered before entering into an agreement with the main contractors, to avoid problems with the retainage.

- **Site safety issues**

Survey data revealed that more than 70% of subcontractors viewed that the site safety of subcontractors' workers was not considered by main contractors while the 38% of main contractors agreed on that. Hence, site safety was at poor level and it can be highly affected on subcontractors' performance as well as on project performance thus, the safety procedure should be improved.

- **Back charging issues**

According to the survey findings, the majority of subcontractors (more than 80%) said that the main contractors collect attendance unnecessarily while more than 60% of main contractors viewed that the subcontractors give up paying for attendance.

- **Critical site coordination**

Results exposed that most of subcontractors complained that the site works were unable to perform efficiently and effectively due to several coordination issues.

- **Involvement of contractors' personnel**

More than 75% of both parties agreed that contractors' personnel were not engaged to the project in approved manner. Thus, the subcontractor's success depends heavily on the capabilities of contractors.

- **Migration of subcontractors' labour**

As viewed by survey findings, most of the subcontractors and main contractors (more than 70%) said that the labour migrations are always happened among the construction sites. Further, labour migration was an uncontrollable issue in construction industry as similarly viewed by both main contractors (68%) and subcontractors (74%).

4.3 Evaluating issues of subcontractors on project performance

According to the survey findings, various issues were identified which can be affected on subcontractors' performance. Those issues can also be influenced on the time, cost and quality of the overall project. As the both main contractors and subcontractors had different opinions, the subcontractors' issues were ranked in terms of the influence on time, cost and quality of overall project with regards to the main contractors' and subcontractors' perspectives separately (refer Table 2).

Table 2: Ranking of subcontractor issues on project performance: main contractor vs. subcontractor

Issues of subcontractors	**Main contractors' perspective**						**Subcontractors' perspective**					
	Time		**Cost**		**Quality**		**Time**		**Cost**		**Quality**	
	RII	**Rank**	**RII**	**Rank**	**RII**	**Rank**	**RII**	**Rank**	**RII**	**Rank**	**RII**	**Rank**
Selection method of SCs for projects	87.86	1	84.0	2	89.33	1	88.00	2	74.00	4	84.67	3
Acquiring bonds and guarantees from SCs	33.33	8	34.67	9	28.00	9	68.67	6	56.67	5	41.33	8
Obtaining insurance for projects through SCs	34.00	7	39.33	7	26.67	8	66.67	7	62.00	7	38.00	6
Delay of subcontractors' payments	62.00	4	44.00	5	41.33	6	86.00	3	86.67	1	83.33	1
Keeping retention from SCs payments	31.33	9	37.33	8	27.00	10	45.33	10	41.33	10	30.00	10
Providing site safety for the SCs	78.67	3	60.47	4	60.67	4	74.00	5	60.00	6	73.33	5
Migration of subcontractors' labours	58.00	5	62.67	3	82.00	3	74.67	4	74.67	3	63.33	4
Back charging	28.67	10	30.67	10	36.00	7	46.00	9	66.00	8	57.33	9
Critical site coordination	82.67	2	85.33	1	86.67	2	91.33	1	75.33	2	92.00	2
Involvement of the MCs' persons for projects	44.67	6	43.33	6	58.67	5	58.00	8	44.67	9	46.00	7

Main contractors' perspective

According to the main contractors' perspective, the selection method of subcontractors, critical site coordination, migration of subcontractors' labours and site safety were identified as most significant factors which can be affected on time, cost and quality of the project. However, back charging, keeping retention from subcontractors' payments, obtaining insurance and acquiring bonds and guarantees from subcontractors were attained as less influenced issues on time, cost and quality performance of the project with lower RII values.

Subcontractors' perspective

However, delay of subcontractors' payments, selection method of subcontractors, critical site coordination and migration of subcontractors' labours were identified as most significant issues which needs high attention to reduce their influence on overall construction project according to the perception of subcontractors.

Table 3: r_s and and t_{cal} values on project performance

Types of performance	**r_s value**	**t_{cal} value**
Time performance	0.890	5.548
Cost performance	0.654	2.448
Quality performance	0.733	3.050

Table 4: Standard for r_s values

$r_s = +1$	Means that the rankings have perfect positive association. Their rankings are exactly alike.
$r_s = 0$	Means that the rankings have no correlation or association.
$r_s = -1$	Means that the rankings have perfect negative association. They have exact reverse ranking to each other.

Time performance

According to the calculations, r_s value for time performance was 0.890, which is closer to the one. Thus, the relationship between main contractors and subcontractors was positive in ranking time performance of the project.

Cost performance

The r_s value for the cost performance was 0.654, which showed positive relationship however it was not strong as time performance.

Quality performance

Quality performance also illustrated a positive relationship same as the time and cost performance, with the r_s value of 0.733. Hence, as identified by both main contractors and subcontractors, issues of subcontractors were affected to poor performance of the construction projects in a same manner.

4.5 Mitigation methods for issues of subcontractors

Survey data revealed that both main contractors and subcontractors were agreed on the requirement of taking actions to mitigate issues of subcontractors.

Hence, several mitigation methods were identified through the questionnaire survey, which were suggested by respondents in construction industry as summarized in Table 5.

Table 5: Proposed mitigation methods for subcontractors' performance issues

Issues	**Mitigation methods**
Selection method	▪ Selection method must be transparent ▪ Consider working capacity and previous experience of the subcontractors

Acquiring bonds and guarantees	▪ Educate the SC's staff about the insurance/bonds
Obtaining insurance for projects	
Delay of subcontractors' payments	▪ clients should pay main contractors punctually
Keeping retention from SCs payments	▪ SCs should consider magnitude of retainage before entering contract
Providing site safety for subcontractors	▪ MCs should provide full-time safety staff ▪ SCs should provide job safety program
Migration of subcontractors' labours	▪ Appoint labours to several projects ▪ Policy enhancement
Back charging	▪ Both party should identify responsibilities
Critical site coordination	▪ MCs have to get direct responsibility
Involvement of MCs' persons	▪ Present during site visit ▪ Involve site meetings with SCs ▪ Make good coordination among workers

4. Conclusions

Performance of the construction projects is one of the major research areas in current practice. The reason is that construction is a major industry in almost all countries, which seriously affects on the economy. Inadequate project performance usually leads to a project failure. Basically construction works are mainly carried out by main contractors. With the lesser time and complex nature the project, main contractors tend to sublet the parts of the projects. In current practice, subcontractors are mainly carrying out finishing works and services rather than the structural works. Main contractors also preferred to subcontract such types of works. However, the satisfaction level of main contractors on the current performance of subcontractors was at inadequate level even though, majority of subcontractors were satisfied.

The survey data further revealed that the performance of subcontractors was poor due to several factors as selection process, bonds and insurance, payment method for subcontractors, retainage issues, site safety, critical site coordination, migration of subcontractors' labour, back charging, and involvement of contractors' personnel. Other than that, the lack of qualified and experienced management supervisory staff, inappropriate contract conditions, and communication difficulties were recognized through the survey findings, as further issues which can be affected on subcontractors' performance. According to the main contractors' point of view, the selection process of subcontractors is a critical issue which was highly affected on the time and quality of the project while critical site coordination and site safety were sequentially influenced on time and cost performance of the overall project. Hence, the selection method of subcontractors, critical site coordination, migration of subcontractors' and site safety were most significant factors as viewed by main contractors. However, subcontractors argued that the delay of subcontractors' payments was also required special attention due to their paramount influence on overall project performance. Even though, in some cases, there were differences between rankings, generally, a comparable picture was shown on the views of both main contractor and subcontractor. Further, the evaluation through 'rank correlation coefficient' clearly mentioned that there was a positive correlation between the opinions of main contractors and subcontractors. Generally, both parties had same view about the poor performance issues of subcontractors and both parties were supposed to implement mitigation procedures to overcome such issues. By concluding this study, the issues of subcontractors were identified and it can be highly influenced on time, cost and quality performance of the project. Hence, people who involved in construction industry can take actions to mitigate major issues of subcontractors in order to complete constructions projects successfully by fulfilling the gap between required and actual performance of subcontractors.

References

[1] Mohammad, S., 2009. A construction subcontractor selection model. *Jordan journal of civil engineering,* 3(4), 375-376.

[2] Piyasoma, W. M., 1994. Interaction between main contractor and subcontractor in construction project. Unpublished dissertation (B.Sc), University of Moratuwa.

[3] Wang, W. and Liu, J. J., 2004. Factor-based path analysis to support subcontractor management. *International journal of project management*, 23(2), 109-120.

[4] Chien, H.K., Cheng, M.Y. and Wu, T.K., 2006. Evaluating sub-contractors performance using EFNIM. *Automation in construction*, 16, 525-526.

[5] Hartmann, A., 2010. Subcontractor procurement in construction the interplay of price and trust. *An International Journal,* 15(5), 354-355.

[6] Errasti, A., Beach, R., Oyarbide, A. and Santos, A., 2006. A process for developing partnerships with subcontractors in the construction industry: An empirical study. *International journal of project management*, 25, 250-251.

[7] Masterman, J.W.E., 2002. *Introduction to building procurement systems*, 2nd ed., Spon Press, London.

[8] Jaggar, D., Ross, A., Smith, J. and Love, P., 2002. *Building design cost management*, Blackwell Science, Oxford.

[9] Arditi, D. and Ranon, C., 2005. Issues in subcontracting practice. *Journal of construction engineering and management*, 131(8), 866-867.

[10] Chiang, Y.H., 2009. Subcontracting and its ramifications: a survey of the building industry in Hong Kong. *International journal of project management*, 27 (1), 80–88.

[11] Hinze, J. and Tracy, A., 1994. The contractor-subcontractor relationship: the subcontractors' views. *Journal of construction engineering and management*, 2(1), 274-287.

[12] Yik, F.W.H., Lai J.H.K., Chan K.T. and Yiu E.C.Y., 2006. Problems with specialist subcontracting in the construction industry. *Building services engineering research and technology,* 27(3), 183-193.

[13] Samuel, L., 2009. Subcontract and supply enquiries in the tender process of contractors. *Journal of construction management and economic*, 27(12), 1220-1221.

[14] Mbachua, J., 2008. Conceptual framework for the assessment of subcontractors' eligibility and performance in the construction industry. *Journal of construction management and economic*, 26(5), 471-473.

[15] Elazouni, A. and Metwally, F., 2000. Decision support system for subcontracting construction works. *Journal of construction engineering and management*, 126 (3), 191-200.

[16] Edwards, D. J., 2003. Accident Trends Involving Construction Plant: An exploratory analysis. *Journal of construction research, 4(2), 161-173.*

[17] James, P. M., 2010. *Subcontractor perspectives: factors that most affect their relationships with general contractors - A Pacific Northwest study*, Thesis (M.Sc.), Washington State University.

[18] Clough, R. and Sears, G., 1994. *Construction contracting*, Wiley, New York.

[19] Russell, J. S., 1991. Insurance industry: Overview. *Journal of management engineering*, 7(1), 98– 118.

[20] Wadick, P., 2010. Safety culture among subcontractors in the domestic housing construction industry. *Structural survey*, 28(2), 108-120.

[21] Kumaraswamy, M. and Matthews, J., 2000. Improved subcontractor selection employing partnering principles. *Journal of management in engineering*, 16, 47-58.

[22] Vilutiene, T., 2008. Automated processing of subcontractor work performance data to improve the quality control and support the subcontractor selection process. ed. *25th International symposium on automation and robotics in construction*, Luthuania, June 26-29. In: Dept of construction technology and management, 507-511.

[23] Manoharan, R., 2005. *Subcontractor selection method using analytic hierarchy process*, Thesis (M.Sc), Universiti Teknologi Malaysia.

[24] Arslan, G., Kivrak, S., Birgonul, M. and Dikmen, I., 2008. Improving subcontractor selection process in construction projects: Web-based subcontractor evaluation system (WEBSES). *Automation in construction*, 17,480-488.

[25] Ford, J.R., Jepson, M., Bryman, A., Keil, E.T., Bresnen, M. and Beardsworth, A., 1983. Management of recruitment in the construction industry. *International Journal of Project Management*, 1, 76 - 82.

[26] Andy, K.W. and Andrew, D. F., 2010. Optimizing the time performance of subcontractors in the building projects. *Australasian journal of construction economics and building*, 10 (1/2), 90-100.

[27] Jayawardane, A. K. W. and Gunawardena, N. D., 1998. Construction workers in developing countries: a case study of Sri Lanka. *Journal of construction management and economics*, 16(5), 521-530.

SECM/15/143

USE OF RICE HUSK ASH BLENDED CEMENT TO MANUFACTURE CELLULAR MASONRY BLOCKS

D.A.R.Dolage[1], A. M. AliRajay[1] and A.Parvathakeethan[1]

[1]The Open University of Sri Lanka, Nawala, Sri Lanka
Email: dadol@ou.ac.lk TP. 0112881289

Abstract: This paper summarises the research work on determining suitability of rice husk ash (RHA) to partially replace cement in manufacturing cellular masonry blocks. The particle size distribution and chemical composition of RHA were measured for samples taken at different temperatures. In this research, mixtures have been prepared in combinations of four binder-sand ratios namely 1:3, 1:4, 1:5 and 1:6, three water-binder ratios namely 0.4, 0.5 and 0.6 and five levels of cement replacement with RHA namely percentages of 0, 5, 10, 15 and 20 by weight. One hundred and twenty cubes were cast (4x3x5x2=120) and tested for compressive strength at 7 and 28 days. Based on the compressive strength values, 1:5 binder-sand ratio was chosen as the appropriate mix proportion to cast cellular masonry blocks for different water-binder ratios namely 0.5 and 0.6 as per SLS 855Part 1:1989.

RHA was blended with cement in percentages of 0, 5, 10, 15 and 20 by weight in producing cellular masonry blocks of size 390 x 190 x 200 mm. These were tested for water absorption in addition to compressive strength. The compressive strengths of cellular masonry blocks at 7, 14 and 28 days for 1:5 binder-sand ratio, water-binder ratio 0.5 and 5 per cent cement replaced with RHA were 2.05 N/mm^2, 2.24 N/mm^2 and 3.37 N/mm^2 respectively. Likewise the values for 1:6 binder-sand ratio for water-binder ratio 0.5 and 5 per cent cement replaced with RHA were 1.6 N/mm^2, 2.18 N/mm^2 and 3.24 N/mm^2 respectively. The minimum compressive strength as per SLS 855 Part I: 1989 is 1.2 N/mm^2. The water absorption rates for water-binder ratios 0.5 and 0.6 are 9.8 and 10.5 respectively, which are within limits; the allowable limit is 10-15% as per BS EN 1996-1-1. The study concludes that 15 per cent cement replacement level is permissible.

Key words: Rice husk ash, Cellular masonry blocks, Blended Cement

1. Introduction

Rice husk is the outer covering of rice grain, generated during the rice milling process. This is an agricultural by-product used mostly as a fuel in brick kilns to generate heat. Still a large amount of rice husk is burnt in heaps in open ground as a measure of disposal. The disposal of rice husk ash (RHA) so generated is still a problem. On the other hand, the cost of producing cellular masonry blocks is increasing due to the escalating prices of cement. This has influenced researchers to investigate the use of waste materials as a supplementary cementitious material, and RHA is thought to be a potential candidate in this cause. Research studies to explore various aspects of using RHA, produced by controlled burning of the rice husk, as a substitute for cement have been in existence for quite some time.

The research reported here is on RHA, with respect to chemical and physical properties at varying temperature, level of replacement of cement and water absorption of RHA blended cement. The main objectives of this study are as follows;

- To explore the chemical and physical properties of RHA in relation to burning temperature.
- To determine the optimum level of replacement of cement with RHA in the manufacture of cellular masonry blocks.

2. Literature Review

2.1 Focus of past studies

Rice is Sri Lanka's staple food, therefore paddy is produced in large scale. Mude *et al.* (2013) have revealed that 22 per cent of the weight of paddy comes as rice husk and 25 per cent of the weight of husk is converted to RHA during the firing process. An important determinant of quality of RHA when considered as an alternative for cement is the extent of silica content. Al-Khalaf and Yousiff (1984) report that when husk is converted to ash by uncontrolled burning below 500^0C, the ignition does not become complete and considerable amount of unburnt carbon is still found in the ash. A study by Boating and Skeete (1990) reveals that the ash produced by controlled burning of the rice husk between 550^0C and 700^0C, and one hour of incineration transforms the formation of silica into amorphous form. The increasing cost of cement has motivated researchers to identify suitable alternative material for block making. Hence an objective of the study is to examine cementitious properties of RHA.

In a pioneering study by Bandara (1994), it is concluded that firing temperature and isothermal firing time for attaining high amount of amorphous silica in fired ash depends on the variety of rice husk ash. The study also reveals that, as an approximation, a firing temperature of 700°C seems to be the optimum for the four Sri Lankan varieties of rice husk examined in that study; an isothermal firing time of 30 to 60 minutes is to be adopted based on the knowledge of the variety of rice husk.

A number of authors namely, De Silva and Uduweriya (2011) and Ganesan *et al.* (2008) have investigated the replacement levels of cement for concrete containing RHA. Dolage *et al.* (2011) investigated the replacement levels of cement to produce cement sand blocks. A study extending the scope of the former by mixing lime with RHA was conducted by Pushpakumara and Subashi (2012). Subsequently, Baskaran *et al.* (2012) have studied the possibility of using RHA in stabilized soil blocks. Most of these studies, in addition, have investigated the particle size distribution of RHA. Since evidently, only a few studies have explored the effect of temperature on the chemical composition and thereby the strength, this study expects to shed some light on this.

2.2 Chemical Reaction of RHA with Cement and Water

The duration of incineration and temperature at which it is incinerated are important parameters influencing the reactivity of RHA. Silica in RHA initially exits in the amorphous form, but may become crystalline when RHA is continued to be burnt at higher temperature. The chemistry of the pozzalonic action of RHA includes the reaction of the amorphous silica in ash with water to form calcium silicate hydrates.

Reactions that take place in the preparation of RHA cellular masonry block are given below. Silicon burnt in the presence of oxygen gives silica.

$$Si + O_2 \rightarrow SiO_2$$
$$C_3S\ (\text{Cement}) + H_2O \rightarrow CSH + Ca(OH)_2$$

The highly reactive silica reacts with calcium hydroxide released during the hydration of cement, resulting in the formation of Calcium Silicate Hydrate, which is responsible for the strength.

$$SiO_2 + Ca\,(OH)_2 \rightarrow CSH + SiO_2$$

2.3 Availability of Rice Husk

Paddy and rice husk production in Ampara district for the year 2014/15 is shown below in Table 1. This indicates if RHA is suitable as an alternative for partial replacement of cement, availability of rice husk would not be a problem in Ampara district.

Table 1: Paddy and rice husk production in Ampara district

Paddy (MT)			Rice husk (MT)
Maha	*Yala*	Total	Rice husk (MT)
307,661	199,265	506,926	101,386

Source: Department of Census and Statistics, 2014

A total of 87 rice mills are located in Ampara district and their milling capacities are shown in Table 2.

Table 2: Milling capacity of rice mills in Ampara district

Milling capacity (kg/day) Capacity = C	Number of mills
<1000	9
1000<C<2500	4
2500<C<5000	8
5000<C<8000	11
C>8000	55

2.4 Cellular Masonry Blocks

Cellular blocks are masonry units that contain one or more formed voids that do not fully penetrate the block. The use of cellular masonry blocks can have significant advantages over solid blocks in situations where weight is a prime consideration. The reduced unit weight results in easy handling, reduced floor/ foundation loading, economic and efficient productivity. There are two block types available in cellular format: dense aggregate cellular block (typical material density range is 1800-2100 kg/m^3) and light weight aggregate blocks (typical material density range is 850-1500 kg/m^3). Cellular masonry blocks are available in various types namely standard common, close textured/paint grade common, standard, facing and architectural masonry facing blocks. The compressive strength of the cellular masonry block ranges from 1.2 N/mm^2 to 10.0 N/mm^2. The standard specification deals with requirements for compliance and specifies materials, sizes and dimensional tolerances and minimum performance levels for cement blocks for construction work. It covers solid, hollow and cellular masonry blocks not exceeding 650 mm in any work size dimension (SLS 855 Part 1: 1989).

3.0 Methodology

3.1 Materials used

OPC conforming to Sri Lankan standard SLS 107: Part 1: 2008 was utilised in preparing the binder. Graded river sand passing through 2.36 mm sieve with fineness modulus of 2.83 (between sieve sizes of 5 mm and 160 micro meters) and having specific gravity of 1.6 was used as fine aggregate, as per Sri Lanka Standard 855:1989. While the RHA sample burnt at approximately 700°C was collected from a thermal power plant, the samples burnt at 650°C and 750°C were obtained from a brick kiln. The RHA samples were sieved through BS standard sieve size 63 micrometer and its colour was grey.

3.2 Casting of solid and cellular masonry blocks

Samples were prepared with four binder-sand ratios, namely 1:3, 1:4, 1:5 and 1:6 for three water-binder ratios, namely 0.4, 0.5 and 0.6. A mixture of cement and RHA was used as the binder; five mixtures of binder were prepared by varying the RHA percentages, namely 0, 5, 10, 15 and 20 by weight. Compressive strength test was carried out on cubes of size 100 x 100 x 100 mm casted using these 120 combinations (4 X 3 X 5 X 2 = 120).

By using the cube strength values the optimum binder sand mix proportion, 1:5 was chosen to prepare cellular masonry blocks. By varying the water-binder ratios 0.5 and 0.6, RHA was blended with cement in percentages of 0, 5, 10, 15 and 20 by weight in producing cellular masonry blocks of size 390 x 190 x 200 mm. Altogether 50 samples of cellular masonry blocks were prepared for both compressive strength and water absorption tests. Out of these, 40 samples were used for testing of compressive strength and the remaining 10 for testing of water absorption. From each mix proportion, five cellular masonry blocks were cast for testing. The details of material usage to cast different masonry block samples is presented in Table 3.

Water was mixed with the dry binder sand mixture until the required workability was obtained. The mixture was then placed in the standard mould fitted to the cellular masonry block manufacturing machine belonging to one of the largest cellular masonry block manufacturers in Sri Lanka. The cellular masonry block was compacted with the use of the vibratory mechanism attached to the machine.

Table 3: Materials usage to cast cellular blocks

Water / Binder	Sample Name	Cement (%)	RHA (%)	Quantities (kg)			
				Sand	Cement	RHA	Water
0.5	X1	100	00	90	18	00	9.0
	X2	95	05	80	15.2	0.8	8.0
	X3	90	10	80	14.4	1.6	8.0
	X4	85	15	80	13.6	2.4	8.0
	X5	80	20	80	12.8	3.2	8.0
0.6	Y1	100	00	90	18	00	10.8
	Y2	95	05	80	15.2	0.8	9.6
	Y3	90	10	80	14.4	1.6	9.6
	Y4	85	15	80	13.6	2.4	9.6
	Y5	80	20	80	12.8	3.2	9.6

3.3 Testing Procedure

Two samples of RHA burnt at 650°C and 750°C were collected from a brick kiln and the third sample of RHA burnt at 700°C from the thermal power plant. The temperature measurement was conducted using an improvised thermo couple connected to a multimeter.

The RHA samples were sieved through BS standard sieve size 63 micrometer. The test for chemical composition was conducted at the research laboratory of the Holcim Pvt. Ltd. After 24 hours, cellular masonry blocks were demoulded and cured for 7 days (10 blocks), 14 days (10 blocks) and 28 days (20 blocks). At the end of these periods cellular masonry blocks were tested for crushing strength.

Figure 1: Cellular block manufacturing machine

The water absorption test was conducted on the cellular masonry blocks. The 10 cellular masonry blocks that had been cured for 28 days were weighed and oven dried for 24 hours at a temperature between 100°C to 115°C. Then the blocks were weighed (dry mass) and immersed completely in water at the room temperature for 24 hours. Thereafter the wet blocks were taken out of the water bath, wiped off with a damp cloth and weighed immediately (wet mass).

4. Results and Discussion

Temperature impact on Chemical composition

The test to determine chemical composition of RHA was carried out at the Holcim Research Laboratory in Puttalam. This was done on a sample of 100 g using the apparatus of X-ray fluorescence (XRF). The results are shown in Table 4.

Table 4: Composition of RHA at different temperatures

Compound	Percentage		
	650°C	700°C	750°C
SiO_2	88.61	89.22	91.11
Al_2O_3	0.94	1.40	1.23
Fe_2O_3	0.22	0.21	0.27
CaO	2.73	2.56	2.43
MgO	0.42	0.41	0.44
SO_3	0.15	0.09	0.11
K_2O	2.17	2.36	2.47

According to the test results, when the temperature increases, percentage of silica content has also increased. All the three samples were examined through a microscope to notice the presence SiO_2 and unburnt carbon. It was observed that the content of crystallised SiO_2 is greater in the sample burnt at 750°C and the presence of unburnt carbon was higher in the sample burnt at 650°C. Since the higher amorphous SiO_2 and lower the unburnt carbon are desirable properties, the sample incinerated at 700°C was selected to cast solid and cellular masonry blocks in this research.

Particle Size Distribution of RHA

The particle size distribution (PSD) curves of OPC and RHA are shown in Figure 1. The particles of RHA are nearly four times coarser than those of OPC and are better well graded in their distribution. The resulting lower surface area of RHA negates the requirement of coating expected of the cementitious material.

Table 5: Summary of Compressive strength of cubes

Sample Set	Water/Binder Ratios	Mix Proportion		28 Days Compressive Strength (N/mm^2)			
				Binder-Sand ratio			
		RHA (%)	OPC (%)	1:3	1:4	1:5	1:6
1	0.4	00	100	12.75	13	11.5	5.5
2		05	95	13.25	14	12.5	5.2
3		10	90	5.25	12	9	3.2
4		15	85	4.50	4.5	4.5	1.5
5		20	80	2.50	3.5	3	-
6	0.5	00	100	13.50	18	16.5	5.2
7		05	95	14.50	18.5	17.5	5.45
8		10	90	11.70	17	13.5	4
9		15	85	5.50	7	7	2.65
10		20	80	4.25	5.5	5	-
11	0.6	00	100	13.00	15.5	13.5	5.15
12		05	95	13.25	16	14.5	5.25
13		10	90	7.00	14	12	3.75
14		15	85	5.25	5.5	6	1.75
15		20	80	4.25	4	4	-

Table 6: Summary of compressive strength of cellular masonry blocks

Binder: Sand Ratio	Water: Binder Ratio	Sample Name	Cement (%)	RHA (%)	Compressive Strength (N/mm^2)		
					7 Days	14 Days	28 Days
1:5	0.5	X1	100	00	1.67	2.18	3.21
		X2	95	05	2.05	2.24	3.37
		X3	90	10	1.22	1.79	2.69
		X4	85	15	1.15	1.54	2.34
		X5	80	20	0.77	1.28	2.12
	0.6	Y1	100	00	1.54	2.12	3.11
		Y2	95	05	1.6	2.18	3.24
		Y3	90	10	1.47	1.73	2.47
		Y4	85	15	1.35	1.67	2.28
		Y5	80	20	1.03	1.47	1.92

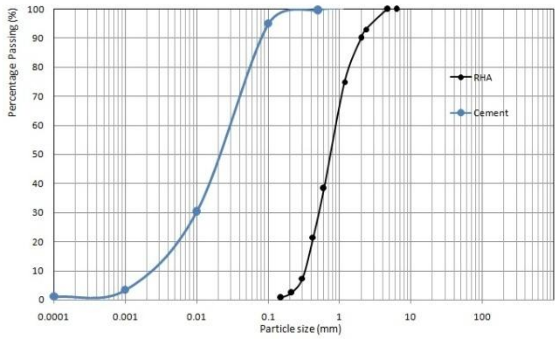

Figure 2: PSD curves for RHA and OPC

Compressive Strength of solid blocks

Table 5 summarises 28 day compressive strength results for binder-sand ratios namely 1:3, 1:4, 1:5 and 1:6, and for the three water- binder ratios namely 0.4, 0.5 and 0.6. According to SLS 855: Part 1:1989, the minimum compressive strength for cement sand blocks is 1.2 N/mm^2. As can be expected, higher the binder-sand ratio, the larger is the compressive strength. Although, binder-sand ratio 1:6 is the most economical, at replacement levels 15 and 20 per cents, it shows compressive strength values lower than 1.2 N/mm^2. According to the above cube testing results, for the binder-sand ratio 1:5 and water-binder ratios 0.4, 0.5 and 0.6, for 7 days and 28 days, compressive strength values satisfy the required compressive strength of cement sand cellular masonry blocks. The prize observation in this study is that when 5 per cent cement is replaced with RHA the compressive strength is increased by 6 per cent.

Compressive Strength of cellular masonry blocks

The compressive strength results of the cellular masonry blocks casted for different mix proportions are computed and presented in Table 6. It is observed that the compressive strength values do not decrease noticeably when water binder ratio is increased from 0.5 to 0.6; decrease only by 3 per cent. Further the results confirm that when 5 per cent cement is replaced with RHA the compressive strength is increased by 6 per cent. Nevertheless, with further increases in cement replacement levels, the strength gradually and noticeably decreases. However, even at the cement replacement level of 15 per cent, the compressive strength (2.34 and 2.28 N/mm^2) is greater than the minimum specified in the SLS 855: Part 1:1989, which is 1.2 N/mm^2.

Water absorption

The water absorption was computed as per SLS 855: Part 2:1989 and a summary of results is presented in Table 7. The water absorption of the cellular masonry blocks with no RHA was 8.3 per cent. However, as per results, when the cement replacement level is increased the water absorption too is proportionately increasing. Water absorption is not a physical requirement as specified in the SLS 855: Part 1. However, it is a useful index to determine whether wetting of block is necessary before the laying of blocks.

Table 7: Summary of water absorption rates

Binder-Sand Ratio	Composition of Binder		Water Absorption (%)	
	RHA (%)	OPC (%)	W/B=0.5	W/B=0.6
1:5	00	100	8.3	9.2
	05	95	9.8	10.5
	10	90	11.4	12.9
	15	85	13.6	14.1
	20	80	14.3	14.6

5. Conclusions

The following conclusions can be made:

1. The chemical composition of RHA and OPC are the same, having the following compounds namely SiO_2, Al_2O_3, Fe_2O_3, CaO, K_2O, MgO, SO_3 and Na_2O. The particle sizes of RHA are coarser than OPC.

2. The rice husk incinerated at temperature 700°C produces the most preferable chemical composition. It contains a high content of amorphous SiO_2 and a low content of unburnt carbon.

3. The compressive strength increase until the cement replacement level of 5 per cent. Thereafter gradually compressive strength

decreases with the increase of cement replacement level. The higher value for the compressive strength can be attributed to the greater compactive effort rendered by the block manufacturing machine.

4. A cement replacement level of 15 per cent can be recommended with respect to producing cellular masonry blocks in keeping with the requirements stipulated in the SLS 855: Part 1.

5. As the cement replacement level is increased the water absorption of cellular masonry blocks too proportionately increases.

References

[1]. Al –Kahalaf, M.N. and .Yousiff H.A. (1984) ‘Use of rice husk ash in concrete’, International Journal of Cement Comp Light Weight Concrete, 1984:6(4): pp.241-8.

[2]. Bandara DHMS, 1994, Development of Blended Cement Utilizing the Pozzolanic Amorphous Silica Component of Rice Husk Ash’, *Journal of National Science Council*, 1994 22(2): pp.189-199.

[3]. Baskaran K, Mallikarachchi H.E. and Jayawickrama, M (2012) ‘Paddy husk Ash Stabilized Soil Bricks’, *International Conference on Sustainable Built Environment*, Kandy Sri Lanka.

[4]. Boating AA and Skeete DH, (1990), Incineration of rice hull for use as a cementations materials; the Gayana experience. Cement Concrete Research, 1990; 20; pp.795-802.

[5]. Central Bank Annual report 2014, Central Bank of Sri Lanka, Colombo Sri Lanka.

[6]. Department of Census and Statistics, Sri Lanka, Statics Report, 2014.

[7]. De Silva S. and Uduweriya, R.B.Y.B (2011), Investigation of the properties of concrete containing rice husk ash, Annual Transaction of IESL, pp. 71-79.

[8]. Dolage.DAR,Mylvaganam.K, Mayoorathan. P and Inparatnam.S, (2012), ‘Use of Rice Husk Ash Blended Cement to Produce Cement Sand Block’, Engineer, vol XXXXIV, No.02, pp (11-19).

[9]. Gaesan K., Rajagopal K., Thangavel K., 2008, Rice husk ash blended cement: Assessment of optimal level of replacement for strength and permeability properties of concrete, Journal of Construction and Building Materials 22,pp.1675-1683.

[10]. Mude, V.D., Bhalme, M.S. and Kamdi, M.S. (2013) ‘Strength Comparison of Ordinary Portland Cement and Rice Husk Ash’, International Journal of Engineering Research and Applications (IJERA), Vol.3, Issue 4, pp.283-284.

[11]. Pushpakumara, B.H.J. and De Silva S. (2012), ‘Characteristics of masonry Blocks Manufactured with Rice Husk Ash (RHA) and Lime, Engineer, vol. XXXXV, No.03,pp (1-10).

[12]. Sri Lanka standard 107: Part 1: 2008 (Specification for Ordinary Portland Cement-Requirements).

[13]. Sri Lanka standard 855: Part 1: 1989 (Specification for Cement Blocks Part 1-Requirements).

SECM/15/147

STUDY ON MODERN METHODS OF CONSTRUCTIONS USED IN SRI LANKA

H.M.M.Uthpala[1*], T.Ramachandra[2]

[1]University of Moratuwa, Moratuwa, Sri Lanka
[2] University of Moratuwa, Moratuwa, Sri Lanka
*E-Mail: madhaveemunasinghe@yahoo.com, TP: +94717418274

Abstract: With the end of world war two, the demand for building construction increased together with inadequate supply of traditional constructions. To cater the increased demand the modern methods of constructions (MMC) came to practice as it yields high quality and less construction time. Nowadays the off-site MMC play a significant role in construction industry worldwide in terms clients' fundamental needs by restraining problems in traditional brick, block constructions. However, the application of MMC seems limited and few building constructions have used MMC in the Sri Lankan construction industry. This research therefore aims to explore current practice of off-site MMC in Sri Lankan construction industry and identify the barriers in adopting MMC.

Questionnaire survey has been carried out among 33 respondents including engineers, quantity surveyors and project managers to identify the applicability of off-site MMC and barriers in using off-site MMC. Data which have been gathered through the questionnaire survey have been analysed through statistical analysis and investigated that volumetric constructions are mostly used for single storey temporary buildings, hybrid constructions are mostly used for single storey office and temporary buildings while panelised constructions are highly used for single storey industrial and temporary buildings and sub-assemblies are mostly used single storey office and commercial buildings. Furthermore main barriers in implementing all above mentioned methods are public perception and poor awareness.

Keywords: Hybrid construction, modern methods of construction, Sri Lanka, volumetric construction.

1. Introduction

Construction, a cannonading industry is preforming a vital role in rapidly growing global economy. In Sri Lanka, construction projects are facing different problems as the industry is labour intensive and wet trade. Off-site Modern Methods of Constructions (Off-site MMC) has been found as a solution to these problems [7]. But the practice of off-site MMC are very less in Sri Lankan construction industry. Therefore this paper focuses to identify the current practice of off-site MMC and the barrier in the construction industry to uplift the usage of off-site MMC.

2. Modern Methods of construction

MMC, which was originated in the United Kingdom used as a common term for both off-site methods of construction and on-site methods of construction [4]. The off-site MMC are prefabricated elements or parts of structures which are transported and assembled on-site even though they are manufactured in a factory. Off-site MMC includes categories of component and subassembly, non-volumetric pre-assembly and volumetric pre-assembly [2]. Moreover off-site MMC can categorized as, modular building, hybrid construction, panelised construction and pre-assembly [1]. However following classification is considered for this research as it can be separately identified in Sri Lankan industry:

- Volumetric construction: volumetric constructions include two categories modular constructions and pod constructions. Modular construction comprises of prefabricated room-sized volumetric units that are normally fully fit-out while manufacture and are installed on-site as load-bearing "building blocks" [5]. Pods are small volumetric rooms which are completed using light steel frame, timber, concrete or glassed reinforced plastic built in factories and finally set in building site [6]. These are usually used in washrooms, bathrooms and kitchens [9].

- Hybrid construction: Hybrid constructions are integration of volumetric units and panelised system. These are also named as semi-volumetric systems. If highly serviced areas such as kitchens or bathrooms can be constructed as volumetric units and rest of the dwelling constructed with panels, they are called as hybrid constructions [9].
- Panelised construction: Panelised constructions are flat panel units which are built in a factory and transported to site for assembly into a three dimensional structure or to fit within an existing structure. Systems can include wall, floor and roof panels to create the complete structural shell [9].
- Sub-assemblies & accessory system: This include larger components that can be incorporated into either conventionally built or MMC dwellings. These items are not full housing systems and are generally factory made [9].

2.1 Barriers in implementing off-site MMC

The use of off-site MMC has been limited in the construction industry due to main aspects:

- Cost: Off-site constructions are 7% to 10% costly than traditional constructions. High quality of off-site MMC and faster construction are responsible for the increased cost [8].
- Industry capacity: The shortage of skilled workers and factory capacity to manufacture parts have hindered the usage [8].
- Public attitudes: most of the public prefer to have traditional brick block constructions over off-site MMC [8].

Moreover logistics also can be identified as a barrier.

- Issues in logistics: transporting fully manufactured houses or partially completed modules is complex, costly, and very difficult [1].

In additionally lack of awareness among public and poor technology are also key barriers [3]. Synthesizing the views cost, public perception, poor awareness, poor technology and capacity of the industry have influenced the limited use of off-site MMC in the industry.

3. Methodology, Data collection and Analysis

The data was gathered using questionnaire survey administered to investigate

- Applicability of off-site MMC in Sri Lankan construction industry and
- Barriers in Sri Lankan construction industry acting on each off-site MMC

Even though professionals in construction industry is high, knowledgeable professionals on this area is difficult to find. Therefore data was corrected from quantity surveyors, engineers, project managers who have involved in at least one off-site MMC used project. In proper recording of constructions companies which are using off-site MMC and limited practice resulted difficulty in identifying the population size. Therefore 33 number of professional having different professional backgrounds had been selected as sample through non-probability convince sampling technique. Data was collected directly as well as via electronic mail.

3.1 Rate of response

Out of the forty eight approached, only thirty three responded to the questionnaire. This yielded 69% response rate.

3.2 Demographic Characteristics of Respondents

The respondents could be categorized as follows based on their professional background as well as their experience on off-site MMC projects.

Table 1: Professional background

Professional Background	Number	(%)
Quantity Surveyors	6	18%
Engineers	19	58%
Project Managers	8	24%

Table 1 presents the participants' professional background and demonstrate that the largest group of respondents were Engineers while others include only 6 quantity surveyors and 8 project Managers.

Moreover respondents were asked about their experience on off-site MMC used projects based on the number of years they had worked in prefabricated building sector. In terms of no of experience 55% had worked in MMC related projects 5-10 years while 33% have less than 5 years' of experience and 12% have more than 10 years' experience as shown in Figure 1.

3.3 Applicability of off-site MMC in Sri Lankan construction industry

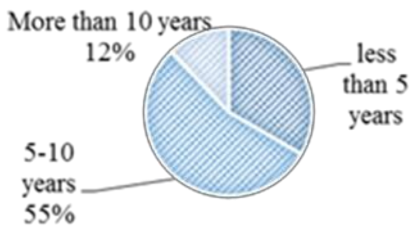

Figure 1: Experience of respondents

All the respondents are asked to respond on the applicability of off-site MMC in Sri Lankan construction industry. According to the responses which are shown in Figure 2, 82% of the respondents have given their response that volumetric constructions are used in temporary buildings and 76% of them have responded that volumetric constructions have been used in residential constructions. Moreover 73%, 64%,58% and 6% have responded that volumetric constructions are used in commercial, industrial, offices and other buildings sectors respectively.

As per the responses volumetric constructions are mostly used for temporary buildings, residential buildings and commercial buildings. Reason for the high usage in temporary building sector is temporary buildings have small scales. It is difficult to transport the units for large scale constructions because of the traffic jam and the road width.

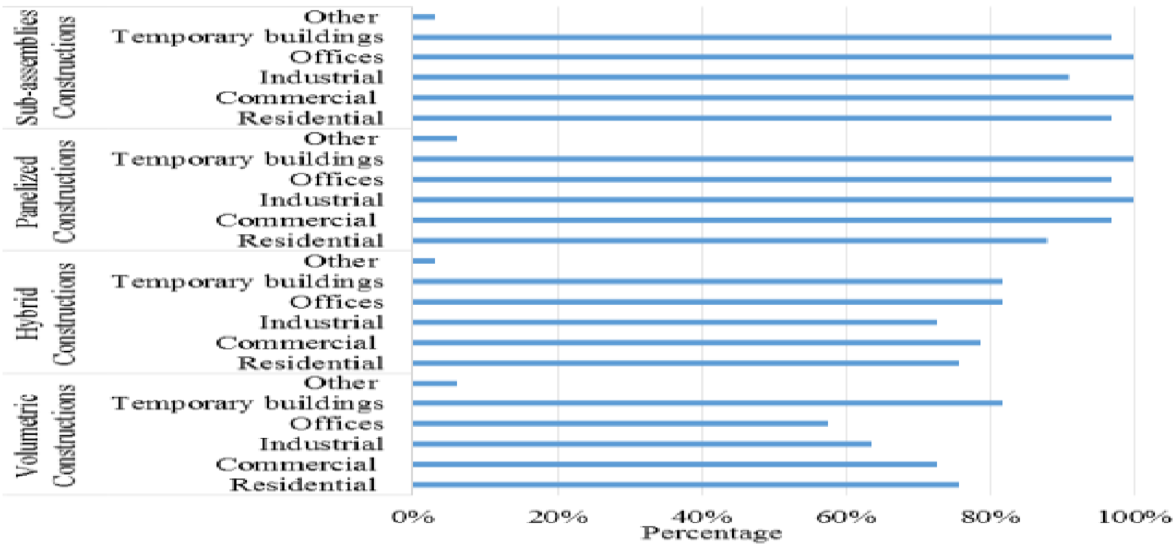

Figure 2: Applicability of off-site MMC in Sri Lankan Construction industry

Therefore for small scale building projects volumetric constructions are mostly used. According to the collected data shown in Table 2, in temporary building sector volumetric constructions are used to build single storey building and 2-11 storey buildings. 27 of the respondents have responded that volumetric constructions are used in single storey temporary buildings and 3 of the respondents have stated that they are also used in 2-11 storey buildings. Even though the category is 2-11 they are not used in more than three storey buildings. Furthermore 25 respondents have stated that volumetric constructions are used in residential buildings and 7 have responded as volumetric constructions are used in 2-11 storey buildings. In additionally 1 has responded that volumetric constructions are used in more than 12 storey residential buildings. In commercial sector it have been responded that 24 respondents to single storey commercial buildings, 6 respondents to 2-11 storey buildings and any of the respondents have not stated that they are used in more than 12 storey commercial buildings.

Table 1: Applications of volumetric constructions

Sector	Scale of the building	Frequency
Residential	Single storey	25
	2-11 storey	7
	More than 12 storey	0
Commercial	Single storey	24
	2-11 storey	6
	More than 12 storey	0
Temporary buildings	Single storey	27
	2-11 storey	3
	More than 12 storey	1

According to Figure 2, 82% of the respondents have responded that hybrid constructions are used in temporary buildings and office buildings. 79% of the respondents have stated that are used in commercial buildings and 76% and 73% respondents have responded that hybrid constructions are used in residential and industrial sectors respectively. Moreover 3% of the respondents have responded that hybrid constructions are used in other sectors than above mentioned sectors. According to the responses hybrid constructions are mostly used in temporary building and offices.

As shown in Table 3 hybrid construction are practiced in single storey offices and temporary buildings as well as 2-11 stories buildings. According to the responses, 27 of the respondents have responded that hybrid constructions are used in single storey offices and single storey temporary buildings and 17 and 6 respondents have said that hybrid constructions are used in 2-11 stories buildings in commercial and temporary buildings respectively. In industrial buildings usage of hybrid constructions have been marked as 24 for single storey and 16 for 2-11 storey buildings.

Table 3: Applications of Hybrid constructions

Sector	Scale of the building	Frequency
Commercial	Single storey	26
	2-11 storey	17
	More than 12 storey	0
Offices	Single storey	27
	2-11 storey	17
	More than 12 storey	0
Temporary buildings	Single storey	27
	2-11 storey	6
	More than 12 storey	0

As per the Figure 2 respondents have responded that panelised constructions are used in industrial and temporary building sector the most. All of the respondents have marked that panelised constructions are used in industrial and temporary building sector. 97% of the respondents have given their response that panelised constructions are used in commercial and offices. 88% of the respondents have responded that panelised constructions are used residential sector and 6% of the reposes have been given that it has been used in other sectors rather than residential, commercial, industrial, offices and temporary buildings. Therefore panelised constructions are mostly practiced in industry building sector and temporary buildings sector. Reason for this higher usage can be identified since most of the factories and warehouses are constructed with steel panels. Because of the easiness in construction and usage.

Table 2: Applications of Panelized constructions

Sector	Scale of the building	Frequency
Industrial	Single storey	33
	2-11 storey	20
	More than 12 storey	5
Temporary buildings	Single storey	33
	2-11 storey	9
	More than 12 storey	0

According to the responses given by the respondents, shown in Table 4 panelised constructions are mostly used in single storey industrial and temporary building sectors. 20 and 9 respondents have responded that panelised constructions are used in 2-11 storey buildings in industrial and temporary building sectors respectively. 5 respondents have identified panelised constructions are used for more than 12 storey industrial buildings.

According to the Figure 2 subassemblies are mostly used in commercial and offices. They have 100% equal usages. 97% has responded that sub-assemblies are used in residential and temporary building sector. 91% and 3% have been responded that sub-assemblies are used in residential and other sectors respectively. Tables, figures and equations should be provided as appropriate and as indicated in this document.

As shown in Table 5, commercial sector and office buildings sector all the respondents have given that sub-assemblies are used in single storey buildings. 24 respondents have answered in commercial sector sub-assemblies are used in 2-11 storey buildings, 6 respondents have answered that they are used in more than 12 stored buildings in commercial sector. Moreover 11 respondents have answered that for 2-11 story office buildings are also construct with panelised constructions. 5 respondents have responded that they are used in more than 12 storey buildings.

Table 3: Applications of sub-assemblies constructions

Sector	Scale of the building	Frequency
Commercial	Single storey	33
	2-11 storey	24
	More than 12 storey	6
Offices	Single storey	33
	2-11 storey	11
	More than 12 storey	5

3.4 Key barriers in implementing off-site MMC methods in Sri Lanka

As per previously described heading off-site MMC are not used in all scales in all sectors of Sri Lankan industry. Therefore usage of off-site MMC is limited in Sri Lankan industry. Limitations or the barriers of implementing each off-site MMC is identified through this heading. In order to fulfil this requirement respondents are requested to mark the barriers in each sector and using MS Excel following graphical representations have been formed.

Barriers in implementing volumetric constructions

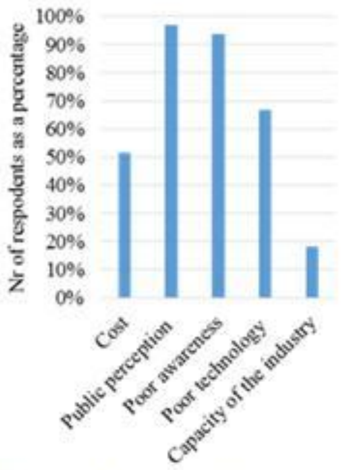

Figure 3: Barriers in implementing volumetric constructions

The professionals' responses on barriers to implement volumetric constructions in Sri Lankan industry is depicted in the following Figure 3.

As per the responses 97% of the professionals have identified public perception as a barrier in implementation of volumetric constructions in Sri Lankan industry. 94%, 67%, 52% and 18% of professionals have identified that barriers in implementing volumetric constructions in Sri Lankan industry as poor awareness, poor technology, cost and capacity of the industry respectively. According to the results volumetric constructions are limited highly in Sri Lanka because public is not well knowledgeable about this method.

Barriers in implementing hybrid constructions

As per the responses of the professionals on barriers to implement hybrid constructions in Sri Lankan industry is depicted in the above Figure 4. 100% of the respondents have identified that poor awareness about hybrid construction as a barrier to implement hybrid constructions in Sri Lankan construction industry. 91% of the respondents have identified that public perception is a barrier and 36%, 24% and 12% have identified poor technology, cost and capacity of the industry respectively as barriers in implementing hybrid constructions in Sri Lanka. As per the responses it can be identified that less awareness on hybrid constructions is the main reason for less usage of this method.

Barriers in implementing panelised constructions

The respondents' opinions about barriers of implementing panelised construction is depicted in above Figure 5. 100% of the respondents have identified that poor awareness about panelised constructions as a barrier to implement panelised constructions in Sri Lankan. 85% of the respondents have identified that public perception as a barrier. 30%, 12% and 6% of respondents have identified poor technology, cost and capacity of the industry respectively as barriers in implementing hybrid constructions in Sri Lanka. Therefore main barrier acting on panelised construction is poor awareness.

Barriers in implementing sub-assemblies constructions

The professionals' responses on barriers to implement sub-assemblies constructions in Sri Lankan industry is depicted in the above Figure 6. 94% of the professionals have identified poor awareness as a barrier in implementation of sub-assemblies constructions in Sri Lankan industry.

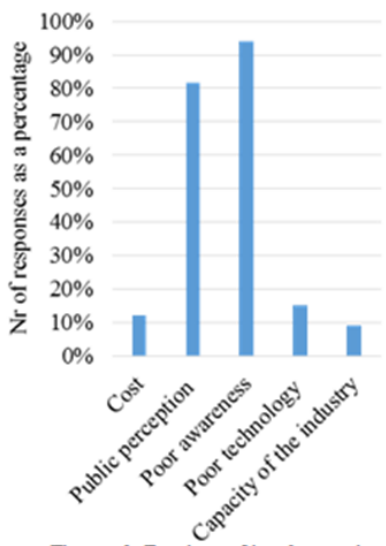

Figure 6: Barriers of implementing sub-assemblies constructions

82%, 15%, 12% and 9% of professionals have identified that barriers for implementing volumetric constructions in Sri Lankan industry as public perception, poor technology, cost and capacity of the industry respectively. Accordingly poor awareness is the key barrier which limited the practical applicability of sub-assemblies.

4. Conclusions

Traditional constructions are facing difficulties with less labour and limited time. Off-site MMC can be identified as an emerging solution for difficulties which a construction client face because of the traditional construction methods. But in Sri Lankan construction industry the practice of off-site MMC are lesser than the other countries. Therefore this research is conducted to find out the current practice and barriers to implement off-site MMC in Sri Lankan industry. Through the research it has been identified that volumetric constructions are mostly used for temporary building construction as the transportation issues as the units are difficult to handle. Hybrid constructions are mostly used in offices and temporary building according to the professional responses. Moreover panelised constructions are mostly used in industrial and temporary building construction as the warehouses and factories can be easily made out of steel panels. Sub-assemblies and accessories are mostly used in commercial and offices and its' usage in other sectors such as residential, industrial, temporary buildings are also more than 95%. As per the responses of the professionals volumetric constructions are limited in Sri Lankan industry mainly because of the public perception. As identified through the research volumetric constructions are used in Sri Lankan industry in the type of container houses. Therefore the knowledge of the public on these area is grey .Therefore the usage is limited. Same as volumetric constructions, hybrid constructions, and panelised constructions and sub-assemblies constructions are also limited due to poor awareness and the poor public perception. Therefore in order to increase the usage of off-site MMC the public perception and awareness have to be made positive.

Acknowledgement

Authors would like to express greatest appreciation for University of Moratuwa and all the professionals in the industry who contributed to this study by actively participating in the data collection process despite their busy work schedules.

References

[1]. Boyd, N., Khalfan, M. M., & Maqsood, T. (2013). Off-site construction of apartment buildings. Journal of Architectural Engineering, 19(1), 51-57. Doi: 10. 1061/ (ASCE) AE.1943-5568.0000 091

[2]. Gibb, A. G. (1999). Off-site fabrication: prefabrication, pre-assembly and modularisation. Whittles, Caithness: John Wiley & Sons publishers. Retrieved from https://books.google.lk/ books?hl =en&lr=&id=uTiN_aGtXzwC&oi =fnd&pg= PR13 &ots=QQrFXMG Znm&sig=mSi8zJsetWle0UwK7zPu93CSfwc& redir_esc=y#v=onepage&q&f=false

[3]. Kamar, K. A., Alshawi, M., & Hamid, Z. (2009). Barriers to industrialised building systems: the case of Malaysia. Proceedings of BuHu 9th International Post graduate Research Conference (IPGRC 2009) (pp. 1-16). Salford: The University of Salford. Retrieved from http://www.Vertili te.asia/f/2012/11/Barriers-of-IBS. Pdf

[4]. Kyjakova, L., Mandicak , T., & Mesaros , P. (2014). Modern methods of construction and their components. Journal of Engineer ing and Architecture, 2(1), 27-35. Retrieved from www. Aripd.org/jea

[5]. Lawson, R. M., Ogden, R. G., & Bergin, R. (2012). Application of modular construction in high-rise buildings. Journal of Architectural Engineering, 148-154. Doi: 10. 1061/ (ASCE) AE. 1943-5568.0000 057.

[6]. Mapston , M., & Westbrook, C. (2010). Prefabricated building units and modern

[7]. Pan, W., Gibb, A. G., & Dainty, A. R. (2008). Leading UK house builders' utilization of offsite. Building Research & Information, 36(1), 56–67. Doi: 10.1080/09613210701204013

[8]. Parliamentary Office of Science and Technology (POST). (2003). Modern Methods of House Building. London: Parliamentary. Retrieved from http://www. parliament.uk/documents/upload/postpn209.pdf

[9]. Ross, K., Cartwright, P., & Novakovic, O. (2006). A guide to modern methods of construction. Amersham: IHS BRE Press.

methods of construction (MMC). In Materials for Energy Efficiency and Thermal Comfort in Buildings (pp. 427-454). United Kingdom: Wood head Publishing Limited. Doi: 10.1533/ 97818 45699277.2.427

SECM/15/152

Potential of Sri Lankan Apatite as a fluoride removal Agent from aqueous solution against Various Apatite Materials

A.A.G.D. Amarasooriya[1*], Hikaru Miyazaki[1], Tomonori Kawakami[1]

[1] Toyama Prefectural University, Toyama, Japan
*E-Mail: gayanamarasooriya @ gmail.com, TP: +819074117511

Abstract: As reported Sri Lanka it has a high fluoride contaminated ground water which was suspected as a cause for chronic kidney failure and there is an urgent need to treat fluoride contaminated drinking water to make it safe for human consumption by a low cost and convenient method. In this study potential of using Sri Lankan Apatite (SAp) as a defloration agent was studied and results were compared with other apatite materials. Adsorption experiments were performed on SAp, Sulphuric treated SAp (SSAp), Chicken bone char (CBC) and pre Hydroxyl Apatite (HAp). Since the raw SAp had no adsorbing capacity of fluoride, it was treated with sulfuric acid to produce HAp, however, sulphuric acid treatment for SAp did not yielded enough amount of hydroxy apatite as a fluoride adsorbent. Accordingly, higher leaching of fluoride into the solution was confirmed by the SSAp than that by the SAp. The fluoride removal capacities were in the order: HAp > CBC > SAp>SSA. The adsorption of fluoride by HAp and CBC was not well expressed by Langmuir isotherm but by Freundlich isotherm. It showed that HAp and CBC was a promising material for fluoride removal, therefore SAp should be further treated to extract phosphates to produce synthetic hydroxyapatite.
Keywords: Hydroxyl apatite, Apatite, Bone char.

1. Introduction

Various treatment technologies were proposed or applied to remove the excess fluoride from drinking water, and these technologies were based on the principle of precipitation, the ion exchange, the membrane or the adsorption processes [1-2]. Among these methods, the adsorption is a simple and attractive one having high efficiency and easy handling. In recent years, much effort has been devoted to investigate and develop new fluoride adsorbent using various synthetic, naturally occurring and waste materials from various industries and requires little processing. Hydroxy apatite is a good adsorption material of fluoride [3]. Since Sri Lanka has apatite deposit in Eppawala, this study was focused on the potential of Sri Lankan rock apatite (SAp) to remove fluoride from drinking water as a low cost material. Its results were compared with other hydroxyapatite materials.

2. Materials and Methods

2.1 Chemicals and analyses

All the chemicals used in the experiment were analytical grade purchased from Wako chemicals, Japan except pure hydroxyapatite (HAp). It was supplied from Taihei Chemical Industrial Co. Ltd. SAp was collected from Eppawala mine and chicken bone was used to produce chicken bone char (CBC). NaF solution was used for the adsorption. Anions were analysed by using anion chromatograph (DIONX-ICS 2000).

2.2 Treatment of SAp

SAp was crushed and passed through 106 µm sieve. Twenty five grams of the sieved SAp was treated with 11.1 ml of H_2SO_4 to produce H_2SO_4 treated hydroxyl Apatite (SSAp). A reaction between SAp and H_2SO_4 produce various products in addition to SSAp (Eq 1).

$$\begin{aligned}&Ca_{10}(PO_4)_6(OH.F.Cl)_2 + H_2SO_4 + H_2O \xrightarrow{yields}\\ &+Ca_{10}(H_2PO_4)_2(OH)_2(s) - \boldsymbol{SSAp}\\ &+ CaSO_4(s) + Ca_{10}(H_2PO_4)_2\,(OH.Cl)_2(s)\\ &+Ca_{10}(PO_4)_6(OH.F)_2(s)\\ &+Ca_{10}(PO_4)_6(OH.Cl)_2(s)\\ &+HF(aq) + HCl(aq) + H_3PO_4(aq) \qquad (1)\end{aligned}$$

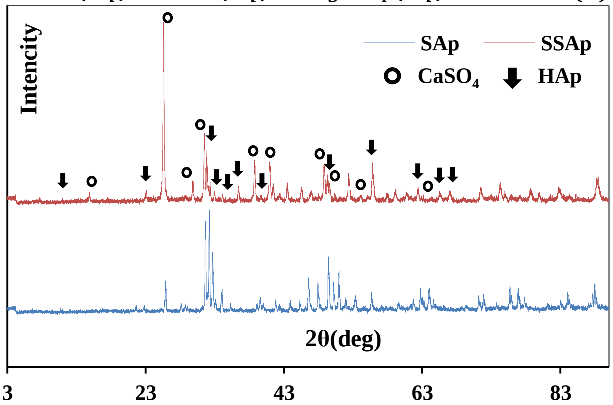

Figure 1: XRD pattern of SAp and SSAp

H_2SO_4 treated SAp was then centrifuged to separate solid portion. The separated solid was washed with excessive ultrapure water several times to remove HF, HCl, H_3PO_4 and excessive H_2SO_4. According to XRD pattern (Fig. 1), it was confirmed SSAp contains HAp and $CaSO_4$ Mixture.

2.3 Treatment of chicken bone

Chicken bone was carbonated at 600°C to make Chicken Bone Char (CBC) of which component is hydroxyapatite. It was crushed, and sieved by a 106 μm sieve for use.

2.4 Effect of sorbent dose on the Adsorbing capacity

The initial pH was adjusted to 7.0, and the initial concentration of fluoride was 10 mg/L. The contact time was 24 hr, and the temperature was kept at 25°C.

2.5 Isotherm

Pure HAp, CBC, SAp, and SSAp were put in 50 mL of NaF solution with a fluoride concentration of 10 mg/L. It was shaken for 24 hours to establish equilibrium between the adsorbent and the solution.

3. Results and Discussion

3.1 Effect of sorbent dose

Fig. 2 shows the effect of adsorbents (HAps, CBC, SAp, SSAp) dose on fluoride adsorption.

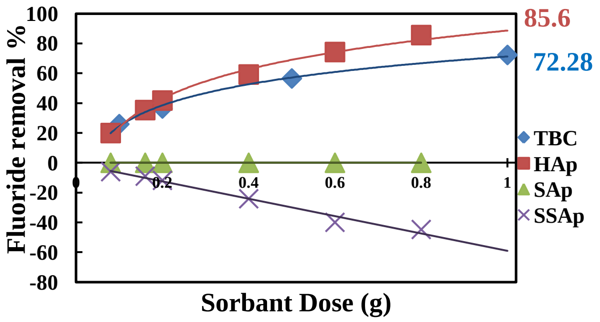

Figure 2: Effect of adsorbent dose

The adsorption capacity of CBC and HAp was significantly influenced by the dose of the materials. SAp and SSAp did not show any adsorption of fluoride. Even though HAp was present in the SSAp it exhibited negligible fluoride removal efficiency. The possible reasons are unstable fluoro Apatite forms and slow release of OH ions from HAp hence far from adsorption; SSAp leached fluoride to the solution.

3.2 Adsorption Isotherms

Fig.3 shows Freundlich isotherm and Fig.4 shows Langmuir isotherm for CBC and HAp. By comparing the results presented in Fig. 3 and Fig.4, the adsorption of fluoride by HAp and CBC was not well expressed by Langmuir isotherm but by Freundlich isotherm. SAp and SSAp did not follow both of the isotherms.

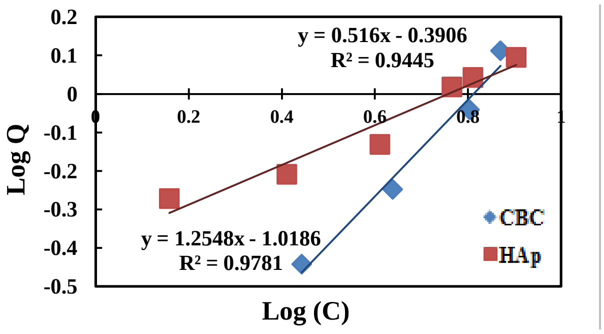

Figure 3: Freundlich Isotherm

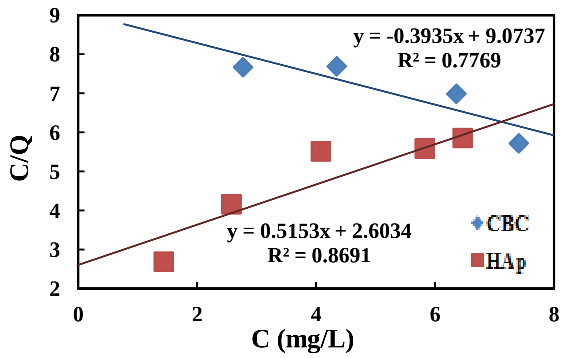

Figure 4: Langmuire Isotherm

4. Conclusion

SAp or SSAp could not remove fluoride from aqueous solution. Further treatment and synthesis are required for producing adsorbent of fluoride. CBC and HAp could be suitable precursor materials for producing high capacity adsorbents of fluoride removal from aqueous solution.

Acknowledgement

We would like to give special thanks to Prof Tafu, National Institute of Technology, Toyama, Japan and Eppawala Apatite mine, Sri Lanka.

References

[1]. Nawlakhe W.G., Kulkarni D.W., Pathak B.N., Bulusu K.R., Indian J. Environ. Health 17 (1975) 26–65.

[2]. Faust S.D., Aly O.M., Adsorption Processes for Water Treatment, Butterworth, Stoneham, MA, 1987, p. 299.

[3]. Gao S., Sun R., Wei Z.G., Zhao H.Y., Li H.X., Hu F.J., Fluorine Chem. 130 (2009) 550–556.

SECM/15/155

Determination of Tensile Strain Capacity of Fresh Concrete: A new test method

T. G. P. L. Weerasinghe[1*] and S.M. A. Nanayakkara[2]

[1] Research Assistant, University of Moratuwa, Moratuwa, Sri Lanka
[2]Professor, University of Moratuwa, Moratuwa, Sri Lanka
*E-Mail: wwpasindu@gmail.com, TP: +94777357981

Abstract: Measuring physical properties of fresh concrete is important to understand the behaviour of the early state of concrete. Plastic shrinkage occurs at the very early stage due to evaporation of water from the concrete surface. When concrete is restrained against plastic shrinkage, tensile strain is developed and when it exceeds the tensile strain capacity, cracks occur. This phenomenon is called as plastic shrinkage cracking. In order to assess the risk of plastic shrinkage cracking tensile strain capacity of fresh concrete should be measured. Fresh concrete means the concrete before the initial setting time which is still in a semi liquid state. The paper presents a test method developed to measure the strain distribution along a fresh concrete sample. Based on this test method tensile strain capacity of a selected mix proportion with three different types of cements, i.e., Ordinary Portland Cement, Fly ash blended and Portland Limestone Cement were determined. Results indicate that concrete with fly ash blended cement has a higher tensile strain capacity than other two cement types.

Keywords: fresh concrete, plastic shrinkage cracking, tensile strain capacity

1. Introduction

Measuring physical properties of fresh concrete is important to understand the behaviour of the early state of concrete. Plastic shrinkage occurs at the very early stage due to evaporation of water from the concrete surface. When concrete is restrained against plastic shrinkage, tensile strain is developed and when it exceeds the tensile strain capacity, cracks occur. This phenomenon is called as plastic shrinkage cracking. Thus evaluation of tensile strain capacity of fresh concrete helps to determine the risk of cracking due to restrained plastic shrinkage.

It has been often reported that cracking had occurred in various types of concrete mixes but there is no procedure to evaluate exactly how vulnerable the mix is for cracking or what mixes has low risk of cracking. As the cracking is mainly due to tensile strain development due to volume change, tensile strain capacity can indicate the probability of such occurrence.

Although there are ample data on strain capacity of hardened concrete, only very few can be found on fresh concrete. Fresh concrete means the concrete before the initial setting time which is still in a semi liquid state. From right after mixing of concrete to 3 – 4 hours is considered as initial setting time period during which concrete changes from plastic state to solid state. According to the studies done by Byfors [1], Hammer [2] and Roziere et al [3] the tensile strain capacity goes through a minimum value as a function of age. It reached approximately 0.05% at 6-8 hours after mixing. However, plastic shrinkage cracking can occur before that as tensile strain developed due to plastic shrinkage could exceed the tensile strain capacity in the plastic state (where tensile strain capacity haven't reached its minimum value). Almost all the tests done in previous studies have started 2 hours after mixing has finished. Therefore those test results do not indicate tensile strain capacities at very early stage of concrete.

2. Development of a test method

2.1 Previous Test methods reported

Developing a sound test method for this purpose is quite challenging. Kasai et al [4] and Hannat et al [5] have been concerned about developing a method with minimum friction as they were to measure both tensile stress and tensile strain. Load was applied vertically or horizontally and displacement was measured with extensometers, electronic deflectometers, LVDTs' and using image processing. Among the various apparatuses Hannat et al [5] has developed a horizontal loading type machine with two air bearing plates to minimize friction. His apparatus was further improved by Hammer [2] and Roziere et al [3] to obtain tensile strain capacity values using LVDTs and image processing. It was also noted that the strain capacity changes with the time, strain loading rate, background temperature and evaporate rate [2][3].

Based on the literature survey following drawbacks were identified that should be addressed when developing a test method to test fresh concrete.

a) Using a rigid container to hold concrete will not ensure a proper grip when applying strain as concrete is in plastic state

b) Measuring average strain along the sample length predicts a lower tensile strain capacity as local strain at the region of cracking could be higher than the average strain

Hence the following key features were identified to be included when developing a test method.

a) Sample should be placed on a mold or casing to support it, as fresh concrete is in semi-liquid state and it can flow. A flexible casing would ensure a proper grip.

b) Strain should be applied to the flexible mold and the mold will transfer it to the concrete.

c) Contactless method should be adopted to measure strain.

d) Local strain will give more accurate results than average strain throughout the sample.

e) Test should be repeatable.

2.2 Test method developed

Taking the above features into account the following test method was developed. (Figure 1)

a)Fresh concrete was placed on a rubber mold (800mm x 100mm x 40mm). It was supported by a steel frame but Perspex sheets were inserted between the mold and the steel frame to allow smooth movement.

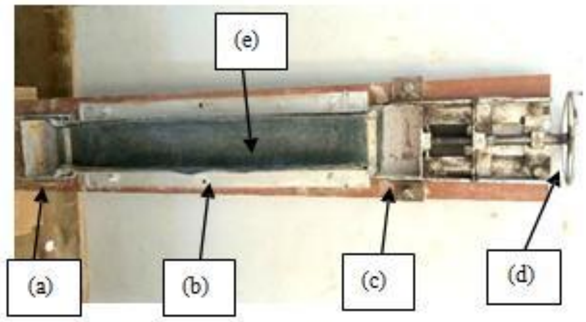

Figure 1: Test apparatus. (a) fixed end, (b) supporting frame, (c) moving end, (d) rotating wheel to apply strain, (e) rubber mold

a) Rubber mold was fixed on to two steel casings (100mm x 100mm x 40mm) at its ends. One end was fixed and pulled from the other end by rotating the wheel attached to the steel casing. Concrete sample inside will move along with it thus the strain applied would be transferred to the sample.

b) Markers were placed on the sample which will act as reference points to measure strain. (Figure 2)

Figure 2: Fresh concrete sample with markers

a) Strain was applied at a rate of 0.3 mm/s. (Tensile strain capacity distribution with time depends on the strain application rate. Higher the strain rate, the variation is more)

b) A camera placed above the sample was used to capture images continuously from the start to until the point of appearance of the first crack. (Figure 3)

c) Images were analysed and pixel count (modified by a scale factor) between two markers at the beginning and at the crack initiation point was used to calculate strain at failure.

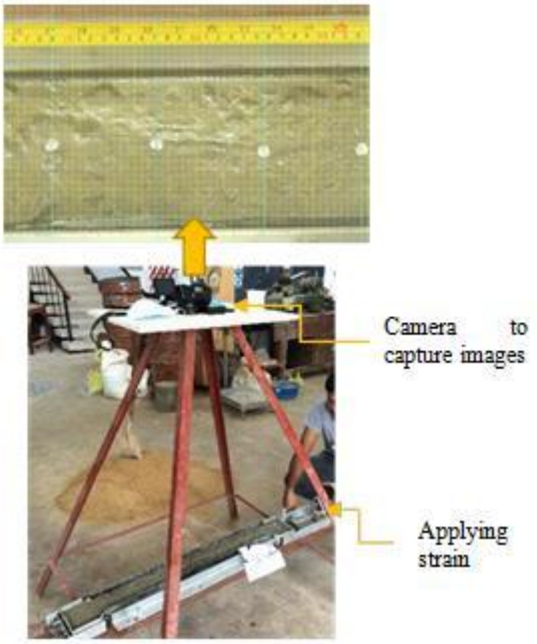

Figure 3: Test procedure and a captured image

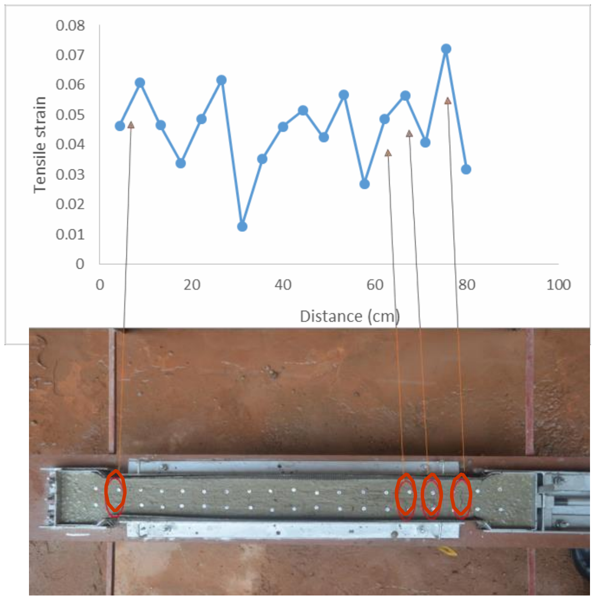

Figure 4: Strain distribution and cracks occurred at initial testing stage

3. Experimental Program

3.1 Initial testing

Initial testing was done using 1:5 cement sand mortar mix. The test was carried out according to the steps mentioned above and the tensile strain capacity was calculated using the following equation.

$$\epsilon_T = \frac{(Px_f \times S_f) - (Px_i \times S_i)}{(Px_i \times S_i)} \qquad (1)$$

ϵ_T – Tensile strain capacity

Pxf – No. of pixels at failure
Sf - Scale factor at failure
Pxi – No. of pixels at start
Si - Scale factor at start

A scale factor was used to account for the distortion of the image due to curvature so that the modified pixel count will give the straight distance between two markers.

Test results showed a strain distribution as shown in Figure 4. It indicates that the peaks corresponded to the cracks appeared which are circled in Figure 4.

3.2 Cement types

After verifying the testing procedure with initial testing with cement mortar, further tests were carried out to study the influence of cement type on the tensile strain capacity. Three common cement types used in Sri Lanka were chosen. They were;

1. Ordinary Portland Cement (OPC)
2. Fly ash blended (20% replacement of OPC)
3. Portland Limestone Cement (PLC)

3.3 Mix proportions

DoE mix design method [6] was used to determine the mix proportions. Cement type was varied keeping other parameters constant. Mixes were designed for a slump of 160mm and a characteristic strength of 30N/mm^2. The selected mix proportions and measured slump and strength results are given in Table 1.

Table 1 Composition of concrete mixtures (kg/m3)

Parameter	OPC	Fly Ash Blended (20%)	PLC
Coarse Aggregates (20mm)	1059	1059	1059
Fine Aggregates	706	706	706
Cement	410	328	410
Fly Ash	-	82	-
Water	205	205	205
W/B	0.5	0.5	0.5
Slump (mm)	155	170	160
$f_{c,28d}$ (N/mm^2)	41.5	40.4	40.3

3.4 Experimental procedure

Test was carried out to simulate the practical situation of placing concrete. Required quantity of concrete was mixed in a concrete mixer at once and kept inside the mixer. The lid mixer drum was closed to prevent evaporation of water. At every 10 minutes concrete was agitated and taken out at the required time for the test. This is to simulate condition of fresh concrete in an agitator truck during transporting.

Acquired Images were processed using Adobe Photoshop CS3. A grid line was created to represent an individual pixel by a square. Number of pixels between adjacent markers were counted. Position of each marker was also recorded using the reference steel measuring tape placed along the sample. So the scale factor corresponding to each region between two adjacent markers can be calculated. Strain was calculated using Eq. (1) and plotted along the sample length.

4. Results and Discussion

4.1 Results

Strain distribution was plotted along the sample length (Figure 5). Distance zero represents the fixed end and distance increases towards the strain application end (moving end). Displacement of each marker relative to its original position before applying the strain was also plotted along sample length. (Figure 6)

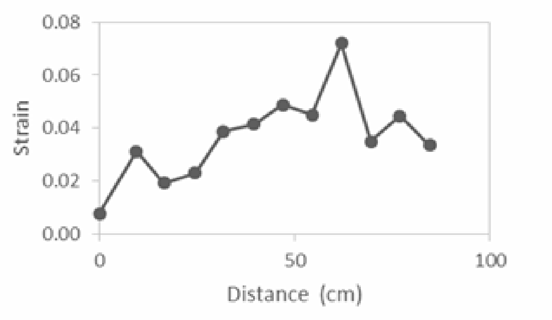

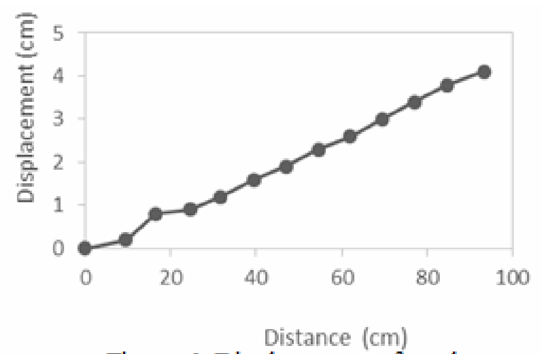

Figure 6: Displacement of markers

Generally the peak strain value corresponds to the cracking location. Therefore it can be taken as the tensile strain at the failure i.e tensile strain capacity. From the strain distribution it is evident that the local strain at the location of cracking is significantly higher than the average strain along the sample.

In order to further clarify the variation of strain, especially the sudden peak at the location of cracking, displacement of adjacent markers to the cracking point were plotted against the duration of strain application (See figure 7).

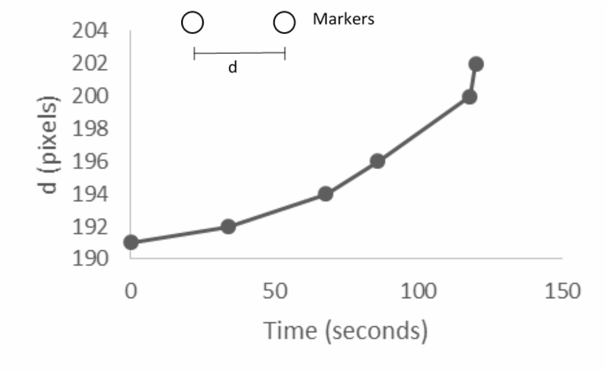

Figure 7: Displacement of two adjacent markers during application of strain

As indicated by figure 7, at the time of cracking there is a sudden increase of displacement between markers which resulted as a peak in strain distribution.

4.2 Tensile strain capacity for concrete with different cement types

Figure 8 shows the variation of tensile strain capacity of each mix with time

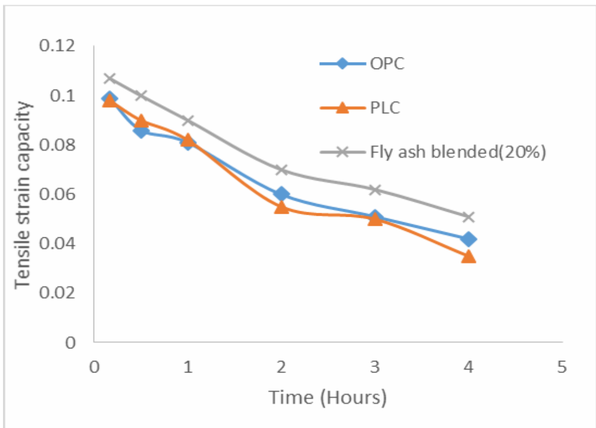

Figure 8: Tensile strain capacity for concrete produced with different cement types

It can be seen that tensile strain capacity decreases non-linearly with time. Concrete becomes stiff and moves from liquid state to semi-liquid state and then to early hardening state. Cohesiveness decreases and becomes minimum and then increases again when concrete hardens. As the test was conducted before the hardening stage strain capacity continuously decreases with time.

Concrete with fly ash blended cement shows a higher tensile strain capacity (8% - 21%) than OPC and PLC. According to Mehta et al [7] Fly ash particles are spherical while OPC and PLC cement particles are irregular shaped. Furthermore studies done by Owens [8] and Thomas [9] disclose that spherical fly ash particles are finer and more cohesive. As a result of that fly ash blended cement concrete can undergo more tensile strain than other two cement types before cracking. According to Owens [8], for equal slump, fly ash blended cement concrete has more free water. Therefore concrete with fly ash blended cement can last longer in the liquid state which has high tensile strain capacity than semi-liquid state. These two phenomenon explains the reason for the results obtained from this experiment.

5 Conclusions

Based on the results obtained from this experimental investigation following conclusions can be made.

- Measuring local strain yields more accurate results than average strain across a sample as the local strain at the location where crack occurs is higher than the average strain calculated from the total length of the sample.
- Tensile strain capacity decreases non-linearly with time during the plastic stage of concrete
- According to results obtained from the experiment, concrete with Fly ash blended cement is less vulnerable to early age cracking than OPC and PLC. The observation is based on the conditions where other external factors contributing to plastic shrinkage were kept same.

Further studies should be conducted to determine the influence of cement type for early age cracking when concrete is placed and kept undisturbed.

Acknowledgement

Authors wish to acknowledge the contribution rendered by academic and non-academic staff of department of civil engineering, University of Moratuwa.

References

[1]. Byfors, J., Plain concrete at early stages, Swedish Cement and Concrete Research Institute, Sweden, 1980.

[2]. Hammer, T.A., “Deformations, strain capacity and cracking of concrete in plastic and early hardening phases”, PhD thesis, Norwegian University of Science and Technology, Norway, 2007.

[3] Roziere, E., Cortas, R., Loukili, A., “Tensile behaviour of early age concrete: New methods of investigation”, Cement & Concrete Composites, Vol. 55, pp. 153-161, 2015.

[4] Kasai, Y., Yokoyama, K., Matsui, I., “Tensile Properties of early-age concrete”, Japan, 1972.

[5] Hannat, D., Branch, J., Mulheron, M., “Equipment for testing of fresh concrete”, Magazine of Concrete Research, Vol. 51, pp. 263-267, 1999.

[6] Building research establishment, Design of normal concrete mixes, 2nd ed., 1997.

[7] Mehta. P., Monterio. P., Concrete: Microstructure, Properties and Materials, 4th ed., McGrawHill education, 2013.

[8] Owens, P., “Fly ash and its Usage in Concrete”, Concrete Magazine, pp. 22-26, 1979.

[9] Thomas, M., “Optimizing the use of Fly Ash in Concrete”, Portland cement association, Illinois, 2007.

SECM/15/159

Experimental study on integrated method of NSM and EBR techniques for flexural strengthening of Concrete Beams using CFRP

N.A.Amarasinghe[1], J.C.P.H. Gamage[2]

[1,2]University of Moratuwa, Moratuwa, Sri Lanka
* E-Mail:narmadhaanjalee@gmail.com, TP: +94773487005

Abstract: This paper is based on an experimental analysis carried out to identify the effectiveness of different installation techniques of CFRP (Carbon Fibre Reinforcement) in concrete elements. Two new methods of integration of externally bonded reinforcement (EBR) and near surface mounted (NSM) methods were also experimented with the objective of increasing the flexural capacity of reinforced concrete beams by increasing the effective area of CFRP strips used. The main objective of this research paper is to identify the adaptability of existing guidelines specified for the EBR and NSM methods separately into the new installation method of integrating the two techniques of EBR and NSM.

Keywords: adhesives, externally bonded reinforcement, near surface mounted CFRP, concrete, method of integration

1. Introduction

Concrete is one of the widely used materials in the construction industry. It has a greater compressive strength but proven to be weak in tension. Without inner reinforcement, concrete will become brittle and fail under tension and make it less appropriate for many of the structures. A traditional way of reinforcing concrete is use of steel bars at the time of casting. Since concrete structures have a relatively longer life span, it is quiet common that the loads imposed on it will increase with time. On the other hand due to material deterioration under severe conditions will also affect badly on structures. This will create a necessity to seek approaches on strengthening these structures.

Rehabilitation and reparation of structures have become a very important, yet a critical factor due to above mentioned factors. Instead of designing a building from the very beginning, it has been identified that rehabilitating an existing building is more difficult and complicated as the structural conditions are already set. It can also be more complicating to reach the areas that need to be strengthened and to recognize the amount of strengthening that needs to be done.

This is generally the case for traditional strengthening systems, namely; reinforced overlays, shotcrete or post tension cables placed on the outer surface of the structure. These techniques require much space, machineries or special equipment. In recent years the development of plate bonding repair technique seems to have shown promising results and applicable to many existing structures. This technique can be acknowledged as a method of binding a sheet or a plate with an epoxy on the outer surface of a structure.

CFRP (Carbon Fibre Reinforced Polymer) was introduced by researchers as a more suitable and convenient solution. It has been identified as a material that can be used for remedying reinforced concrete, pre stressed concrete, masonry, timber and also steel. High in strength, lightness in weight, resistance to corrosion and ease in application of CFRP have earned the trust among its users and proved to be more promising in the construction industry. Introduction of CFRP to the construction industry eradicated most of the mentioned issues prevailed in the industry.

CFRP can be installed mainly in two different methods; Near Surface Mounted **(**NSM) and Externally Bonded Reinforcement (EBR) on the element. For both these methods of application, an adhesive needs to be used. This could be either any specified epoxy or cement grout. Out of the two methods of installation, near surface mounted (NSM) CFRP has demonstrated a competitive advantage over externally bonded reinforcement due to many reasons [1]. NSM allows better adhesion compared to EBR, provides a larger specific area for binding with concrete, durable, thermal protection becomes easier, more convenient in installation since there is less preparation of the surface. It has also been recognised as a better method of installation if CFRP bars are expected to be used in pre stressing [2].

Even though the NSM method has been identified as an effective method of installing CFRP in qualitative terms, experimental values have not been provided to verify its effectiveness in terms of flexural strengthening when the same effective area of CFRP is used. This research was designed to bridge the gap existed due to lack of experimental verifications. Therefore in this current study it has been proven that the NSM method provides better flexural strengthening compared to the EBR method and also an integrated method of EBR and NSM can also be effectively used.

Furthermore according to the guidelines of ACI 440-2R.08 [6] [6], the moment capacity of a beam strengthened by NSM and EBR methods can be measured separately. If an integrated method is used a combination of those calculation methods should be adopted along with an additional safety factor. In this paper the additional safety factor has been investigated through experimental data and analysis.

2. Test program

2.1 Objectives

The main objective of this research is to identify the best method of installing CFRP strips in reinforced concrete beams when the same effective area of CFRP is being used. It has also been investigated and experimented on new methods of installing CFRP strips using the NSM and the EBR method together both in parallel and perpendicular directions. Eventually the moment capacity of the integrated method was calculated according to the guidelines provided in ACI 440-2R.08 [6] and an additional safety factor was introduced by comparing the theoretical values with actual experimental results. The research was carried sequentially as follows;

- A thorough literature review was conducted in order to identify the new trends of CFRP uses and emerging technologies
- The research gap was identified and the experimental programme was planned in order to achieve the objectives
- Experiment was carried out and data was gathered
- A complete analysis was carried out eventually to achieve the pre-defined**.**
- Theoretical results were compared with experimental values to introduce a safety factor when equations specified in design guidelines are used.

2.2 Experimental procedure

Six concrete beams of 150 mm × 150 mm × 750 mm dimensions were cast using G35 concrete. Cubes cast out of the same concrete were tested after 28 days and the average compressive strength was recorded as 39.7 N/mm^2. Two 6mm diameter mild steel bars were used for main bars and 6 mm diameter galvanized iron bars were used as shear links with 75 mm spacing in the concrete beams.

Properties of CFRP strips used for strengthening the reinforced concrete beams are mentioned below in Table 1. Two part epoxy adhesive was used for bonding. The mixing ratio was 4:1 by weight according to manufacturer's technical data sheet.

Table 1: CFRP Manufacturer Specifications [7]

Parameters	Value
Elastic modulus (GPa)	>170
Tensile strength (MPa)	>2800
Elongation at rupture	≥1.6
Fibre volume content	>68
Bond strength (MPa)	≥1.5
Strip thickness (mm)	1.2

Table 2: Epoxy specifications [7]

Parameters	Value
Elastic modulus (N/mm^2)	>7100
Compressive strength (N/mm^2)	>70
Tensile strength (N/mm^2)	≥3
Shear strength (N/mm^2)	>26
Density (g/cm^3)	1.7-1.8

2.2.1 Test matrix

Table 3: Description of test specimens

Description	Beam No
Beams strengthened in EBR method	B1,B2

Beams strengthened in NSM method	B3, B4
NSM and EBR method in parallel direction	B5
NSM and EBR method perpendicular to each other	B6

2.2.2 Specimen preparation

After the beams were cured the surface of the beams were prepared for the installation of CFRP strips. Four different categories of test specimen were needed to be prepared as shown in Table 3.
In the NSM method two grooves of 5 mm width and 15 mm depth were cut with a centre to centre spacing of 30 mm at the bottom surface of the beams. Then an air compressor was used to clean the grooves and there after acetone was used to clean them further. When the groves were prepared an edge distance of 60 mm were allocated in each beam to eliminate the overlapping of tensile stresses induced by the CFRP strips at the point of loading.

In the EBR method, the surface was prepared by grinding and acetone was used to wipe off the dust. In the method of integration of the EBR and NSM methods, the surface was prepared first by grinding and then in one beam two grooves were cut parallel to main reinforcement and in the other beam, six grooves were cut perpendicular to the main reinforcement. (Figure 1 and Figure 2)

Figure 1: Grooves prepared perpendicular to main steel reinforcement

Figure 2: Grooves prepared parallel to main reinforcement

Surface preparation methodologies and groove dimensions were referred to from ACI 440-2R.08 [6]. 10 mm wide CFRP strips were used and the length used was 450 mm. The length was determined according to the effective bond length mentioned in the ACI codes.

In both NSM and integrated systems, the grooves were first half filled with epoxy and then the CFRP strips were installed. The rest of the grooves were filled after inserting CFRP strips. In addition to this, in the two integrated systems, after installing CFRP strips in NSM method, two CFRP strips of the same length as used in EBR method, were pasted on top of the grooves. (Figure 3 and Figure 4).

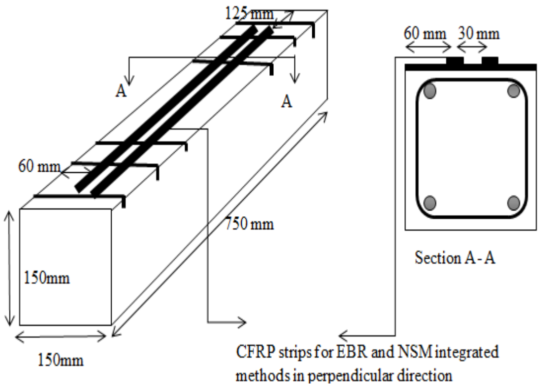

Figure 3: Integrated in perpendicular direction

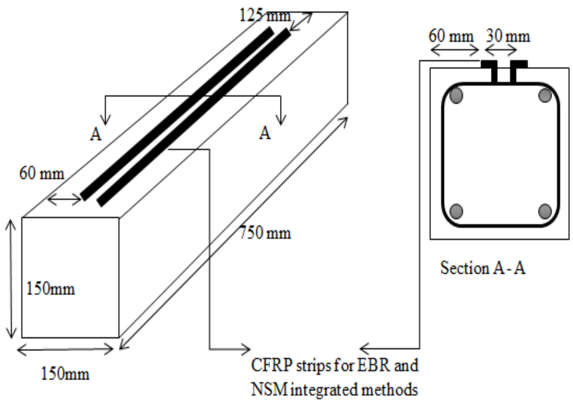

Figure 4: Integrated in parallel direction

2.2.3 Testing methodology

The Amsler machine was used for the four point bending test. Concrete beams were simply supported with a test span of 600 mm. The supports were located at 75 mm away from the CFRP strips to avoid creating end anchorage to CFRP strips from external supports. The experimental set up is shown in Figure 5.

The specimens were gradually loaded and mid span deflection was recorded using dial gauges. The failure load was considered as the load recorded at the point of 0.3 mm crack initiation. The concrete beams were loaded further after reaching its failure loads to clearly observe the failure patterns.

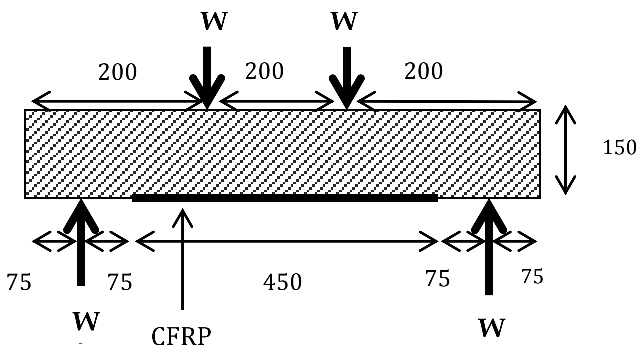

Figure 5 - Experimental set up (in mm)

3. Results and analysis

3.1 Load deflection curve

A ductile system displays sufficient warning before catastrophic failure. It becomes a significant property of a beam which becomes important for seismic design, and since retrofitting is sometimes concerned with upgrading a structure to resist seismic forces, identifying the retrofitting material which gives better ductility is important [5].

From the results obtained from beam testing, the load-deflection curve was drawn. It is shown in Figure 6. According to experimental data the beams strengthened in the NSM method shows the least deformation for a given load. The NSM method showcases the best performance under loading, and it is proven to be more ductile, in return displaying sufficient warning before collapse and being ideal for seismic designing as well.

However with the increase in loading the integrated method in parallel direction also yields better results. Higher the load, greater the ductility is.

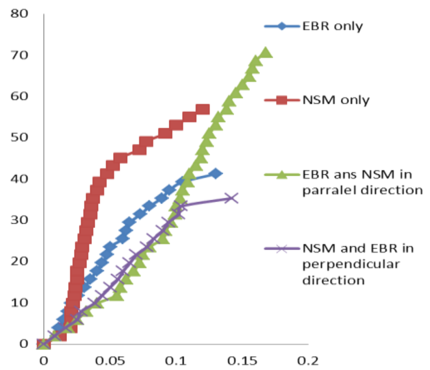

Figure 6: Load

This hints at the anticipatory future of CFRP applications for seismic designs in both existing and emerging building; especially for high rises.

3.2 Flexural strength gain

Of the four methods of installation, the integrated method in parallel direction demonstrated the highest strength gain. In the below Figure 7, increase in percentage with comparison to theoretical load of unstrengthen beam is shown. In the y axis of the graph 1, 2, 3 and 4 indicates the EBR method (B type), NSM method (C type), integrated in parallel (D type) and integrated in perpendicular directions (E type) respectively.

This has been proven in similar experiments carried out in other countries as well. Lack of information about the effective area used inhibits those results from verifying the fact that NSM method performs better in terms of flexural strength. The latest similar experiment that had been carried out by El-Hacha, and Rizkalla in 2004 [2] yields the same conclusion. According to their experiment the NSM method is nearly 54% more effective than the EBR method. In their experiment an anchorage length of 2400 mm had been used and the strips installed by EBR method had further been confined with U- wrap CFRP sheets at the two ends in order to eliminate de-bonding .This is the main reason for not being able to compare the NSM method and EBR method under same effective areas of CFRP strips. The CFRP sheet or the textile too comes into effect in that experiment making the effective areas of CFRP unequal.

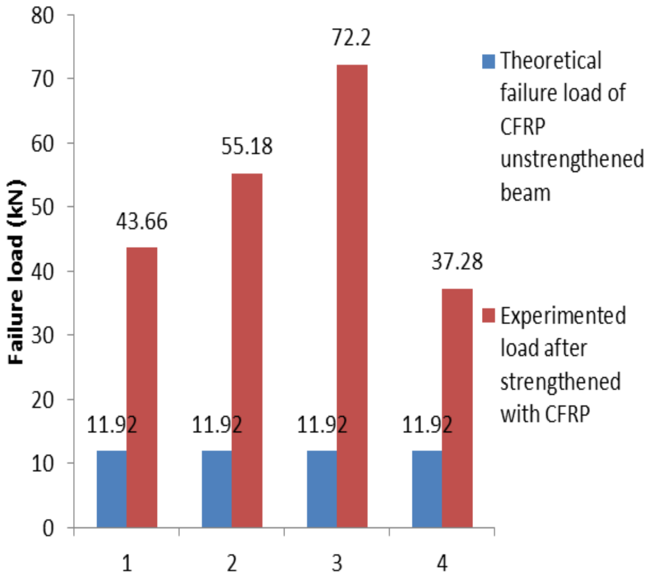

Figure 7: Comparison of loads with unstrengthen CFRP beam

The experimental programme explained in this paper, was planned to make sure that the same effective area of CFRP strips is used through-out without incorporating other CFRP materials to eliminate de-bonding and peeling off. The results obtained exhibits a 26% increment of flexural strength of NSM method Vis a Vis the EBR method (Figure 7).

Another important fact to be identified is that, the external reinforcement is provided as tension reinforcement. For a simply supported beam it is the bottom face of the beam which needs to be reinforced. The beams tested for this research had highly limited surface area due to space allowances provided for edge splitting, cover delamination and generation of excessive tensile stresses at grooves. So the flexural gain cannot be easily enhanced with attempt to mount more CFRP strips on a beam surface. This can be easily and effectively achieved by integrating the NSM and EBR methods together. Not that this method has provided more space for mounting CFRP strips but also has enhanced the flexural capacity by 67% compared to sole EBR method. Compared to the NSM method it is an increment of 31% (Figure 7).

3.3 Failure modes

Not many different types of failure modes were observed. Even though the methods of installation varied significantly from each other, the failure modes did not differ much from each other. B1, B2 (EBR method) beams failed due to strip end de-bonding (Figure8). This type occurs with a loss in the composite action between the bonded CFRP and the RC member. De-bonding in CFRP strengthened RC members occurs in regions of high stress concentrations, which are often associated with material discontinuities and with the presence of cracks. If de-bonding from end plate was avoided by transverse clamping with CFRP U-wraps or steel plates with anchor bolts at the end, the failure load could have been increased. The transverse clamping could have prevented de-bonding at the end and delay the failure.

Figure 8: De-bonding at plate end

C1, C2 beams that were strengthened in NSM method failed due to the splitting of epoxy (Figure 9). This is the usual method of crack initiation in an NSM mounted method according to Zsombor K. Szabo`[3].

Figure 9: Surface splitting in NSM method

In the experiment carried out, the surface splitting of the adhesive occurred closer to the supports. So the splitting of epoxy that is known as a secondary failure can be the result of shear failure around the reinforcement. The flexural strength of the beam had been enhanced by this arrangement and now that the failure occurs due to lack of shear strength.

Splitting in the epoxy cover is a result of high tensile stresses at the CFRP and epoxy interface. Increasing the thickness of the epoxy cover can reduce the tensile stresses induced. [4] In order to increase the thickness of the epoxy cover, the groove has to be cut deeper into the beam. However this is impossible unless the cover is greater in the beam. The cover in the beams used was 25 mm. And the depth of the groove was nearly 15 mm. This could have been extended a bit further, but will be restricted at the depth of 25 mm. Instead of this solution an epoxy with higher tensile stress can be used. These remedies can increase the failure load of the strengthened beams under NSM method.

Figure 10: Crack initiation in the epoxy cover in the integrated method

D1 beam which was strengthened in the integrated method in parallel direction failed in a similar way to C2 beams and E1 beams that was strengthened by the integrated method (perpendicular to the main reinforcement direction) failed at a very low ultimate load due to de-bonding of the CFRP strips.

This emphasises the fact that in beam D1, even though it is an integration of both NSM and EBR methods, the same failure pattern seen in the NSM method could be seen here as well. It depicts that the NSM method is more predominant in the integration method. And the externally bonded CFRP strips in D1 beam behaved as if they had been clamped, (Figure 10) which means that the CFRP strips installed in NSM method have reduced the stress concentration induced at plate ends. Instead it had increased the shear stress at the supports and made the beam fail in shear failure. This indicates that this method has improved the flexural strength, and now it had been the shear strength which had weakened the beam's capacity. If proper shear reinforcement was provided through CFRP the failure load could have been increased.

3.4 Moment capacity

According to ACI 440-2R.08 [6] design recommendations CFRP strengthening systems should be designed to resist tensile forces while maintaining strain compatibility between the CFRP and the concrete substrate. In section 9 of ACI 440.2R-08 the design philosophy of calculating the moment capacity of a CFRP strengthened beam is discussed. According to the researches carried out it has been recommended to use an environmental reduction factor of 0.9 for CFRP strengthening systems with the assumption that the exposure condition is interior. Additional safety factors need to be applied when CFRP reinforcement is used to reflect uncertainties inherent in CFRP systems compared with steel reinforced and pre-stressed concrete.

3.4.1 EBR method

When the moment capacity of the reinforced concrete beam strengthened by the EBR method was calculated it could be seen that the effective strain in CFRP reinforcement is limited by the de bonding strain of the CFRP strip. Hence the flexural moment provided by the CFRP strengthening system is dictated by the stress induced at the point at which the CFRP de bonds from the substrate.

$$\varepsilon_{fd} = 0.41 \sqrt{(fc'/nE_f t_f)} \leq 0.9\varepsilon fu \text{ in SI units} \quad (1)$$

ε_{fd} is the strain level at which de bonding occurs and fc', n, E_f, εfu and t_f represent the design compressive strength of concrete, number of CFRP strips used, elastic modulus of CFRP strips, design rupture strain of CFRP strips and thickness of the strips respectively.

fc' = 35 N/mm^2, n = 2, E_f = 170000 N/mm^2 , εfu = 0.0152 ($\varepsilon fu = C_E\, \varepsilon fu^*$ *in which* C_E =0.9 *and* εfu^* =0.016*) and* t_f = 1.2 mm

In the EBR method when the strain level at de bonding was calculated it was found that the value is 0.0038 and it was less than the given limit.

$$\varepsilon_{fe} = 0.003\left(\frac{d_f - c}{c}\right) - \varepsilon_{bi} \leq \varepsilon_{fd} \quad (2)$$

Equation 2 calculates the effective strain in the CFRP strip (ε_{fe}) when the concrete is at its crushing point. It is calculated using the strian at the substrate which is indicated by ε_{bi} and d_f and c representing the effecticve depth to CFRP strips and depth to the neutral axis respectively. d_f is observed to be 150 mm as the CFRP strips are pasted at the bottom surface for the EBR method. This could be taken as 142.5 mm for the NSM method as CFRP strips are inserted inside the beam by cutting a groove in the bottom surface of the beam. c is found through an iteration process and the last iteration value was taken as 24.98 mm. Equations used to arrive at c value is clearly shown in ACI 440-2R.08 [6] under section 9.

The strain at the substrate can be found using separate equations specified in ACI 440-2R.08 [6] under section 9. When determining the strain at the substrate only the dead loads are taken into account. When data was insereted to eqaution 2 it was seen that the maximum effective strain at the CFRP strips at failure was greater than its de bonding strain which was stated as 0.0038 in the earlier paragraph. So the effective strain at the CFRP strips at failure was restriced to its de bonding failure strain. So it was concluded that the failure occurs due to de bonding of the strips and the moment capacity was found accordingly.

$$f_{fe} = E_f \varepsilon_{fe} \quad (3)$$

$$M_{nf} = A_f f_{fe}\left(d_f - \frac{\beta_1 c}{2}\right) \quad (4)$$

The stress of the CFRP strips can be calculated using equation 3 and this stress (f_{fe}) is used to determine the moment capacity of CFRP strengthened beams as shown in equation 4. M_{nf} represents the moment achieved only due to CFRP strengthening and A_f represents the CFRP area while β1 gives the ratio of depth of equivalent rectangular stress block to depth of the neutral axis. The total flexural strength comes as a combination of M_{nf} and moment due to steel reinforcement.

According to design philosophy in section 9 of ACI 440.2R-08 the theoretical increment of moment capacity in the EBR strengthened method due to CFRP strengthening using all the equations given, is 78% and the total flexural strength obtained is 4.19 kNm.

3.4.2 NSM method

If the same procedure was applied for the NSM strengthening method, the de bonding strain will once again govern the maximum strain level that can be achieved in the CFRP reinforcement. But the de bonding strain limit can be applied only for externally bonded method as the NSM model hardly fails under de bonding failure. So in this case the maximum strain is decided by the crushing of concrete.

Thus the maximum strain obtained will be determined from equation 2 and the de bonding strain will be ignored. This strain is then applied to equation 3 and 4 sequentially. Hence the theoretical increment of moment capacity due to NSM strengthening would be nearly 250% and the total flexural strength obtained was 8.82 kNm.

3.4.3 Integrated method

When these two methods were integrated in the parallel direction the experimental value obtained for the failure load was 72.2 kN. The calculated moment capacity at the mid span was 9.06 kNm via equation 5

$$M = \frac{wl^2}{8} + \frac{Wl_1}{2} \qquad (5)$$

In equation 5, w (0.54 kN/m) is the self-weight of the beam and W (72.2 kN) is the point load imposed at the point of failure (This load was imposed on the beam as two point loads at the four point bending test). l (750 mm) is the length of the beam. l_1 (250 mm) is the distance between the support and the point load.

One of the most significant observations at the experimental program of the integrated beam was that the CFRP strip end de bonding did not occur even though they had been pasted at the bottom surface of the beam in EBR method. Instead the beam failed due to concrete crushing as in NSM method. So the strain of the CFRP strips at failure should be determined via equation 2. The ultimate moment capacity obtained from the above mentioned set of equations as specified in ACI 440-2R.08 [6] is 14.5 kNm. This value is obtained when four strips of CFRP strips were used; two strips inserted in NSM method and another two pasted in EBR method. An issue encountered in this theoretical calculation is that the guidelines tend to consider both CFRP strips installed in NSM and EBR methods to have been installed in NSM method only. This is mainly due to the similar failure patterns of the integrated method and the NSM method.

A modification factor can be proposed as a ratio between the theoretical value calculated according to the guidelines in ACI 440-2R.08 and the experimental value obtained from this test series. This additional safety factor can be calculated as 0.6 but needs to be verified further by using a numerical analysis method as well.

4. Recommendations

If transverse clamping had been used in beams B1 and B2, the failure load could have been increased. If an adhesive with better tensile strength was used, beams C1 and C2 could have failed under heavier loads. The deepening of the groove in C1 and C2 also could have enhanced the failure load. However the space allocations required in installation of CFRP strips in accordance with ACI 440-2R.08 [6] and the minimum cover of a beam hinder such procedures.

When the moment capacity of the integrated method was found it could have been summarised as follow;

The ultimate moment capacity of a CFRP strengthened beam is given by the equation 6 below

$$\Phi M_n = \phi\left[M_{ns} + \Psi_f M_{nf}\right] \qquad (6)$$

M_n, M_{ns} and M_{nf} represent the flexural strength gain due to the addition of steel and CFRP reinforcements, strength gain due to steel reinforcement only and strength gain due to CFRP reinforcement only respectively.

The rest of the symbols represent various modification factors specified in the guidelines. This equation is used in both NSM and EBR installations. Hence the new modification factor of 0.6 can be incorporated in equation 6 when it is being used for the integrated method.

ϕ in equation 6 sets the reduction factor at 0.90 for ductile sections and 0.65 for brittle sections where the steel does not yield, and provides a linear transition for the reduction factor between these two extremes. When this model is being used for the integrated method it can be recommended to use ϕ as 0.54 for brittle sections and 0.4 for ductile sections after incorporating the safety factor of 0.6 mentioned above.

5. Conclusions

After examining the failure loads it can be concluded that when the same effective area of CFRP strips are used, the more effective method of installation is the NSM method. In a given area, it is not easy to install as many strips as desired since there are space allowances that need to be allocated. In the method of integration, the effective area of CFRP strips was doubled without causing excessive tensile stresses due to congestion of grooves and CFRP strips. It also improved the flexural capacity nearly by two times compared to the typical EBR method.

Different methods of CFRP installation systems can enhance the flexural capacity of a reinforced concrete beam, so that the beams tend to fail under shear. In order to eliminate this, the beams should be adequately strengthened in shear as well.

When the two methods are integrated in parallel direction, the NSM method dominates and this method of integration also acts as transverse clamping to the CFRP strips bonded in EBR method on the surface. If the integration of the two methods were done in perpendicular direction to each other, the EBR method dominates the failure pattern of the beam.

A modification factor of 0.6 can be introduced for the determination of flexural strength of the integrated method in parallel direction. This additional safety factor should be incorporated in the moment equation presented in ACI 440-2R.08 guidelines under section 9. This factor needs to be further investigated through a numerical analysis model.

The NSM method and the integrated system in parallel direction perform better in terms of ductility, which makes them much appropriate in earthquake resistivity.

Acknowledgements

This study was financially supported by a University Research Grant (Grant No. SRC/ST/2013/01) from the Senate Research Committee, University of Moratuwa, Sri Lanka. Special gratitude is extended to the company "Airowsolution" and Mr. Mohamad Sathik for co-operating towards the success of the experiment.

References

[1]. Tanarslan, H. M., "The effects of NSM CFRP reinforcements for improving the shear capacity of RC beams", Construction and Building Materials, 2663-2673, 2011.

[2]. EI-Hacha, R., and Rizkalla, S. H., "Near surface mounted fiber reinforced polymer reinforcement for flexure strengthening of concrete structures", ACI Structural Journal, American Concrete Institute, Vol. 101, N0. 06, pp. 717-726, 2004.

[3]. Szabo, A. K., & Balazs, G. L., "Near surface mounted FRP reinforcement for strengthening of concrete structures", Periodica polytechnica, 33-38, 2007

[4]. Hassan, T. K., & Rizkalla, S. H., "Bond Mechanism of Near-Surface-Mounted Fibre-Reinforved Polymer Bars for Flexural Strengthening of Concrete Structures", *ACI Structural*, 830-839, 2004.

[5]. Bsisu,K., Hunaiti Y., and Younes R., "Flexural Ductility Behavior of Strengthened Reinforced Concrete Beams Using Steel and CFRP Plates", Jordan Journal of Civil Engineering, Vol 6,No 3, 2012.

[6] ACI 440-2R.08 Guide for the Design and Construction of Externally Bonded FRP Systems for Strengthening Concrete Structure

[7] Simpson Strong-Tie, C-FRP-2014/15, www.strongtie.com, accessed on 2.12.2014

SECM/15/160

ACI guidelines to assess the performance of CFRP-strengthened concrete beams with transverse end U wraps

M.R.E.F. Ariyachandra[1*], J.C.P.H. Gamage[1]

[1]Department of Civil Engineering, University of Moratuwa, Sri Lanka
*E-Mail: ariyachandra88erandi@gmail.com, TP: +94719085399

Abstract: In this comprehensive study, firstly, the theoretical model described in ACI 440 committee report to calculate the area of transverse U wraps provided for anchored CFRP-strengthened concrete beams was examined. Then, an experimental study was carried out with a total of 10 small-scale test specimens and test parameters were set to inspect the validity of the limitations given in the above theoretical model. Theoretical calculations were performed in accordance with ACI guidelines for the above test specimens as well as for the previous research studies. Finally, the constraints of applicability of the theoretical model given in ACI 440 committee report was discussed presenting new recommendations for different scenarios.

Keywords: CFRP, debonding, flexural capacity, transverse end U wraps

1. Introduction

Impacts of environmental degradation due to numerous ageing mechanisms, accidental damage and increased loading decline structural integrity and prolonged service life of reinforced concrete (RC) structures. The use of Carbon Fiber Reinforced Polymers (CFRPs) to rehabilitate the RC structures has become more popular among conventional strengthening methods such as external pre-stressing, the use of externally bonded steel plates and section enlargement [1, 2]. This can be mainly attributed to its excellent material characteristics such as light weight, high tensile strength, durability, low maintenance and ease of installation.

However, inherent deficiencies have reduced the effectiveness of CFRP systems due to the occurrence of premature failure modes causing structures to fail at much lower loads than expected. These debonding failure modes are typically caused by the loss of composite action between the concrete and CFRP [3]. FRP debonding generally initiates within the bond line due to high interfacial stress concentrations and results in primarily two types of failures [4, 5]. The first type is "mid-span debonding", which may initiate at flexural or shear cracks close to the mid-span and then propagates towards the plate end. Debonding may also occur near the plate end and this type is identified as "end debonding". This type of failure commonly exhibits crack propagation in the direction of mid-span caused by a predominant shear crack induced at the plate end [4, 5].

The provision of anchorages for externally bonded CFRP laminates to soffits is identified as a promising technique to prevent or delay premature debonding failures and thereby greatly improves the failure loads of CFRP-concrete systems [6, 7]. To enhance the flexural performance of CFRP-strengthened concrete beams, numerous research studies have been focused on the use of end anchorages in the form of transverse FRP end U wraps. These research studies concluded that the provision of transverse FRP end U wraps not only increases the failure loads, but also improves the ductility of CFRP/concrete composite beams.

Although provision of transverse FRP end U-wraps has proven its efficiency as a promising technique to delay premature end debonding failure, to the best of the authors' knowledge, there are no well-documented guidelines to assess the performance of CFRP-concrete beams anchored with transverse end U-wraps. As a result, the extensive use of anchorage systems in the form of end U-wraps has been restricted. Xiang *et al.* [8] proposed a new theoretical model to calculate the moment capacity of anchored CFRP/concrete beams with transverse end U-wraps which is only applicable for low-strength concrete beams.

In the ACI 440 Committee report [9] for externally bonded FRP systems, Section 10.1.1 in chapter 10 and section 13.1.2 in chapter 13 emphasize the importance of provision of transverse FRP U-wraps which offer a clamping effect against cover separation failure for the improved bond behaviour of CFRP-strengthened concrete beams. Moreover, a set of equations is presented to compute the area of transverse clamping of FRP U-wraps to prevent concrete cover separation failure, as proposed by Reed et al, 2005. Nevertheless, none of these equations estimate the resultant percentage strength gains compared to the provided anchorage area.

2. Literature review

Even though the provision of transverse U wraps, W wraps or L wraps to increase the shear capacity of CFRP-strengthened concrete beams has been comprehensively scrutinized and documented, few research studies have been focused on the influence of flexural capacity of CFRP-concrete composite beams due to the provision of transverse U wraps placed at the two ends of longitudinal CFRP laminate within the effective bond length. However, significant strength improvements have been observed in CFRP/concrete composite beams anchored with transverse end U wraps compared to non-anchored CFRP-strengthened concrete beams.

Buyle-Bodin & David [10] tested a 150 mm×300 mm×3000 mm size concrete beam strengthened using externally bonded 100 mm wide CFRP sheet anchored with two 300 mm wide transverse CFRP end U wraps and observed 33.58% strength gain compared to non-anchored CFRP-strengthened concrete control beam. Buyukozturk et al. [11] prepared two 150mm × 180mm × 1500mm concrete beams strengthened with 38 mm wide CFRP sheet bonded to the soffits and anchored with 80 mm and 160mm wide CFRP end U wraps. These specimens (S4PS1M & S4PS2M) were tested using four point bending test and observed failure loads were 205.8kN and 231.3kN, which is equivalent to 22.14% and 37.27% strength increments over non-anchored CFRP/concrete control composite beam. Ceroni [12] tested one CFRP-strengthened concrete beam with dimensions 100 mm×180 mm×2000 mm strengthened using 100 mm wide externally bonded CFRP sheet together with 100 mm transverse CFRP U wraps. The reported failure load was 41.3 kN with 10.43% strength increment compared to CFRP-strengthened beam without end U wraps. Pham & Al-Mahaidi [13] observed significant strength gains of 57.50% and 81.17% for concrete beams of 140 mm×260 mm×2900 mm dimensions strengthened with 100 mm wide CFRP laminates and anchored with 50 mm and 150 mm wide transverse end U wraps. These test specimens (A1a and A1b) were subjected to four point bending test and the above strength improvements were reported with respect to non-anchored CFRP/concrete control beam (E3b2). Pimanmas & Pornpongsaroj [14] prepared two CFPR/concrete beams with 120 mm×220 mm×2200 mm dimensions strengthened with 100mm wide CFRP sheets. These test specimens, A-420-U and B-200-U were anchored with 300 mm wide transverse CFRP U wraps and achieved 41.41% and 24.90% strength gains compared to CFRP-strengthened control beam. Anchored test specimens, CU2-d/2 and CU2-d with 80mm and 160 mm wide GFRP end U wraps were prepared by Sadrmomtazi et al. [15] and observed strength gains of 5.02% and 11.88% respectively in comparison to non-anchored CFRP/concrete beams. Smith & Teng [16] prepared two CFRP-strengthened concrete beams (4A & 5B) with 75 mm and 125 mm wide transverse end U wraps. The longitudinal CFRP sheet has 150 mm width which is bonded externally to the soffits of the beams. These test specimens were subjected to three point bending test and reported strength increments were 19.44% and 15.86% for 4A and 5B respectively. Sobuz et al. [17] tested one 150 mm×200 mm×2000 mm CFRP-strengthened concrete beam with 100 mm wide transverse CFRP end U wraps and observed 22.50% strength improvement over CFRP/concrete composite control beams. According to the experimental studies carried out by Valcuende et al. [18], they observed 8.24% increment in failure loads for anchored CFRP/concrete beams (with 300 mm wide CFRP U wraps) with respect to control concrete beams strengthened with 50 mm wide CFRP laminates. The dimensions of concrete beams were 100 mm×150 mm×1200 mm. Valivonis & Skuturna [19] used 100 mm wide end U wraps to anchor externally bonded CFRP/concrete beams with 100 mm wide CFRP laminate. They observed a significant strength increment of 40.02% due to the addition of transverse end U wraps.

3. ACI guidelines for anchored beams with transvers end U wraps

As stated in ACI 440 committee report [9], provision of transverse clamping FRP U-wraps along the length of the flexural FRP reinforcement has been observed to result in increased FRP strain at debonding. Thus, higher loads can be transferred to the flexural FRP laminates by utilizing material properties effectively, which in turn improves the overall efficiency of the strengthening system. The area of the transverse clamping CFRP U-wrap,

$A_{f\,anchor}$ can be computed in accordance with Eq. 13-1 given in the ACI 440 Committee report [9].

$$(A_f)_{anchor} = \frac{(A_f f_{fu})_{longitudinal}}{(E_f k_v \varepsilon_{fu})_{anchor}} \quad (1)$$

The bond reduction coefficient k_v depends upon the concrete strength, the type of wrapping scheme and the stiffness of the laminate. Thus, k_v can be calculated from Eq. 11-7 to 11-10, as stated in the ACI guidelines.

$$k_v = (k_1 k_2 L_e)/11{,}900\, \varepsilon_{fu} \leq 0.75 \quad (2)$$

The active bond length L_e is the length over which the majority of the bond stress is maintained. L_e can be obtained by Eq. 3.

$$L_e = 23{,}300/(n t_f E_f)^{0.58} \quad (3)$$

k_v depends on two other modification factors k_1 (Eq. (4) and k_2 (Eq. (5):

$$k_1 = (f_c'/27)^{\frac{2}{3}} \quad (4)$$

$$k_2 = \left(d_{fv} - L_e\right)/d_{fv} \quad \textit{for U wraps} \quad (5)$$

Where f_c' is compressive strength on concrete and d_{fv} is height of the U wrap above tensile reinforcement bars as illustrated in Figure 1(a). As a result, if the height of end U wraps are lesser than a_s, Equation (5) is inapplicable and hence cannot compute the theoretical area of U wraps. Thus, according to the above theoretical model, transverse end U wraps should have a minimum height greater than a_s to be effective in delaying premature debonding failure. To examine the applicability of this constraint in terms of minimum height of the U wraps, an experimental programme was devised to inspect the influence of height of the transverse end U wraps. Even though addition of end U wraps which provides enhanced performances, in practice for rehabilitation, it may be difficult to bond transverse end U wraps with greater heights due to external barriers. In addition, provision of U wraps with greater heights does not always offer economical solutions due to lack of material efficiency. Thus, one objective of the test programme was to evaluate the strength gains correspond to shorter U wrap heights which is not specified in ACI guidelines. The test programme comprised both transverse FRP end U wrap configurations illustrated in Figure 1(a) and Figure 1(b). As shown in Figure 1(b), the provided height

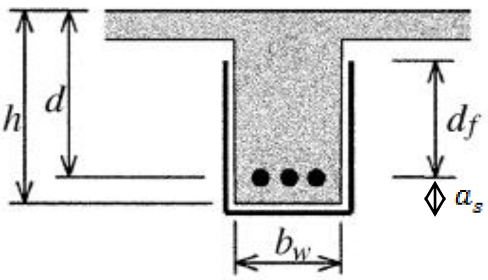

Figure 1(a) : Configuration of transverse end U wraps according to ACI report [9]

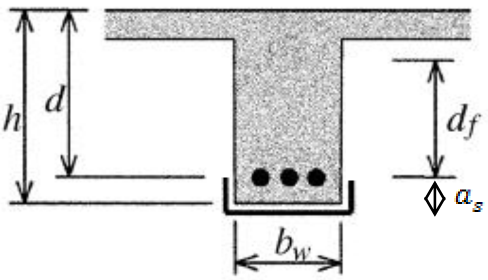

Figure 1(b) : Configuration of transverse end U wraps used in present test programme

of the U wrap was lesser than d_f as defined in Figure 1(a). For both end U wrap configurations, corresponding strength improvements were observed with respect to the provided height of end U wraps.

4. Test programme

To assess the validity of limitations considered in the theoretical model described in previous section, authors carried out an experimental study with a total of 10 numbers of small-scale reinforced concrete test specimens with dimensions 100 mm × 150mm × 750 mm (width × depth × length). The strengthening scheme of CFRP-strengthened test beams anchored with transverse FRP end U wraps is illustrated in Table 1. The test specimens were cast using grade 30 concrete mix with a maximum aggregate size of 20 mm and a water-cement ratio of 0.55. Standard size concrete cubes of 150 mm × 150 mm × 150 mm were also prepared and cured under similar laboratory conditions and measured average compressive strengths was 31.99 N/mm^2. Mild steel bars of 6 mm in diameter were used as the longitudinal reinforcement and galvanized iron bars of 4 mm in diameter were used to prepare shear links. The tensile strengths of 250 N/mm^2 and 363 N/mm^2 were obtained for mild steel and galvanized steel respectively using standard laboratory tests. Both CFRP and glass fibre reinforced polymer (GFRP) sheets were used for specimen preparation. A commercially available two-part epoxy adhesive was used to bond the FRP sheets. The material properties of both FRP sheets and the epoxy adhesive are listed in Table 2, in accordance with the manufacturers’ specifications [20].

Table 1: Strengthening scheme of test specimens

Designation	Description	Strengthening scheme	Figures
B/2/CC	Non-strengthened control concrete beam	None	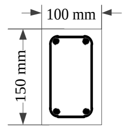
B/2/CF	CFRP-strengthened concrete beam	Strengthened with one externally bonded 100mm×600mm CFRP sheet	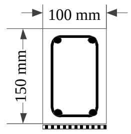
B/2/CF$_{50}$	Anchored beams with CFRP U wraps	Strengthened with one externally bonded 100mm×600mm CFRP sheet + 50 mm wide two CFRP end U wraps	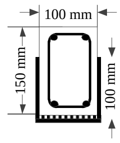
B/2/CF$_{100}$	Anchored beams with CFRP U wraps	Strengthened with one externally bonded 100mm×600mm CFRP sheet + 100 mm wide two CFRP end U wraps	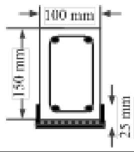
B/2/GF$_{100}$	Anchored beams with GFRP U wraps	Strengthened with one externally bonded 100mm×600mm CFRP sheet + 100 mm wide two GFRP end U wraps	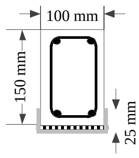

Table 2: Material properties of FRP and two part epoxy adhesive [20]

FRP sheet			Two-part epoxy adhesive		
Parameters	CFRP	GFRP	Parameters	Primer	Saturant
Fibre Density (g/cm^3)	2.1	2.6	Yield Strength(MPa)	24.1	138
Fibre Modulus (GPa)	640	73	Strain at Yield (%)	4%	3.8%
Thickness (mm)	0.19	0.31	Elastic Modulus(MPa)	595	3724
Ultimate Tensile Strength (MPa)	2600	2400	Ultimate Strength(MPa)	24.1	138
Ultimate Tensile Elongation (%)	0.4	4.5	Glass Transition Temperature (°C)	77	71

The bottom surfaces of the concrete beams were sand-blasted prior to bonding of the FRP and resulted concrete substrates were reasonably rough. The wet lay-up system [9] was used to bond CFRP sheets onto the concrete beams. Primer part A (hardener) and part B (base) were mixed at 1:2 ratio by weight and a thin layer of primer was applied immediately after cleaning which resulted in a dry and slightly sticky film. The prepared concrete beams were set aside for about 45 minutes. The result was a dry, non-sticky surface that could be protected from contamination until epoxy adhesive was ready to be bonded to the substrate. Saturant part A (hardener) and part B (base) were mixed using a 1:2 ratio by weight as per the manufacturer’s specifications [20]. Next, the prepared concrete substrates and FRP sheets were saturated with epoxy saturant. CFRP sheets with dimensions of 100 mm × 600 mm impregnated with saturant were pressed onto the concrete substrates and a ribbed roller was used to remove air entrapped in the bond line. Ribbed rolling was carried out in the direction parallel to the fibres. The epoxy adhesive had a pot life of 40 minutes and it was cured for 7 days at room temperature [20]. All CFPR-strengthened concrete control test beams were prepared following the above procedure.

The prepared test specimens were simply supported and subjected to three-point bending using an Amsler testing machine. Roller supports were placed 75 mm from the bonded CFRP sheet. A point load was applied at the top of the beam at mid-span. Mid-span deflections were recorded using a dial gauge and initiation of cracks was observed. The test specimens were further loaded to determine the corresponding failure modes. The average failure loads of non-strengthened concrete control beams were 14.71 kN.

5. Test results

The highest strength gain of 14.64% was found for the CFRP-concrete test beams with 100 mm wide CFRP U wraps (B/2a/CF_{100}), compared with the non-anchored CFRP-strengthened control beams (B/2a/CF). The resultant failure behaviour of test beams B/2a/CF_{100} comprised separation of the concrete cover along the steel reinforcements. However, the test beams anchored with GFRP U wraps with a similar width (B/2a/GF_{100}) achieved only a 2.44% strength gain compared to the non-anchored CFRP-strengthened control beams. This was mainly due to the inappropriate thickness of the GFRP fibres, which hindered complete impregnation with epoxy adhesive, resulting in a poor bond between the longitudinal CFRP sheet and the transverse GFRP U wraps. A major shear crack was initiated at the end of CFRP sheet followed by delamination of the longitudinal CFRP sheet. A similar strength gain was achieved by anchored CFRP-strengthened specimens with 50 mm CFRP U wraps (B/2a/CF_{50}) and the resultant failure mode consisted of shear cracks at the innermost edge of the CFRP U wrap. All non-anchored CFRP-strengthened control beams failed due to cover separation failure and all non-strengthened control beams failed due to a single flexural crack initiated at mid-span. Although the implemented U wrap configurations were ineffective in delaying end debonding failure, type B/2a/CF_{100} successfully achieved a noticeable strength gain.

6. Predictions from ACI guidelines

As explained in section 3, the theoretical area of transverse end U wraps were computed using Equations (1-5) for the test specimens in the present study as well as for the previous research studies reviewed in Section 2. The calculated areas of the end U-wraps are listed in Table 3. The theoretical widths of U-wraps, b_{ACI} were computed by dividing the calculated area of the transverse end U wrap by the total length of the U-wrap provided experimentally. As revealed in Table 3, most of the theoretical widths of U-wraps obtained from the ACI guidelines are considerably greater than the experimentally investigated widths of U wraps b_{exp} selected in this paper, although noticeable strength gains were reported.

Figure 2 shows the variation of percentage strength increments (compared to non-anchored CFRP-concrete beams) with the ratios of the theoretical widths of U-wraps over the experimental widths of U-wraps. As indicated in the graph, the behaviours of the above two parameters are quite scattered and hence it can be concluded that no strong relationship exists between these two parameters.

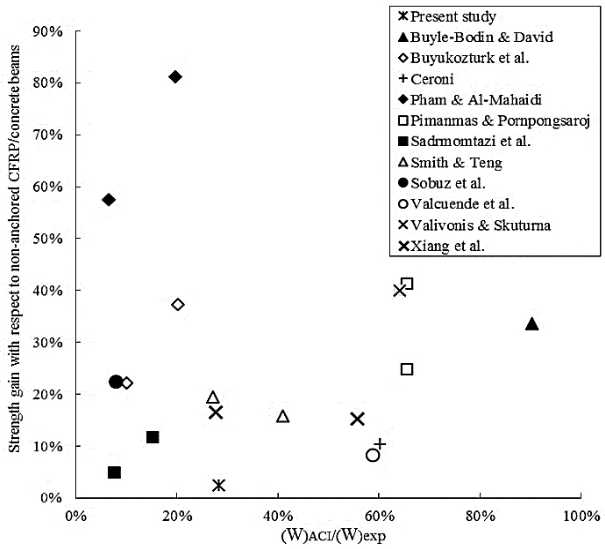

Figure 2: Variation of percentage strength increments (compared to non-anchored CFRP-concrete beams) with the ratios of theoretical width of U-wraps over experimental width of U-wraps

7. Conclusions and recommendations

CFRP-concrete composite beams exhibit several types of failure modes, of which premature end-debonding is the most critical type of failure, which takes place at the interface of the bond line or within the concrete cover zone. The provision of anchorages in the form of transverse end U wraps for externally bonded CFRP/concrete composites offers an excellent method of preventing or delaying premature debonding failure and thereby remarkably increasing the failure capacity of CFRP-concrete systems. As a result, higher loads can be transferred to the CFRP laminate, utilizing the material properties of CFRP more efficiently. However, the extensive use of FRP anchorage systems is restricted due to the lack of reliable design guidelines and also very few research studies have focused on enhancing the flexural capacity of CFRP-concrete composite beams using transverse U-wraps placed at both ends of the longitudinal CFRP laminate within the effective bond length. ACI 440 Committee report emphasizes the importance of provision of transverse FRP U-wraps to offer a clamping effect against cover separation failure for the improved bond behaviour of CFRP-strengthened concrete beams. A theoretical model is presented to compute the area of transverse clamping of FRP U-wraps to prevent concrete cover separation failure. Nevertheless, none of these equations estimate the resultant percentage strength gains compared to the provided anchorage area. According to the ACI theoretical model, transverse end U wraps should have a minimum height specified in the latter guideline to be effective in delaying premature debonding failure. In the present study, an experimental investigation was devised to examine the applicability of this constrain to inspect the influence of height of the transverse end U wraps. According to reported test results, anchored test beams with U wraps having shorter heights than minimum required heights defined in ACI guidelines also offered significant strength improvements with respect to non-anchored CFRP-strengthened control beams. Moreover, most of the theoretical widths of U-wraps obtained from the ACI guidelines are considerably greater than the experimentally provided widths of U wraps b_{exp}, although noticeable strength gain were reported from the previous experimental investigations in literature. Furthermore, it can be concluded that no strong relationship exists between the calculated theoretical area of U wraps and resulted strength improvements due to the provision of U wraps. Hence, the design guidelines should be reconsidered in order to design anchored CFRP/concrete beams with transverse end U wraps which also predict the corresponding strength gains to optimize the performance of CFRP/concrete composites in terms of material efficiency.

Table 3 : Theoretical and experimental areas of transverse end U wraps

Reference	Beam	$(A_f)_{anchor}$ mm^2	L^* mm	W_{ACI} mm	W_{exp} mm	$\frac{W_{exp}}{W_{ACI}}$	Strength gain † %
Present study	B/2/CF$_{50}$	52905.41	300	176.4	50	28%	2.44%
	B/2/CF$_{100}$	N/A	150	N/A	100	N/A	14.64%
	B/2/GF$_{100}$	N/A	150	N/A	100	N/A	2.44%
Buyle-Bodin& David [10]	F	249212.56	750	332.3	300	90%	33.58%
Buyukozturk et al. [11]	S4PS1M	405089.50	510	794.3	80	10%	22.14%
	S4PS2M	405089.50	510	794.3	160	20%	37.27%
Ceroni [12]	A7	76477.27	460	166.3	100	60%	10.43%
Pham & Al-Mahaidi [13]	A1a	503205.43	660	762.4	50	7%	57.50%
	A1b	503205.43	660	762.4	150	20%	81.17%
Pimanmas & Pornpongsaroj [14]	A-420-U	256523.15	560	458.1	300	65%	41.41%
	B-200-U	256523.15	560	458.1	300	65%	24.90%
Sadrmomtazi et al.[15]	CU2-d/2	443806.76	420	1056.7	80	8%	5.02%
	CU2-d	443806.76	420	1056.7	160	15%	11.88%
Smith & Teng [16]	4A	179313.26	650	275.9	75	27%	19.44%
	5B	198263.11	650	305.0	125	41%	15.86%
Sobuz et al.[17]	FBF-1LU	691097.40	550	1256.5	100	8%	22.50%
Valcuende et al.[18]	B-SF	204514.08	400	511.3	300	59%	8.24%
Valivonis & Skuturna [19]	SD6	78053.69	500	156.1	100	64%	40.02%
Xiang et al. [8]	B12	201810.22	750	269.1	150	56%	15.17%
	B22	408825.01	753	542.9	150	28%	16.51%

Acknowledgements

This study was financially supported by a University Research Grant (Grant No. SRC/ST/2013/01) from the Senate Research Committee, University of Moratuwa, Sri Lanka. The assistance of the technical staff of the Structural Testing Laboratory and Building

Materials Laboratory at University of Moratuwa is gratefully acknowledged.

References

[1]. Heiza K, Nabil A, Meleka N, Tayel M. State-of-the Art Review: Strengthening of Reinforced Concrete Structures – Different Strengthening Techniques. Sixth International Conference on Nano-technology in construction (NTC 2014) Cairo, Egypt, Volume 6.

[2]. Jumaat MZ, Rahman MM, Alam MA. Flexural strengthening of RC continuous T beam using CFRP laminate: A review. International Journal of the Physical Sciences 2010; 5(6): 619-625

[3]. Review of strengthening techniques using externally bonded fibre reinforced polymer composites: Report 2002-005-C-01. Australia: Construction Innovation 2002; 1-48.

[4]. Aram MR, Czaderski C, Motavalli M. Debonding failure modes of flexural FRP-strengthened RC beams. Composites: Part B 2008; 39: 826–841.

[5]. Yao J, Teng JG. Plate end debonding in FRP-plated RC beams—I: Experiments. Engineering Structures 2007; 29:2457–2471.

[6]. Kalfat R, Al-Mahaidi R, Smith ST. Anchorage devices used to improve the performance of reinforced concrete beams retrofitted with FRP composites: State - of - the - Art review. Journal of Composites for Construction 2013; 17(1): 14–33.

[7]. Grelle SV, Sneed LH. Review of anchorage systems for externally bonded FRP laminates. International Journal of Concrete Structures and Materials 2013; 7(1): 17-33.

[8]. Li X, Gu X.L, Song X.B, Ouyang Y, Feng Z.L. Contribution of U shaped strips to the flexural capacity of low-strength reinforced concrete beams strengthened with carbon fibre composite sheets. Composites: Part B 2013; 45: 117-126.

[9]. ACI Committee 440. Guide for the design and construction of externally bonded FRP systems for strengthening concrete structures (ACI 440.2R-08). Farmington Hills, MI: American Concrete Institute.

[10]. Buyle-Bodin F, David E. Use of carbon fibre textile to control premature failure of reinforced concrete beams strengthened with bonded CFRP plates. Journal of Industrial Textiles 2004; 33(3): 145 –157.

[11]. Buyukozturk O, Gunes O, Karaca E. Characterization and modeling of debonding in RC beams strengthened with FRP composites. 15th ASCE Engineering Mechanics Conference, Columbia University, New York, June 2002: 1-8.

[12]. Ceroni F. Experimental performances of RC beams strengthened with FRP materials. Construction and Building Materials 2010; 24(9):1547–1559.

[13]. Pham HB, Al-Mahaidi R. Prediction models for debonding failure loads of carbon fiber reinforced polymer retrofitted reinforced concrete beams. Journal of Composites for Construction, ASCE 2006; 10(1): 48–59.

[14]. Pimanmas A, Pornpongsaroj P. Peeling behaviour of reinforced concrete beams strengthened with CFRP plates under various end restraint conditions. Magazine of Concrete Research 2004; 56(2): 73-81.

[15]. Sadrmomtazi A, Rasmi Atigh H, Sobhan J. Experimental and analytical investigation on bond performance of the interfacial debonding in flexural strengthened RC beams with CFRP sheets at tensile face. Asian Journal of Civil Engineering (BHRC) 2014; 15(3): 391-410.

[16]. Smith ST, Teng JG. Shear-bending interaction in debonding failures of FRP-plated RC beams. Advances in Structural Engineering 2003; 6(3): 183 –199.

[17]. Sobuz HR, Ahmed E, Sutan NM, Hasan NMS, Uddin MA, Uddin MJ. Bending and time-dependent responses of RC beams strengthened with bonded carbon fiber composite laminates. Construction and Building Materials 2012; 29: 597-611.

[18]. Valcuende M, Benlloch J, Parra CJ. Ductility of reinforced concrete beams with CFRP strips and fabrics. Proceedings of 6th International Symposium on Fibre-Reinforced Polymer (FRP) Reinforcement for Concrete Structures FRPRCS-6, Singapore, 8–10 July 2003: 337-346.

[19]. Valivonis J, Skuturna T. Cracking and strength of reinforced concrete structures in flexure strengthened with carbon fibre laminates. Journal of Civil Engineering and Management 2007; 13(4): 317-323.

[20]. MBrace CF 640/2600, Manufacturer specifications, BASF Chemical Company, 2013.

SECM/15/162

Embodied Energy Analysis of a Pre-cast Building System

D.M.K.W. Dissanayake[1*] and C. Jayasinghe[2]

[1]Research Assistant, University of Moratuwa, Moratuwa, Sri Lanka
[2]Professor, University of Moratuwa, Moratuwa, Sri Lanka
*E-Mail: kasurikad@gmail.com, TP: +94717600489

Abstract: The embodied energy of a building can represent up to 40% of life cycle energy use of residential buildings. Residential buildings in Sri Lanka serve as one third of the local construction sector. However, extraction materials which are extensively used in building construction in Sri Lanka are being limited by the environmental regulations and depletion of resources. Precast concrete products are generally chosen for achieving sustainability in buildings since they incorporate holistic design, efficient use of material and minimize the construction waste and site disturbance. This paper presents a comparative analysis of embodied energy of a conventional in-situ building system and a precast building system: a case study for two identical buildings constructed at the same location using the two building systems. The results of the analysis reveal that the embodied energy of the precast building system is 19% less than the conventional in-situ building system.

Keywords: Building Materials, Embodied Energy, Expanded Polystyrene, Pre-cast Building

1. Introduction

Buildings consume more than 40% of global energy and contributes about 33% of greenhouse gas emissions, both in developed and developing countries. [1] The ever increasing population and commercial needs, demands for more and more buildings, each year and it results in a large consumption in material, energy and natural resources. In European building sector, residential buildings represent about 63% of total energy consumption and 77% of total CO2 emissions. [2] In the UK, residential buildings accounts for around 30% of the total final energy use of the country and responsible for more than 25% of CO2 emission. [2] And upto 40% of the energy consumend by a residential building over its life cycle will be represented by the embodied energy.

Sri Lanka’s residential buildings represent about one third of the construction sector, in terms of fixed capital formation. [3] 92% of occupied housing units, of the country are collectively single storied or two storied, while 58% of the houses are constructed with brick walls and 33.8% are constructed with blocks, which are the major walling materials of permanent housing in Sri Lanka. [4] According to Reddy [5], bricks, cement and steel are the major contributors to the energy cost of building construction. With the depletion and environmental restrictions on natural resources like clay, sand, stones and with the increasing cost of labour in Sri Lanka, the conventional housing systems are challenged with new alternative building systems.

Precast concrete products have become a natural choice of achieving sustainability in buildings since they incorporate holistic design, efficient use of material and minimize the construction waste and site disturbance. The system which is studied under this research consists of a precast pre-stressed concrete beam, column and slab system, with wall panels constructed out of Expanded Polystyrene (EPS). The foundation of the house is generally constructed as the in-situ concrete isolated pad footings. The characteristics of those building elements in the precast system are listed down in table 1.

This research paper is based on a comparison of total embodied energy, for construction using the conventional in-situ building system and the studied precast building system of a residential building with two stories located in Kandana area.

2. Embodied Energy Analysis

Embodied energy is the energy consumed by processes associated with the total production of a building, from the acquisition of natural resources from processes including mining and manufacturing, through transport and other functions. [5] The importance of embodied energy is growing as a consequence of new regulations introduced to reduce the building consumption during the operation phase. [6]

Embodied energy analysis of a building or any product depends on several parameters. System boundary defines how much upstream or downstream processes are included in the scope of the study. Geographical location of the study is also important, because the climate conditions, material properties, transport distances and methods, and many other parameters can change depending on the location of study. Source of data, age of data completeness of data and technology of the manufacturing process can also have an impact on the analysis. Another major factor which governs the final result of an embodied energy analysis is the method of embodied energy analysis. There are three widely used methods of energy analysis, which can assess how much energy is used for a certain activity. [7]

Table 1: Characteristics of the Precast Building System

Building System	Specific Characteristics
Structure	Precast pre-stressed beams (150mm×350mm) / columns (200mm×200mm)
Foundation	In-situ isolated pad footings with precast pre-stressed tie beams
Floors	Ground floor: 50mm G20 screed and 1st floor with precast pre-stressed slab panels (thickness 65mm×1m×4m)
Walls	Both interior and exterior walls out of EPS panels (100mm×600mm×2400mm)
Windows	Timber flamed single glass windows
Doors	Timber and plastic (PVC)
Roof	Timber truss and asbestos sheets
Ceiling	Steel grid, 68% recycled content ceiling tiles (600mm×600mm)
Flooring	Ceramic Tiles

2.1 Process-based Analysis

Process-based analysis is one of the most widely used methods for the embodied energy analysis. Final production process of the building material is taken into account first, considering all possible direct energy inputs or sequestered energy of each contributing material. Then it works backwards as the energy of each contributing material or energy input needs to be ascertained. [7] It is like obtaining energy figures for each material.

Process based energy analysis has its own limitations because of the exclusion of many upstream processes as a result of truncation of system boundaries. The reason for this is the enormous efforts required to identify and quantify each small energy and product input of the complex upstream process. It is said that the magnitude of system incompleteness and error in process analysis is estimated to be as high as 50 percent and 10 percent respectively.

2.3 Input-Output Analysis

Input/output-based analysis can be considered as relatively complete, since it can account for most direct and indirect energy inputs in the process of production of building materials. The economic data of money flow among various sectors of industry are used, in the form of input/output tables which are made available by the national government, thereby transcribing economic flows into energy flows by applying average energy tariffs. The Embodied Energy is calculated by multiplying the cost of the product by the energy intensity of that product expressed in MJ or GJ/$1000 and dividing it by $1000[7]

It can capture that every dollar transaction, and hence every energy transaction, across the entire national economy. But the assumptions of homogeneity and propotionality across the economic sector, errors and uncertainty of economic data can make this analysis unreliable.

2.3 Hybrid Analysis

A hybrid analysis attempts to incorporate the most useful features of input-output analysis and process analysis by eliminating the fundermental errors. It starts with the readily available data for a process analysis. Sometimes it can go one stage more in the upstream where those energy data are usually the direct energy inputs of the final production stage and possibly the materials acquisition stages immediately upstream of that final stage. Then these values are substituted with the input-output method when it is difficult to achieve reliable and consistent information regarding complex upstream processes. [7]

Considering the availability of resources and availability of data in the Sri Lankan construction industry, process based embodied energy analysis is used in this research study.

3. Scope of study

Same location of the house with identical architectural house plans is assumed for the two building systems. *(Figure 1 & 2)* The total embodied energy analysis of the building includes energy consumed in the production process of raw material and energy needed for transportation at various stages of the production till they arrive to the construction site. Energy used in installation/assembling of products or at the construction stage is also included in the calculations since it provides a comprehensive comparison between the precast building system and the conventional building system. So, this paper will present the embodied energy of the following 3 aspects of embodied energy.

1. Energy consumption at production of building materials *(E_p)*
2. Energy in transportation of building materials *(E_t)*
3. Energy at construction stage of the building *(E_c)*

There for total embodied energy *(EE_T)* may expressed by,

$$(EE_T) = (E_p) + (E_t) + (E_c) \qquad (1)$$

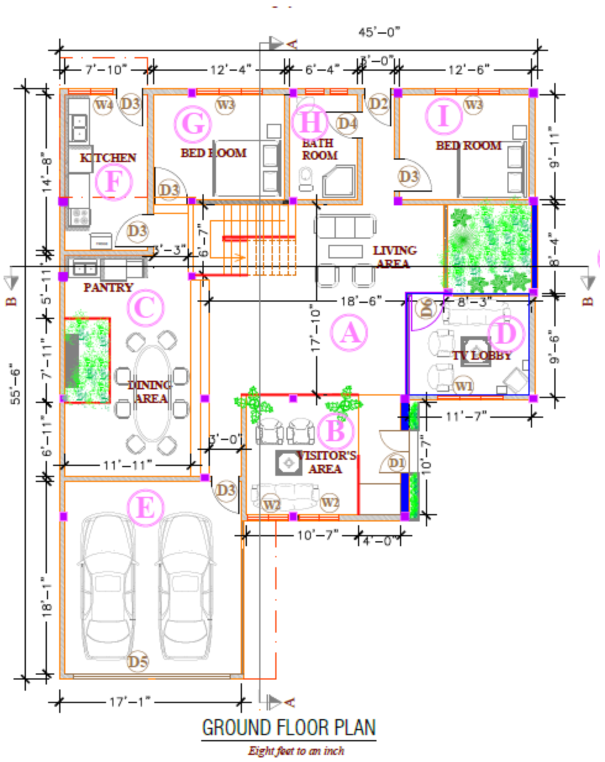

Figure 1: Ground floor plan

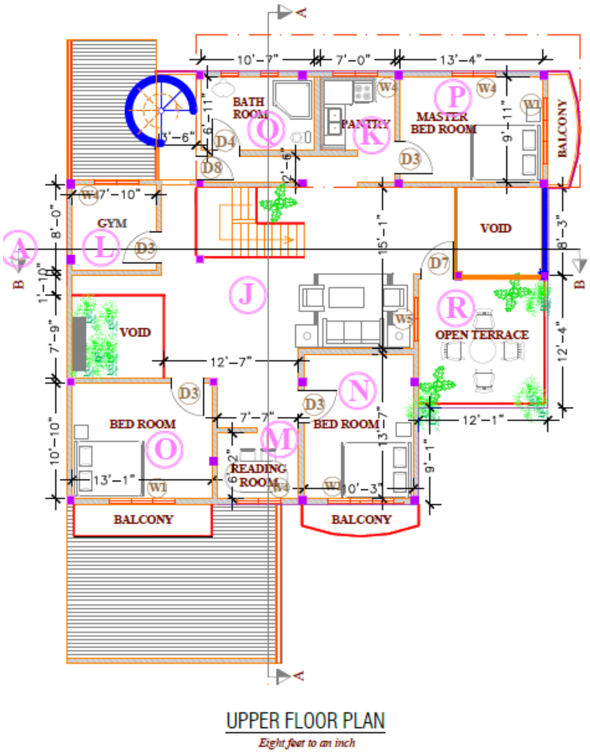

Figure 2: Upper floor plan

4. Methodology

The Bill of Quantities (BOQ) and the architectural/structural drawing prepared for the building are taken as the basis for to obtain the quantities of materials. To calculate the embodied energy of these materials, three data sources were used, namely, Sri Lankan data [8], Indian data [5] [9] [10] and Inventory of Carbon and Energy (ICE) which is prepared by University of Bath [11]. Due to unavailability of information about the manufacturing procedure and energy spent on the manufacturing of products used in plumbing and wiring, most of the embodied energy is calculated considering the particular material energy only. The embodied energy of electrical work and wiring of the house has been eliminated in the calculation because of non availability of details. Work studies and interviews with industry related people are used to calculate the energy spent in the construction stage of the building. Generally the equipment intensive activities are taken for the energy calculation since it is difficult to estimate the energy consumed as physical labour by humans at labour intensive activities. Fuel usage data of different vehicles used in plants and sites as well as general transport equipment were collected and used to estimate the fuel consumption in transportation and then those data was converted to energy.

5. Energy consumption at production of building materials (Ep)

The bill of quantities of the conventional in-situ house was used to obtain the amount of the building materials, required for each building component. Since the same house plan is used to estimate the quantity of embodied energy of the precast building system, several elements of bill of quantities remain same such as excavation and earth work, ceiling, roof, floor finishes, waterproofing, etc. Material quantities of other structural elements such as beams, columns, slabs and wall panel are estimated individually and embodied energy of each building element is calculated separately. Number of each elements required to construct the house is obtained according to the architectural drawings of the house. The embodied energy of some of the materials are given in the table 2

Table 2: Main construction materials and their energy density

Materials	Energy Intensities (MJ/kg)	Source
Aggregate	0.11	SL
River Sand	0.08	SL
Aluminium	155	ICE
Cement	4.9	SL [12]
Cement Motar	2.55	SL
Ceramic tiles	12	ICE
Sanitary products	20	ICE
Bricks	2.3	SL [8]
Wood	10.8	IND [1]
Plywood	15	ICE
Steel	35.1	IND [1]
Stainless steel	56.7	ICE
Brass	62	ICE
Asbestos	7.4	ICE
PVC	105	IND [1]
Glass	15	ICE
Paints	70	ICE
Putty	5.3	ICE
Primer	144	IND [1]
Lime	5.63	IND [5]
EPS	36	EU [13]

SL: Sri Lanka, IND: India, ICE: Inventory of Carbon & Energy V1.6a

The embodied energy of aggregates was estimated from a result of work-study related to production of aggregates in a crusher plant. Diesel fuel usage and electricity usage of the crusher plant was collected for a 6 month period and those data were converted to energy. For a one litre of diesel 45.71 MJ was considered and 1kWh of electricity was taken as 3.6MJ, for this study.

The precast element construction yard of this particular precast building system is located in Ekala area. So, the transportation energy of different materials in the precast yard has to be considered in calculating the embodied energy of final products. Precast concrete elements are manufactured with Grade 40 concrete and in current practice ready-mix concrete is used where the supplier's plant is located in Kandana area, which is within 50km from the precast yard. Building materials which are used predominantly are given here with the transportation distances to the construction yard/ building site in the table 3. However the energy usage to manufacture expanded polystyrene (eps) wall panels is not based on any work-study but it was calculated based on literature. [13] The manufacturer of these panels in Sri Lanka is yet to start the production of panels and with that more reliable value for the analysis can be obtained.

Table 3: Transportation distances of several construction materials

Material	Transportation Distance (km)		
	to construction site	to redimix plant	to precast yard
Cement	200	200	180
Sand	100	100	100
Aggregate	50	50	50
Steel	30	-	50
EPS	-	-	30
Fly ash	-	200	200
Bricks	40	-	-
Plywood	130	-	-
Wood	100	-	-

6. Energy in transportation of building materials (Et)

As described above transportation of building materials may happen in different stages of manufacturing of products. At the production stage, transportation, energy usage at raw material extraction and in-plant transportation are included. The fuel consumption data and the transportation distances or waiting/idle times at different activities with those machinery related to this building construction were studied. In table 4, energy consumption of several vehicles which are heavily used in construction site are given.

However, to estimate the energy at transportation the amount of material/equipment transported by the vehicle, and transportation distance alone will not be enough, since the vehicle is not loaded fully at each time. So, enough work-study was done to identify the details of the payload per trip, at different activity happen in constructing this building. For example, precast slab panels are transported in a 25 ton truck with only 10 slab panels per trip. The weight of the payload is approximately 6 tons, but fuel consumption is almost the same as 25 ton load.

Table 4: Energy consumption of some of the vehicles used in transportation [7]

Vehicle	Energy Consumption	Unit
25 Ton truck (while operating)	0.76	MJ/(t*km)
25 Ton truck (idle)	15.21	MJ/h
7.5 Ton truck	2.08	MJ/(t*km)
750kg mini truck	3.17	MJ/(t*km)
7 m^3 truck mixture	66.53	MJ/km
Container ship [14]	0.054	MJ/(t*km)

7. Energy at construction stage of the building (Ec)

For a small scale construction like this, the energy usage at construction stage is minimized, since most of the work is labour intensive and machinery usage is minimized. At in-situ building construction, a concrete mixture is used and several electrical machinery is in used like grinders, bar-cutters, arc-welding plant, and electrical drill. So, the quantification of energy for different activities were done along with the data from the work-studies, considering the time duration of each machinery are in use and its wattage or fuel consumption.

8. Results and discussion

Using the process based embodied energy analysis of the conventional in-situ building system, it was found that 1231.34 GJ of energy is used for the completion of building construction. Table 5 shows the final results of the analysis at different stages/activities of the construction process. It is 3.8 GJ/m^2 for residential house construction. Previous studies conducted in several other countries have found embodied energy for a residential house is within the range of $3.6GJ/m^2$ -$6.8GJ/m^2$. [7] So the value obtained from this study is a reasonable value in a country like Sri Lanka, since human labour is extensively used in house construction which is not accounted for calculations. Since the whole study was conducted as a process based embodied energy analysis, it is invertible of having certain errors in the calculations. These calculations can be fine tuned if the analysis is conducted as a hybrid analysis, where data from the process based analysis is substituted with the input-output method, since it is difficult to achieve reliable and consistent information regarding complex upstream processes. [15]

Table 5: Embodied energy calculation for the conventional in-situ building

On site construction activity	Embodied Energy (GJ)
Excavation and earthwork	2.80
Total in-situ concrete	138.13
Total formwork items	89.20
Total Reinforcement	86.25
Masonry Works	231.13
Floor finishes with ceramic tiles	78.41
Wall finishes (plastering and painting)	280.36
Ceiling construction	128.80
Metal Work	5.63
Roof construction	39.48
Windows/ Doors	49.65
Plumbing & sanitary work	101.49
Total embodied energy of the house	1231.34

Calculated embodied energy values for different precast elements are given in the table 6. The embodied energy analysis for the precast building system shows that the total embodied energy of the house after construction is 995.1 GJ and it is about 3.06 GJ/m^2 of energy for the house. (Table 7) It is a reduction of 19% of embodied energy, compared to the conventional building system.

Table 6: Embodied energy results for precast elements in the alternative building system

Building element	EE per item	Unit	No of units	Weight	EE (GJ)
columns	2166	MJ	41	11808	89.19
beams	543.25	MJ/m	92	11592	50.36
slabs	2480	MJ	48	29491.2	120.56
EPS panels	420.8333	MJ/m^2	433	38104	182.98
Screed	1828	MJ/m^3	5.85	14040	10.88
Total embodied energy for precast elements					453.97

Table 7: Embodied energy calculation for the precast building system

On site construction activity	Embodied Energy (GJ)
Excavation and earthwork	2.80
Total in-situ concrete (10% from in-situ)	13.81

Total formwork items	0.50
Total Reinforcement (5% from in-situ)	4.31
Masonry Works	0.10
Floor finishes with ceramic tiles	78.41
Wall Finishes (painting 50% less)	116.14
Precast concrete elements	453.97
Ceiling construction	128.80
Metal Work	5.63
Roof construction	39.48
Windows/ Doors	49.65
Plumbing & sanitary work	101.49
Total embodied energy of the house	995.10

9. Conclusions

Residential buildings represent a reasonable proportion of the construction sector. Resource depletion and environmental restrictions provide strong case for new alternative building systems over conventional buildings. This paper presents a comparative analysis of embodied energy of a conventional in-situ buililding system and a precast building system using process-based analysis has been used for the study. Energy consumption at production, transportation and construction stages were considered in the calculations. The results showed that total embodied energy of the precast building system (3.06 GJ/m^2) is 19% less than the conventional building (3.8 GJ/m^2). So it can be concluded that the studied precast building system is a more sustainable alternative to the residential house construction than a conventional building system.

Further studies on the production process of EPS wall panels and construction stage the energy usage of the building will help to improve the accuracy of the results. The ongoing research is seeking to optimize the section sizes and strength properties of EPS panels, which will help to further reduce the embodied energy as well as the cost of the precast building system.

Acknowledgements

The authors would like to express their gratitude to the Mr. Neranjan Fernando, Mr. J.R.M. Bogahawatta and Mr. K.S.M.R. Priyadarshana for the valuable support given at data collection.

References

[1] P. Devi L and S. Palanippan, “A case study on life cycle energy use of residential building in South India,” *Energy and Buildings,* no. 80, pp. 247-259, 2014.

[2] D. Li, H. X. Chen, C. Eddie, J. Zhang and Q. Li, “A method for estimating the lide-cycle carbon efficiency of a residential building,” *Building and environment,* vol. 59, no. 2013, pp. 448-455, 2013.

[3] CBSL, “Annual Report,” Central Bank of Sri Lanka, Colombo, 2014.

[4] “Census of Population and Housing 2012: Key Findings,” Department of Census and Statistics, Sri Lanka, Colombo, 2012.

[5] B. V. Reddy and K. Jagadish, “Embodied energy of common and alternative building materials and technologies,” *Energy and Buildings,* no. 35, pp. 129-137, 2001.

[6] U. S. B. &. C. Initiative, “Buildings and Climate Change: Summary for Design Makers,” UNEP, Paris, France, 2009.

[7] M. K. Dixit, J. L. Fernández-Solís, S. Lavy and C. H. Culp, “Identification of parameters for embodied energy measurement: A literature review,” *Energy and Buildings,* no. 42, p. 1238–1247, 2010.

[8] C. Jayasinghe, “Embodied energy of alternative building materials and their impact on life cycle cost parameters”.

[9] K. Jagadish and B. V. Reddy, “Embodied energy of common and alternative building materials and technologies,” *Energy and Buildings,* no. 35, pp. 129-137, 2003.

[10] W. K. Biswas, “Carbon footprint and embodied energy consumption assessment,” *International Journal of Sustainable Built Environment,* no. 3, pp. 179-186, 2014.

[11] P. G. Hammond and C. Jones, “Inventory of Carbon & Energy (ICE),” University of Bath, 2008.

[12] D. D. A. Namal, “Analysis of energy embodied in cement produced in Sri Lanka,” Moratuwa, 2003.

[13] “Reducing Climate Change with EPS insulation,” European Manufacturers of EPS.

[14] D. J. MacKay, “Sustainable Energy – without the hot air,” 29 08 2015. [Online]. Available: http://www.withouthotair.com/c15/page_95.shtml. [Accessed 29 10 2015].

[15] M. Lenzen, “Errors in conventional and input output base life cycle inventories,” *Journal of*

Industrial Ecology, vol. 4, no. 4, pp. 128-148, 2006.

[16] T. J. Wen, H. C. Siong and Z. Noor, "Assessment of embodied energy and global warming potential ofbuilding construction using life cycle analysis approach: Case studiesof residential buildings in Iskandar Malaysia," *Energy and Buildings*, no. 93, pp. 295-302, 2015.

[17] C. Scheuer, G. A. Keoleian and P. Reppe, "Life cycle energy and environmental performance of a new university building: modeling challenges and design implications," *Energy and Buildings*, no. 35, pp. 1049-1064, 2003.

SECM/15/165

Rheological Behaviour of Cement Paste with Fly Ash in the Formulation of Self-Compacting Concrete (SCC)

A.K. Manawadu[1]*, W.M.K.B. Wijesinghe[1], H. Abeyruwan[1]

[1]Department of Civil Engineering, University of Peradeniya, Sri Lanka

*E-Mail: ayumi2391@gmail.com, TP: +94713345831

Abstract: The use of Self-Compacting Concrete (SCC) is growing rapidly due to its ability to compact solely under its own weight. But, due to the unavailability of a universally approved mix design procedure, the industry uses trial and error methods to proportion mixes leading to high material and time wastage.

Unlike traditional concrete, SCC possesses a very high workability. Thus, it is worthwhile to be evaluated through a rheological point of view. But, to facilitate high workability, SCC requires a sufficient amount of paste to fill the voids and confine its aggregates. However, if the binder or the cement content is raised to achieve this purpose, it will result in many negative structural and non-structural impacts. It will not only increase the cost, but will also lead to cracks due to the increased heat of hydration. It will also harm the environment through excessive use of resources, while contributing to the emission of large amounts of carbon dioxide, a greenhouse gas. Therefore, Supplementary Cementitious Material (SCM) such as fly ash could be identified as a better supplement to overcome these problems.

This study focuses on determining the yield shear stress and plastic viscosity (Bingham constants) of paste having varying constituent proportions, by using coaxial type rheometer. Both individual and combined effect of water/cement (w/c) ratio and fly ash content on the rheological behaviour is observed and analysed to determine the optimum SCM composition for a mix for two common w/c ratios. The results for optimum material quantities could be used as a guide for initial trial mixes, minimizing the time and material wastage.

Keywords: Rheology, Self-Compacting Concrete, Bingham model, coaxial concentric rheometer, Fly Ash

1. Introduction

Self-Compacting Concrete (SCC) was first developed in Japan in 1988 to overcome inefficiencies in the traditional concreting procedure. Insufficient compaction leads to increase the presence of air voids and a reduction in both strength and durability, whereas, too much compaction leads to segregation, creating non-homogeneous products. Therefore, SCC has been identified as a valuable substitute in structures where complex shapes and congested reinforcements are involved.

1.1 Criteria for Self-Compactability

For a concrete to be categorized as self-compacting, the following criteria should be fulfilled [1].

Filling ability: Ability to flow freely, both in the horizontal and the vertical directions and fill the formwork completely under its own weight without any other form of external compactive effort.

Passing ability: Should not cause any type of blockage when passing through a narrow gap

Stability: Should not segregate during mixing, placement and after casting. Otherwise, it may lead to a non-homogeneous mix.

The above criteria are mainly associated with the flowability of SCC. Therefore, SCC is much suitable to be evaluated in a rheological perspective. Bingham model, which depicts a linear relationship between shear stress and shearing rate, is useful in this regard.

1.2 Rheology

Rheology is the science dealing with flow and deformability of material. Even though, slump flow is the most common method to assess SCC, the flow values may differ with differences in the formwork geometry and reinforcement. Therefore, studies based on rheology are much more important to evaluate the functionality of SCC [2].

1.3 Bingham model

There are many models, such as, Bingham model, Herschel Bulkley model, and modified Bingham model developed to characterize the rheological properties of thick suspensions. The latter two are nonlinear models, whereas the former is the simplest, which depicts a linear relationship between shear stress and shearing rate. However, there are some evidences where the yield shear stress has given very small negative values probably because, SCC has a yield shear stress which is closer to zero [1],[3].

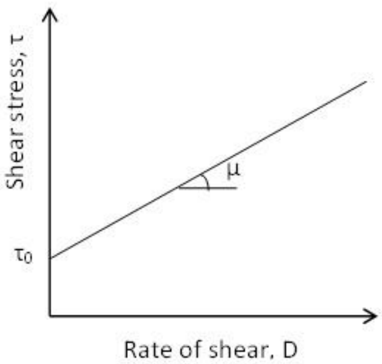

Figure 1: Bingham model

Figure 1 elaborates the Bingham model, which gives the simplest relationship of all. Rheological properties of a paste could be simply defined using the Bingham constants; Yield shear stress and Plastic viscosity, which are defined as follows:

- Yield shear stress: The critical shear stress at which a thick suspension (e.g., concrete) initiates its flow (different to Newtonian fluids). It is given by the intercept of the line (τ_0)

- Plastic Viscosity: Rate of increase of the resistance to flow with the increase in shearing rate, once the flow has initiated. It is represented by the gradient of the line (μ)

To satisfy the filling ability criterion, it is necessary to incorporate a high capacity of deformation. Thus, a low yield shear stress is required. To ensure a uniform suspension without segregation of aggregates and mortar, the SCC must have a moderate viscosity. Therefore, it is necessary for a concrete to have a low yield shear stress and a moderate plastic viscosity, to be categorized as a self-compacting concrete. Nevertheless, there are interdependencies between these two parameters. For example, increasing the water content to reduce the yield stress would also reduce the plastic viscosity, and it may lead to segregation of particles. If the cement content is kept constant this would result in a decrease of strength as well. Therefore, the use of high range water reducing admixtures (HRWRA)/ superplasticizers are necessary to support high water reduction without compromising the workability. However, it should be noted that the effect of superplasticizer diminishes with time [1]. Performance of superplasticizer mainly depends on the inherent properties of the product and will not be discussed in this paper. Nevertheless, it is necessary to consider its effect as well in the formation of SCC.

1.4 Paste and the rheology

The paste volume must be sufficient to fill the voids and to create an enveloping layer around aggregates to lubricate the relative movement between particles [4]. This could be accompanied by increasing the cement content, which may result in high costs. Furthermore, it will contribute to release large amounts of heat of hydration, resulting in cracks, which raises concern on serviceability and durability of the structure. In addition, it contributes to environmental issues such as greenhouse effect, with the release of carbon dioxide to the atmosphere. To overcome such problems, substitutes should be identified, which could replace the cement partially. Fly ash is one of such material which will help to reduce the above mentioned problems.

1.5 Objectives and scope

Despite the wide use of SCC in the construction industry, there is no universally accepted mix design methodology to formulate concrete with target self-compactable properties. Therefore, SCC is formed based on trial and error methods, leading to a large amount of material and time wastage. This could be avoided if the characteristics of the self-compacting concrete are to be adjusted at the earliest possible point in the mixing process. Therefore, linking the rheological properties of the paste to that of the final SCC mix is of great importance. To do so, the behaviour of the mix with the addition of each material should be studied thoroughly.

This study focuses on identifying the rheological behaviour of paste when fly ash is added to paste comprising cement and water. The relationships are determined in terms of Bingham constants, yield shear stress and plastic viscosity. The study is based on two common w/c ratios that are used in the industry, and the experiment is carried out using a coaxial type rheometer. However, testing the time-dependent rheological properties and the hardened concrete properties of the SCC are left outside the scope of this study.

2. Literature Review

There has been extensive research on the formation of self-compacting concrete. But, only a handful of research concentrates on the rheological characteristics.

SCC can be treated as a two-phase material, composed of coarse aggregate and suspending mortar. Similarly, mortar is a two phase material composed of fine aggregate and paste. Therefore, the workability of the mortar must be dependent upon the physical properties and the quantity of fine aggregates, as well as the rheological characteristics of paste [5].

2.1 Excess thickness theory

Experimental studies have shown that the fluid mortar volume must be sufficient to fill voids between coarse aggregate particles and also to create an enveloping layer to lubricate the relative movement of coarse aggregates [3].This layer is known as the mortar film and its thickness is half of the spacing between aggregate particles. Similarly, excess paste thickness is referred to as the thickness of the film layer which is in excess of the paste, after the paste fills the void spaces in between fine aggregate particles [4].

Paste film thickness relates the combined effect of the content and the physical properties of the fine aggregate. In a similar manner, mortar film thickness account for the content and the physical properties of the coarse aggregate. When the mortar film thickness is kept constant, the rheology of SCC can be determined by the rheological characteristics of the mortar. Similarly, when the paste film thickness is kept constant there will be such relationship between the paste and the mortar as well. Thus, when both paste film thickness and mortar film thickness are kept constant, the rheology of SCC could be directly related to the rheology of paste. Experimental studies have been carried out to directly relate the paste to SCC by means of Bingham constants. Thus, SCC mix could be altered at the earliest possible point to avoid unnecessary wastage of material and time, using a simple mini slump cone test. However, this concept has been evaluated only by varying the superplasticizer dosage and the water/cement ratio (w/c). It has also been assumed that the mortar film thickness around gravel particles are same for all gravel sizes, particles are spherical and the equivalent diameter can be obtained through sieve analysis. However, future research has been proposed on the investigation of mortar film thickness and the paste film thickness [5].

2.3 w/p ratio and SCC

Water-cement ratio is the most significant single parameter that governs the strength of concrete while, w/p (water/powder) ratio governs the workability of the concrete. The term "powder" is defined as a material of particle size less than 0.125 mm [6]. This includes cement, supplementary cementitious material, and even non-cementitious material falling in to that size. In traditional concrete, the w/c ratio is altered and through that, the required strength is achieved. In contrast, design of SCC concentrate more on the workability and thus, the governing factor would be w/p ratio, and the paste content. Extensive research has been carried out to link the variation of w/p to SCC properties (i.e. by varying water, cement, filler and the superplasticizer dosage). One method of carrying out mix design for SCC has been identified as to keep the fine and coarse aggregate contents constant and to vary the powder characteristics to achieve self-compatibility [7]. However, neither single method nor combination of methods has been approved universally as a mix design method for SCC.

2.4 Supplementary Cementitious material (SCM)

As mentioned previously, in order to achieve adequate self-compatible properties, it is always necessary to achieve a moderate viscosity in the SCC mix. So, it is necessary to obtain a low w/p compared to the traditional concrete, and in order to do this, the finer material content has to be increased [1],[8],[9].This helps to enhance the cohesion and ultimately result in good segregation resistance between the binder phase and the aggregate particles. However, if the binder or the cement content is increased it will increase the cost, increase the heat of hydration and lead to cracks, while contributing to the emission of a large amount of carbon dioxide, a greenhouse gas, to the environment. Therefore, SCM could be identified as a better replacement to overcome these problems.

There has been investigations on how the rheological properties of SCC varies with the addition of various SCMs such as; Silica Fume (SF), Metakaolin (MK), Ground Granulated Blast furnace slag (GGBS), Siliceous Fly ash (class F fly ash - FAF) and Calcareous fly ash (class C fly ash -FAC) [9]. The summary of the outcomes are listed below.

- SF and MK : reduce workability, plastic viscosity and permeability of SCC; gives a high early strength; increase HRWRA demand & yield shear stress.
- GGBS: improve workability; reduce early strength, HRWRA demand and plastic viscosity
- FAC: higher HRWRA demand than the FAF, increase plastic viscosity
- FAF: reduce HRWRA demand, reduce (maintain somewhat constant) plastic viscosity
- Water/binder ratio: reduce HRWRA demand, reduce plastic viscosity
- Viscosity Modifying Admixture (VMA): enhance plastic viscosity

Among these SCMs, class F fly ash is the most commonly found material which could be used to enhance the properties of the SCC. Class F fly ash meets pozzolanic properties while class C fly ash meets latent hydraulic properties (cementitious properties), in addition to weaker pozzolanic properties. Both Fly ash types may contain carbon in significant amounts, which in turn reduce the strength of concrete and reduce the efficiency of air entrainment. However, out of these two categories class F fly ash has a spherical morphology and a smooth surface texture of grains, leading to a higher ball bearing effect to reduce inter-particle friction. Therefore, it reduces the plastic viscosity and enhances the workability. Other than that, low porosity of particles and a lower fineness has contributed to the low HRWRA demand. In contrast, class C fly ash contains irregular grain shapes reducing some of these benefits [9].

2.5 Typical ranges of proportions for SCC to achieve self-compatibility

Following guidelines are stated in literature as the most appropriate proportions in the formation of SCC [6].

- Water/ Powder ratio by volume : 0.8-1.1
- Total powder content : 160 - 240 L/m^3 (400-600 kg/m^3)
- Water content, typically less than 200 L/m^3

2.6 Testing

Some of the most common tests used to evaluate the characteristics of SCC are: slump flow test, V-funnel test, J-ring test, L-box test, U-box test and sieve segregation test. In the laboratory, the most commonly used type of tests applied on cement paste are the mini slump cone test, Marsh cone test, and the coaxial rheometer test. Out of these three, the most convenient and simple test is the mini slump cone test which is an indirect test used to estimate the yield shear stress and plastic viscosity of flowable paste. However, the geometry of the cone largely affects the test results [10]. Equations have been identified to link the plastic viscosity and yield shear stress to the slump flow and flow time.

The other common apparatus used is the coaxial type rheometer, which is a direct method of measurement. However, the results depend highly on the accuracy of measurement and the geometry of the cylinder. There, are several equations obtained to relate the Bingham constants with the rheometer readings (torque and rotational velocity). There have also been attempts to relate the mini slump cone test results with the rheometer test results [10].

3. Methodology

3.1 Material

Material required for the experiment are defined according to the ASTM standard as in Table1.

Table 1: Properties of ingredients

Material	Description	
Cement	Type	ASTM Type 1 OPC
	Specific gravity	3.15
	Blaine fineness	326m^2/kg
Fly ash	Type	ASTM C618 Class F fly ash
	Specific Gravity	2.15
	Blaine fineness	438m^2/kg
	Particle size	Passing 75 µm sieve

3.2 Procedure

The results of the experimental program was analysed using the Bingham model. Each specimen was tested with coaxial type rheometer as stated in ASTM guidelines [11]. The equations to convert experimental data to yield shear stress and plastic viscosity are stated in a later section.

The effect of fly ash on cement paste mix was observed, for w/c ratios of 0.50 and 0.55. The fly ash content by mass of cement was varied as 0%, 6%, 12%, 18%, 24%, 30%, and 36% for each w/c ratio. It was expected that only a certain amount of fly ash to contribute to the hydration reaction. The rest was expected to stay in the matrix as an inert compound contributing to the powder, enhancing the workability.

3.3 Apparatus, tests and mixing procedures

The Bingham constants were evaluated using a coaxial type rheometer as indicated in Figure 2 (a). This is a direct test method of obtaining yield shear stress and plastic viscosity. The test was performed according to the guidelines given in ASTM C1749-12: "Standard Guide for the measurement of rheological properties of a hydraulic cementitious paste using a rotational rheometer". For the apparatus to be categorized as a narrow gap concentric cylinder, it had to satisfy the following requirement as per the guideline, where R_1 and $R_2$is the radius (m) of the inner stationary cylinder and the outer rotating cylinder respectively.

$$\frac{R_1}{R_2} \geq 0.92$$

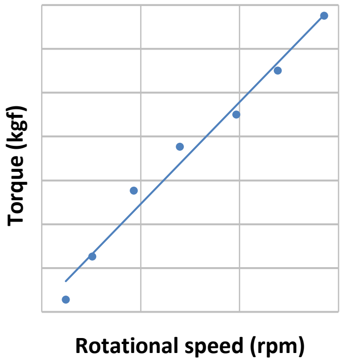

(a) (b)

Figure 2 : (a) Concentric cylindrical rheometer , (b) Rheometer observations and trend line

The available rheometer satisfied the above requirement and was categorized as a narrow gap concentric cylinder. The following equations were used in the determination of shear stress and shearing rate from the torque and rotational speed respectively.

$$\text{Shear stress} = \frac{T}{2\Omega R_1^2 L}$$

$$\text{Shearing rate} = \frac{\Omega i.\ R_2}{R_2 - R_1}$$

Ω_i - rotational speed of the outrer cylinder (r/s)
T - torque (N·m)
L - cylinder length (m)

In the coaxial type cylindrical rheometer (Figure 2(a)), the outer cylinder is rotated, while the inner cylinder is kept stationary. Thus, to prevent slip through the development of a liquid layer on the wall of the rotating cylinder, the cylinder surfaces are made rough.

The initial torque reading had to be obtained 20s after continuous rotation at the lowest speed. All the readings were first taken in the ascending order and then, in the descending order. The torque and the rotation was recorded at each stage and it was converted to shear stress and shearing rate values as stated in the ASTM standard specification. The expected variation of torque with the rotational velocity is indicated in the Figure 2(b).

In the presence of only cement, water and fly ash, the approach to mixing is different than the concrete, due to the absence of aggregates. The ASTM C1738/C1738M-14 [12], provides the guidelines to carry out the tests. As stated in the standard, the method has been useful in testing the rheology of the paste because it gives similar results to those obtained in a concrete mix where the aggregates have been removed. Mixing of paste does not falls under ASTM C305,since, it should not be thoroughly mixed due to the absence of sand. This practice is known as high shear mixing, because, it imparts a significantly higher amount of shear than in ASTM C305 [13].

4. Results and Discussion

4.1 Influence of fly ash content on yield shear stress of paste

The fly ash content of the paste was varied from 0% to 36% by mass of cement at w/c 0.5 and w/c 0.55. The only constituents in the paste while carrying out this experiment was cement, water and fly ash. The extracted results for the yield shear stress of those samples are shown in the Table 2.

Figure 3 is the graphical representation of variation of yield shear stress with the fly ash content by the mass of cement. As shown, the yield shear stress of the paste has increased, approximately following a polynomial function with the addition of fly ash. It further shows a significant change after 18% of fly ash by mass of cement. Even though, fly ash could be used to reduce the heat of hydration as a partial substitute for cement, adding excessive amounts would increase the yield shear stress creating a high resistance to initiate flow. Thus, it is better to keep the maximum substitution level of fly ash for cement, below 18% as indicated.

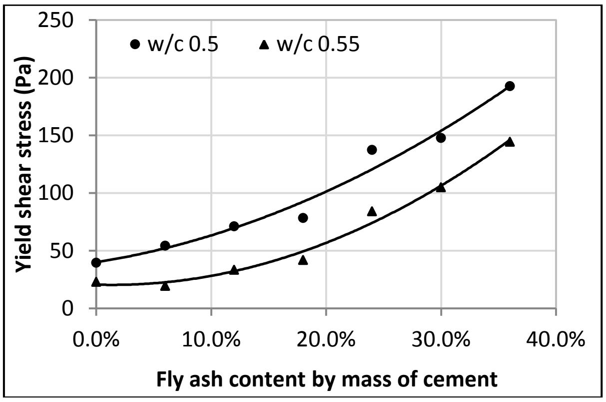

Figure 3: Variation of yield shear stress with fly ash content from (0 to 36%)

It also shows a reduction in yield shear stress with the addition of water (higher w/c ratio). However, near zero fly ash content, the two trend lines converges to closer values. The increase of yield shear stress with the addition of fly ash is more significant at w/c 0.50 compared to w/c 0.55. Table 3 indicates results in detail. The two equations given by the two polynomial trend lines are as indicated in Table 4.

Table 3: Yield shear stress result for different fly ash contents (*FA : Fly Ash)

Sample	w/c	Fly ash	Abs vol of *FA/ total vol	Yield shear stress (Pa)
LFA(0)	0.50	0	2.00	40
LFA(0.06)	0.50	0.06	1.45	54
LFA(0.12)	0.50	0.12	1.34	71
LFA(0.18)	0.50	0.18	1.25	78
LFA(0.24)	0.50	0.24	1.17	137
LFA(0.30)	0.50	0.30	1.09	148
LFA(0.36)	0.50	0.36	1.03	193
HFA(0)	0.55	0	1.82	23
HFA(0.06)	0.55	0.06	1.59	19
HFA(0.12)	0.55	0.12	1.47	33
HFA(0.18)	0.55	0.18	1.37	42
HFA(0.24)	0.55	0.24	1.28	85
HFA(0.30)	0.55	0.30	1.20	105
HFA(0.36)	0.55	0.36	1.13	144

Table 4: Functions for yield shear stress variation with fly ash by mass of cement (FA)

w/c	Yield shear stress (τ)	R^2
0.50	$734.5(FA)^2 + 159.8(FA) + 39.86$	0.972
0.55	$1047.(FA)^2 - 28.12(FA) + 20.46$	0.986

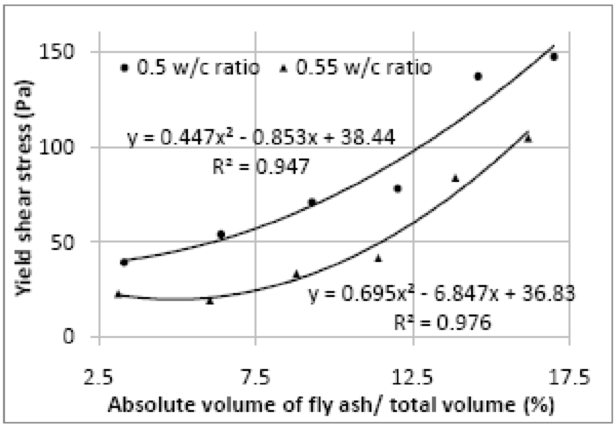

Figure 4: Variation of yield shear stress with the ratio between absolute volume of particles to total volume

The variation of the yield shear stress with the absolute volume of fly ash as percentage of the total volume of paste is indicated in Figure 4. Here, the absolute volume is the mass divided by specific gravity of each material. The total volume is the addition of absolute volumes of water, cement and fly ash. After 12% of absolute fly ash volume with respect to the total volume, the yield shear stress of the mix has increased dramatically.

4.2 Influence of fly ash on plastic viscosity of paste

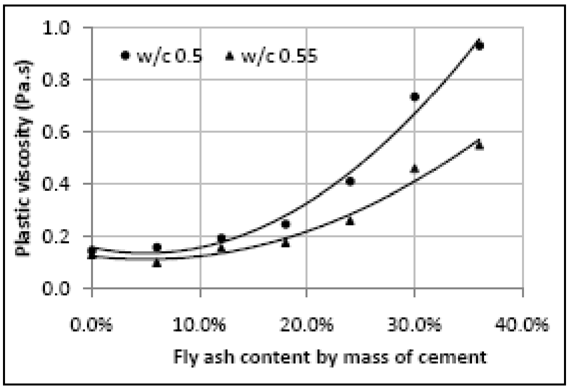

Figure 5: Variation of plastic viscosity with fly ash content from (0 to 36%)

The details of the variation of plastic viscosity with the fly ash content is given in the Table 5. Figure 5 indicates that in general, the plastic viscosity increase with the fly ash content for the two different w/c ratios. However, the polynomial functions vary and the lower w/c ratio (0.5 w/c) shows a higher plastic viscosity value compared to the one with the higher w/c ratio as expected. Nevertheless, in both cases, the rate of variation has differed after 18% fly ash by mass of cement. After this point there is an increase in the rate of change of plastic viscosity. More detailed results are shown in the Table 5. The functions of the two trend lines are given in the Table 6, which indicates a quadratic relationship between the two parameters.

Table 5: Plastic viscosity result for different fly ash contents (*FA : Fly Ash)

Sample	w/c	Fly Ash	Abs vol of *FA/ total vol	Plastic viscosity (Pa.s)
LFA(0)	0.50	0	2.00	0.147
LFA(0.06)	0.50	0.06	1.45	0.160
LFA(0.12)	0.50	0.12	1.34	0.195
LFA(0.18)	0.50	0.18	1.25	0.249
LFA(0.24)	0.50	0.24	1.17	0.411
LFA(0.30)	0.50	0.30	1.09	0.735
LFA(0.36)	0.50	0.36	1.03	0.931
HFA(0)	0.55	0	1.82	0.132
HFA(0.06)	0.55	0.06	1.59	0.101
HFA(0.12)	0.55	0.12	1.47	0.157
HFA(0.18)	0.55	0.18	1.37	0.177
HFA(0.24)	0.55	0.24	1.28	0.262
HFA(0.30)	0.55	0.30	1.20	0.460
HFA(0.36)	0.55	0.36	1.13	0.549

Table 6 : Functions for plastic viscosity variation with the fly ash content for different w/c ratios

w/c	Plastic viscosity	R^2
0.50	8.520(FA)2 - 0.855(FA) + 0.159	0.986
0.55	4.762(FA)2 - 0.478(FA) + 0.125	0.976

For convenience, the results have been presented as the absolute volume of fly ash as a percentage of total volume of the paste, as indicated in Figure 6. A similar, trend exist here as well, where there is a significant variation in the rate of change of plastic viscosity after 12% of absolute fly ash volume with respect to the total volume of the mix.

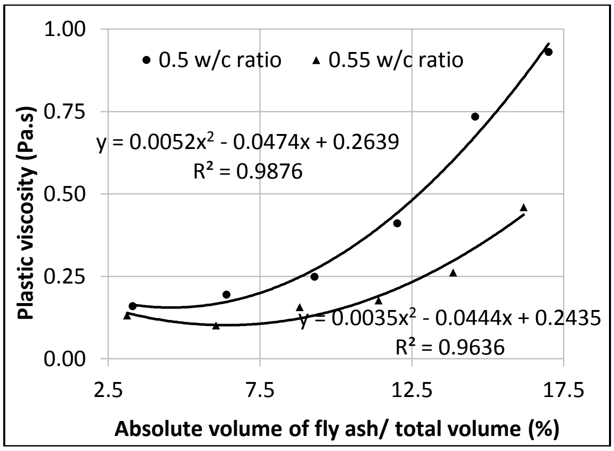

Figure 6: Variation of yield shear stress with the ratio between absolute volume of particles to total volume of paste

4. Conclusions and Recommendations

With the addition of fly ash to a paste the yield shear stress and the plastic viscosity of the mix increases according to a polynomial function. Both parameters shows significant rises in their values after 18% of fly ash by mass of cement. Even though fly ash is a good SCM which partially substitute cement, adding excessive amounts would increase both yield shear stress and plastic viscosity creating a high resistance to flow. The diminished self-compactibility will compromise the benefits from reduction of cement. Thus, 18% can be used as the optimum level of fly ash to proportion initial trial mixes.

If the optimum value is to be represented as a ratio between absolute fly ash volume to total volume, it would fall around 12%. This representation is more convenient in terms of proportioning.

Nevertheless, the hardened properties of the concrete, has not been linked to the rheology of the fresh mix within the scope of this publication.

Acknowledgement

Support from the following parties is greatly appreciated.

- Non-academic staff of the Materials Laboratory for their technical support.
- Holcim Lanka Ltd. and Tokyo fund for the financial and material support provided.

References

[1]. Feys, Verhoeven, D., and Schutter, R., Evaluation Of Time Independent Rheological Models Applicable to Fresh Self-Compacting Concrete, Vol. 17, Issue 5, 2007

[2]. Barnes, H. A., Hutton, J. F., and Walters, K. F. R. S., What is rheology; An Introduction to rheology, Amsterdam, Netherlands, Elsevier Science Publishers, 1993

[3]. Bui, V. K., Akkaya, Y., and Shah, S. P., Rheological Model for Self-Consolidating Concrete, ACI Material Journal, pp. 549-559, 2002

[4]. Ganaw, A., and Ashour, A., Rheological Properties Of Mortars Prepared with Different Sands, ACI Material Journal, Vol. 5, pp. 561-568, 2014

[5] Wu, Q., and An, X., Development of mix design method for SCC based on the

Rheological characteristics of paste, Construction and Building Material, Vol. 53, pp. 642-651, 2014

[6] http://www.efnarc.org, visited ,19th March 2015
Standard EFNARC 2002, Specification and Guidelines for Self-Compacting Concrete

[7] Felekoglu, B., Turkel, S., and Baradan, B., Effect of Water/cement ratio on the fresh and hardened properties of self-compacting concrete, Building and Environment, Vol. 42, pp. 1795-1802, 2006

[8] Okamura, H., and Ouchi, M., Self-Compacting Concrete, Journal of Advanced Concrete Technology, Vol. 1, pp. 5-15, 2003

[9] Ahari, R. S., Erdem, T. K., and Ramyar, K., Effect of various supplementary cementitious materials on rheological properties of self-consolidating concrete, Construction and Building Materials, Vol. 75, pp. 89-98, 2015

[10] Bouvet, A., Ghorbel, E., and Bennacer, R., The mini-conical slump flow test; Analysis and numerical study, Cement and Concrete Research, Vol. 40, pp. 1517-1523, 2010

[11] Measurement of the Rheological Properties of Hydraulic Cementitious Paste Using Rotational Rheometer, Standard ASTM C1749-12, 2012

[12] High-Shear Mixing of Hydraulic Cement Pastes, Standard ASTM C1738/C1738M-14, 2014

[13] Mechanical Mixing of Hydraulic Cement Paste and Mortar of Plastic Consistency, Standard ASTM C305-14, 2014